COMPOSITION, REGULATION, AND FUNCTION OF PROTEIN SERINE/THREONINE PHOSPHATASE•KINASE SIGNALING MODULES

By

Matthew David Mazalouskas

Dissertation
Submitted to the Faculty of the
Graduate School of Vanderbilt University
in partial fulfillment of the requirements
for the degree of

DOCTOR OF PHILOSOPHY

in
Pharmacology
May, 2014
Nashville, Tennessee

Approved:

Brian E. Wadzinski, Ph.D.

Vsevolod Gurevich, Ph.D.

Claus Schneider, Ph.D.

BethAnn McLaughlin, Ph.D.

Albert Reynolds, Ph.D.

To my wife, Abigail, whose love, and patience, knows no bounds

and

For Ambriella, Braeleigh, and Brecklyn, each equally my pride and joy.

ACKNOWLEDGEMENTS

The path towards completing this dissertation has been a journey of ups and downs, both professionally and personally. The highs of serendipitous results and studies that progressed forward were punctuated by the lows of inconsistent data, diminutive differences, and the occasional need to recalibrate the direction of my project. The joys of marrying my wife and the birth of three daughters was juxtaposed with the challenges of raising a chronically ill child and her untimely death a few months shy of her third birthday. Always looking forward, and with the support of many people, I optimistically traversed this undulating path towards my doctoral degree.

I would like to thank my mentor, Dr. Brian Wadzinski, for the help and guidance he has given me over the years. He provided me the freedom to openly explore biological questions with ever increasing independence. He has also been an exemplary scientific and parental role model. This dissertation would not have been possible without the members of my Committee: Drs. Vsevolod Gurevich, BethAnn McLaughlin, Claus Schneider, and Al Reynolds, for their patience in allowing me time to address experimental questions, their honesty when the data just was not working, and their flexibility as my project aims changed. I would like to acknowledge our collaborators, Drs. Richard Honkanen and Danna Zimmer, who provided expert advice and reagents critical to my studies on the PP5•ERK complexes in Chapter IV.

Over the years, the members of the Wadzinski lab have been a constant source of moral support and have provided an entertaining environment that made scientific-time fly by. Regrettably, I cannot acknowledge all of them by name. In particular, I would like to thank Dr. Guy Watkins for his candor when challenging my experimental ideas and his

assistance in strengthening the caliber of my studies, as well as Dr. Kelie Reece for her tenacity and cheerful spirit as we tackled many scientific challenges in studying the CaMKIV•PP2A complexes found in Chapter II. I want to thank Rey Gomez, M.S. in providing technical guidance and sound advice, as well as Dr. Ning Wang for his scientific recommendations and knowledge about *in vivo* animal models that placed my studies within a larger perspective. I would also like to recognize Dr. Ana Carneiro for her thoughtful suggestions that improved the quality of my experiments. I am appreciative of my family, my wife's family, and friends for their encouragement during my graduate studies. I will always be grateful to the staff of Monroe Carell Jr. Children's Hospital at Vanderbilt for their kindness, empathy, and friendship. I owe my gratitude to the Vanderbilt Pediatric Liver Transplant Program, in particular, Dr. Burnett "Beau" Kelly Jr., Dr. Lynette A. Gillis, and Nurse Practitioner Carly Bhave, as well as the organ donor families whose loved ones provided the "gift of life" for my daughter. Finally, I'd be remiss if I didn't acknowledge the innumerable sacrifices made by my wife, Abigail, in shouldering far more than her fair share of the parenting and household burdens while I pursued this doctoral degree.

Lastly, the work presented in this dissertation would not have been possible without the financial support of the Cellular, Biochemical and Molecular Sciences Predoctoral Training Grant T32 GM08554 (awarded to Matthew D. Mazalouskas), Predoctoral Training in Pharmacological Sciences Grant 2-T32-GM07628 and an NIGMS Predoctoral Fellowship (awarded to Kelie M. Reece), and the National Institutes of Health Grants GM051366 and 354DK070787 (awarded to Brian E. Wadzinski).

Imagination is more important than knowledge.
– Albert Einstein –

I know it's easy to imagine,
But it's easier to just "do."
See, if you can't "do" what you imagine,
Then, what is imagination to you?
– Kid Cudi –

TABLE OF CONTENTS

LIST OF TABLES

Page

LIST OF FIGURES

Page

CHAPTER I

INTRODUCTION

Cellular signaling and reversible phosphorylation

Cellular processes are regulated by a complex communication system of signal transduction pathways that govern cellular responses to both external and internal cues. Post-translational modifications (PTMs) of intracellular proteins are a crucial mechanism by which eukaryotic cells dynamically regulate signal transduction pathways. As a result, PTMs like phosphorylation, ubiquitylation, glycosylation, and acetylation are involved in orchestrating fundamental cellular activities, including cell cycle progression, apoptosis, DNA damage response, autophagy, and metabolism. Phosphorylation is the process by which a phosphate (PO_4^{3-}) group is added to a protein or other organic molecule and commonly occurs in eukaryotic proteins on serine, threonine, and tyrosine amino acids. The reversibility of protein phosphorylation arises from the integrated actions of protein kinases and protein phosphatases that catalyze the opposing processes of protein phosphorylation and dephosphorylation, respectively (Fig. 1). Phosphorylation ranks, by an order of magnitude, as the most experimentally observed PTM in prokaryotes and eukaryotes and is the second most common, putative PTM in the Swiss-Prot database, underscoring the importance of these events in regulating protein function (1,2). Since deregulation of proteins involved in signal transduction pathways can lead to disease, the enzymes catalyzing the addition or removal of site-specific phosphorylation events have emerged as prominent therapeutic targets.

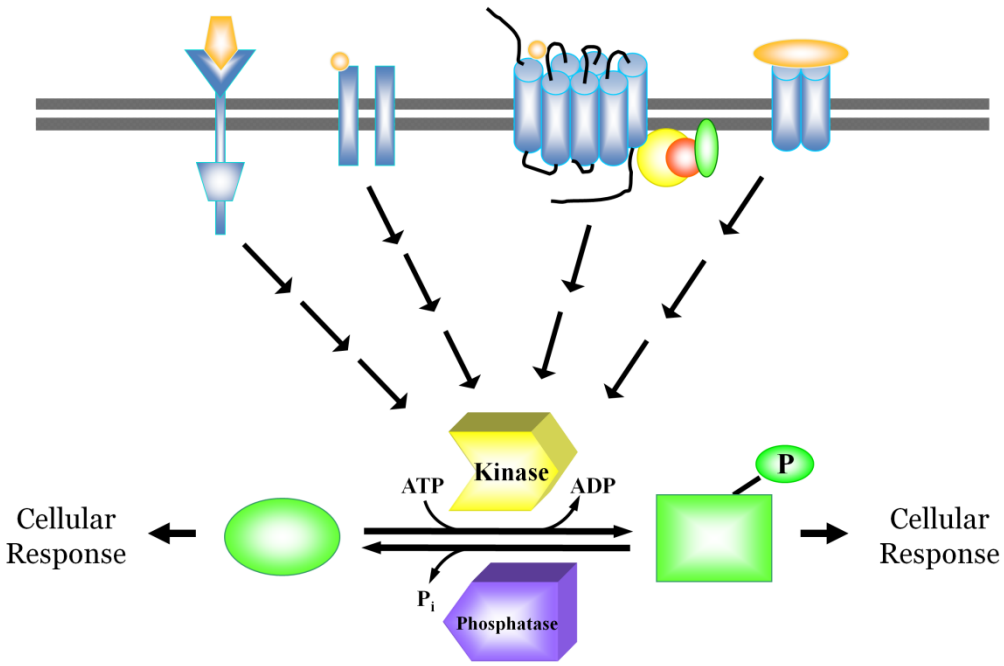

Figure 1. Reversible phosphorylation of proteins.
Cells respond to their environment by interpreting extracellular derived signals and altering intracellular signaling networks, often through the widely used mechanism of reversible protein phosphorylation. The phosphorylation state of target proteins within signaling pathways is controlled by a delicate balance of protein kinase and protein phosphatase activities.

Protein kinases

Protein kinases are ATP-dependent phosphotransferases that transfer a single phosphate group from the γ position of ATP to the hydroxyls of serine, threonine, and tyrosine residues in protein substrates. An essential divalent metal ion, usually Mg^{2+} or Mn^{2+}, binds ATP and facilitates the phosphoryl transfer reaction. The human kinome contains 518 putative protein kinase genes divided into two superfamilies. Kinase genes within the much smaller, atypical protein kinase (aPK) superfamily (40 members) lack sequence similarity to a conserved catalytic domain that is found within members of the eukaryotic protein kinase (ePK) superfamily (3,4). ePK kinase domains are divided into 12 subdomains that structurally form a bi-lobed catalytic core, where the active site lies in a deep cleft between the two lobes. The N-terminal lobe coordinates the binding of the donor ATP while the larger, C-terminal lobe binds the protein substrate (5). Most kinases transition from an inactive, "off" state to an active, "on" state (or vice versa) following phosphorylation of at least one residue (i.e., Ser, Thr, Tyr) in the activation loop, which induces conformational changes that facilitate substrate binding and catalytic transfer of the phosphate group. Phosphorylation and stabilization of the activation loop occurs via autophosphorylation (i.e., *in cis* or *in trans*) or following transphosphorylation by a separate kinase.

The ePK superfamily is subdivided into classes, families, and subfamilies based upon the sequence similarities of the catalytic domains, but kinases can also be divided into two main groups based upon their ability to phosphorylate serine/threonine or tyrosine residues. The covalent addition of a negatively charged phosphoryl group alters the conformation of the targeted protein and, consequently, its functional state. Besides

modulating a protein's localization, catalytic activity, or ability to interact with other proteins, the phosphorylation event can also provide a binding site for enzymes catalyzing additional PTMs. The removal of phosphate groups from targeted proteins by protein phosphatases can similarly regulate protein function.

Protein phosphatases

Protein phosphatases are phosphoric monoester hydrolases that utilize a water molecule to hydrolyze the phosphoester bonds of phospho-serine, phospho-threonine, or phospho-tyrosine residues in protein substrates. Akin to the protein kinases, protein phosphatases can be grouped according to their ability to dephosphorylate phospho-serine and phospho-threonine residues (protein serine/threonine phosphatases, PSTPs), phospho-tyrosine residues (protein tyrosine phosphatases, PTPs), or both phospho-tyrosine and phospho-serine/threonine residues (dual specificity phosphatases, DUSPs). Several large scale, proteomic analyses of phospho-peptides from a variety of mammalian cell lines have estimated that approximately 86.3-90.1% of all phosphorylation occurs on serine residues, 9.2-11.8% of all phosphorylation occurs on threonine residues, and 1.3-4.5% of all phosphorylation occurs on tyrosine residues (6,7). Thus, PSTPs play a prominent role in regulating over 98% of all protein phosphorylation events. PSTPs are subclassified into three families according to sequence, structure, and catalytic function: phosphoprotein phosphatases (PPPs), metal-dependent protein phosphatases (PPMs), and aspartate based phosphatases such as FCP (TFIIF-associating component of RNA polymerase II CTD phosphatase) and SCP (small CTD phosphatase) (8). The PPM family is the largest family, composed of 16 genes encoding at least 22 isozymes that require Mn^{2+} or Mg^{2+} for activity and are activated or inhibited by other

divalent ions; Fe^{2+} or Co^{2+} activate, whereas Cd^{2+}, Ca^{2+}, Zn^{2+}, or Ni^{2+} inhibit (9-13). The FCP/SCP family comprises 8 members that utilize a Mg^{2+} ion coordinated by two aspartic acid residues to dephosphorylate protein substrates. FCP acts on RNA polymerase II to regulate transcription , whereas SCP1, SCP2, and SCP3 have been found to modulate growth factor signaling by targeting Smads (13,14).

The PPP family consists of 13 genes (several of which are alternatively spliced; Fig. 2) giving rise to phosphatase catalytic subunits that are classified by their substrate specificity, sensitivity to toxins, and other biochemical characteristics. In 1983, Ingebritsen and Cohen developed a two subtype classification system for the then known mammalian PSTPs (15,16). Type-1 protein phosphatases (i.e., PP1) preferentially dephosphorylate the β-subunit of phosphorylase kinase and are sensitive to inhibition by two heat- and acid-stable, cytosolic proteins termed inhibitor-1 and inhibitor-2 (I-1 and I-2). Type-2 protein phosphatases (i.e., PP2) preferentially dephosphorylate the α-subunit of phosphorylase kinase and are insensitive to inhibition by I-1 or I-2. Additional studies further divided the PP2 family into three subtypes based on their catalytic requirement for divalent cations; PP2A members are active in the absence of divalent cations, PP2B requires Ca^{2+}/calmodulin, and PP2C requires Mg^{2+} or Mn^{2+}. Subsequent studies revealed that the PP2A and PP2B catalytic subunits exhibit strong conservation of their primary amino acid sequence while PP2C was found to be structurally distinct and warranted its own gene family, thus PP2C (i.e., PPM1) became the founding member of the PPM family (17). Over the years, additional PSTPs were discovered and added to the PPP family (reviews (18-21)). PP3 was first purified from detergent extracts of whole bovine brain (22), and is very likely the same enzyme as PP5, which was identified in a human

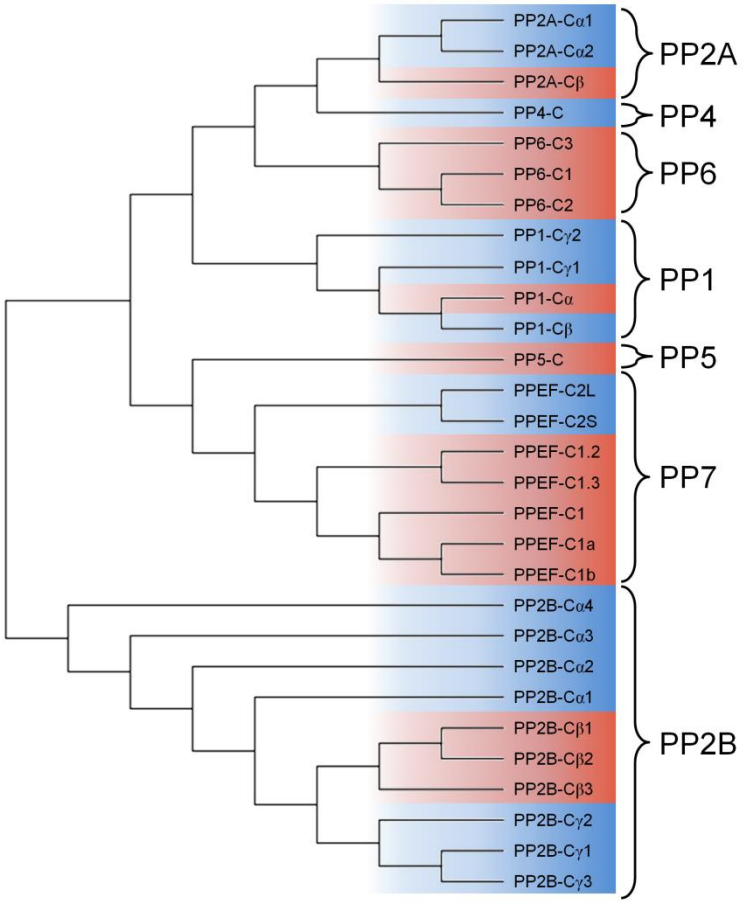

Figure 2. Molecular phylogenetic analysis of the Phosphoprotein Phosphatases (PPP). The evolutionary history was inferred by using the Maximum Likelihood method based on the Le_Gascuel_2008 model (355). The tree with the highest log likelihood (-4851.4602) is shown. Initial trees for the heuristic search were obtained automatically by applying Neighbor-Join and BioNJ algorithms to a matrix of pairwise distances estimated using a JTT model, and then selecting the topology with superior log likelihood value. A discrete Gamma distribution was used to model evolutionary rate differences among sites [5 categories (+G, parameter = 1.5496)]. The analysis was performed using 29 amino acid sequences of PPP proteins, including variant proteins produced by alternative splicing of PPP genes. Sequences, for which there is experimental evidence available, were obtained from UniProtKB/Swiss-Prot protein knowledgebase release 22 January 2014. All positions with less than 95% site coverage were eliminated (i.e., fewer than 5% alignment gaps, missing data, and ambiguous bases were allowed at any position). There were a total of 232 positions in the final dataset. Evolutionary analyses were conducted in Molecular Evolutionary Genetics Analysis (MEGA) Version 6.0.5 (356,357). Splice variants of the same PPP gene are grouped and shaded blue or red. Related PPP proteins have been grouped into their respective PPP subfamilies.

teratocarcinoma cell line cDNA library (23), a yeast two-hybrid screen (24), and in a rat adipose tissue cDNA library (25). The official name for PP3/PP5 was established as PP5 to prevent confusion with the PP2B phosphatase gene, which was designated as PPP3 by the human genome project (Richard E. Honkanen, personal communication). PPX was identified from a rabbit liver cDNA library and subsequently termed PP4 (26,27). Homology-based reverse-transcription polymerase chain reaction of HeLa S3 cell RNA led to the discovery of PP6, which is highly homologous to the *S. cerevisiae* SIT4 phosphatase (28,29). A Mg^{2+}-dependent, Ca^{2+}-activated phosphatase, termed PP7, was identified from human retina RNA (30,31) and by exon mapping of the human X chromosome (32). PP7 is placed in the PPP family since its catalytic core possesses 28-35% identity with the cores of PP1-PP6, and contains all 53 of the conserved amino acids found in PP1-PP6 (30).

The number of protein tyrosine kinases and protein tyrosine phosphatases are similar (85 and 81, respectively) (33); however, there is a disparity in the number of protein serine/threonine kinases and protein serine/threonine phosphatases (344 and 37, respectively) (5). Diversity in protein phosphorylation seems to have favored an evolutionary expansion in the number of kinase genes, but questions arise as to how PSTPs are able to regulate a diverse array of phosphorylated targets while maintaining substrate specificity with so few gene products. Functional diversity in PSTP signaling is achieved through the binding of catalytic subunits to numerous regulatory and targeting subunits, which create different oligomeric forms (i.e., holoenzymes) of the same phosphatase with distinct functions. In addition, a variety of PTMs (i.e., phosphorylation by protein kinases) have been shown to modulate phosphatase function.

Dephosphorylation of phosphorylated phosphatases can occur by an autocatalytic intra- (i.e., *in cis*) or inter-molecular (i.e., *in trans*) mechanism as well as by a different phosphatase. Since protein phosphatases are substrates for protein kinases, they can participate in kinase cascades, phosphatase cascades, or mixed cascades to regulate a variety of cellular functions.

Protein phosphatase 2A (PP2A)

PP2A is the prototypical member of the PP2A subfamily of PPPs, which includes PP4 and PP6. Present in all eukaryotic phyla, PP2A has been estimated to account for 0.2-1% of the total cellular protein (34,35). PP2A plays a prominent role in the regulation of a variety of cellular processes, including metabolism, apoptosis, DNA damage response, translation initiation and termination, cell cycle, growth, proliferation, and differentiation (36). Accordingly, dysfunctional regulation of PP2A has severe consequences on cell physiology. Genetic studies have established that a disrupted PP2A catalytic subunit is lethal in yeast (37), in *Drosophila* during embryogenesis (38), and in mice at E5-6.5 (39). The naturally occurring PP2A inhibitor okadaic acid (produced by dinoflagellates and several marine sponge species) causes diarrhetic shellfish poisoning and has been demonstrated to promote skin tumor formation in mice (40). Additionally, two other natural PP2A inhibitors, microcystin-LR and nodularin (produced by cyanobacterium), are known to induce hepatocarcinomas (40). PP2A is also the target of a number of viral proteins that subjugate host cell processes. The polyoma middle tumor (T) and small t antigens, as well as the SV40 small t antigen, directly associate with PP2A to promote cellular transformation (41). Adenovirus type 5 E4orf4 protein and HIV-1-encoded NCp7 and vpr proteins also form stable complexes with PP2A to

deregulate cell growth and survival (42,43). Besides playing a role in the development of cancers, PP2A has also been implicated in the pathophysiological development of diabetes and several neurodegenerative diseases (44-47).

PP2A exists in a variety of oligomeric complexes in cells (48). The catalytic activity of PP2A, contained within the catalytic subunit ($PP2A_C$), is encoded by two highly conserved genes, $PP2A_C$ alpha (Cα) and beta (Cβ), which are evolutionarily conserved in plants (49) and animals (50). Human Cα and Cβ are 97% identical in sequence and ubiquitously expressed; however, the subunits are not functionally equivalent. Disruption of the Cα gene is embryonic lethal in mice and the presence of Cβ is unable to compensate for the loss of Cα (39). Most cells express 10 times as much Cα as Cβ (51), but Cα knockout embryos contain similar levels of total $PP2A_C$ as wildtype embryos, suggesting that Cβ does not target the same substrates as Cα (39). In support of this, Cα was found to be predominately localized to the plasma membrane during early murine embryogenesis while Cβ was found primarily in the cytoplasm and nucleus (52). Differences in the subcellular localization of these isoforms may stem from Cα-specific targeting signals (7 of the 8 amino acids different between the two isoforms is contained within a 30 amino acid stretch at the N-terminus) and/or differences in the association of these catalytic subunits with regulatory subunits.

The 36 kDa $PP2A_C$ subunit associates with a 65 kDa regulatory/scaffolding A subunit ($PP2A_A$) to form the core dimer (AC). $PP2A_A$ exists as two isoforms (Aα and Aβ) that are 86% identical and ubiquitously expressed in all tissues, although several differences have been established: the Aα isoform is expressed ~10-fold more abundantly in mammalian tissues, Aβ binds more weakly to $PP2A_C$, Aβ expression appears to be

suppressed in a number of tumor lines, and SV40 small t antigen binds Aα but not Aβ while polyoma middle T antigen binds both isoforms (53,54). There is also an N-terminal extension of 12 amino acids present in Aβ, probably acquired during mammalian evolution since it is absent in *Xenopus* Aβ, that may elicit some unknown functional effect (54). Biochemical analyses of the four core dimers (AαCα, AβCα, AαCβ, AβCβ) have revealed that there are no differences in the ability of Cα and Cβ to interact with any one $PP2A_A$ isoform (though there is a difference between $PP2A_A$ subunits in their capacity to bind $PP2A_C$) nor any differences in the phosphatase activities of any of the core dimers (55). Thus, the different roles played by Cα and Cβ in early embryogenesis are more likely the result of their differential association with canonical regulatory B subunits and atypical regulatory subunits.

PP2A canonical regulatory B subunits

PP2A canonical regulatory B subunits associate with the core dimer in a mutually exclusive manner to form a heterotrimeric holoenzyme complex (ABC), the predominate form of PP2A that exists in cells. $PP2A_A$ is composed of 15 tandem HEAT (Huntingtin, Elongation factor 3, PP2A subunit, TOR) motifs, a 39-amino acid sequence that forms two anti-parallel α helices, which stack to form an elongated horseshoe-shaped protein that accommodates the binding of both $PP2A_C$ and a B subunit (56). The human genome contains 15 B subunit genes that yield 23 different regulatory subunits, once alternative transcripts and splice variants are taken into account (57). The B subunits are classified into 4 families designated B (58), B′ (59), B″ (60), and B‴ (61) (Fig. 3). While extensive sequence homology exists within the members of the B and B′ families, there is little sequence similarity between B subunit families. However, a common structural core

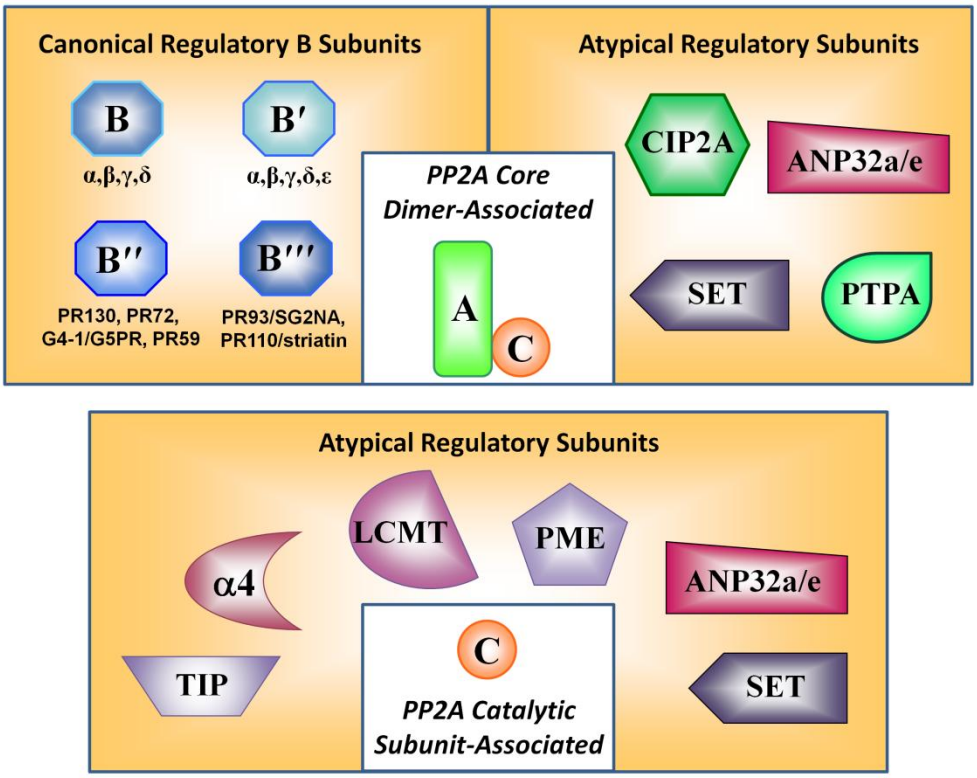

Figure 3. PP2A canonical regulatory B subunits and PP2A atypical regulatory subunits.

Four major PP2A canonical regulatory B subunit families (B, B′, B″, B‴), each containing multiple isoforms and splice variants, associate with the PP2A core dimer (*AC*). PP2A atypical regulatory subunits can associate with AC and/or the PP2A catalytic subunit (*C*).

allows a conserved mode of interaction between the B subunits and HEAT repeats 2-7 of $PP2A_A$ (62,63). An analysis of purified PP2A holoenzymes indicated that both Cα- or Cβ-containing holoenzymes exhibited identical phosphatase activity towards myelin basic protein and histone H1 when associated with the same B subunit (Bα, B′α1, or B″/PR72) and Aα (55). However, a difference in the magnitude of the dephosphorylation rates towards these substrates was observed amongst the different ABC complexes, suggesting that regulatory B subunits can dictate the substrate specificity of $PP2A_C$ (55). It is interesting to note that besides Aβ exhibiting a 7-fold reduction in the binding of $PP2A_C$, it also displays a 3-fold reduction in the binding of B′α1 and B″/PR72, as well as an inability to bind any Bα, when compared to Aα (54). The concept that canonical regulatory B subunits generate substrate specificity for $PP2A_C$ is further supported by studies revealing that many B subunits are regulated in a temporal manner, differentially expressed in tissues, and localized to different subcellular compartments within cells. Crystal structures of AαBαCα, AαB′γ1Cα, and AαB″/PR70Cα holoenzymes have also revealed that the B subunit directly controls substrate specificity by altering the physiochemical environment of the active site in the adjacent $PP2A_C$, restricting the accessibility of the active site to substrates, as well as by providing additional binding sites for potential substrates (58-60,64). $PP2A_C$ regulates a various array of cellular processes, which is likely explained by the diversity of PP2A heterotrimeric holoenzymes that can form to modulate signaling pathways and substrates in a spatiotemporal manner.

PP2A atypical regulatory subunits and post-translational modifications

Recent experimental evidence has indicated that the assembly of PP2A heterotrimeric holoenzymes, as well as the stability and activity of $PP2A_C$, is modulated

via atypical regulatory subunits. Unlike the canonical regulatory B subunits that require $PP2A_A$ for association with $PP2A_C$, the majority of the atypical regulatory subunits bind $PP2A_C$ in the absence of $PP2A_A$ (Fig. 3). Two such subunits, leucine carboxyl methyltransferase (LCMT) and PP2A methyl esterase (PME), are enzymes that catalyze the reversible methylation of $PP2A_C$. Variations in the methylation state of $PP2A_C$ have been found in a number of physiological settings and have been shown to be decreased in Alzheimer's disease; however, the precise cellular consequences of changes in $PP2A_C$ methylation remain poorly characterized (65). Methylation of $PP2A_C$ at its C-terminal leucine residue (Leu309) appears to play a crucial role in determining the type of regulatory B subunits able to bind (66). While several members of the B′, B″, and B‴ families are able to form holoenzyme complexes with both methylated and demethylated $PP2A_C$, members of the B family require $PP2A_C$ methylation in order to form complexes (67). Chronic downregulation of LCMT expression results in the degradation of Bα subunits and induces a G_1 phase arrest in cells, which eventually culminates in apoptosis (67). The methylation state of $PP2A_C$ is regulated, in part, through the spatial localization of LCMT and PME; LCMT is located within the cytoplasm, whereas PME is primarily housed within the nucleus. Conformational changes in PME following its association with $PP2A_C$ shifts PME into an active conformation that facilitates demethylation of Leu309 and also shifts $PP2A_C$ into an inactive state, most likely through the loss of Mn^{2+} ions from its active site (68). The inability of LCMT to re-methylate PME-inactivated $PP2A_C$ provides supporting evidence that $PP2A_C$ must be in an active conformation to facilitate LCMT-mediated methylation of Leu309 (68,69).

Initially termed Phosphatase Tyrosyl Phosphatase Activator (PTPA) for its ability to induce tyrosine phosphatase activity in $PP2A_C$ (70), PTPA has since been backronymed Phosphatase Two A Phosphatase Activator because it reactivates PME-bound, inactivated $PP2A_C$ (67). PTPA is an atypical subunit that requires the presence of $PP2A_A$ to associate with $PP2A_C$. In contrast to PTPA, other proteins have been identified that directly inhibit $PP2A_C$ activity. PP2A Inhibitor 1, or ANP32a, and a related family member, ANP32e, inhibit $PP2A_C$ activity until they become phosphorylated at an unknown tyrosine site (71,72). SET, also known as PP2A Inhibitor 2 (71), has been shown to inhibit $PP2A_C$ in its monomeric, core dimer, or holoenzyme form, indicating it directly associates with the catalytic subunit. SET can be selectively cleaved into two fragments and both have been shown to inhibit PP2A phosphatase activity (73). Like PP2A Inhibitor 1, SET is a phosphoprotein and the phosphorylation of key serines, potentially by PKC, appears to play a role in its regulation of PP2A (74). The recently identified CIP2A, or Cancerous Inhibitor of PP2A, appears to require the presence of $PP2A_A$ for binding, is upregulated in multiple tumor types, and inhibits PP2A-mediated dephosphorylation of c-Myc through an unknown mechanism (75). The 41 kDa protein TIP (Type 2A Interacting Protein) also acts as an inhibitor of $PP2A_C$ activity *in vitro*, while its 20 kDa splice variant, TIP_i2, fails to associate with and inhibit $PP2A_C$ (76). Modulation of TIP levels in cells, as well as okadaic acid treatment, alters the phosphorylation state of an unknown 32 kDa substrate of ATM and ATR kinases, thereby implicating PP2A in the regulation of this phospho-protein in the DNA damage response pathway. Since PP4 and PP6 are also sensitive to okadaic acid and bind TIP, it is unclear which of these phosphatases are acting downstream of ATM/ATR (76).

Studies in yeast on the rapamycin-sensitive TOR signaling pathway, a pathway required for protein synthesis in response to nutrient availability, determined that phosphorylation of Tap42 by TOR kinase facilitates the interaction of Tap42 with the yeast homologs of $PP2A_C$ (77). Moreover, $PP2A_C$, $PP4_C$, and $PP6_C$ were found to interact with the mammalian homolog of Tap42, alpha4 (*IGBP1*), which alters phosphatase activity in a substrate-dependent manner (78-80). Alpha4 has been demonstrated to modulate the polyubiquitination state of $PP2A_C$, acting to both prohibit and promote polyubiquitination (81,82). The mechanism for the dual protective/destructive nature of alpha4 was recently established in our lab; my contributions to these studies earned me co-authorship on a JBC publication (83). We demonstrated that alpha4 is itself targeted for monoubiquitination by MID1, a microtubule-associated E3 ubiquitin ligase, and subsequent calpain-mediated cleavage of the C-terminus. Alpha4-mediated protection of a polyubiquitin site in $PP2A_C$ appears to fine tune the level of PP2A activity at microtubules. Interestingly, alpha4 cleavage was found to be decreased in patients with Opitz syndrome and increased in patients with Alzheimer's disease, further supporting a role for defective alpha4-regulation of PP2A in the generation of hypophosphorylated (Opitz) and hyperphosphorylated (Alzheimer's) microtubule associated proteins.

Dr. Ning Wang in our laboratory developed a platform to explore the *in vivo* role of *Drosophila melanogaster* Tap42 in the development of *Drosophila* imaginal discs (84). Tap42 null animal models are nonviable (85,86). Therefore, our group engineered the tissue-specific knockdown of Tap42 expression in *Drosophila* by combining the Gal4/UAS tissue-specific expression system with Tap42-targeted RNAi driven by wing imaginal disc drivers (i.e., *pnr*- and *ap*-). A pleiotrophic phenotype was observed that

included a thoracic cleft, undeveloped wings, and low survival rates. Tap42 interacts with Mts, PP4, and PPV, the *Drosophila* homologs of $PP2A_C$, $PP4_C$, and $PP6_C$, respectively; indicating that the interaction of alpha4/Tap42 with PP2A family members is evolutionarily conserved (80). Importantly, expression of a phosphatase-binding defective mutant of Tap42 failed to rescue the Tap42 RNAi-induced phenotypes, suggesting that the observed phenotypes are specifically due to Tap42's ability to associate with these phosphatases and regulate key signaling pathways, including JNK, Hedgehog, and Decapentaplegic (DPP; a homolog of mammalian bone morphogenic proteins (BMPs)). I collaborated with Dr. Wang on some of these studies and also demonstrated that *Drosophila* Tap42 is targeted for monoubiquitination (data not shown), as is human alpha4 (83), indicating that alpha4 regulation of PP2A function is evolutionarily conserved. These contributions warranted my co-authorship on Dr. Wang's paper (84).

Besides methylation at Leu309 and ubiquitylation at Lys41 (87,88), $PP2A_C$ is subject to several other important PTMs that regulate $PP2A_C$ function (Fig. 4). The carboxy-terminal tail of $PP2A_C$, "TPDYFL" (304-309), has been reported to be subject to phosphorylation events at Thr304 and Tyr307 (89). Threonine phosphorylation by a still unidentified "autophosphorylation-activated protein kinase," originally isolated from bovine kidney, inhibits the catalytic activity of the core dimer (90). Tyrosine phosphorylation of $PP2A_C$ by p60v-src, p56lck, epidermal growth factor receptor, and insulin receptor has been demonstrated to inhibit the catalytic activity of monomeric $PP2A_C$ by over 90% (91,92). Threonine and tyrosine phosphorylation of $PP2A_C$ is

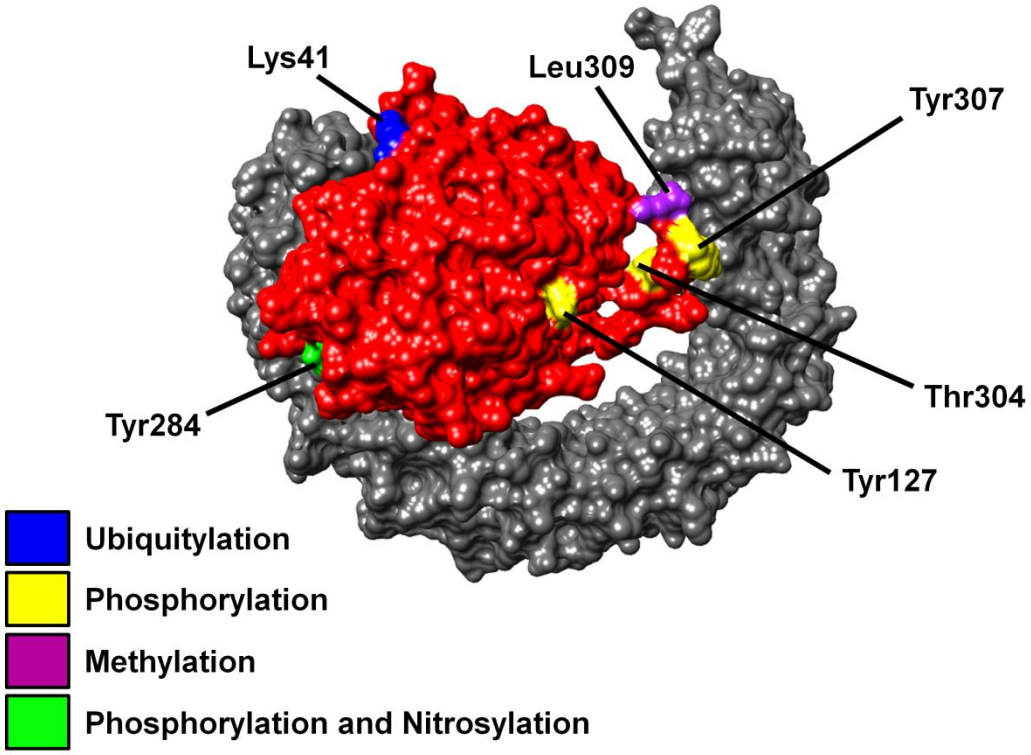

Figure 4. Post-translational modifications of $PP2A_C$.
Crystal structure of the AαB′γ1Cα holoenzyme with the regulatory B′γ1 subunit removed to display the PP2A scaffolding ($PP2A_A$; dark gray) and catalytic ($PP2A_C$; red) subunits. The protein surface is colored according to the ability of $PP2A_C$ residues to be ubiquitylated (blue), phosphorylated (yellow), methylated (purple), or phosphorylated and nitrosylated (green). Structure was generated using UCSF Chimera version 1.8.1 and Protein Data Bank ID code 2NPP.

enhanced in the presence of okadaic acid, indicating that autodephosphorylation of these phospho-sites may occur (91). Deletion of nine residues at the C-terminus of $PP2A_C$ renders a protein that is unable to associate with regulatory subunits from the B family, indicating that modifications at the C-terminus are important in regulating holoenzyme formation (89). $PP2A_C$ phosphorylation also appears to modulate its methylation state and hence its interaction with members of different B subunit families (67). Detailed biochemical analyses of various point mutants of $PP2A_C$ (at Thr304, Tyr307, or Leu309) have revealed that binding to $B\alpha/\beta_1$ subunits requires methylation and is inhibited by phosphorylation, binding to $B'\alpha/\beta_1/\varepsilon$ subunits is unaffected by methylation and may be inhibited by phosphorylation, while binding to $B'\delta_1$ and B″PR70/PR72 subunits is unaffected by both (67,93). Of note, unpublished studies from our laboratory have raised significant question about $PP2A_C$ tyrosine phosphorylation; our studies indicate that $PP2A_C$ is subject to phosphorylation on Tyr127 and Tyr284 but not Tyr307. $PP2A_C$ is also targeted for nitrosylation at Tyr284. Induced in the presence of elevated levels of nitric oxide when $PP2A_C$ is associated with the protein VCP/p97, nitrosylation at Tyr284 results in an increase in the expression/stability of cellular $PP2A_C$ as well as a disruption of the association of $PP2A_C$ with $PP2A_A$ (94). Thus, the extant data indicate that holoenzyme composition, association with atypical regulatory subunits, and PTMs play important roles in regulating phosphatase activity and creating functional diversity in $PP2A_C$.

Protein phosphatase 5 (PP5)

Protein phosphatase 5 (PP5) is encoded by a single gene, *PPP5C*, in humans. In contrast to other members of the PPP-superfamily of phospho-serine/threonine protein phosphatases, the regulatory, substrate targeting, and catalytic domains of PP5 are expressed within a single polypeptide chain. PP5 is ubiquitously expressed in mammalian tissues, with the highest levels detected in brain, and is present in both the cytoplasm and nucleus of multiple cell types. However, the physiological roles of PP5 have been difficult to elucidate.

PP5 structure

PP5 is a 58 kDa protein (499 amino acids) that contains 4 major domains: a tetratricopeptide (TPR) domain, a peptidyl-prolyl *cis-trans* isomerase like (PPI-like) domain, a catalytic domain, and a regulatory domain (Fig. 5). Discovered in 1990 by two independent groups, the TPR motif is named after the degenerate 34 amino acids that make up the α-helical motif (95,96). TPR motifs can be individually dispersed in a protein, but are usually associated in tandem repeats of 3-16 motifs in a host of proteins from bacteria to man. Defined by a pattern of small and large hydrophobic residues, the TPR motif lacks invariant residues and only a few amino acid positions have a strong preference for a particular class of amino acid (e.g., small, large, aromatic). Nevertheless, this helical motif is structurally versatile in accommodating small insertions, loops, and helical extensions to generate diversity in the structures adopted by these tandem repeats (97). In fact, the first solved crystal structure of a TPR-motif containing protein was PP5 (98). Located within the N-terminal region of PP5, each of the three TPR motifs in its TPR domain adopts a helix-turn-helix arrangement. These three pairs of antiparallel,

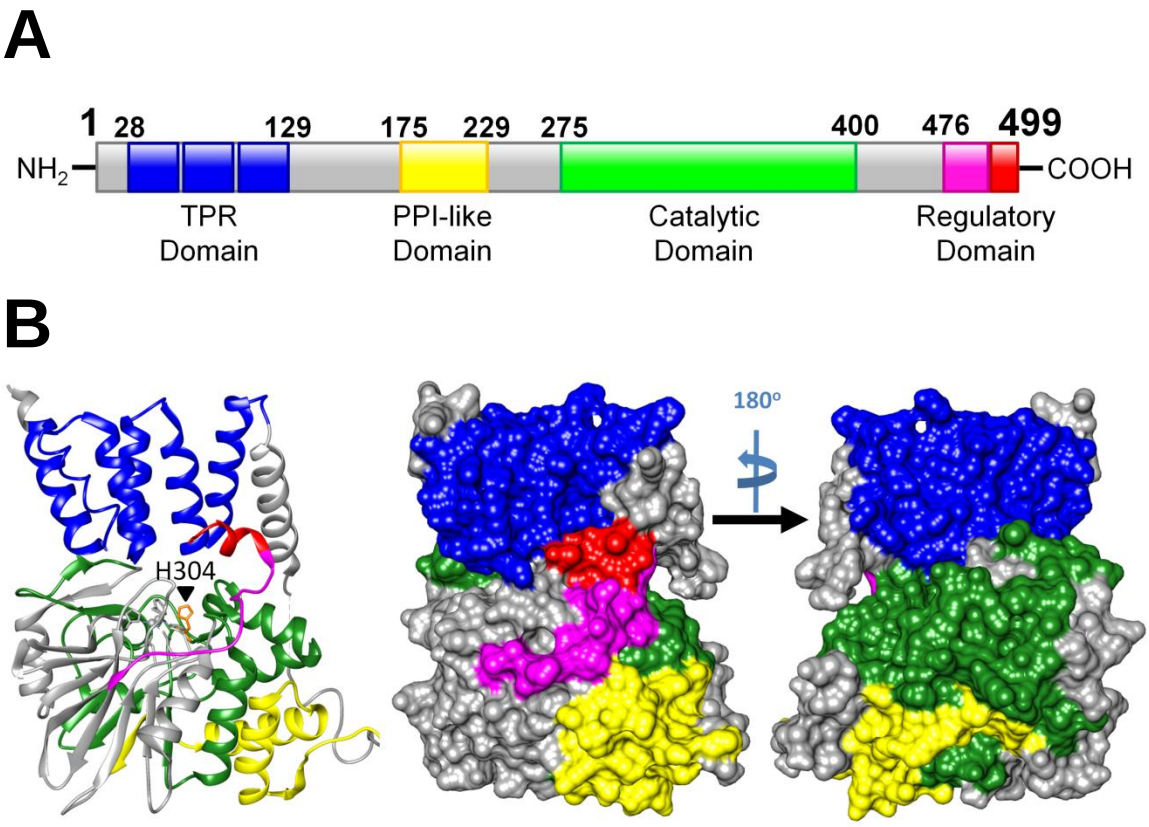

Figure 5. Functional domains of PP5.

A, Schematic representation showing the functional domains present in the PP5 protein. PP5 has an N-terminal autoregulatory domain containing the tetratricopeptide (TPR) domain, which is composed of three TPR motifs (blue). The globular C-terminal domain of PP5 contains a peptidyl-prolyl cis-trans isomerase like (PPI-like) domain (yellow), the catalytic domain (green), and a regulatory domain that contains a putative nuclear localization sequence (NLS) (pink) and the J-helix (red). ***B***, The PP5 protein, depicted as a ribbon diagram (*left*) and as a solid surface in two views rotated 180^{o} (*right*), is color coded to correspond to the functional domains. The catalytic histidine (H304) side chain is shown in the ribbon diagram and colored orange. Structures were generated using UCSF Chimera version 1.8.1 and Protein Data Bank ID code 1WAO.

α-helical bundles are rotated 24^{o} relative to one another and pack to form a globular domain with a right-handed superhelical arrangement that forms a concave surface on one face and a convex surface on the other. The 35 residues flanking the C-terminus of the last TPR motif fold into an extended α-helix when the TPR domain is separated from the rest of the protein, but is partially unwound in the full protein, forming a disordered linker that connects the TPR domain to the C-terminal globular domain that contains the PPI-like, catalytic, and regulatory domains (99).

The PPI-like domain in PP5 is a stretch of 55 amino acids that shares 60% similarity to a consensus FK-506 Binding Protein (FKBP) motif (100). FKBP is a family of proteins that have prolyl isomerase activity and function as protein folding chaperones. An alignment with the PPI domain of FKBP52 shows that PP5 contains 9 of the 12 residues involved in the high affinity interaction with FK-506 (100), an immunosuppressant drug primarily utilized for preventing organ rejection in transplant patients (101). An FK-506 affinity matrix weakly binds purified PP5, but more importantly PP5 can be eluted from the matrix with FK-506 but not cyclosporin A, suggesting that PP5 exhibits weak FK-506 binding activity and that it can be eluted in a stereospecific manner (100). However, its ability to isomerize proline residues has not yet been demonstrated.

The catalytic domain of PP5 is 42-43% identical to the catalytic domains of mammalian PP1, PP2A, and PP2B at the primary amino acid level (102). Furthermore, the catalytic domain of the yeast homolog, PPT, is 42% identical and 63% similar to PP5 if conservative substitutions are taken into account, indicating that this phosphatase is well conserved from yeast through humans (23). A bimetallic active site [Asp271-

M1:M2-His427-W1-His304-Asp274 (where M1/M2 and W1 are metal ions and a water molecule, respectively)] common to all PPP gene members is located in a shallow grove on the surface of the catalytic domain of PP5 (103). The extreme C-terminus of PP5 contains the regulatory domain, which harbors a putative nuclear localization signal (NLS) and the J-helix, an α-helix formed from the last 8 amino acids, which modulates phosphatase activity by associating with the N-terminal globular domain to regulate substrate access to the catalytic site.

PP5 regulation

Unlike PP1 and PP2A, the basal activity of PP5 is very low. Early studies examining the catalytic activity of PP5 indicated that bacterially purified human PP5 exhibits phosphatase activity >100-fold lower than that of PP2A towards phospho-histone H1 (23). However, incubation of PP5 with trypsin removes the N-terminal domain to produce a 39 kDa fragment containing the catalytic domain that exhibits enhanced phosphatase activity towards casein (26-fold) and myelin basic protein (260-fold) (104). The initial purification of PP5 (i.e., PP3) similarly resulted in the formation of a 36 kDa protein that exhibited phosphatase activity because of the removal of the N-terminus (22). This finding suggests that the N-terminal domain shields the active site from substrates. Later crystallographic studies of full-length PP5 revealed that the residues comprising the turns connecting the α-helices within each TPR motif form a continuous labium that juts into the catalytic groove of the phosphatase domain (99). The initial characterization of PP5 revealed that it was activated in response to arachidonic acid (22). This was confirmed by other groups showing that arachidonic acid and other similar polyunsaturated fatty acid derivatives of arachidonic acid enhanced the activity of

non-trypsinized, full-length PP5 26-fold (104). These studies also showed that the isolated catalytic domain of PP5 was unresponsive to arachidonic acid, concluding that lipid binding to the N-terminal, autoinhibitory domain modulates phosphatase activity. The regulatory domain of PP5 was identified when deletion of the C-terminal 13 amino acids resulted in a form of PP5 that was just as active as the full length, lipid-activated phosphatase (105,106). Crystal structures show that the C-terminal J-helix does not physically block access to the catalytic cleft but instead stabilizes the interaction of the N-terminal domain with the catalytic domain to generate the autoinhibited conformation of PP5 (99). Interestingly, the J-helix also plays an important role in the arachidonic acid-induced increase in phosphatase activity, thereby implicating this regulatory domain in both inhibiting and promoting phosphatase activity (106).

TPR motifs mediate protein-protein interactions (107). One protein that interacts with PP5 at its TPR motifs is the chaperonin heat shock protein 90 (HSP90). Several key basic residues (Lys32, Arg74, Lys97, and Arg101) within the N-terminal domain of PP5 interact with an acidic EEVD sequence located within the C-terminal tail of HSP90 (108) (Fig. 6). Mutation of any of the basic residues within the concave face of the TPR domain to alanine dramatically reduce or eliminate binding to HSP90 (108). Scanning mutagenesis of the TPR motifs also indicated that mutations of these basic residues do not affect the autoinhibitory conformation of PP5, revealing that the concave and convex faces of the TPR domain are separately involved in binding HSP90 and inhibiting PP5 (106). In addition to binding PP5, HSP90 is a moderate activator of PP5 activity, as both full-length yeast HSP90 and a peptide derived from human HSP90α (TSRMEEVD) increase the activity of PP5 7-fold towards the small molecule substrate

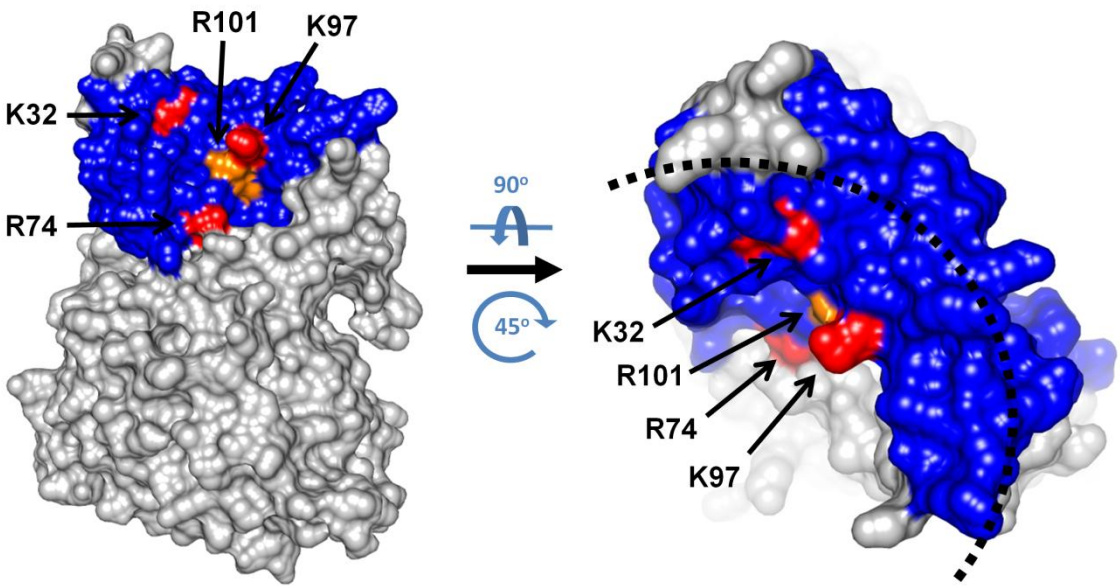

Figure 6. Interaction between PP5 and HSP90 is mediated by key residues within the TPR domain of PP5.

A, Surface representation of the PP5 protein, with the TPR domain colored blue. Basic residues within the N-terminal domain of PP5 important in the PP5-HSP90 interaction are colored red (*K32, R74, and K97*) or orange (*R101*). ***B***, A second view of the PP5 protein, rotated orthogonally and then clockwise 45°, highlights the curvature of the TPR domain, which is emphasized by the dashed arc (black). Residues important in the PP5-HSP90 interaction are located within the concave face of the TPR domain. Structures were generated using UCSF Chimera version 1.8.1 and Protein Data Bank ID code 1WAO.

para-nitrophenylphosphate (pNPP) (99). Very recently, HSP70 was also shown to bind PP5 and activate it ~5-fold greater than HSP90 (109). Whereas two HSP90 molecules associate with each PP5, HSP70 interacts with PP5 in a 1:1 stiochiometric ratio. Several additional PP5-interacting proteins associate with the TPR domain of PP5 and increase phosphatase activity (e.g., activated Rac1, $G\alpha_{12}$ and $G\alpha_{13}$, and select Ca^{2+}-bound S100 proteins) (110-112).

PP5 function

Immunofluorescent studies examining the cellular distribution of PP5 initially revealed that it was primarily located within the nucleus (23). Deletion and mutational analyses concluded that a putative nuclear localization signal (NLS) located at the C-terminus (Phe476-Asn491) promoted nuclear translocation of PP5 in a phosphatase activity-independent manner (113). The identification of HSP90, predominately cytoplasmic in its distribution, as an interacting partner for PP5 demonstrated for the first time the presence of PP5 within the cytoplasm (108). Although the specific cellular functions regulated by PP5 remains unclear, PP5 has been implicated in the control of cell proliferation, migration, differentiation, electrolyte balance, apoptosis, survival, and DNA damage repair (114,115). Several of PP5's functions have been ascertained following the identification of PP5-interacting proteins. For example, Chinkers and colleagues demonstrated an interaction between PP5 and the atrial natriuretic peptide (ANP)/guanylate cyclase receptor of the heart and proposed that PP5 plays a role in desensitizing the receptor following ligand binding and activation (24). Subsequent studies indicated that the interaction between PP5 and the ANP/guanylate cyclase receptor involved HSP90, as did the interaction of PP5 with the estrogen and

glucocorticoid receptors (100,116-118). PP5 appears to have opposing roles in regulating glucocorticoid signaling and it may be that PP5 regulates the system at multiple steps in the pathway (119). The interactions of PP5 with p53 and the mammalian anaphase promoting complex implicate the phosphatase in the modulation of cell cycle progression, while the association of PP5 with the mammalian cryptochrome, CRY2, suggests that PP5 regulates or is regulated by circadian rhythm. PP5 also regulates the phospho-state of the voltage-gated potassium channel KCNH2 (i.e., hERG1) and large-conductance Ca^{2+}- and voltage-activated K^{+} channels (BK channels), and is involved in several stress-induced signal transduction pathways (120,121).

Genotoxic stress, induced by ionizing radiation or hydroxyurea treatment, activates the Ataxia-telangiectasia mutated (ATM) or ATM- and Rad3-related (ATR) kinases following the formation of double-stranded or single-stranded DNA breaks, respectively (122). These kinases play an important role in activating the DNA damage checkpoint that precedes cell cycle arrest and DNA damage repair. PP5 interacts with both kinases, promoting the autophosphorylation and activation of ATM as well as the phosphorylation of downstream ATR substrates (123,124). Recent studies have refined the role of PP5 in the ATR response, placing the phosphatase in a position to regulate the phosphorylation of Chk1, an important substrate of ATR (125). PP5 also plays a role in the DNA repair process. It interacts with the DNA-dependent protein kinase catalytic subunit (DNA-PKcs) and dephosphorylates at least two inhibitory sites to allow repair of DNA double-stranded breaks (126). Cellular exposure to hypoxia, oxidative stress, and rapamycin activates apoptosis signal regulated kinase 1 (ASK1), a mitogen activated protein kinase kinase kinase (MAP3K) for p38 mitogen activated protein kinase

(p38MAPK) and c-Jun N-terminal Kinase (JNK) (127-129). PP5 negatively regulates the activation of ASK1 to reduce downstream signaling to JNK, mostly likely by directly dephosphorylating Thr845 in ASK1, without affecting p38MAPK activity (110,128).

Interestingly, a yeast two-hybrid screen revealed that PP5 could associate with the A subunit of PP2A and subsequent immunoprecipitation experiments from HeLa cell extracts revealed that a regulatory B″/PR72 subunit associated with the PP5-PP2A_A heterodimer to form a heterotrimeric holoenzyme containing PP5 in lieu of PP2A_C (130). Although few studies have followed up on this finding, a separate group found that rapamycin treatment of Rh30 cells reduced the amount of regulatory B″/PR72 subunit present in PP5 immune complexes in an mTOR-dependent manner, without altering levels of co-precipitated PP2A_A (129). PP5 has also been shown to associate with another B″ member. Studies by other groups have demonstrated that the B″ subunit GPR5/G4-1 will associate with IKKβ, acting to recruit PP5 to IKKβ to inhibit kinase activity and downstream signaling to NF-κB (131), and with P-glycoprotein, promoting interactions with PP5 which negatively regulates P-glycoprotein expression and function (132).

Recently, two-dimensional liquid chromatography and mass spectrometry identified PP5 as a Raf1-interacting protein (133). Raf1 is a MAP3K for extracellular signal-regulated kinase (ERK) and undergoes a complex series of phosphorylation and dephosphorylation events as part of its activation-inactivation cycle (Chapter III). Detailed biochemical analyses demonstrated that PP5 negatively regulates Raf1 signaling and inhibits neuritogenesis in PC12 cells by dephosphorylating an activating site on Raf1 (Ser338). The identification of PP5 interacting proteins, including transcription factors (e.g., p53, estrogen receptors, and glucocorticoid receptors), small G proteins (e.g., Rac1,

$G\alpha_{12}$, and $G\alpha_{13}$), and protein kinases (e.g., ATM, ASK1, Raf1) has provided key insights into the functional roles of this phosphatase.

Phosphatase•kinase complexes

Multiprotein signaling modules are increasingly recognized as crucial components of a variety of signaling pathways. Many such modules are composed of both protein kinases and protein phosphatases, which play a key role in maintaining the proper phosphorylation state of target proteins within cell signaling pathways. These modules may also contain anchoring or scaffolding proteins that spatially regulate substrate phosphorylation by targeting the kinases and/or phosphatases to specific subcellular compartments. Furthermore, the close positioning of these enzymes near their substrates facilitates the temporal regulation of a variety of phospho-proteins. Several macromolecular complexes have been identified in which crosstalk between the kinase and phosphatase occurs, where the kinase regulates the phosphorylation state of the associated phosphatase or vice versa. As mentioned previously, PP5 has been found to associate with a number of protein kinases, including ATM, ATR/Chk1, DNA-PKcs, ASK1, Raf1, eIF2α kinase, and IKKβ (123-127,131,133,134). Likewise, studies from our laboratory and others have shown that PP2A forms complexes with several protein kinases, including CaMKIV (135), Raf1 (136,137), p70S6K (138-140), PAK (140), CK2 (141), TGFβR1 (142), PKC (143), Akt (144,145), JAK-2 (146), KSR (147), and IκB kinase (148,149).

Summary

The goals of my research were to increase our understanding of the oligomeric composition, regulation, and function of select protein serine/threonine phosphatase•kinase signaling modules. Following the purification of stable CaMKIV•PP2A complexes, we showed that the kinase-associated phosphatase was a heterotrimeric holoenzyme containing a regulatory Bα subunit (135). Additional studies from our group indicated that PP2A negatively regulated CaMKIV signaling and the suggested that PP2A targeted phospho-Thr200. The studies outlined in Chapter II describe the development and characterization of a phospho-Thr200-CaMKIV antibody that allowed us to monitor stimulus-induced activation and inactivation of endogenous CaMKIV•PP2A complexes (150). We found that ectopically expressed CaMKIV required the co-expression of Bα or Bδ regulatory subunits to recruit $PP2A_C$ to the kinase, but the Bα- and Bδ-containing holoenzymes failed to dephosphorylate phospho-Thr200-CaMKIV in cells and *in vitro*, calling into the question the role of these holoenzymes in the dephosphorylation of this site. Unexpectedly, immunoprecipitation assays uncovered an interaction between CaMKIV and alpha4•$PP2A_C$ in cells, which may play an important role alongside the holoenzymes in regulating CaMKIV function.

In contrast to the inhibitory role that Bα- and Bδ-containing PP2A holoenzymes play in CaMKIV signaling, our laboratory determined that ABαC and ABδC positively regulate Raf1 signaling and that the PP2A-Raf1 interaction was increased following EGF stimulation (137). The studies outlined in Chapter III focus on determining the molecular mechanism(s) responsible for the EGF-mediated alterations in the composition of the PP2A•Raf1 module. My examination of EGF-dependent alterations in the PP2A-Raf1

interaction revealed relatively small and often variable changes in the association. Therefore, I exploited a chemical crosslinking strategy to stabilize PP2A-Raf1 interactions and associated proteins for subsequent mass spectrometry studies to identify putative interacting proteins that may regulate the PP2A•Raf1 complex. This proteomic approach identified several candidate PP2A•Raf1 complex-interacting proteins that will require further characterization to establish their role in the regulation of this phosphatase•kinase complex.

In Chapter IV, I present studies revealing the identification of several novel PP5•kinase complexes, whose interactions are facilitated, in part, by HSP90 (151). Focusing on PP5•ERK complexes, I showed that PP5 forms stable complexes with ERK2, ERK1, and the ERK1 splice variants ERK1b and ERK1c. Similar to PP2A•CaMKIV complexes, the formation of PP5•ERK1/2 complexes do not require phosphatase or kinase activity. However, small G proteins are capable of modulating the PP5-ERK1/2 interaction. Surprisingly, I found that PP5•ERK2, but not PP5•ERK1, complexes are altered in the presence of select oncogenic RAS proteins. The RAS-dependent decrease in PP5-ERK2 binding does not require MEK activity but paradoxically requires ERK2 activity. Importantly, I found that PP5•ERK2 complexes regulate the phosphorylation state of Raf1, which may be dysregulated in certain human tumors characterized by select gain-of-function mutations in *RAS* genes.

CHAPTER II

OLIGOMERIC COMPOSITION AND REGULATION OF CAMKIV•PP2A COMPLEXES

CaMKIV background

One of the first reports detailing the formation of a phosphatase•kinase complex was from our laboratory and showed that calcium (Ca^{2+})/calmodulin (CaM)-dependent protein kinase IV (CaMKIV) stably interacts with PP2A (135). The Ca^{2+}/calmodulin (CaM)-dependent protein kinase (CaMK) family contains protein serine/threonine kinases that are activated in response to increases in intracellular Ca^{2+} and are subdivided into two groups. One group, the "dedicated kinases," have specific protein substrates and includes phosphorylase kinase, myosin light chain kinase (MLCK), and eukaryotic elongation factor-2 kinase (a.k.a. CaMKIII). A second group of "multifunctional kinases" has broad substrate specificity and regulates multiple physiological processes following increases in intracellular calcium. This group is composed of several subfamilies: CaMKI (α, β, γ, δ genes), CaMKII (α, β, γ, δ genes), CaMIV (one gene), and CaMKK (α and β genes) (152).

Alternative splicing of the CaMKIV gene yields two isoforms, CaMKIVα (65 kDa) and CaMKIVβ (67 kDa); the larger CaMKIVβ has an N-terminal extension of 28 amino acids (153). An alternative start site within exon XI of the CaMKIV gene generates calspermin, a 32 kDa protein exclusively expressed in the testis, which lacks catalytic activity and may inhibit the function of CaM during spermatogenesis (154). CaMKIV contains several important functional domains: a serine-rich N-terminal

domain, a catalytic domain, an autoregulatory domain, and a highly-acidic C-terminal domain (155). In the absence of Ca^{2+}, CaMKIV is maintained in an autoinhibited state via the association of the autoregulatory domain with the catalytic domain, which blocks substrate access. Increases in intracellular Ca^{2+}, via the opening of voltage-gated Ca^{2+} channels or following its release from internal stores, allows binding of Ca^{2+} to CaM. Ca^{2+}/CaM binds to the autoregulatory domain of CaMKIV, which repositions the autoregulatory domain and exposes a threonine residue (Thr200 in the human enzyme and Thr196 in the rat enzyme) critical in the activation of CaMKIV (Fig. 7). Ca^{2+}/CaM-bound CaMKIV exhibits low basal activity that promotes autophosphorylation of Ser12 or Ser13 in the serine-rich N-terminal domain, relieving a second site of intrasteric autoinhibition. Only one of the serine residues needs to be autophosphorylated, as single point mutants exhibit full activity but a double point mutant can not be activated (156). The binding of Ca^{2+}/CaM not only exposes Thr200, but also a CaMKK docking site to which Ca^{2+}/CaM-bound CaMKK binds to, facilitating the subsequent phosphorylation of Thr200. Located within the activation loop of CaMKIV, phosphorylation of Thr200 activates the enzyme further, by lowering the K_m for substrates 10-fold, and generates a Ca^{2+}/CaM-independent enzyme (157,158). CaMKIV directly phosphorylates a number of transcription factors (159), including cyclic adenosine monophosphate (cAMP) response element binding protein (CREB) on Ser133 (160), activating transcription factor-1 (ATF-1) on Ser63 (161), and serum response factor (SRF) on Ser103 (162). By functioning as a key mediator of Ca^{2+}-induced gene expression in the brain, thymus, testis, ovary, spleen, bone marrow, and adrenal gland, CaMKIV plays important roles in neuronal physiology

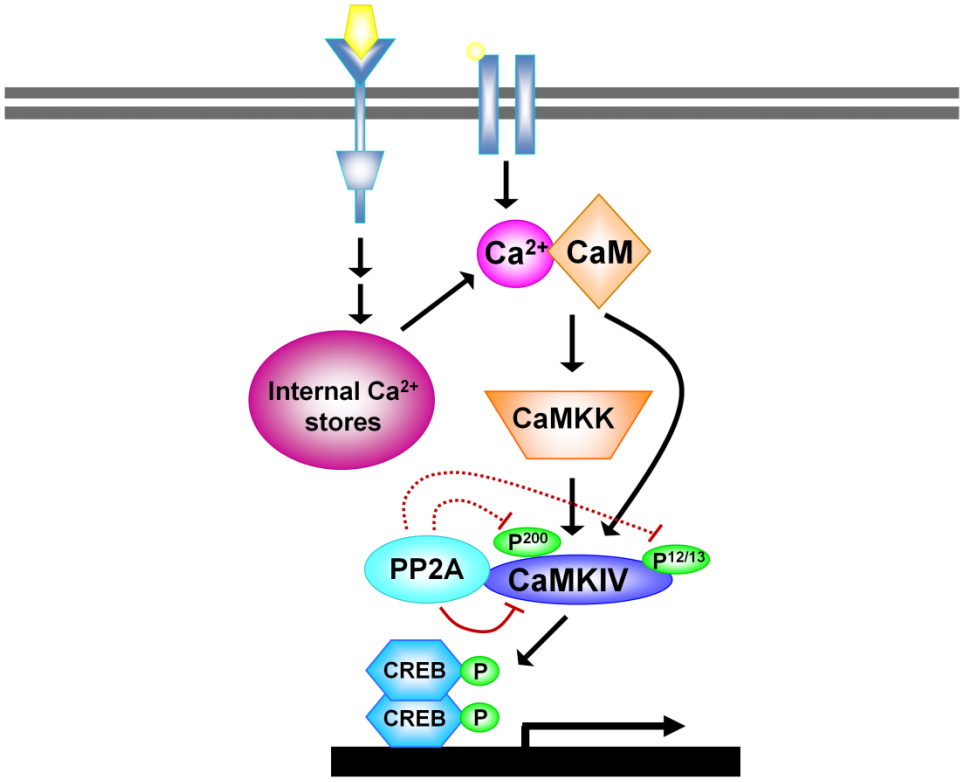

Figure 7. Diagram of the CaMKIV•PP2A signal transduction pathway.
In response to T cell receptor activation, increases in intracellular calcium facilitate Ca^{2+}/calmodulin (*CaM*) binding to CaM-dependent protein kinase IV (*CaMKIV*). This interaction facilitates autophosphorylation of the N-terminal serines (i.e., Ser12/Ser13; $P^{12/23}$) and permits CaM kinase kinase (*CaMKK*) mediated phosphorylation of CaMKIV at threonine-200 (P^{200}), which fully activates CaMKIV. Activated CaMKIV phosphorylates transcription factors (e.g., *CREB*) responsible for immediate early gene expression. PP2A holoenzymes, ABαC or ABδC, negatively regulate an associated CaMKIV (solid red line); potential phospho-residues targeted by PP2A are indicated by dashed red lines. See text for additional details.

(e.g., learning and memory), the activation of T lymphocytes, and spermatogenesis (163,164).

$PP2A_C$ interacts with CaMKIV

The activation of CaMKIV occurs through kinase-mediated phosphorylation events. Therefore, inactivation of CaMKIV is likely mediated by dephosphorylation of these activating sites. Studies from our group and others have provided key insights into the termination of CaMKIV signaling by phosphatases. CD3 receptor-stimulated T cells exhibit a robust increase in CaMKIV phosphorylation that peaks at 1 min but rapidly returns to basal levels at 5 min, suggesting that a phosphatase in close proximity to CaMKIV swiftly terminates kinase activity (165). A preformed kinase•phosphatase complex would conceptually facilitate rapid changes in the activation state of CaMKIV and early *in vitro* studies demonstrating the inactivation of CaMKK-phosphorylated CaMKIV by $PP2A_{AC}$, and not by PP1, raised the possibility that CaMKIV could form stable complexes with PP2A (165). Our group determined that CaMKIV associates with a PP2A holoenzyme in a 1:1 stoichiometric ratio (135). The isolation of CaMKIV•PP2A complexes from rat brain extracts and Jurkat T cells using catalytically inactive GST-CaMKIV or microcystin-Sepharose (a phosphatase affinity resin) demonstrated that neither kinase nor phosphatase activity was required for their association. However, data from our lab indicated that CaMKIV was a substrate for the associated PP2A, as we observed enhanced levels of CaMKK-mediated phosphorylation of CaMKIV in the presence of okadaic acid in a partially purified CaMKIV•PP2A preparation (135). Additional experiments using a CREB reporter assay revealed that the expression of small t antigen to inhibit PP2A holoenzyme activity led to an increase in CaMKIV-

mediated CREB transcription, thus demonstrating that PP2A negatively regulates CaMKIV activity in cells and that this activity requires a regulatory B subunit. Subsequent collaborative studies from us and Anthony Means's group identified a PP2A binding site within the autoregulatory domain of CaMKIV, and showed that PP2A competes with Ca^{2+}/CaM for binding to this region in order to regulate CaMKIV activity (166).

The data presented in this chapter represent a collaborative effort with another graduate student, Kelie Reece, to examine the role played by the regulatory B subunit in the assembly and function of the CaMKIV•PP2A complex (150). To study the functional role of PP2A holoenzymes in the regulation of CaMKIV signaling, we exploited a novel CaMKIV phospho-specific antibody and sought to identify differences in the regulation of endogenous and ectopic CaMKIV by cellular phosphatases. We showed that Bα and Bδ regulatory subunits facilitate the formation of CaMKIV•PP2A complexes by recruiting endogenous $PP2A_C$ to the kinase. Also included in this chapter are additional unpublished findings that I generated, including data demonstrating that Bα- and Bδ-containing holoenzymes can not dephosphorylate phospho-Thr200-CaMKIV in cells or *in vitro*, as well as evidence supporting the existence of CaMKIV•alpha4•$PP2A_C$ complexes in cells.

Materials and Methods

Antibodies and reagents

Anti-FLAG M2-agarose, FLAG peptide, and rabbit and mouse anti-FLAG antibodies were from Sigma (St. Louis, MO). Monoclonal CaMKK, CaMKIV, and

PP2Ac antibodies were from BD Biosciences Pharmingen (San Diego, CA). Alpha4, phospho-Thr200-CaMKIV, and CaMKIV polyclonal antibodies were from Bethyl Laboratories, Inc. (Montgomery, TX). Generation and characterization of affinity-purified Bα/Bδ antibodies were reported previously (167,168). Secondary antibodies for fluorescence detection were from Rockland (Gilbertsville, PA) or Molecular Probes (Eugene, OR). Normal rabbit IgG and normal mouse IgG were from The Jackson Laboratory (Bar Harbor, ME), and Protein A-Sepharose was from Zymed Laboratories Inc. (San Francisco, CA). Protein G-Sepharose 4B conjugate was from Invitrogen (Carlsbad, CA). Lipofectamine 2000 was from Invitrogen (Carlsbad, CA), while TransIT-LT1 and TransIT-293 transfection reagents were from Mirus (Madison, WI). Okadaic acid and ionomycin were from Alexis Biochemicals (San Diego, CA) and Sigma (St. Louis, MO), respectively. The CaMKK inhibitor, STO-609, was from Tocris Bioscience (Ellisville, MO). GSH-agarose and bovine serum albumin were from Sigma-Aldrich (St. Louis, MO), while Bio-Rad Protein Assay Dye Reagent Concentrate for Bradford protein assays was from Bio-Rad Laboratories, Inc. (Hercules, CA). Odyssey Blocking Buffer was from LI-COR (Lincoln, NE).

Plasmid constructs

Generation of FLAG-tagged Bα and Bδ mammalian expression plasmids were described previously (137). pcDNA5/TO was from Life Technologies and GST-Bα was a kind gift from Verle Janssens (KU Leuven; Leuven, Belgium). Mammalian expression plasmids for untagged CaMKIV, FLAG-CaMKIV, and FLAG-T200A-CaMKIV were kindly provided by Dr. Tony Means (Duke University; Durham, NC). The HA-CaMKIV construct was generated by subcloning human CaMKIV cDNA into the BglII and NotI

sites of the pCMV-HA vector (Clontech, Palo Alto, CA). Proper construction of the plasmid was verified by automated DNA Sequencing (Vanderbilt DNA Core Facility).

Cell culture and transfection

The human embryonic kidney cell line QBI-293A (HEK-293A) was a gift from Dr. Tony Means (Duke University; Durham, NC), and the HEK-293FT cell line was from Invitrogen (Carlsbad, CA). Cells were grown at 37^{o}C in a humidified atmosphere with 5% CO_2 in DMEM supplemented with 10% fetal calf serum, 2 mM L-glutamine, and antibiotics; 110 mg/L sodium pyruvate was also added to the HEK-293A media. Jurkat T cells were maintained in RPMI media supplemented with 10% fetal bovine serum, 2 mM L-glutamine, and antibiotics. HEK-293A cells grown to ~90% confluency in a 100 mm dish were transfected with the appropriate expression vectors using Lipofectamine 2000. HEK-293FT cells grown to 45% confluency in 60 mm dishes were transfected with the appropriate expression vectors using TransIT-LT1 or TransIT-293.

Co-immunoprecipitations

For immunoprecipitations using antibody-conjugated agarose beads, cells were harvested in 500 µl lysis buffer (25 mM NaH_2PO_4, 2 mM EDTA, 2 mM EGTA, 10 µg/ml leupeptin, 100 µg/ml Pefabloc SC, and 100 nM okadaic acid). Lysates were incubated on ice for 30 min and centrifuged at 13,000xg for 10 min at 4^{o}C. Clarified lysates were then incubated with 20 µl of a 50% slurry of anti-FLAG agarose beads overnight at 4^{o}C, and bound proteins were eluted with 300 ng/µl FLAG peptide, followed by SDS-PAGE and immunoblot analysis. In some experiments, bound proteins were directly eluted from the anti-FLAG agarose beads in SDS sample buffer. For immunoprecipitations shown in Fig.

13, cells were lysed in buffer containing 20 mM Tris-HCl, pH 7.6, 150 mM NaCl, 0.5% Igepal, 3 mM EDTA, 3 mM EGTA, 1 mM PMSF, 17 µg/ml aprotinin, and 5 µg/ml leupeptin. Clarified lysates were incubated overnight with rotation at 4^{o}C with 2 µg of rabbit polyclonal CaMKIV or 2 µg of normal rabbit IgG, and then incubated for 1 h with rotation at 4^{o}C with 20 µl of a 50% slurry of Protein A-Sepharose beads. Bound proteins were washed, eluted in SDS sample buffer, and subjected to Western analysis. Immunoprecipitations to compare different CaMKIV antibodies (Figs. 10, 11 and 20) were performed using extracts of unstimulated (Figs. 10 and 20) or serum starved (1 h at 37^{o}C) (Fig. 11) Jurkat T cells prepared in Phospho-Buffer (20 mM Tris-HCl, pH 7.2, 2 mM EGTA, 5 mM EDTA, 30 mM sodium fluoride, 20 mM sodium pyrophosphate, and 0.5% Igepal CA-630) containing inhibitors (40 mM β-glycerophosphate, 1 mM Na_3VO_4, 3 mM benzamidine, 5 µM pepstatin A, 10 µM leupeptin, and 1 mM phenylmethylsulfonyl fluoride). Approximately 300 µg of total protein was incubated with 1 µg of anti-CaMKIV antibody, normal rabbit IgG, or normal mouse IgG for 4 h (Fig. 20) or overnight (Figs. 10 and 11), followed by subsequent incubation with protein G-Sepharose 4B (20 µl of a 50% slurry) and rotation for 1 h at 4^{o}C. After three 1 ml washes with lysis buffer, bound proteins were eluted with 30 µl 2xSDS sample buffer and subjected to Western analysis. The interaction of HA-CaMKIV and FLAG-alpha4 was examined using Buffer B (20 mM Tris-HCl, pH 8.0, 137 mM NaCl, 10% glycerol, and 1% Igepal CA-630) containing inhibitors (17 µg/ml aprotinin, 10 µM leupeptin, 1 mM phenylmethylsulfonyl fluoride, and 1 mM Na_3VO_4). FLAG immunoprecipitations from cellular extracts were performed using 10 µl of a 50% slurry of anti-FLAG resin,

overnight incubations at 4^{o}C with rotation, and elution of bound proteins with 2xSDS sample buffer.

Analysis of CaMKIV phosphorylation

For characterization of the CaMKIV phospho-T200 antibody, HEK-293FT cells were transfected with pcDNA3 (empty vector), FLAG-CaMKIV (FLAG-KIV), or a FLAG-CaMKIV construct containing a single threonine to alanine mutation (FLAG-KIV-T200A). Twenty-four h post-transfection, the media was replaced with serum-free DMEM containing 5 µM STO-609 or an equivalent volume of vehicle (DMSO). Following overnight incubation, cells were treated for 5 min with serum-free DMEM containing 2 µM ionomycin or an equivalent volume of DMSO. Cells were washed once with PBS and harvested from the dish in 300 µl Phospho-Buffer containing inhibitors. Clarified cell lysates were incubated with anti-FLAG agarose beads and bound proteins were eluted with SDS sample buffer. To analyze endogenous CaMKIV phosphorylation, Jurkat T cells were serum-starved for 1 h prior to treatment with 2 µM ionomycin, 1 µM okadaic acid, or a combination of both reagents for the indicated time points; for the combination treatments, okadaic acid was added 10 min before ionomycin stimulation. To compare endogenous versus ectopic CaMKIV phosphorylation in response to stimuli, HEK-293A cells were transfected with FLAG-CaMKIV. At 48 h post-transfection, cells were stimulated for the indicated time points with ionomycin alone or a combination of okadaic acid and ionomycin as described above. Clarified cell lysates were incubated with anti-FLAG agarose beads, and bound proteins were eluted from the resin with 300 ng/µl FLAG peptide. Aliquots of the cell lysates and FLAG immune complexes were subjected to Western analysis.

Dephosphorylation assays

For the in-cell dephosphorylation experiments (Fig. 16), HEK-293FT cells were transfected with 0.5 µg untagged CaMKIV and 2.0 µg FLAG-Bα. After 48 h, cells were serum starved for 70 min before being treated with nothing or 2 µM ionomycin for increasing amounts of time. Cells were then lysed with Phospho-Buffer containing inhibitors and prepared for Western analysis as noted above. For the *in vitro* dephosphorylation experiments (Figs. 17 and 18), HEK-293FT cells (10-cm plates) were untransfected or transfected with 7 µg of FLAG-KIV, GST-Bα, or FLAG-Bα plasmid and allowed to express protein for 48 h. Phospho-Thr200-FLAG-KIV was purified from cells stimulated with 2 µM ionomycin for 5 min and then lysed in Phospho-Buffer containing inhibitors. Active PP2A holoenzymes containing GST-Bα or FLAG-Bα were purified from cell extracts prepared in NP40 lysis buffer (20 mM Tris-HCl, pH 7.6, 150 mM NaCl, 3 mM EDTA, 3 mM EGTA, and 0.1% Igepal CA-630) containing inhibitors (1 mM phenylmethylsulfonyl fluoride, 17 µg/ml aprotinin, 5 µg/ml leupeptin). Forty µl of a 50% slurry anti-FLAG or anti-GST resin were added to the appropriate extracts and incubated overnight at 4^{o}C with rotation. Bound FLAG-CaMKIV was first washed once with 700 µl Phospho-Buffer lacking inhibitors. FLAG-CaMKIV, GST-Bα, and FLAG-Bα were then washed twice with 700 µl NP40 PAN Buffer (10 mM PIPES, pH 7.0, 100 mM NaCl, 0.5% Igepal CA-630, and 17 µg/ml aprotinin), once with 700 µl PAN Buffer (10 mM PIPES, pH 7.0, 100 mM NaCl, and 17 µg/ml aprotinin), and once with 700 µl Phosphatase Assay Buffer (PAB) [25 mM Tris-HCl, pH 7.5 (pH 8.0 for GST-Bα), 1 mM EDTA, 1 mM EGTA, 1 mM DTT, and 0.25 mg/ml bovine serum albumin]. FLAG-tagged proteins were eluted with two washes of 50 µl PAB containing 100 µg/ml FLAG

peptide; for each elution the beads were gently rotated for 20 min at 4^{o}C. The pooled eluates were combined with 100% glycerol to yield a final concentration of 30% glycerol. The amount of CaMKIV and ABαC protein was determined by SDS-PAGE and staining of the gels with Bio-Safe Coomassie G-250 (Bio-Rad Laboratories, Inc.; Hercules, CA); serial dilutions of bovine serum albumin (Pierce; Rockford, IL) were used as standards. Quantification was accomplished using the Odyssey infrared imaging system and Odyssey application software version 3.0 (LI-COR; Lincoln, NE).

Experiments examining the dephosphorylation of CaMKIV by PP2A holoenzymes (Fig. 17) were performed by combining 80 ng phospho-Thr200-FLAG-CaMKIV with PAB, 90 ng ABα_{FLAG}C, or 1/10 of the ABα_{GST}C-bound beads in a final reaction volume of 90 µl. Reactions were carried out at 37^{o}C for 30 min with agitation every 10 min. The dephosphorylation of CaMKIV by cellular lysate and purified PP2A$_C$ [a kind gift from Dr. Gregg Moorhead (University of Calgary; Calgary, Alberta, Canada)] (Fig. 18) was performed by incubating 120 ng phospho-Thr200-FLAG-CaMKIV with PAB, increasing amounts of untransfected HEK-293FT lysate (0.1-50 µg total protein as determined by Bradford protein assay), or 100 ng purified PP2A$_C$ in a final reaction volume of 20 µl. Reactions were incubated for 60 min at 37^{o}C with agitation every 15 min. Reactions were terminated following the addition of 5xSDS sample buffer and heating to 95^{o}C for 5 min. One-third of the holoenzyme reactions and all of the cell lysate/purified PP2A$_C$ reactions were analyzed by Western.

Western analysis

Western analysis was carried out as previously described (76). All membranes were blocked in Odyssey Blocking Buffer for detection with the Odyssey Infrared Imaging System (LI-COR, Lincoln, Nebraska).

Results

Characterization of a phospho-Thr200-specific CaMKIV antibody

Previous studies by our laboratory demonstrated that PP2A regulates CaMKIV activity and that phosphorylation of Thr200 in CaMKIV is altered when its association with PP2A is disrupted (166); however, the precise site of CaMKIV dephosphorylation by PP2A had not been determined. Our analysis of a rabbit antibody raised against a peptide encompassing phospho-Thr200 (New England Peptide, Inc.), the residue most likely to be targeted by PP2A, revealed that it recognized ectopic phospho-CaMKIV (166) but failed to recognize endogenous phospho-CaMKIV in HEK-293A cells (data not shown). Western analysis of HEK-293 variants, including HEK-293A cells, for endogenous CaMKIV demonstrated that the kinase is expressed in these cell types (data not shown). In collaboration with a second company (Bethyl Laboratories, Inc.), we screened a new affinity-purified, rabbit phospho-Thr200-CaMKIV (p-Thr200) antibody. To characterize the specificity of the p-Thr200 antibody, we analyzed extracts of HEK-293FT cells transfected with empty vector, FLAG-CaMKIV, or a phospho-null point mutant of CaMKIV (FLAG-T200A-CaMKIV) that were subjected to overnight treatment with a CaMKK inhibitor, STO-609, or vehicle (DMSO). Both lysates and FLAG immune complexes from FLAG-CaMKIV-expressing cells exhibited a robust increase in p-

Thr200 levels in the presence of ionomycin (Fig. 8). Pretreating cells with a CaMKK inhibitor (STO-609) reduced the levels of ionomycin-stimulated p-Thr200 in wildtype FLAG-CaMKIV, and the p-Thr200 antibody failed to recognize the FLAG-T200A-CaMKIV mutant in ionomycin-stimulated cells. These data demonstrate that the p-Thr200 antibody in recognizes the CaMKK phosphorylated residue (p-Thr200) within the activation loop of CaMKIV. Additional testing also revealed that this antibody exhibits some cross-reactivity with phosphorylated CaMKI and CaMKK, most likely as a result of the high sequence homology between these CaM kinases in the region of CaMKIV used to generate the p-Thr200 antibody (data not shown). We next examined the ability of the p-Thr200 antibody to detect endogenous, phosphorylated CaMKIV in Jurkat T lymphocyte lysates. Western analysis of extracts from Jurkat T cells treated with ionomycin or okadaic acid alone failed to exhibit a p-Thr200 response (Fig. 9). However, cells pretreated with okadaic acid 10 min prior to ionomycin stimulation showed a time dependent increase in p-Thr200, indicating that the phosphorylation of CaMKIV at Thr200 was tightly regulated by an okadaic acid-sensitive phosphatase. Similar okadaic acid/ionomycin co-treatments were necessary to observe CaMKIV phosphorylation in primary cultures of rat neurons (forebrain neurons from E17 Sprague Dawley rat fetuses) as well as in HEK-293FT and HEK-293A cells (data not shown).

Regulated changes in endogenous CaMKIV•PP2A$_C$ complexes

Previous attempts to isolate an endogenous CaMKIV•PP2A complex from native tissues required a multi-step chromatographic purification procedure or affinity matrices (e.g., calmodulin-Sepharose or microcystin-Sepharose). Since 43% of the total cellular CaMKIV interacts with PP2A$_C$, but less than 1% of the cellular PP2A$_C$ interacts with

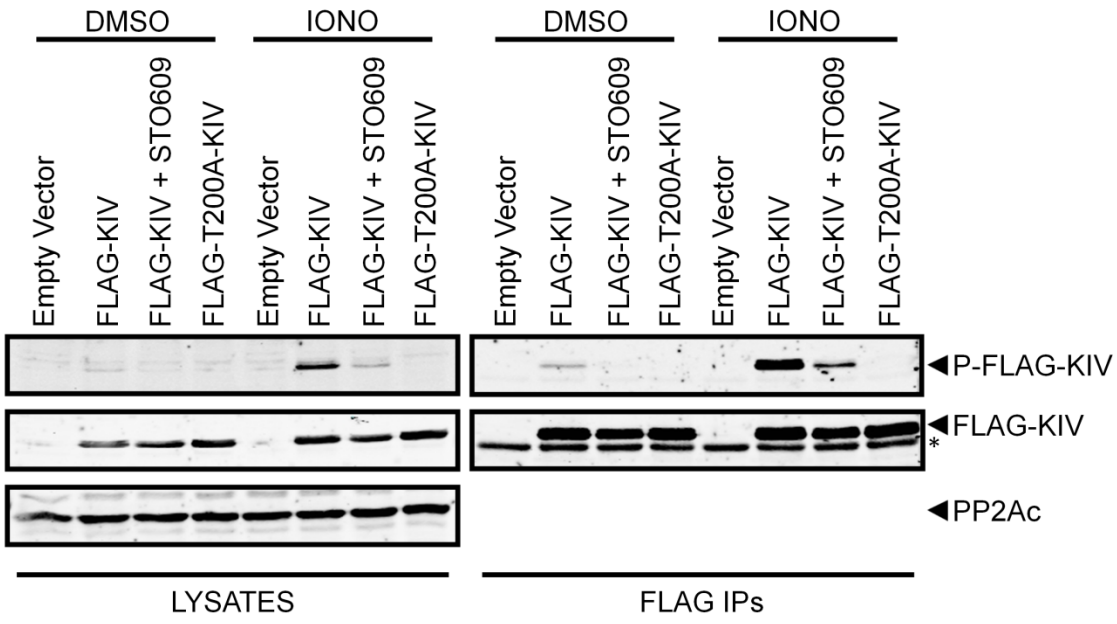

Figure 8. Characterization of a phospho-Thr200-CaMKIV antibody.
HEK-293FT cells were transfected with empty vector, FLAG-CaMKIV (*FLAG-KIV*), or a FLAG-CaMKIV mutant (*FLAG-T200A-KIV*). At 24 h post-transfection, cells were pre-treated overnight with STO-609 or vehicle (*DMSO*), and then treated with ionomycin (*IONO*) or DMSO for 5 min. Lysates (15 μg of protein) and FLAG immune complexes were subjected to Western analysis using antibodies recognizing phospho-T200-CaMKIV (*P-FLAG-KIV*) and the FLAG epitope (*FLAG-KIV*). The cell lysates were also subjected to Western analysis using a $PP2A_C$ antibody (n = 4). *, denotes IgG heavy chain recognized by the secondary antibody.

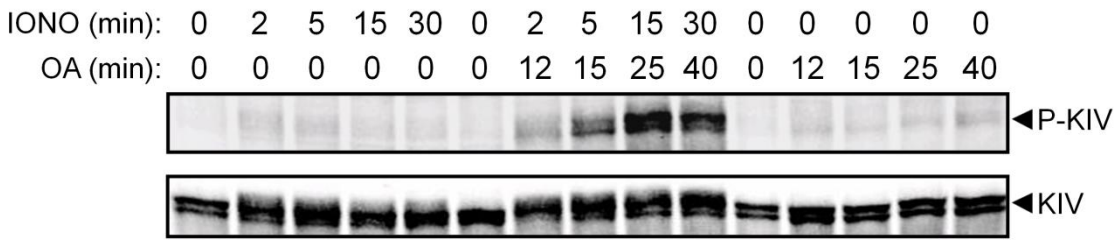

Figure 9. Inhibition of PP2A enhances ionomycin-induced phosphorylation of endogenous CaMKIV.

Jurkat T cells were treated with ionomycin (*IONO*), okadaic acid (*OA*), or a combination of both reagents for the indicated times as described in *Materials and Methods*. Cell lysates (15 μg of protein) were immunoblotted for phospho-T200-CaMKIV (*P-KIV*) and total CaMKIV (*KIV*) (n = 3).

CaMKIV (135,169), we predicted that CaMKIV immunoprecipitations would markedly enrich for the CaMKIV•$PP2A_C$ complex over methods used to purify the associated phosphatase. Our collaboration with Bethyl Laboratories, Inc. allowed us to test a panel of affinity-purified, rabbit antibodies recognizing various epitopes that span the CaMKIV primary sequence. Western analysis of immune complexes from unstimulated Jurkat T cell extracts revealed that all four CaMKIV antibodies could immunoprecipitate the kinase and that no CaMKIV was present in the control rabbit IgG lane (Fig. 10). Although Bethyl Labs Antibody #2 (BL#2) immunoprecipitated the least amount of CaMKIV, it was the only CaMKIV antibody that could co-immunoprecipitate $PP2A_C$. Given our interest in understanding the molecular role that $PP2A_C$ plays in CaMKIV activation/inactivation, we examined whether the CaMKIV-$PP2A_C$ interaction was regulated in Jurkat T lymphocytes in response to cell stimulation. After treating cells with nothing (-) or a combination of okadaic acid and ionomycin (+), the cell extracts were subjected to immunoprecipitations using control rabbit IgG, BL#2, or BL#3. Western analysis of the resulting immune complexes from unstimulated cell extracts confirmed the findings in Fig. 10 - BL#3 precipitated more CaMKIV then BL#2 and only BL#2 co-precipitated $PP2A_C$ (Fig. 11). Levels of $PP2A_C$ in BL#2-derived CaMKIV complexes were decreased following stimulation, without altering the amount of precipitated CaMKIV, indicating that the CaMKIV-$PP2A_C$ interaction may be regulated in response to cell stimulation. Since the binding of CaMKIV to $PP2A_C$ was decreased in stimulated cells, we expected to observe a corresponding increase in the amount of phospho-CaMKIV in the BL#2 immune complexes. However, phosphorylated CaMKIV was only detected in BL#3 immune complexes isolated from stimulated cells.

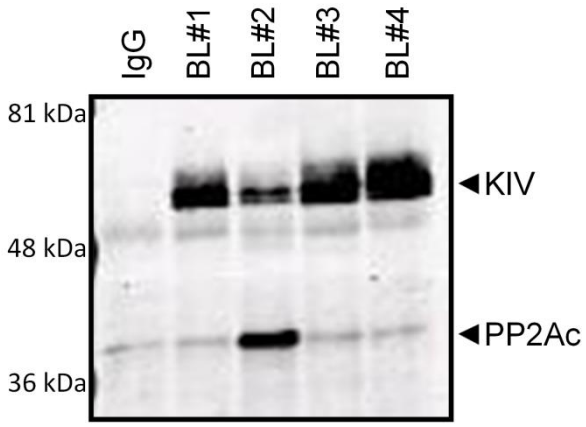

Figure 10. $PP2A_C$ interacts with a pool of CaMKIV in Jurkat T lymphocytes.

CaMKIV immunoprecipitations from Jurkat T cell extracts were performed using control rabbit IgG (*IgG*) and a panel of CaMKIV polyclonal antibodies from Bethyl Laboratories, Inc. (*BL#1-4*). Bound proteins were eluted with SDS sample buffer and analyzed by Western using antibodies recognizing CaMKIV (*KIV*) and $PP2A_C$ (n = 2).

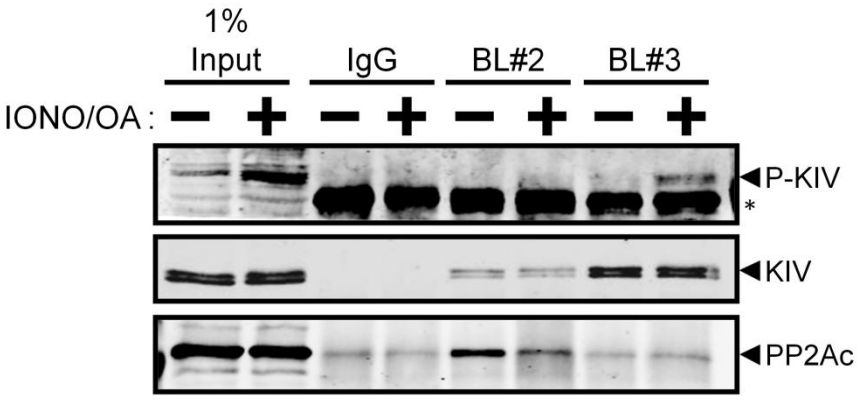

Figure 11. CaMKIV-PP2A$_C$ interactions and CaMKIV Thr200 phosphorylation are regulated in response to ionomycin and okadaic acid.

Jurkat T cell lymphocytes were serum starved for 1 h and then pretreated with (+) or without (-) 1 µM okadaic acid (*OA*) for 10 min followed by stimulation with 2 µM ionomycin (*IONO*) for 5 min. Cell lysates were prepared in a buffer containing a cocktail of phosphatase inhibitors and immunoprecipitations were performed using normal rabbit IgG (*IgG*) and two CaMKIV-specific antibodies (*BL#2* and *BL#3*). A fraction of the starting material (*1% Input*) and the immune complexes were subjected to SDS-PAGE and Western analysis using antibodies directed against P-Thr200-CaMKIV (*P-KIV*), total CaMKIV (*KIV*), and PP2Ac (n = 3). *, denotes IgG heavy chain recognized by the secondary antibody.

PP2A-dependent regulation of CaMKIV phosphorylation

Our analysis of endogenous CaMKIV•$PP2A_C$ complexes revealed that the kinase-phosphatase interaction may be regulated in response to cell stimulation (Fig. 11). Therefore, we sought to further characterize the association of PP2A with CaMKIV using a heterologous expression system by examining the ionomycin-induced activation of endogenous and ectopic CaMKIV using the p-Thr200 antibody. Whereas peak activation of endogenous CaMKIV in Jurkat T cells occurred at 1 min and returned to basal levels within 5 min, ectopic CaMKIV in HEK-293A cells displayed a peak at 5 min that returned to baseline by 15 min (165,166). Given that HEK-293A cells appear to have the protein machinery to regulate CaMKIV signaling, we examined the activation/inactivation profile of endogenous CaMKIV and ectopically-expressed FLAG-CaMKIV in HEK-293A cells. We observed a time-dependent and sustained increase in endogenous CaMKIV phosphorylation that could only be observed when cells were pretreated with okadaic acid (Fig. 12), consistent with what we observed in Jurkat T cells (Fig. 9). Although the p-Thr200 profile of FLAG-CaMKIV in ionomycin-only treated cells matched our published findings (166), FLAG-CaMKIV phosphorylation was unaffected by okadaic acid pretreatment. In both FLAG immune complexes and lysates, we detected a robust increase in FLAG-CaMKIV phosphorylation at Thr200 at 5 min that was rapidly decreased to basal levels regardless of whether okadaic acid was present or not (Fig. 12). These data suggest that while endogenous CaMKIV is regulated by an okadaic acid-sensitive phosphatase, the ectopic FLAG-CaMKIV is regulated by an okadaic acid-insensitive phosphatase. Since the subcellular distribution of FLAG-CaMKIV parallels that of endogenous CaMKIV (data not shown), we hypothesized

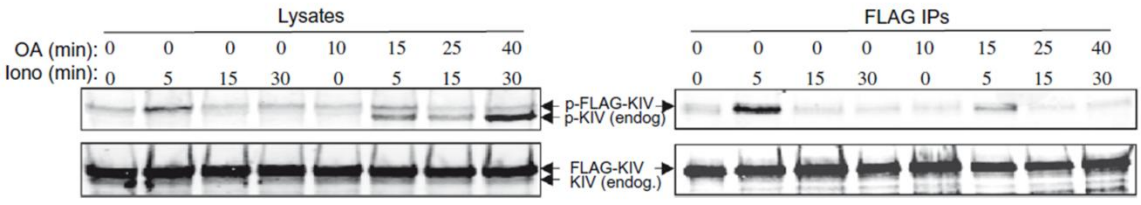

Figure 12. Differential regulation of endogenous and ectopic phospho-CaMKIV dephosphorylation.

HEK-293A cells transfected with FLAG-CaMKIV were treated with ionomycin (*Iono*) or both Iono and okadaic acid (*OA*) as described in *Materials and Methods*. Lysates (30 μg of protein) and FLAG immune complexes were subjected to Western analysis using antibodies recognizing phospho-T200-CaMKIV and total CaMKIV (n = 3). These data were generated by Kelie Reece.

that the differential regulation of these kinases was a result of differential binding to $PP2A_C$. Extracts of untransfected and FLAG-CaMKIV expressing HEK-293A cells were incubated with normal rabbit IgG (IgG IPs), a polyclonal CaMKIV antibody (CaMKIV IPs), or anti-FLAG resin (FLAG IPs). Western analysis of the immune complexes demonstrated that endogenous $PP2A_C$ co-precipitated in the CaMKIV IPs from untransfected cells but not in the FLAG IPs from FLAG-CaMKIV expressing cells (Fig. 13). Although more CaMKIV was present in the CaMKIV IPs from transfected cell lysates, when compared to CaMKIV IPs from untransfected cell lysates, the levels of $PP2A_C$ were similar, further confirming that ectopic CaMKIV does not associate with endogenous $PP2A_C$.

Given that regulatory B subunits are thought to direct $PP2A_C$ to specific substrates within the cell and that the initial purification of CaMKIV•PP2A complexes revealed the presence of PP2A holoenzymes containing a regulatory Bα subunit (135), we hypothesized that the Bα subunit may target $PP2A_C$ to CaMKIV. We also examined if Bδ, a regulatory subunit cloned by our laboratory that is 89% identical to Bα at the protein level (168), could promote the formation of CaMKIV•PP2A complexes. Western analysis of FLAG immune complexes from cells transfected with untagged CaMKIV or a combination of untagged CaMKIV and FLAG-Bα or FLAG-Bδ indicated that both regulatory B subunits could co-precipitate CaMKIV (Fig. 14). Our observation that Bα- and Bδ-containing holoenzymes interacted with CaMKIV led us to next examine the ability of these regulatory subunits to recruit endogenous $PP2A_C$ to FLAG-CaMKIV. To address this question, we performed CaMKIV immunoprecipitations from extracts of cells expressing untagged-Bα, untagged-Bδ, FLAG-CaMKIV, or a combination of

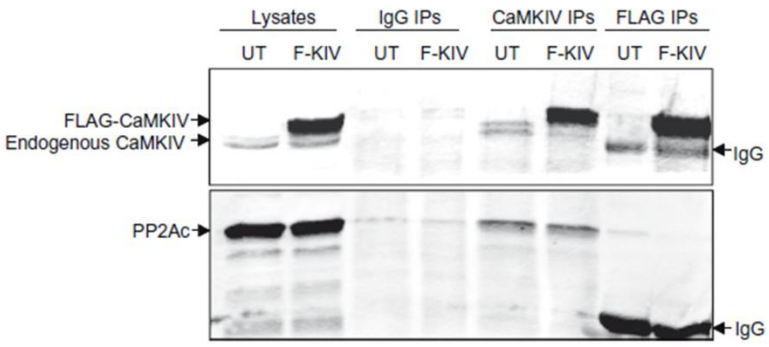

Figure 13. PP2A$_C$ associates with endogenous, but not ectopic CaMKIV.
HEK-293A cells were either untransfected (*UT*) or transfected with FLAG-CaMKIV (*F-KIV*). After 48 h, immunoprecipitations were performed from the cell lysates using rabbit IgG and protein A-Sepharose (*IgG IPs*), a CaMKIV rabbit antibody and protein A-Sepharose (*CaMKIV IPs*), or anti-FLAG agarose beads (*FLAG IPs*). Bound proteins were eluted with SDS buffer followed by immunoblot analysis with antibodies recognizing CaMKIV and PP2A$_C$; an aliquot of each solubilized extract (*Lysates*) was also analyzed (n = 3). IgG heavy (*upper panel*) and light (*lower panel*) chains are noted. These data were generated by Kelie Reece.

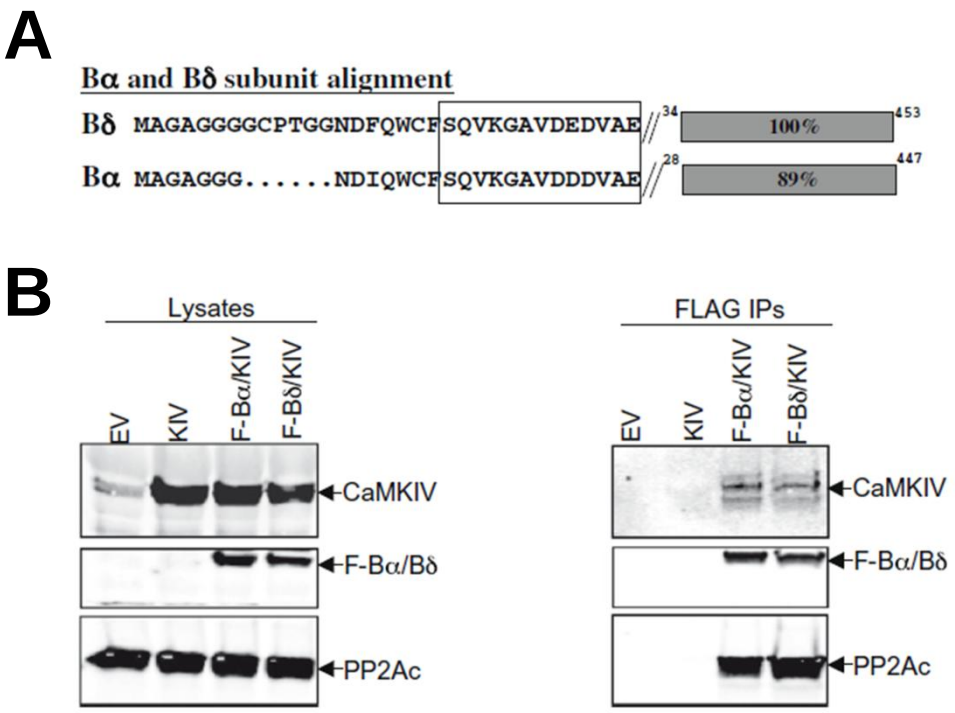

Figure 14. The PP2A regulatory Bα and Bδ subunits interact with CaMKIV.
A, Amino acid sequence alignment of the N-termini of the Bα and Bδ subunits is depicted. The boxed area represents the epitope to which the ‘‘Bα-specific” antibody was directed. The shaded boxed area indicates the percent amino acid sequence identity relative to Bδ. ***B***, HEK-293A cells were transfected with empty vector (*EV*), untagged CaMKIV (*KIV*), or FLAG-tagged B subunit (*F-Bα/F-Bδ*) and KIV. At 48 h post-transfection, cells were lysed and FLAG immune complexes were isolated. Bound proteins were eluted with SDS sample buffer and analyzed by SDS-PAGE and Western using antibodies recognizing CaMKIV, the FLAG epitope, and $PP2A_C$ (n = 9). These data were generated by Kelie Reece.

FLAG-CaMKIV and either Bα or Bδ. Western analysis of FLAG immune complexes (FLAG IPs) from cells expressing FLAG-CaMKIV alone demonstrated that no endogenous PP2A Bα/δ or $PP2A_C$ associated with the kinase (Fig. 15). However, when Bα or Bδ was co-expressed with CaMKIV we observed that binding of these subunits to FLAG-CaMKIV enhanced the levels of endogenous $PP2A_C$ co-precipitating with CaMKIV. Thus, the regulatory B subunits, Bα and Bδ, promote the assembly of CaMKIV•PP2A complexes by recruiting $PP2A_C$ to the kinase.

We next examined the regulation of ectopic CaMKIV phosphorylation in cells co-expressing the regulatory Bα subunit. HEK-293FT cells expressing untagged CaMKIV alone or together with FLAG-Bα were stimulated with ionomycin for increasing amounts of time, and cellular lysates were analyzed for p-Thr200 levels by Western. In the absence of FLAG-Bα, ionomycin generated a rapid increase in ectopic phospho-CaMKIV levels at 5 min, which were followed by a slight decrease at 30 min (Fig. 16). Surprisingly, co-expression of FLAG-Bα failed to alter the ionomycin-induced p-Thr200 profile, suggesting that the Bα-containing holoenzyme was unable to regulate CaMKIV phosphorylation at Thr200 under these experimental conditions. We next performed *in vitro* dephosphorylation assays to examine if Bα-containing PP2A holoenzymes can directly dephosphorylate p-Thr200. Phospho-FLAG-CaMKIV, purified from ionomycin stimulated HEK-293FT cells, was incubated with two forms of Bα-containing holoenzyme: $AB\alpha_{GST}C$ immobilized on resin and FLAG-peptide eluted $AB\alpha_{FLAG}C$. Following incubation in a reaction buffer supporting phosphatase activity, we observed no dephosphorylation of p-Thr200 (Fig. 17). The PP2A holoenzymes containing FLAG-Bα were catalytically active, as dephosphorylation of phospho-Histone H3 was observed

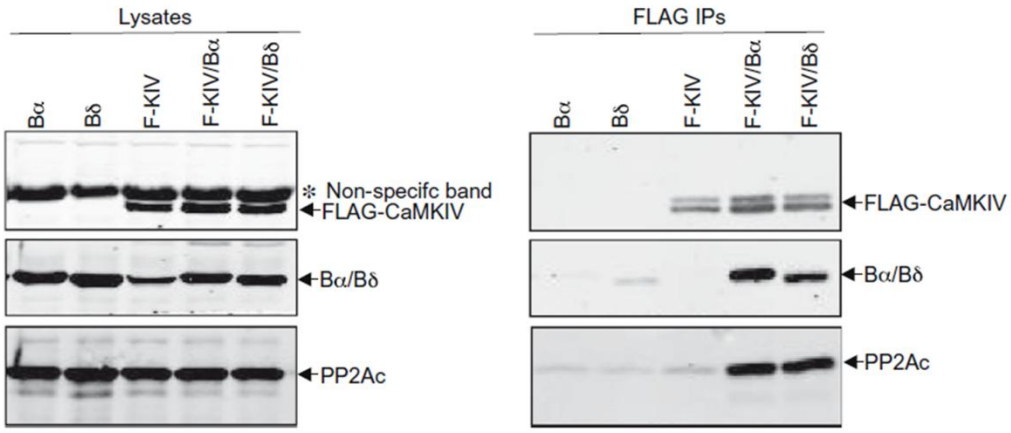

Figure 15. The PP2A regulatory Bα and Bδ subunits recruit PP2A$_C$ to CaMKIV. HEK-293A cells were transfected with untagged Bα or Bδ alone, FLAG-CaMKIV (*F-KIV*) alone, or a combination of F-KIV and untagged Bα or Bδ. Cells were lysed, followed by immunoprecipitation with anti-FLAG agarose beads and FLAG peptide elution of the bound proteins. Cell lysates (45 μg of protein) and FLAG peptide eluates were resolved by SDS-PAGE. Immunoblot analysis was carried out with antibodies recognizing CaMKIV, Bα/Bδ, and PP2A$_C$ (n = 4). *, denotes a non-specific band recognized by the secondary antibody. These data were generated by Kelie Reece.

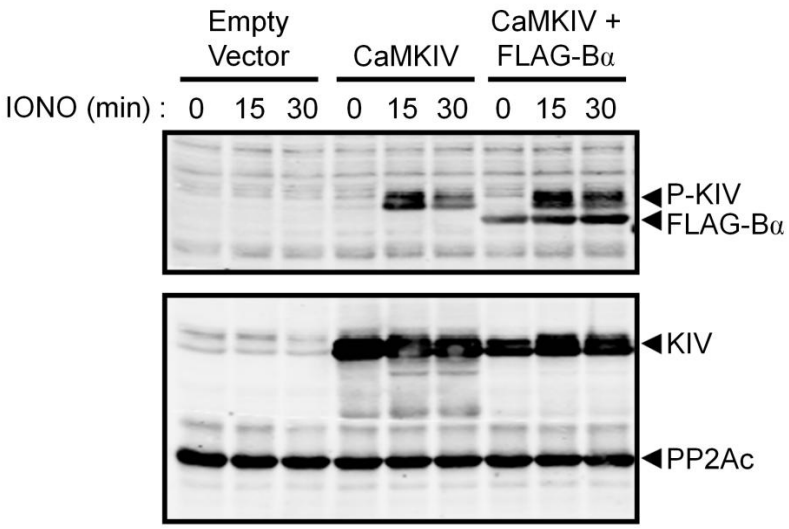

Figure 16. Overexpression of Bα does not affect phospho-Thr200-CaMKIV levels in cells.

HEK-293FT cells were transfected with pcDNA5/TO (*Empty Vector*), untagged CaMKIV, or untagged CaMKIV and FLAG-Bα. Cells were stimulated with 2 μM ionomycin (*IONO*) for increasing amounts of time (min) and then lysed in a buffer containing a cocktail of phosphatase inhibitors. Western analysis of clarified extracts was performed using antibodies recognizing phospho-T200-CaMKIV (*P-KIV*), CaMKIV (*KIV*), the FLAG epitope, and PP2Ac (n = 2).

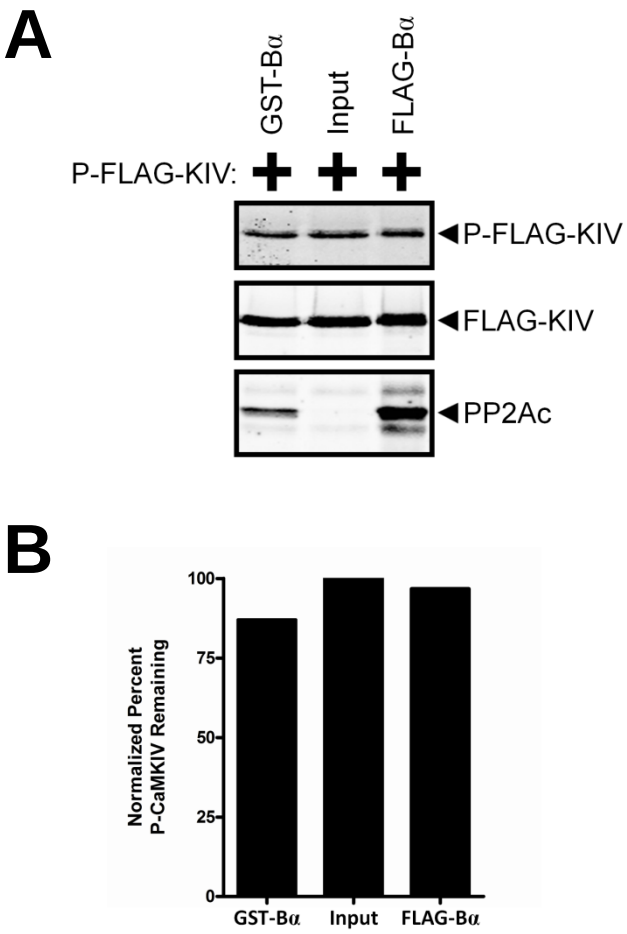

Figure 17. ABαC does not dephosphorylate phospho-Thr200-CaMKIV *in vitro*.
A, Dephosphorylation reactions were carried out by combining phospho-FLAG-Thr200-CaMKIV purified from ionomycin-stimulated cells with buffer alone (*Input*), purified $AB\alpha_{GST}C$ (*GST-Bα*), or purified $AB\alpha_{FLAG}C$ (*FLAG-Bα*). Following a 30 min incubation at 37°C, reactions were terminated with SDS sample buffer and subjected to immunoblot analysis using antibodies recognizing phospho-T200-CaMKIV (*P-FLAG-KIV*), the FLAG epitope (*FLAG-KIV*), and $PP2A_C$ (n = 2). ***B***, Quantification of the immunoblot in *A* for remaining P-FLAG-KIV signal (normalized to total FLAG-KIV) relative to Input, which was set to 100.

using the same reaction conditions (data not shown). Additional phosphatase assays demonstrated that the purified phospho-Thr200-FLAG-CaMKIV can be dephosphorylated, as incubation of the purified phospho-kinase with increasing amounts of cellular lysates led to dephosphorylation of p-Thr200 (Fig. 18). Interestingly, we also observed pThr200 dephosphorylation in the presence of purified $PP2A_C$ (Fig. 18). These observations indicate that the kinase was in a conformation susceptible to dephosphorylation. Collectively, our *in vitro* phosphatase assays support the notion that phospho-Thr200 is regulated by $PP2A_C$; however, this site does not appear to be directly dephosphorylated by Bα-containing PP2A holoenzymes. The regulation of p-Thr200 by PP2A will require further studies and may be more complex than initially thought.

Identification of CaMKIV•alpha4•PP2A$_C$ complexes in cells

The inability to detect the presence of $PP2A_A$ in CaMKIV•$PP2A_C$ immune complexes isolated using the BL#2 antibody (data not shown) led us to examine the possibility that an atypical PP2A regulatory subunit may be present in the kinase•phosphatase complex. Specifically, we investigated whether alpha4 could associate with CaMKIV. Western analysis of FLAG immune complexes from HEK-293FT cells expressing HA-CaMKIV and FLAG-alpha4 indicated that both endogenous $PP2A_C$ and HA-CaMKIV co-precipitated with FLAG-alpha4; we did not detect any HA-CaMKIV non-specifically associating with the anti-FLAG resin (Fig. 19). To determine if an endogenous alpha4•CaMKIV complex existed in cells, we analyzed CaMKIV immune complexes from Jurkat T lymphocyte extracts for the presence of alpha4. Using a panel of antibodies to immunoprecipitate CaMKIV, we detected the presence of alpha4

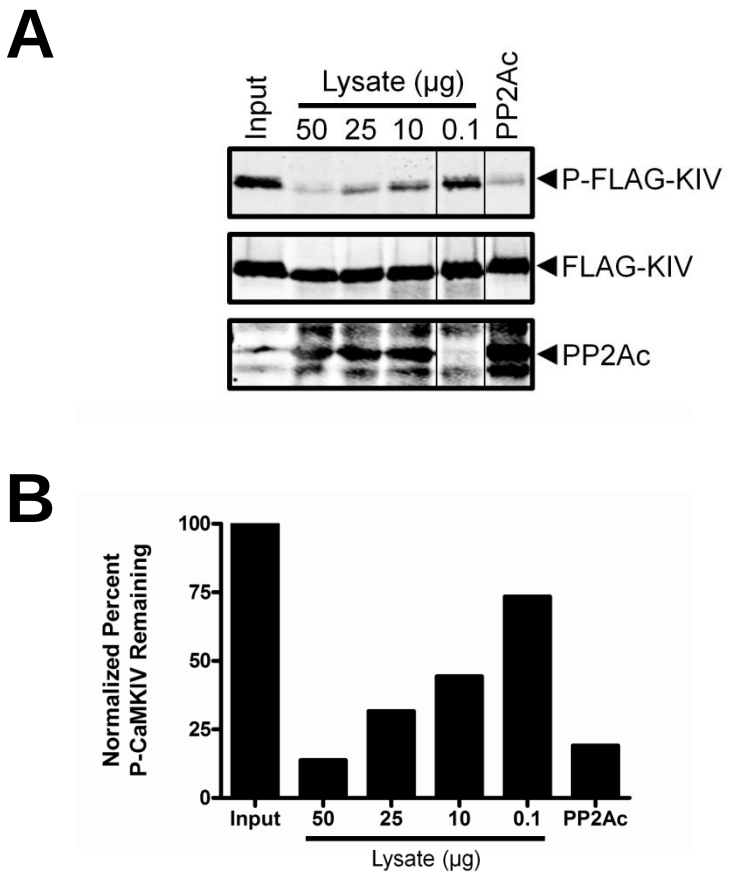

Figure 18. Dephosphorylation of phospho-Thr200-CaMKIV *in vitro*.
A, Dephosphorylation reactions were carried out by combining phospho-FLAG-Thr200-CaMKIV purified from ionomycin-stimulated cells with buffer alone (*Input*), increasing amounts of HEK-293FT extract (*Lysate*; 0.1-50 µg), or purified $PP2A_C$. Following a 60 min incubation at 37°C, reactions were terminated with SDS sample buffer and subjected to immunoblot analysis using antibodies recognizing phospho-T200-CaMKIV (*P-FLAG-KIV*), the FLAG epitope (*FLAG-KIV*), and PP2Ac (n = 1). ***B***, Quantification of the immunoblot in *A* for remaining P-FLAG-KIV signal (normalized to total FLAG-KIV) relative to Input, which was set to 100.

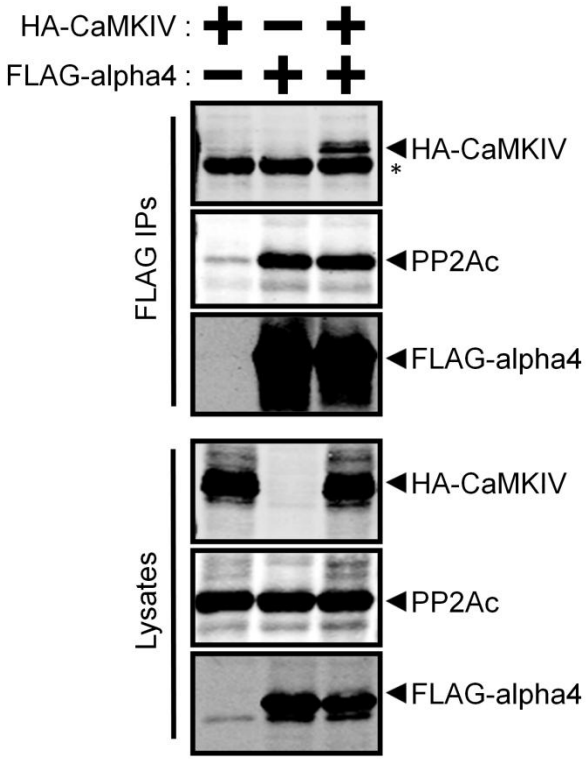

Figure 19. Alpha4 interacts with CaMKIV.
HEK-293FT cells were transfected with HA-CaMKIV, FLAG-alpha4, or both HA-CaMKIV and FLAG-alpha4. Clarified cell extracts were incubated with anti-FLAG agarose beads and bound proteins were eluted with SDS sample buffer. Western analysis of the FLAG eluates (*FLAG IPs*) and lysates was performed using antibodies recognizing the HA epitope (*HA-CaMKIV*), the FLAG epitope (*FLAG-alpha4*), and $PP2A_C$ (n = 2). *, denotes IgG heavy chain recognized by the secondary antibody.

only in BL#2-derived CaMKIV complexes, which also co-precipitates endogenous $PP2A_C$ (Fig. 20). Since alpha4 directly binds $PP2A_C$, these data indicate that alpha4•$PP2A_C$ complexes may play a role in regulating CaMKIV function.

Discussion

CaMKIV plays important roles in memory, learning, T cell development, spermatogenesis, and follicular development (170-173). As such, understanding the molecular mechanisms that regulate CaMKIV signaling may provide insight into dysregulated neuronal and immune processes, as well as infertility and paternal age effects. A lack of reagents (e.g., phospho-specific antibodies) has hampered studies examining the activation and inactivation of CaMKIV. Although the phospho-Thr200-CaMKIV antibody developed in collaboration with New England Peptide, Inc. allowed us to track the activation of ectopically expressed CaMKIV, it fell short in allowing us to monitor the activation of endogenous CaMKIV. However, our collaboration with Bethyl Laboratories, Inc., led to the generation of an antibody that specifically recognizes the phospho-Thr200 epitope within CaMKIV (Fig. 8). This antibody was used to study the kinetics of CaMKIV signaling, revealing that CaMKIV signaling in Jurkat T cells is tightly regulated by an associated, okadaic acid-sensitive PSTP (Fig. 9). Studies by our group and others have demonstrated that PP2A is the associated-PSTP (135,165,166). However, none of these studies examined the direct dephosphorylation of p-Thr200 by $PP2A_C$ or Bα-containing PP2A holoenzymes.

The CaMKIV-$PP2A_C$ interaction appears to be regulated in response to cellular treatment with ionomycin and okadaic acid (Fig. 11). The lack of p-Thr200 signal in the BL#2-derived CaMKIV complexes could be because the phospho-signal was below the

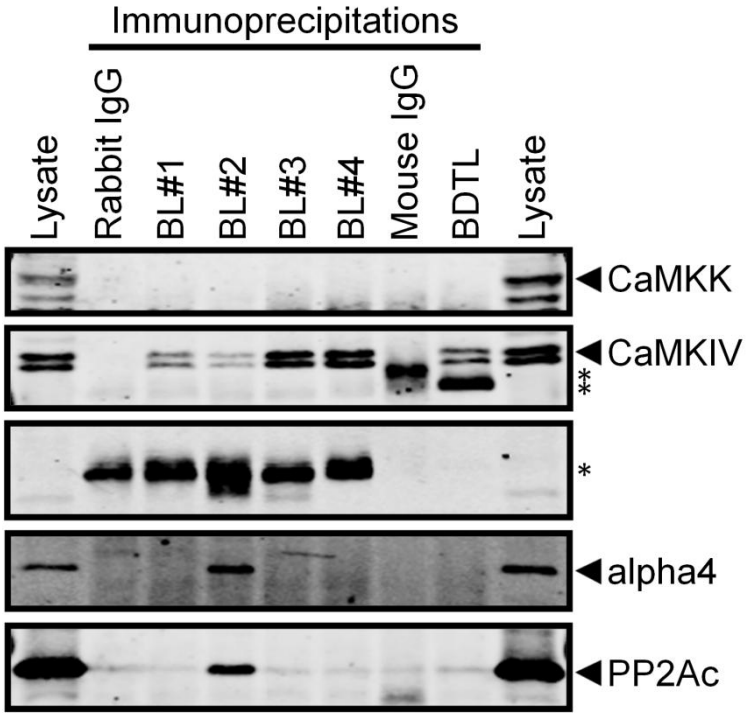

Figure 20. CaMKIV•alpha4•PP2A$_C$ complexes exist in cells.
CaMKIV immunoprecipitations from Jurkat T cell extracts was performed using control rabbit IgG, control mouse IgG, a panel of CaMKIV polyclonal antibodies (*BL#1-4*), and a CaMKIV monoclonal antibody (*BDTL*). Bound proteins were eluted with SDS sample buffer (*Immunoprecipitations*) and analyzed alongside starting material (*Lysate*) by Western using antibodies recognizing CaMKK, CaMKIV, alpha4, and PP2A$_C$ (n = 2). *, denotes IgG recognized by the secondary antibody.

limits of detection. Given that CaMKIV•PP2A$_C$ complexes can be isolated with microcystin-Sepharose (135), it is unlikely that okadaic acid binding disrupted the CaMKIV-PP2A$_C$ interaction. Instead, it appears that the ionomycin-induced increase in intracellular Ca^{2+} alters the kinase-phosphatase association. These unpublished data showing stimulus-induced changes in the endogenous CaMKIV-PP2A$_C$ interaction are consistent with a molecular model generated from our studies of ectopic CaMKIV. In this model, CaMKIV is constitutively bound to PP2A$_C$ to prevent activation of the kinase until a stimulus threshold is met, leading to Ca^{2+}/CaM-mediated displacement of PP2A$_C$ and the subsequent phosphorylation of CaMKIV by activated CaMKK (166). An alternative explanation for the lack of pThr200 in BL#2-derived CaMKIV complexes is that BL#2 and BL#3 may target separate pools of CaMKIV. For example, BL#2 may isolate only PP2A$_C$-bound inactive CaMKIV, whereas BL#3 may selectively target multiple conformations of CaMKIV and exclude the PP2A$_C$-bound form.

Unlike endogenous CaMKIV, which is inactivated by an associated PP2A, inactivation of ectopically-expressed CaMKIV is regulated by an okadaic acid-insensitive phosphatase (Figs. 12 and 13). Since the interaction of PP2A$_C$ and ectopic CaMKIV was enhanced following overexpression of Bα or Bδ subunits (Fig. 15), it is possible that cellular levels of these regulatory subunits may be insufficient to generate functional CaMKIV•PP2A complexes in the presence of excess CaMKIV. Nonetheless, these data further support the role regulatory B subunits play in targeting PP2A$_C$ to specific cellular substrates, and demonstrate that at least two different holoenzyme forms of PP2A can associate with CaMKIV (Fig. 14). Other PP2A substrates have been shown to interact with different holoenzyme forms, including the kinase Raf1, which interacts with Bα-

and Bδ-containing holoenzymes (137), and the neurotrophin receptor TrkA, which associates with B′β- and B′δ-containing holoenzymes (174). Despite the recruitment of $PP2A_C$ to CaMKIV in HEK-293A cells, we did not detect any difference in Thr200 phosphorylation between ionomycin-stimulated HEK-293FT cells expressing CaMKIV and those co-expressing CaMKIV and FLAG-Bα (Fig. 16). Further examination of the ability of PP2A to dephosphorylate phospho-Thr200-CaMKIV *in vitro* revealed that Bα-containing holoenzymes were unable to dephosphorylate p-Thr200 while purified $PP2A_C$ could (Figs. 17 and 18). These unpublished data indicate that different forms of PP2A may regulate CaMKIV phosphorylation, and suggest that the associated PP2A holoenzyme may not directly target the Thr200 site.

Endogenous CaMKIV complexes isolated from Jurkat T cells not only contain endogenous $PP2A_C$, but also alpha4, an atypical PP2A regulatory subunit (Fig. 20). The closely related CaMKII has also been shown to associate with alpha4•$PP2A_C$ complexes, signifying that this form of PP2A has precedent for playing a role in Ca^{2+}-mediated, CaMK-dependent gene transcription (175). Interestingly, tissue specific knockout of alpha4 expression in the thymus generates T cells that exhibit impairments in CD3 signaling, where CaMKIV has been shown to play a critical role in T cell maturation downstream of CD3 receptors, and abnormal development of the T cells in the thymus (176). Likewise, alpha4 plays a role in B lymphocyte maturation, where it was identified to play a role in the regulation of S6 kinase 1 (S6K1) by PP2A (177,178). In those studies, alpha4 failed to directly associate with S6K1 and required the presence of $PP2A_C$ to interact with S6K1, suggesting that alpha4 does not directly bind the kinase. Although

we did not test for a direct association of alpha4 with CaMKIV, we found that the CaMKIV-alpha4 interaction occurs only when $PP2A_C$ is present (Figs. 19 and 20).

Alpha4 has been reported to enhance as well as inhibit phosphatase activity in a substrate-dependent fashion (179-182); however, newer studies have demonstrated a role for alpha4 in the biogenesis of PP2A holoenzymes. Viral-mediated deletion of *alpha4* in mouse hepatocytes results in the loss of $PP2A_A$ and $PP2A_C$ protein levels, revealing that PP2A holoenzyme complexes are subject to rapid turnover, with alpha4 playing a role in binding inactive, core dimer- and holoenzyme-disrupted $PP2A_C$ to prevent the polyubiquitination and degradation of the liberated $PP2A_C$ (81,82,87,183). Alpha4•$PP2A_C$ complexes exhibit little to no phosphatase activity and most likely serve as a reserve of inactive $PP2A_C$ that is utilized to generate active core dimers and/or holoenzyme complexes when needed by the cell (87). While the precise role of alpha4•$PP2A_C$ complexes in regulating CaMKIV signaling remains unclear, it may work in concert with Bα- and Bδ-containing holoenzyme forms of PP2A to modulate CaMKIV activity at specific phospho-sites or direct the formation/disassembly of the holoenzymes that dephosphorylate CaMKIV residues. It is tantalizing to speculate that the PP2A holoenzymes regulate the phospho-state of the N-terminal serines in CaMKIV, which in turn modulates the permissibility of CaMKIV to phosphorylation at Thr200. Perhaps the role of alpha4•$PP2A_C$ complexes as regulators of CaM Kinases (i.e., CaMKII, CaMKIV) should be more generalized to signify their role in regulating CaM Kinase Kinase substrates, especially in light of recent data demonstrating that deletion of *alpha4* enhances levels of phospho-Thr172-AMPKα, a CaMK-like (CaMKL) kinase subfamily member recently found to be phosphorylated by CaMKKβ (183,184).

CHAPTER III

REGULATION OF PP2A•RAF1 COMPLEXES AND IDENTIFICATION OF PUTATIVE BINDING PROTEINS

RAF Background

In screening for novel tumor-inducing viruses, Ulf Rapp identified a murine sarcoma virus, isolate 3611 (3611-MSV), that induced the formation of fibrosarcomas (185). He determined that the virus carried an oncogene encoding a protein lacking tyrosine kinase activity, which was peculiar at the time because tyrosine kinase activity was commonly associated with the products of oncovirus genomes (185). The viral-induced rapidly accelerated fibrosarcoma (*v-raf*) gene had both murine and human homologs, termed C-*RAF*, that were later identified to code for proteins that harbor serine/threonine kinase activity (186). The human genome contains six *RAF* genes, A-*RAF*-1, A-*RAF*-2, B-*RAF*-1, B-*RAF*-2, C-*RAF*-1, and C-*RAF*-2, where the genes denoted with a "2" are pseudogenes and those with a "1" code for the functional proteins A-Raf, B-Raf, and C-Raf/Raf1 (hereafter referred to as Raf1) (187-192). B-*RAF*-1 appears to represent the original precursor gene, retaining more features in common with *Drosophila melanogaster RAF* (D-*Raf*) and *Caenorhabditis elegans RAF* (*lin-45*) and first appearing in invertebrates (since yeast do not express any RAF kinases) (193).

All three RAF isoforms share a common architectural structure containing three conserved regions (CR), known as CR1, CR2, and CR3 (Fig. 21). RAF proteins can be functionally divided into a regulatory amino-terminus, containing CR1 and CR2, and a

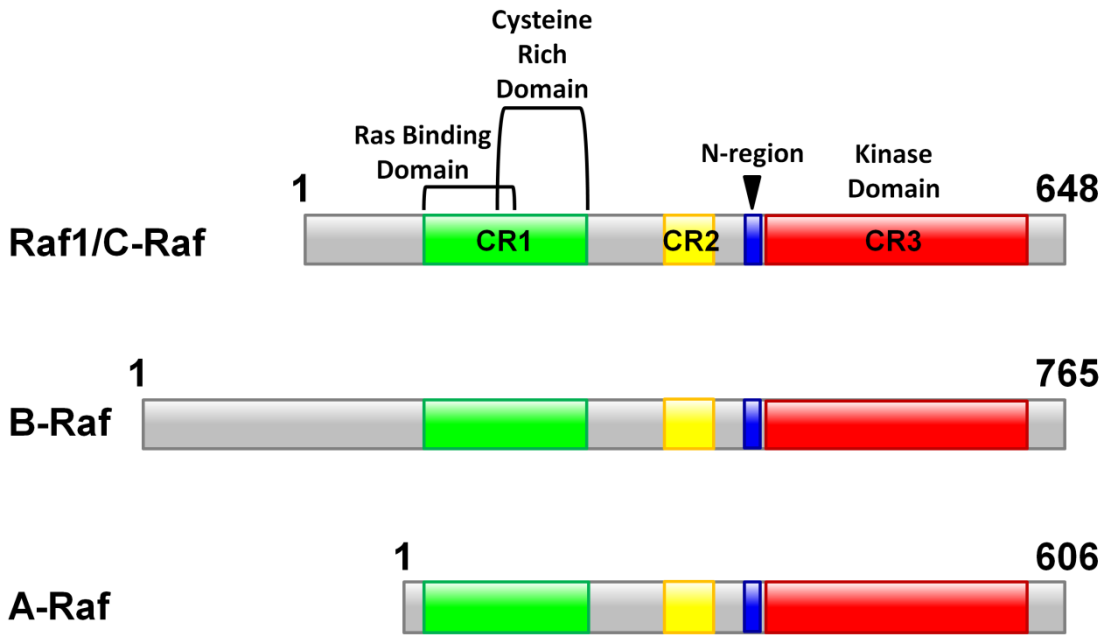

Figure 21. RAF kinase isoforms and functional domains.
Schematic representation showing the functional domains present in Raf1/C-Raf (648 amino acids), B-Raf (765 amino acids) and A-Raf (606 amino acids). The regulatory N-terminus of RAF proteins contains the Ras Binding and Cysteine Rich Domains within Conserved Region 1 (CR1; green) as well as the serine/threonine rich CR2 (yellow), which contains the inhibitory Ser259 phosphorylation site. The C-terminal domain contains the Negative-charge regulatory region (N-region; blue), which harbors residues Ser338, Tyr340, and Tyr341 (in Raf1), and CR3 (red), the kinase domain.

catalytic carboxy-terminus that houses CR3. The N-terminus of RAF functionally suppresses kinase activity as a result of the cysteine-rich domain (CRD) in CR1 making contact with sequences in CR3 to generate an autoinhibitory conformation (194-196). Active, membrane-bound RAS dis-inhibits RAF's autoinhibitory conformation by first associating with the RAS-binding domain (RBD) of RAF, also located within CR1, and then secondarily interacting with the CRD to disrupt the CRD-CR3 interaction (197). The association with RAS promotes the recruitment of RAF to membranes, a process facilitated by the presence of lipophilic binding domains in RAF. These domains exhibit differences in binding to particular lipids, which contributes to isoform-specific RAF functions (198-201). CR2 is a serine/threonine rich region containing important inhibitory phosphorylation sites that modulate RAS binding, as well as residues that mediate protein-protein interactions important in determining the localization of RAF. The C-terminus of RAF features the kinase domain (CR3) and a negative-charge regulatory region (N-region) just upstream of CR3 that is postulated to tightly associate with the catalytic domain to inhibit RAF activity (202).

RAF Signaling

RAF kinases play important roles in the integration of various signaling events, switching heterotrimeric G protein signaling and tyrosine kinase signaling to serine/threonine kinase signaling. Receptors that regulate RAF kinases include members of the G-protein coupled receptors (GPCRs), transmembrane receptor tyrosine kinases (RTKs), and cytokine receptors that regulate intracellular protein tyrosine kinases (PTKs). The discovery of epidermal growth factor (EGF) by Nobel Laureate Stanley Cohen and the characterization of its receptor, by Cohen and Graham Carpenter at

Vanderbilt University, has been paramount to understanding the development of cancer and developing anti-cancer drugs (203,204).

Epidermal growth factor receptor (EGFR, a.k.a. ErbB-1) is a cell-surface RTK that associates with several ligands to regulate a variety of cellular processes, including cell growth, proliferation, migration, and differentiation (205). Following formation of a ligand•RTK complex, EGFR undergoes a complex series of intra- and inter-molecular conformational shifts that switch the inactive monomeric RTK to an active homodimer or heterodimer (if EGFR associates with ErbB-2) (206,207). Reorientation of the intracellular kinase domains allows for transphosphorylation of the RTK activation loops and stabilization of the active state of the catalytic domain. Additional phosphorylation at other tyrosine residues along the cytoplasmic tail creates recruitment sites for the adaptor proteins Grb2 (growth factor receptor-bound protein 2) and Shc (Src homology 2 domain containing). Besides directly associating with activated EGFR, Grb2 can be indirectly recruited to the receptor by associating with EGFR-phosphorylated Shc (208). Interestingly, the presence of Shc governs which subgroups of mitogen-activated protein kinase (MAPK) pathways are activated downstream (209,210). The recruitment of Grb2 complexes containing son of sevenless (SOS), a RAS guanine nucleotide exchange factor, to the plasma membrane facilitates the activation of RAS proteins (211).

There are three *RAS* genes in humans giving rise to four RAS proteins (H-Ras, N-Ras, K-Ras4A, K-Ras4B), which exhibit differences in their binding affinities to the RBDs of the various RAF isozymes and therefore differences in their ability to activate each RAF kinase (212,213) (Fig. 22). Additional differences in individual RAS proteins

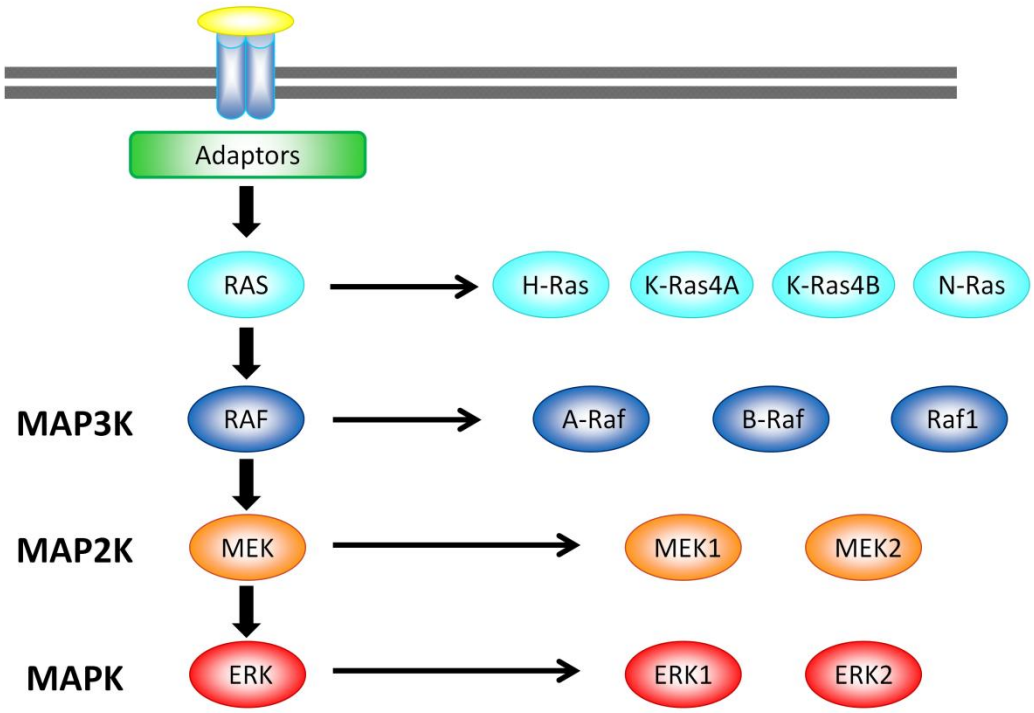

Figure 22. Components of the MAPK signaling pathway.
Schematic overview of the extracellular signal-regulated kinase (*ERK*) subgroup of MAPKs. RAF proteins (MAP3Ks) are activated by RAS proteins in response to receptor tyrosine kinase stimulation. Active RAF signals downstream to MEK proteins (MAP2Ks), which subsequently activate ERK proteins (MAPKs). Activated ERK regulates cell growth, differentiation, and development. Abbreviations: MAPK, mitogen-activated protein kinase; MAP2K, MAPK kinase; MAP3K, MAPK kinase kinase.

will be discussed further in Chapter IV. Activated RAF proteins phosphorylate and activate the dual-specificity MAPK/ERK kinases (MEK1 and MEK2) that are responsible for mediating the phosphorylation of threonine and tyrosine residues in the activation loop of extracellular signal-regulated kinases (ERK1 and ERK2). Activated ERK1/2 can then regulate cytosolic or nuclear targets to modulate transcription, metabolism, and cytoskeletal rearrangements (214).

The only widely accepted downstream targets of the mammalian RAF proteins *in vitro* and *in vivo* are MEK1 and MEK2. However, other substrates have been proposed, including the CDC25A phosphatase (215), the tumor-suppressor protein retinoblastoma (Rb) (216), and the inhibitor of nuclear factor (NF)-κB (IκB) (217). After initial reports that Raf1 could phosphorylate IκB, it was later discovered that a contaminant in the preparation, casein kinase II (CK2), was instead responsible for the phosphorylation of IκB (218). Unfortunately, the phosphorylation of CDC25A and Rb by Raf1 has not been studied further; thus, the biological relevance of these events is currently unclear. In line with the genetic evidence that B-*RAF*-1 evolutionarily preceded A-*RAF*-1 and C-*RAF*-1, several scientific observations suggest that B-Raf is the main activator of MEK in cells and that the other RAF isoforms play supportive roles (219). One such study demonstrated that B-Raf can activate MEK1 10-fold greater than Raf1, and 500-fold greater than A-Raf (220). Nevertheless, the modulatory effect of A-Raf and Raf1 on ERK signaling cannot be underestimated, as these isoforms appear to play key roles in determining the magnitude and duration of ERK activity and, ultimately, cell fate decisions (221).

Regulation of Raf1

The regulation of Raf1 is complex, involving intramolecular interactions, phosphorylation and dephosphorylation events, and protein-protein interactions. In its basal, unstimulated state Raf1is phosphorylated at three inhibitory sites – Ser43, Ser259, and Ser621 (222). Phosphorylation of Ser43 by protein kinase A (PKA) prevents the association of RAS and Raf1, while binding of 14-3-3 proteins to phospho-Ser259 and phospho-Ser621 stabilizes contacts between the N-terminal and C-terminal domains to lock Raf1 in an autoinhibitory conformation (223). Paradoxically, the binding of 14-3-3 to phospho-Ser621 also plays a critical role in the activation of Raf1, as mutation of this site has been shown to ablate kinase activity (222). Fortunately, recent studies have clarified the dual nature of this phospho-site. Ser621 must remain phosphorylated to allow binding of ATP to the active conformation of Raf1 and the association of 14-3-3 with this residue acts to prevent its dephosphorylation by unknown protein phosphatases, which appears to result in proteasome-mediated degradation of Raf1 (224,225). These studies also confirmed earlier reports that Ser621 can be autophosphorylated by Raf1 or targeted for phosphorylation by mitogen-stimulated kinases (225). Since 14-3-3 must remain bound to phospho-Ser621, it is the displacement of 14-3-3 from phospho-Ser259 that functions as an early step in the activation of Raf1 by RAS (Fig. 23). Both PP1 and PP2A have been implicated in the dephosphorylation of phospho-Ser259-Raf1, which relieves the autoinhibited state of Raf1 and promotes translocation of the kinase to different plasma membrane microdomains (226). Interactions between RAS and Raf1 at the plasma membrane leads to the phosphorylation of four other residues that are critical for full activation of Raf1: Ser338, Tyr341, Thr491, and Ser494. p21 activated kinases

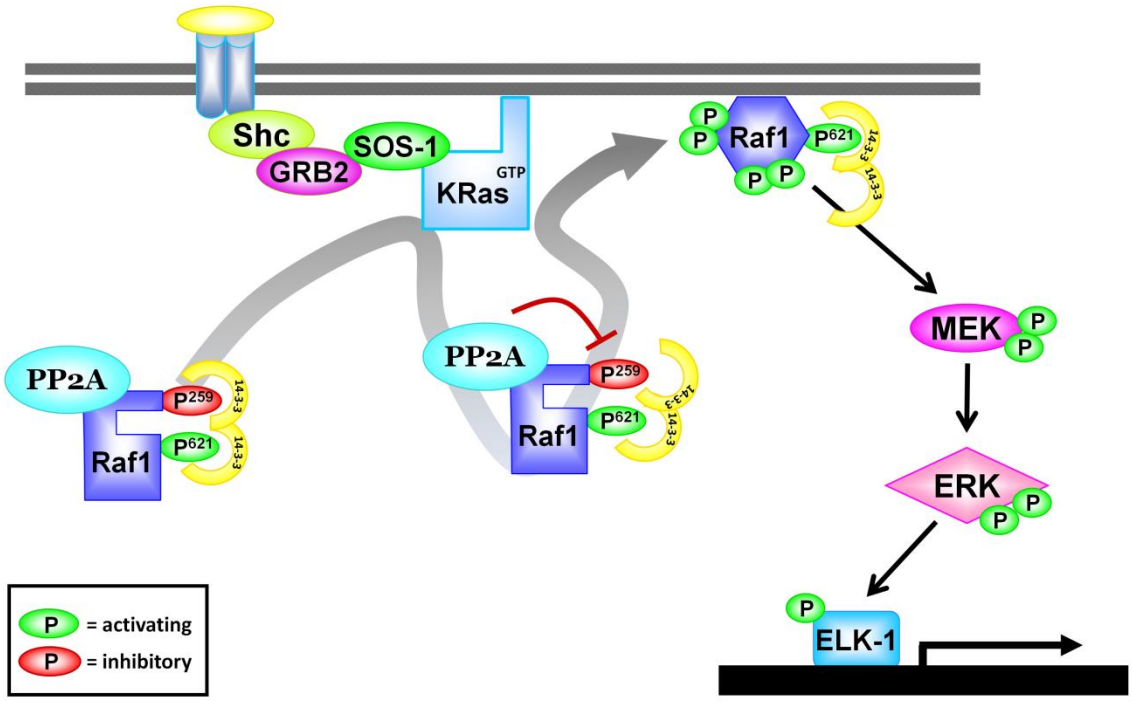

Figure 23. Displacement of 14-3-3 and PP2A dephosphorylation of an inhibitory residue in Raf1 positively regulates MAPK signaling.

14-3-3 dimers bind to phospho-Ser259 (P^{259}) and phospho-Ser621 (P^{621}) to lock cytosolic Raf1 in an autoinhibitory conformation that is associated with. The details are unclear, but the coordinated actions of GTP-bound KRas and PP2A displace 14-3-3 and expose P^{259}. PP2A holoenzymes containing Bα or Bδ subunits positively regulate this pathway by dephosphorylating P^{259}, which relieves autoinhibitory contacts within Raf1 and promotes translocation of the kinase to the plasma membrane. Additional phosphorylation events and conformational changes lead to the full activation of Raf1 and promote signaling downstream to MEK1/2 and ERK1/2. Activated ERK1/2 facilitates phosphoactivation of transcription factors (e.g., *ELK-1*) responsible for immediate early gene expression.

(PAK1 and PAK2) have been implicated in the phosphorylation of Ser338, but other kinases may be involved (e.g., CK2, Raf1) (227,228). Src and Src-family kinases target Tyr341 for phosphorylation (229). The phosphorylation of Ser338 and Tyr341, located within the N-region of Raf1, creates a negative charge that relieves the autoinhibition imposed by the N-terminal domain, reconfigures the MEK1/2 binding sites, and stabilizes an active Raf1 conformation (195,230). Phosphorylation of the activation segment residues in CR3 (i.e., Thr491 and Ser494) by unknown kinases further stabilizes the active Raf1 conformation and exposes the catalytic cleft. These five activating phospho-sites in Raf1 (i.e., Ser338, Tyr341, Thr491, Ser494, and Ser621) are functionally conserved in A-Raf. However, B-Raf exhibits a constant negative charge in its N-region, containing a constitutively phosphorylated Ser445 and an aspartic acid in lieu of a tyrosine (Asp448), which is responsible for the elevated basal activity of B-Raf relative to Raf1 (231).

Raf1 interacts with ABαC and ABδC holoenzymes

As previously mentioned, dephosphorylation of phospho-Ser259 by PSTPs promotes translocation of Raf1 to the plasma membrane and its association with RAS. A report from the Baccarini group not only confirmed prior studies by other groups that PP2A can regulate Raf1 phosphorylation (226), but also established a physical interaction between Raf1 and the PP2A core dimer (i.e., AC) in cells (136). While no PP2A regulatory B subunit was implicated in this PP2A•Raf1 complex, a genetic screen examining RAS-mediated *C. elegans* vulval development showed that a B subunit gene (i.e., *sur-6*) acted downstream of, or in parallel with, *RAS* and upstream of *lin-45* (i.e., *RAF*) to positively regulated RAS signaling (232). Our studies of Bα (i.e., mammalian

homolog of *C. elegans* SUR-6) and the closely related Bδ indicated that Bα- and Bδ-containing holoenzymes upregulate Raf1 activity by associating with the kinase and dephosphorylating the inhibitory phospho-Ser259 residue (137). However, the signaling events that regulate ABαC•Raf1 and ABδC•Raf1 complexes to promote Raf1-MEK-ERK signaling remain poorly understood.

The initial characterization of a PP2A•Raf1 complex in BAC-1.2F5 cells, a murine macrophage cell line, indicated that the formation of this complex was unaffected by mitogenic stimulation with CSF-1 (136). However, subsequent studies by this same group demonstrated that EGF stimulates the association of Raf1 and $PP2A_C$ in both cytosolic and membrane fractions of COS-1 cells (233). Furthermore, studies from the Morrison laboratory demonstrated that the PP2A core dimer was constitutively bound to Raf1 in Cos cells and that the binding of the regulatory B subunit was promoted following stimulation with platelet-derived growth factor (PDGF) (147). Together, these data suggest that PP2A-Raf1 interactions may be regulated through distinct mechanisms that are dependent on the cell type as well as the cell stimulus. Our prior studies indicate that Bα-Raf1 and Bδ-Raf1 interactions are enhanced by 47% and 38%, respectively, following EGF treatment (137). Therefore, we decided to further examine the regulatory mechanisms controlling ABαC-Raf1 and ABδC-Raf1 interactions.

In this chapter, I present data demonstrating EGF-dependent changes in the ABδC-Raf1 interaction and stimulus-induced alterations in Raf1 activity in cells overexpressing Bδ. Since these changes were relatively small and often variable, we utilized cell-permeable, chemical crosslinkers to capture transient associations in ABδC•Raf1 complexes. Although we observed enhanced binding of ABδC and Raf1

with one crosslinker, we did not observe a difference in the ABδC-Raf1 interactions between crosslinker treated and untreated samples. Using mass spectrometry to identify PP2A-interacting proteins, we determined that different crosslinkers stabilize overlapping, but distinct ABδC interactomes. Using the crosslinker that enhanced ABδC-Raf1 interactions, we examined ABδC, Raf1, and the ABδC•Raf1 complex for novel binding partners. These unpublished proteomic studies on ABδC•Raf1-interacting proteins identified several putative candidates that await further characterization to determine if they regulate the ABδC•Raf1 complex. Lastly, I present evidence revealing an association between AB′βC and Raf1 that suggest other PP2A holoenzymes may be involved in the complex regulation of Raf1 function.

Materials and Methods

Antibodies and reagents

The mouse anti-FLAG M2 antibody, mouse anti-FLAG M2 affinity gel and FLAG peptide were from Sigma-Aldrich (St. Louis, MO). Human epidermal growth factor (EGF) and Protein G-Sepharose 4B conjugate were from Invitrogen (Carlsbad, CA). Rabbit anti-Raf1 (sc-133) and goat anti-ERK2 (C-14-G) antibodies were from Santa Cruz Biotechnology, Inc. (Santa Cruz, CA). Rabbit anti-phospho-p44/42 MAPK (ERK1/2; pThr202/pTyr204) was from Cell Signaling Technology, Inc. (Danvers, MA). Monoclonal $PP2A_C$ and Raf1 (53/c-Raf-1) antibodies were from BD Transduction Laboratories (San Diego, CA). Generation of rabbit $PP2A_A$ antibodies was previously described (234). Secondary antibodies for fluorescence detection were from Rockland (Gilbertsville, PA) or Molecular Probes (Eugene, OR). Normal rabbit IgG (sc-3888) and

mouse IgG (catalog #553452) were from Santa Cruz and BD Pharmingen, respectively. Bio-Rad Protein Assay Dye Reagent Concentrate for Bradford protein assays was from Bio-Rad Laboratories, Inc. (Hercules, CA). Odyssey Blocking Buffer was from LI-COR (Lincoln, NE). Dithiobis(succinimidyl propionate) (DSP) and dithiobis-maleimidoethane (DTME) were from Thermo Scientific Pierce (Rockford, IL). All other reagents were purchased from Sigma-Aldrich (St. Louis, MO) or Thermo Fisher Scientific Inc. (Lafayette, CO).

Cell culture and induction

Monoclonal cell lines stably expressing tetracycline-inducible expression plasmids encoding Bα-FLAG, Bδ-FLAG, or FLAG-B′β, as well as control cell lines stably expressing pcDNA5/TO, were described previously (137). Expression of PP2A B subunits was accomplished by treating the respective cells with 1 μg/ml tetracycline for 20-48 h at 37^{o}C. Wildtype C57BL/6 mouse embryonic fibroblasts (MEFs) were a kind gift from Dr. Catrin Pritchard (University of Leicester; Leicester, United Kingdom). Stable cells were maintained at 37^{o}C and 5% CO_2 in DMEM supplemented with 10% fetal bovine serum, 5 μg/mL blasticidin, and 175 μg/mL hygromycin B; MEFs were maintained in similar conditions in the absence of antibiotics.

Regulation of Raf1-Bδ_{FLAG} interactions

Control and Bδ-FLAG stable cells were treated with tetracycline and then serum starved for 20 h prior to treatment with 50 ng/ml EGF. Cells were washed twice with ice-cold PBS, pH 7.4 and then lysed using ice-cold Buffer B (20 mM Tris-HCl, pH 8.0, 137 mM NaCl, 10% glycerol, and 1% Igepal CA-630) containing inhibitors (17 μg/ml

aprotinin, 10 µM leupeptin, 1 mM phenylmethylsulfonyl fluoride, and 1 mM Na_3VO_4). Clarified lysates were generated following centrifugation at 16,300xg for 10 min at 4°C. For FLAG immunoprecipitations, the clarified lysates were gently rotated with 20 µl of a 50% slurry of resin for 4 h at 4°C. Bound proteins were washed three times with 200 µl Buffer B lacking inhibitors and eluted with 2xSDS sample buffer.

In cell crosslinking

For each experiment, crosslinkers were freshly prepared as a 20 mM solution in dimethyl sulfoxide (DMSO) and subsequently diluted to the indicated, final working concentrations in phosphate-buffered saline (PBS), pH 7.0 containing 10 mM EDTA. Cells were washed twice with room temperature PBS pH 7.0 + EDTA and then incubated at room temperature with PBS + EDTA containing DMSO, 0.5 mM DSP (or the indicated concentration), 1.0 mM DTME (or the indicated concentration), or 0.5 mM DSP and 1.0 mM DTME for 10-30 min at 25°C. The crosslinker solution was then removed by gentle aspiration and cells were subsequently incubated for 10-15 minutes at 25°C with quenching solution (50 mM Tris-Cl, pH 7.4 and 5 mM L-Cysteine). Quenching solution was then removed and cells were lysed in ice-cold RIPA (50 mM Tris-HCl, pH 8.0, 150 mM NaCl, 1% Igepal CA-630, 0.5% sodium deoxycholate, and 0.1% SDS) or ice-cold $RIPA^{++}$ (RIPA containing 30 mM NaF, 40 mM β-glycerophosphate, and 20 mM sodium pyrophosphate) containing inhibitors (17 µg/ml aprotinin, 10 µM leupeptin, 1 mM phenylmethylsulfonyl fluoride, and 1 mM Na_3VO_4). Clarified lysates were generated following centrifugation at 16,300xg for 10 min at 4°C. Samples to be reduced were incubated with 50 mM DTT for 30 min at 37°C and diluted with 5xSDS sample buffer containing β-mercaptoethanol (βME) prior to heating to 95°C

for 5 min. Non-reduced samples were prepared by adding additional lysis buffer, in lieu of DTT, and diluted with 5xNon-reducing sample buffer (250 mM Tris, pH 6.8, 20% glycerol, 5% SDS, and 0.02% bromophenol blue), without heating above 25^{o}C. Non-crosslinker treated cells were washed twice with ice-cold PBS, pH 7.4 and then lysed using ice-cold Buffer B containing inhibitors and prepared using 5xSDS sample buffer containing βME. For FLAG immunoprecipitations, the clarified lysates were gently rotated with 15 µl of a 50% slurry of resin for 4 h at 4^{o}C. Bound proteins were washed three times with 300 µl of the respective lysis buffer lacking inhibitors and eluted with 2xSDS sample buffer.

In vitro *crosslinking*

Following induction of Bδ-FLAG expression, cells were lysed in Buffer B containing inhibitors. FLAG immunoprecipitations were carried out using 15 µl of a 50% slurry of resin and incubated for 4 h at 4^{o}C with rotation. Bound proteins were washed three times with 300 µl Buffer B lacking inhibitors and then incubated with the indicated concentration of crosslinker(s) for 30 min at 25^{o}C with agitation every 5 min. Bound proteins were washed three times with 300 µl Buffer B lacking inhibitors and eluted with 2xSDS sample buffer.

Silver and Colloidal Blue staining

Following treatment with tetracycline, control and Bδ-FLAG cells were treated with crosslinker as described above. For FLAG immunoprecipitations, the clarified lysates were gently rotated with 15 µl of a 50% slurry of anti-FLAG resin for 4 h at 4^{o}C. Bound proteins were washed three times with 300 µl RIPA or RIPA^{++} buffer and eluted

with 2xSDS sample buffer containing 50 mM DTT (Silver) or 25 µl $RIPA^{++}$ containing 50 mM DTT followed by a 30 min incubation at 37°C with agitation (Colloidal Blue). Colloidal Blue samples were subsequently mixed with 5xSDS sample buffer and heated at 95°C for 5 min. Samples were analyzed by SDS-PAGE and visualized by Silver Stain (235) or Colloidal Blue staining (Invitrogen; Carlsbad, CA) according to the manufacturer's protocol.

Tandem affinity purification

Using four plates (10-cm) of control or Bδ-FLAG cells per immunoprecipitation, tetracycline-induced cells were treated with crosslinker as described above. Clarified lysates of the same cell type were pooled and incubated with 60 µl of a 50% slurry of anti-FLAG resin and incubated for 4 h at 4°C with rotation. FLAG immune complexes were washed twice with 500 µl $RIPA^{++}$ lacking inhibitors and once with 500 µl Buffer B lacking inhibitors. Bound proteins were eluted with 500 µl Buffer B containing 100 µg/ml FLAG peptide for 1 h at 4°C with rotation. A portion of eluted proteins (10 µl) was reserved for subsequent analysis and diluted with 5xSDS sample buffer. The remaining eluate was transferred to a new eppendorf and incubated with 250 ng mouse anti-Raf1 antibody plus 200 ng rabbit anti-Raf1 antibody overnight at 4°C with rotation. Samples were then incubated with 15 µl of a 50% slurry of Protein G-Sepharose 4B for 1.25 h at 4°C with rotation. Bound proteins were washed three times with 300 µl Buffer B, eluted with 15 µl 2xSDS sample buffer, and analyzed by Western.

Mass spectrometry

Using four plates (10-cm) of control or Bδ-FLAG cells per immunoprecipitation, tetracycline-induced cells were treated with crosslinker as described above. Clarified lysates of the same cell type were pooled and incubated with 2.5 µg normal mouse IgG plus 2.0 µg normal rabbit IgG, 2.5 µg mouse anti-Raf1 antibody plus 2.0 µg rabbit anti-Raf1 antibody, or 75 µl of a 50% slurry anti-FLAG resin (FLAG IPs). Raf1/IgG immunoprecipitations were incubated 3.5 h at 4^{o}C with rotation and subsequently incubated with 20 µl of a 50% slurry Protein G-Sepharose 4B for 1 h at 4^{o}C with rotation. Raf1/IgG immune complexes and single-step FLAG IPs were washed four times with 500 µl RIPA^{++} lacking inhibitors and bound proteins eluted with 80 µl RIPA^{++} containing 50 mM DTT with incubation at 37^{o}C for 40 min and agitation every 5 min. Eluted proteins were transferred to a new eppendorf and submitted for mass spectrometry analysis.

FLAG IPs destined for tandem affinity purification were incubated 4 h at 4^{o}C with rotation and then washed three times with 500 µl RIPA^{++} lacking inhibitors and once with 500 µl Buffer B lacking inhibitors. Bound proteins were eluted with 500 µl Buffer B containing 100 µg/ml FLAG peptide for 1 h at 4^{o}C with rotation. The remaining eluate was transferred to a new eppendorf and incubated with 750 ng mouse anti-Raf1 antibody plus 600 ng rabbit anti-Raf1 antibody overnight at 4^{o}C with rotation. Samples were then incubated with 20 µl of a 50% slurry Protein G-Sepharose 4B for 1 h at 4^{o}C with rotation. Bound proteins were washed three times with 300 µl Buffer B, eluted with 40 µl 2xSDS sample buffer and submitted for mass spectrometry analysis.

Proteins were either eluted using RIPA^{++} buffer containing 50 mM DTT (Fig. 33) or 2xSDS sample buffer (Table 2). The DTT-eluted proteins were precipitated using 25% TCA (w/v), washed twice with ice cold acetone, and then subjected to in solution trypsin digestion in 2 M urea. The SDS solubilized samples were resolved approximately 1 cm onto a 10% Novex protein gel (Life Technologies) and then stained with Colloidal Blue. The entire contents of each immunoprecipitation were subjected to an in-gel trypsin digestion. Resulting peptides were analyzed by a 70 minute data dependent LC-MS/MS analysis. Briefly, peptides were autosampled onto a 200 mm by 0.1 mm (Jupiter 3 micron, 300A), self-packed analytical column coupled directly to an LTQ (ThermoFisher) using a nanoelectrospray source and resolved using an aqueous to organic gradient. A series of full scan mass spectrum followed by 5 data-dependent tandem mass spectra (MS/MS) were collected throughout the run and dynamic exclusion was enabled to minimize acquisition of redundant spectra. MS/MS spectra were searched via SEQUEST against a human database (UniprotKB – reference proteome set) that also contained reversed versions for each of the entries (236). Identifications were filtered and collated at the protein level using IDPicker version 1.0 (237) or Scaffold version 3.3.1 (Proteome Software Inc.; Portland, Oregon).

Western analysis

See "Materials and Methods" in Chapter IV for details of this methodology.

Statistics

Statistical comparisons were performed using GraphPad Prism version 4.03 (GraphPad Software; San Diego, CA).

Results

EGF-induced changes in PP2A-Raf1 interactions and Raf1 activity

To address the molecular mechanism(s) that regulates ABδC-mediated dephosphorylation of Raf1, we exploited monoclonal HEK-293 TREx cells that can be induced (via tetracycline) to express a C-terminal, FLAG-tagged Bδ regulatory subunit (Bδ-FLAG) (137). Following induction with tetracycline (36-48 h), serum-starved control cells and Bδ-FLAG cells were stimulated with 50 ng/ml EGF and solubilized extracts were monitored for changes in phospho-ERK1/2, a readout of upstream Raf1 activity, by Western. Control cells demonstrated a robust increase at 5 min followed by a time-dependent decrease in phospho-ERK1/2 levels (Fig. 24). Consistent with published findings from our laboratory (137), expression of Bδ-FLAG significantly enhanced ERK phosphorylation at several time points (Fig. 24). Western analysis of the FLAG immune complexes demonstrated the presence of Bδ-FLAG•Raf1 complexes in unstimulated cells and a subtle, but statistically significant, EGF-induced decrease in their interaction between the 30 min and 120/240 min time points (Fig. 25). Surprisingly, changes in the association of Bδ-containing PP2A holoenzymes ($AB\delta_{FLAG}C$) and Raf1 did not temporally correlate with the observed differences in ERK phosphorylation (Fig. 24). A number of assay conditions were manipulated to optimize and enhance the relatively weak levels of Raf1 found in the FLAG immune complexes, but despite slight gains in total Raf1 signal, the data trends remained unchanged (data not shown).

In addition to monitoring PP2A-Raf1 interactions in stimulated cells, we also examined EGF-induced changes in Raf1 kinase activity using an *in vitro* MEK

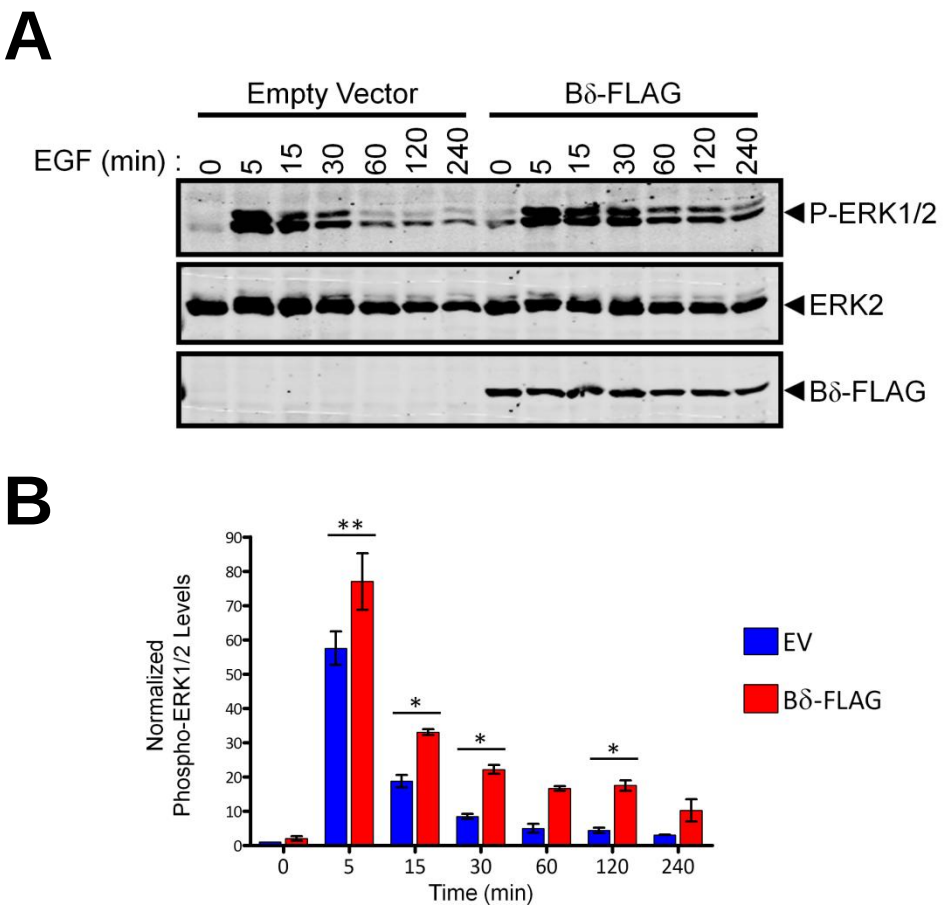

Figure 24. Elevated cellular levels of Bδ enhance ERK1/2 phosphorylation.
A, Control (*Empty Vector*) and Bδ-FLAG monoclonal cell lines were treated with tetracycline for 24 h and then serum-starved overnight in serum-free medium containing fresh tetracycline. Prior to harvest, cells were treated with 50 ng/mL EGF for increasing amounts of time (min). Cell lysates were analyzed by Western with antibodies recognizing phospho-ERK1/2 (*P-ERK1/2*), ERK2, and the FLAG epitope (*Bδ-FLAG*). ***B***, Quantification of phospho-ERK1/2 levels normalized to total ERK2 from Control (blue bars) and Bδ-FLAG (red bars) extracts relative to unstimulated control cells, which were set to 1. Two-way analysis of variance followed by Tukey post- tests identified statistically significant elevations in ERK1/2 phosphorylation: *, $p < .05$; **, $p < .01$ ($n = 4$).

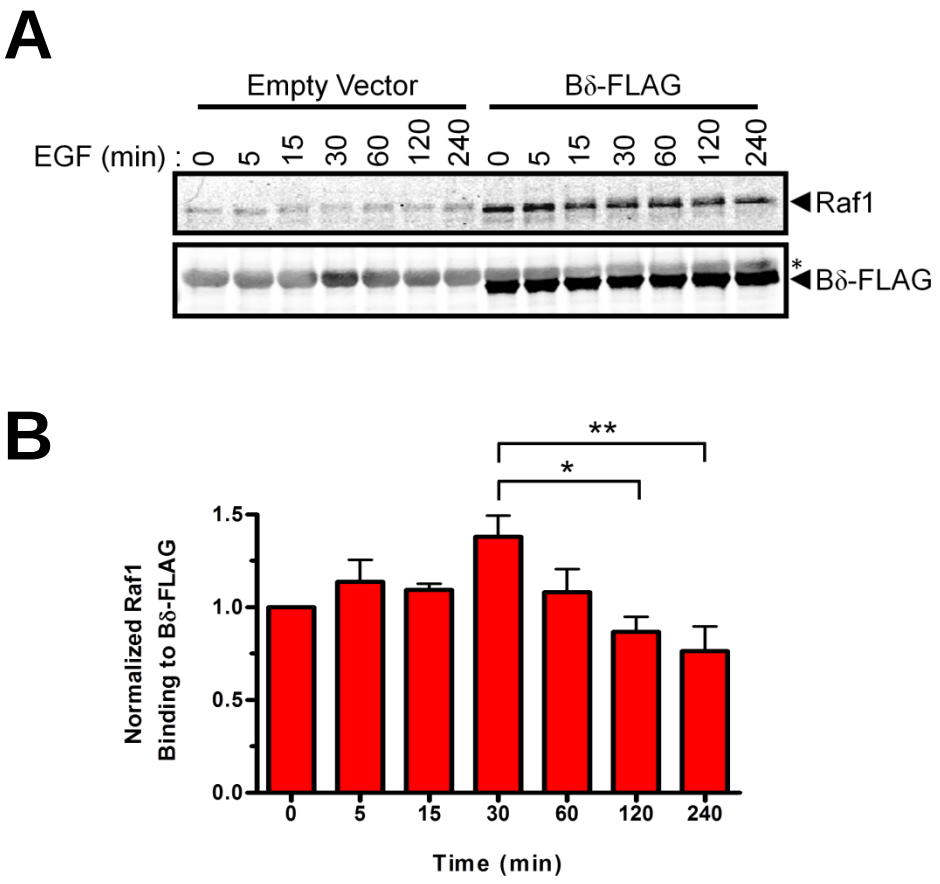

Figure 25. EGF stimulation of cells disrupts ABδC-Raf1 interactions.
A, Cellular extracts from Fig. 24 were incubated with anti-FLAG resin and bound proteins were eluted with SDS sample buffer. Immunoblot analysis of FLAG eluates was performed using antibodies recognizing Raf1 and the FLAG epitope (*Bδ-FLAG*). *, heavy chain IgG. ***B***, Quantification of Raf1 present in FLAG immune complexes normalized to levels of Bδ-FLAG as compared to unstimulated Bδ-FLAG samples, which were set to 1. One-way analysis of variance followed by Tukey post-tests identified statistically significant differences in Raf1 binding: *, $p < .05$; **, $p < .01$ ($n = 4$).

phosphorylation assay. Raf1 immune complexes from EGF-stimulated Bδ-FLAG cells exhibited a small increase in kinase activity (~50-60%) relative to EGF-treated control cells (data not shown). We also discovered that expression of constitutively active MEK prevented an EGF-induced increase in Raf1 activity (data not shown). Additionally, we observed a small decrease (~30-35%) in the binding of PP2A and Raf1 in Bδ-FLAG cells expressing constitutively active MEK (data not shown), implicating an unknown feedback loop in the control of $AB\delta_{FLAG}C$•Raf1 complexes. Prior findings from our group have demonstrated that the association of the regulatory Bα/δ subunit and $PP2A_C$ with Raf1 immune complexes was enhanced following EGF treatment (137), but given the relatively small difference and variability of these assays, we concluded that alterations in the PP2A•Raf1 complex may be quite dynamic and difficult to capture. Therefore, we employed cell-permeable chemical crosslinkers to trap transient $AB\delta_{FLAG}C$-Raf1 interactions following EGF stimulation.

"ReCLIP'ing" $AB\delta_{FLAG}C$ and Raf1 interacting proteins

Transient protein-protein interactions can be strong or weak in magnitude and temporally fast or slow. Purification of labile protein complexes can be accomplished using Reversible Cross-Link Immuno-Precipitation (ReCLIP), a relatively new method developed by the Reynolds group at Vanderbilt University (238). By coupling ReCLIP with mass spectrometry, transient binding partners for any given protein can be identified in an unbiased, discovery-based approach. In our application of ReCLIP, we utilized cell-permeable, thiol-cleavable homobifunctional crosslinkers with distinct reactive chemistries. Dithiobis(succinimidyl propionate) (DSP, a.k.a. Lamont's Reagent) has a 12 Å spacer arm and reacts with primary amines (found in lysine residues as well as the N-

terminal methionine residue) at pH 7-9 to form stable amide bonds; dithiobis-maleimidoethane (DTME) has a 13.3 Å spacer arm and reacts with sulfhydryl groups (found in cysteine residues) at pH 6.5-7.5 to form stable thioether bonds (Fig. 26). There are three potential outcomes for proteins reacting with DSP or DTME: i) crosslinking of residues on the same protein (intra-molecular crosslinking), ii) crosslinking of residues between two different proteins (inter-molecular crosslinking), and iii) reaction of one end of the crosslinker with an amino acid while the second reactive group fails to react with another amino acid (dead-end crosslinking) (Fig. 27).

To establish the legitimacy of this method to effectively crosslink cellular proteins of interest to us (i.e., Raf1 and Bδ), wildtype mouse embryonic fibroblasts (MEFs) were treated with increasing doses of DSP and analyzed by Western under non-reducing conditions. Raf1 exhibited a dose-dependent shift towards higher molecular weight, crosslinked complexes, which were readily reversed following reduction of the thiol bond within the DSP spacer arm with dithiothreitol (DTT) (Fig. 28). We then monitored Raf1 crosslinking in the presence of increasing doses of DSP, DTME, or both DSP and DTME in cells expressing Bδ-FLAG. These experiments revealed the minimal concentration of crosslinker needed to crosslink the majority of Raf1 (i.e., 1 mM DSP and 0.5 mM DTME) and also suggested that different Raf1 interactomes could be isolated in a crosslinker-dependent manner (Fig. 29). Similar results were obtained when examining crosslinked Bδ-FLAG complexes from cells expressing this PP2A regulatory subunit (data not shown). We next examined the effect of the chemical crosslinkers on the association of $AB\delta_{FLAG}C$ and Raf1. Analysis of FLAG immune complexes from untreated Bδ-FLAG cells solubilized in a mild lysis buffer (i.e., Buffer B) indicated that

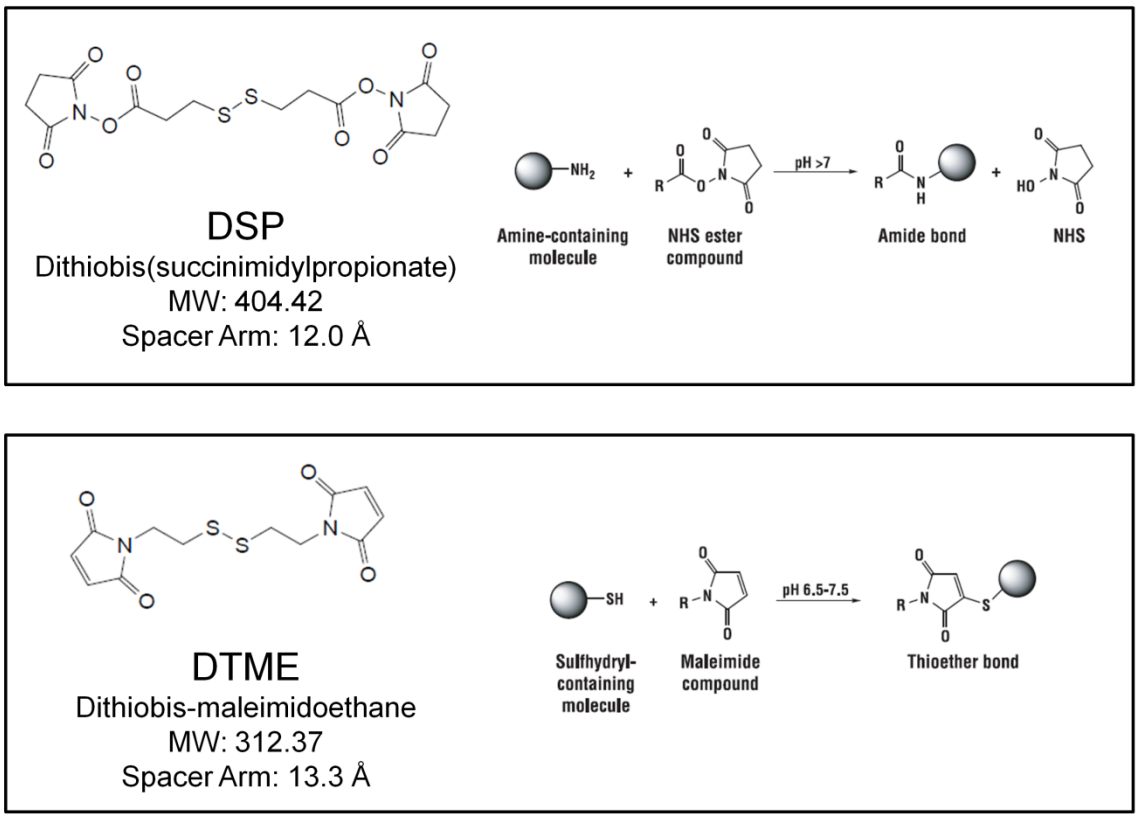

Figure 26. Properties of chemical crosslinking reagents.
The chemical structure, name, molecular weight (*MW*), spacer arm length, and coupling reactions of DSP (*top*) and DTME (*bottom*) are shown.

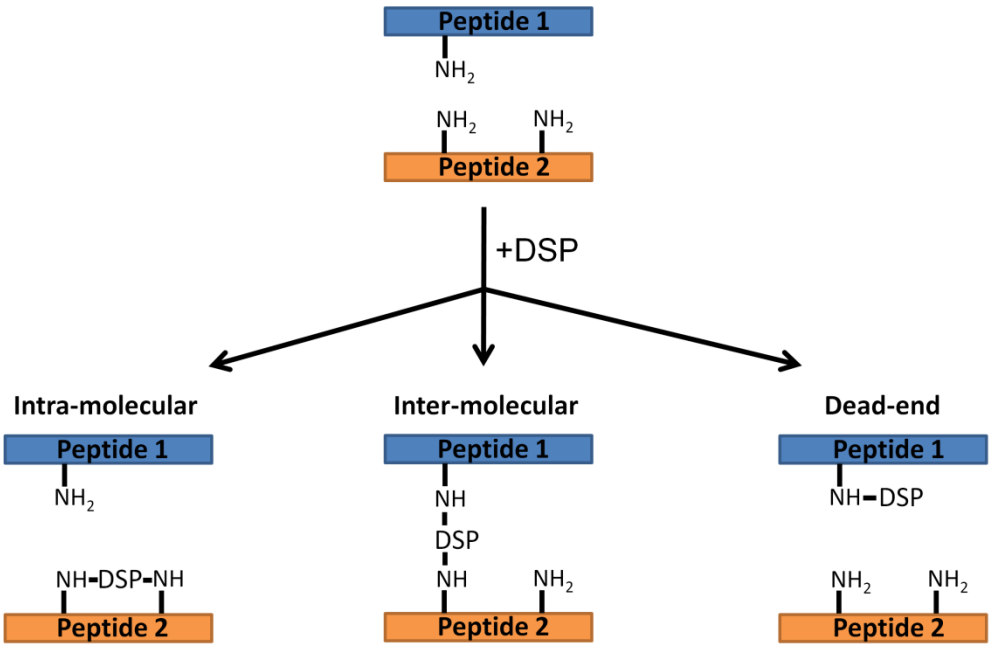

Figure 27. Crosslinking of primary amines by the chemical crosslinking reagent DSP.

There are three potential outcomes when crosslinking proteins with DSP. Intra-molecular crosslinking: crosslinking of primary amines on the same protein (*Peptide 2*). Inter-molecular crosslinking: crosslinking of primary amines between two different proteins (*Peptide 1* and *2*). Dead-end crosslinking: reaction of one end of the crosslinker with a primary amine on one protein (*Peptide 1*) while the second reactive group fails to react with another primary amine.

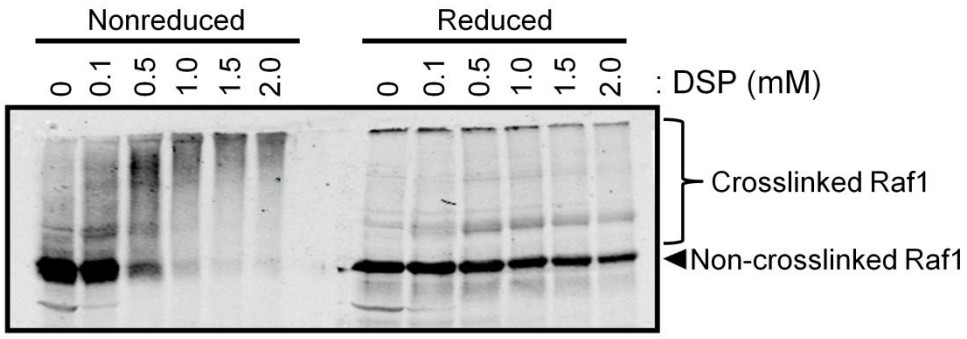

Figure 28. Intracellular crosslinking of Raf1 with DSP.
Wildtype C57BL/6 mouse embryonic fibroblasts were treated with solutions lacking (0 mM) or containing increasing concentrations of DSP (0.1-2.0 mM). Nonreduced and Reduced cell extracts were prepared and analyzed by Western using a Raf1 antibody (n = 3).

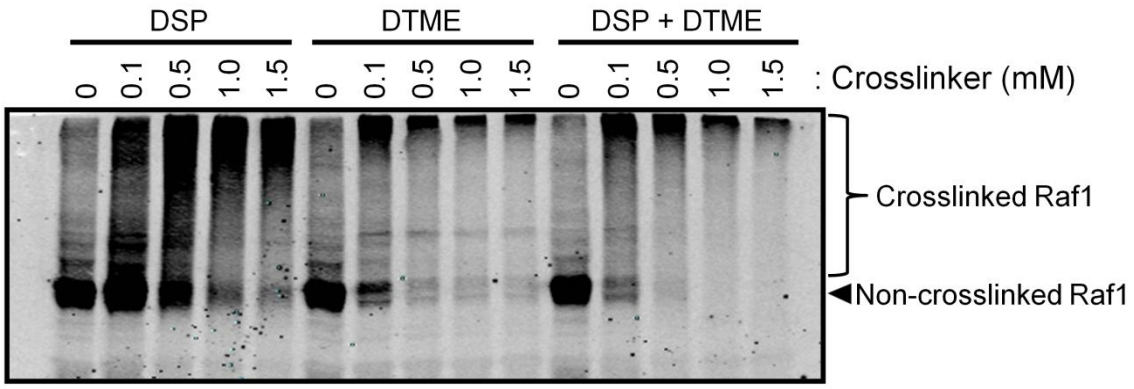

Figure 29. Comparison of intracellular crosslinking of Raf1 using DSP, DTME, or both DSP and DTME.

Bδ-FLAG monoclonal cell lines were treated with tetracycline for 36-48 h and then incubated with solutions lacking (0 mM) or containing the indicated concentrations of DSP, DTME, or both DSP and DTME. Immunoblot analysis of nonreduced cell extracts were performed using a Raf1 antibody (n = 3).

endogenous Raf1, as well as the structural ($PP2A_A$) and catalytic ($PP2A_C$) subunits of PP2A, co-precipitated with the regulatory Bδ-FLAG subunit; these proteins were not detected in FLAG immune complexes from empty vector-expressing cells (Fig. 30A, top panel). FLAG immune complexes from Bδ-FLAG cells treated with vehicle (i.e., DMSO) and solubilized in a stringent lysis buffer (i.e., RIPA buffer) co-precipitated much less Raf1 when compared to the FLAG immune complexes isolated from cells lysed in Buffer B. Crosslinking with DSP enhanced the amount of Raf1, $PP2A_A$ and $PP2A_C$ co-precipitating with Bδ-FLAG, indicating that DSP stabilized both $AB\delta_{FLAG}C$-Raf1 interactions and interactions between the core dimer and regulatory subunit. Crosslinking with DTME or both DSP and DTME drastically enhanced the association of Raf1 with Bδ-FLAG. However, a dramatic loss of $B\delta_{FLAG}$-associated $PP2A_A$ and $PP2A_C$ was observed following DTME treatment and a mild loss of these subunits was observed in immune complexes from cells treated with both DSP and DTME. As expected, Western analysis of cellular extracts for Raf1 under non-reducing and reducing conditions revealed the effectiveness and reversibility of the crosslinking with DSP, DTME, and DSP plus DTME (Fig. 30A, middle and bottom panels).

The loss of $B\delta_{FLAG}$-associated $PP2A_A$ and $PP2A_C$ subunits following DTME treatment was unexpected. To rule out the possibility that this was due to crosslinker-modified epitopes that would result in a loss of antibody binding to the target proteins and a subsequent inability to detect these proteins by Western, we silver stained SDS-polyacrylamide gels containing $AB\delta_{FLAG}C$ holoenzymes isolated from DTME treated cells. Silver stain analysis revealed that DTME dose-dependently decreased the amount of $PP2A_A$ and $PP2A_C$ subunits co-precipitating with the Bδ-FLAG subunit (Fig. 31), thus

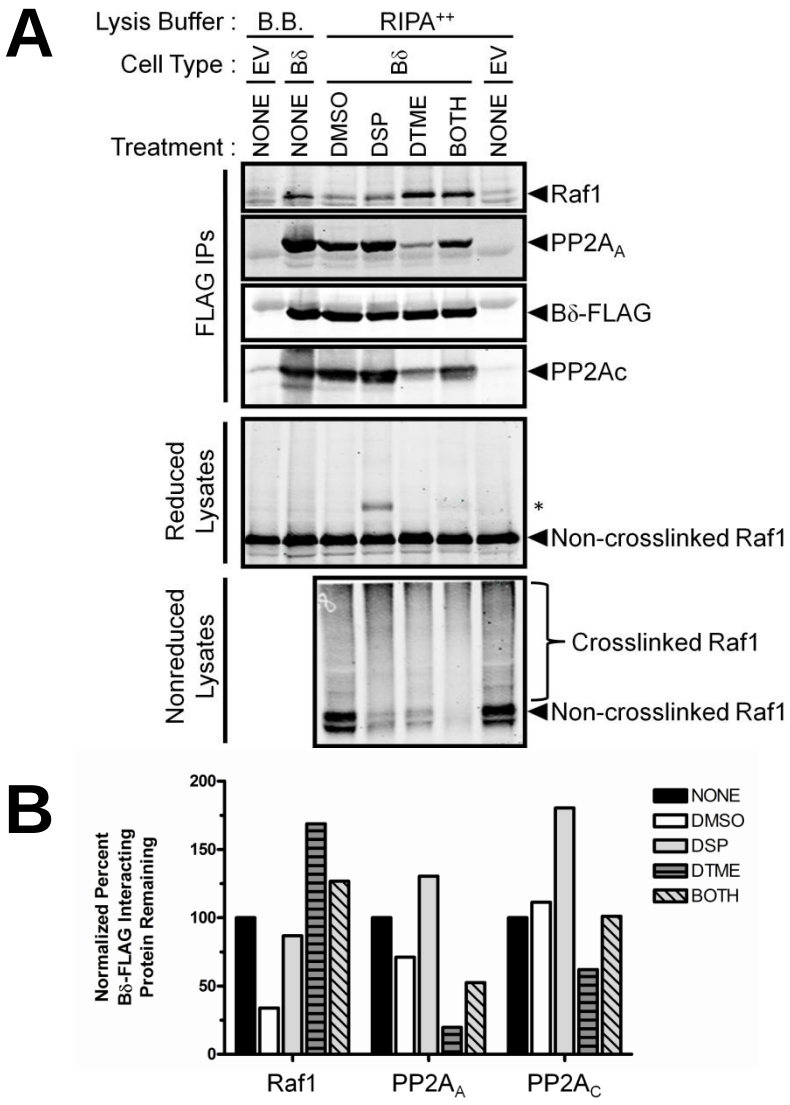

Figure 30. DTME enhances the association of Bδ-FLAG and Raf1, but disrupts Bδ-FLAG binding to the PP2A core dimer.

A, Control (*EV*) and Bδ-FLAG (*Bδ*) cells were treated with tetracycline for 36-48 h and then solubilized without treatment (*NONE*) or following incubation with solutions lacking (*DMSO*) or containing crosslinker [1 mM DSP, 0.5 DTME, or 1 mM DSP and 0.5 mM DTME (*BOTH*)] using low stringency (Buffer B; *B.B.*) or high stringency ($RIPA^{++}$) lysis buffers. Extracts were incubated with FLAG resin and bound proteins were washed with the appropriate lysis buffer before being eluted with SDS sample buffer. Western analysis of FLAG immune complexes (*FLAG IPs*) (*upper panel*) and lysates prepared under Nonreducing (*middle panel*) or Reducing (*lower panel*) conditions was performed using antibodies recognizing Raf1, $PP2A_A$, the FLAG epitope (*Bδ-FLAG*), and $PP2A_C$ (n = 2). *, DSP crosslinked Bδ-FLAG recognized by the secondary antibody, see Fig. 32. ***B***, Quantification of the above immunoblot for FLAG resin bound Raf1, $PP2A_A$, and $PP2A_C$ normalized to Bδ-FLAG levels and compared to FLAG immune complexes from untreated Bδ-FLAG cells (*NONE*), which were set to 100.

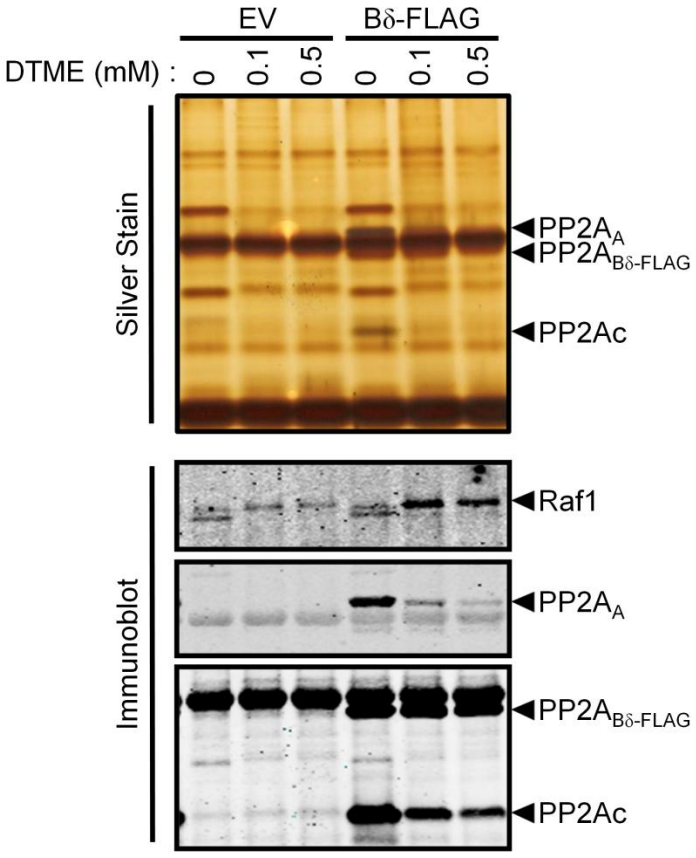

Figure 31. DTME does not modify the PP2A$_A$ and PP2A$_C$ antibody binding epitopes.

Control (*EV*) and Bδ-FLAG (*Bδ*) cells were cultured with tetracycline for 36-48 h and then treated with solutions lacking (0 mM) or containing increasing concentrations of DTME (0.1-0.5 mM). FLAG immune complexes isolated from solubilized EV and Bδ extracts were eluted with SDS sample buffer and analyzed by silver staining SDS-polyacrylamide gels (*Silver Stain*) or Western analysis (*Immunoblot*) using Raf1, PP2A$_A$, FLAG, and PP2A$_C$ antibodies (n = 1).

demonstrating that the crosslinking treatment did not mask an antibody binding epitope. We also observed a parallel increase in Raf1 binding to Bδ-FLAG, thereby confirming earlier results that crosslinking of cysteines enhances the association of Bδ-FLAG and Raf1 while simultaneously disrupting $PP2A_A$ and $PP2A_C$ interactions with the Bδ subunit (Fig. 31). To address the possibility that DTME acted *in situ* to actively disrupt preformed $AB\delta_{FLAG}C$ holoenzymes, we treated purified, FLAG resin-bound $AB\delta_{FLAG}C$ complexes with the crosslinkers and examined bound proteins following several washes with Buffer B. When compared to $AB\delta_{FLAG}C$ complexes treated with buffer only (NONE), the presence of the crosslinker (DSP, DTME, or both DSP and DTME) did not alter the binding of $PP2A_A$ and $PP2A_C$ with Bδ-FLAG (Fig. 32). Based on these findings, we concluded that DTME does not disrupt heterotrimeric $B\delta_{FLAG}$-containing holoenzymes *in vitro*. Since DTME enhanced $AB\delta_{FLAG}C$-Raf1 interactions, we moved forward to investigate if transient, EGF-dependent changes in PP2A-Raf1 binding could be stabilized in the presence of DTME. Previous studies revealed that 1 mM DSP effectively crosslinks over 71% of the Raf1 proteins and 84% of the Bδ-FLAG proteins within 5 min of treatment, highlighting the rapidity with which these crosslinkers work (data not shown). $B\delta_{FLAG}$-expressing cells stimulated with EGF for increasing amounts of time and then treated with DTME displayed enhanced $B\delta_{FLAG}$-Raf1 interactions (data not shown); however, the trends in binding between Bδ-FLAG and Raf1 did not overtly differ from the data generated in the absence of crosslinker (Fig. 25).

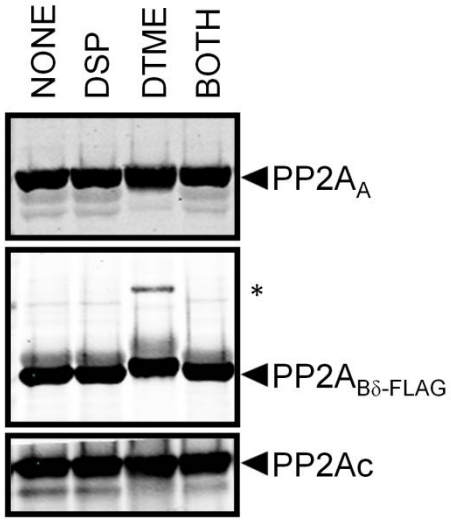

Figure 32. DTME does not disrupt heterotrimeric Bδ-FLAG-containing holoenzymes *in vitro*.

FLAG resin-bound ABδ_{FLAG}C complexes were treated *in vitro* with buffer only (*NONE*) or crosslinker (1.0 mM DSP, 0.5 mM DTME, or 1.0 mM DSP and 0.5 mM DTME (*BOTH*)) for 30 min at 25^{o}C with agitation. Bound proteins were washed and then eluted with SDS sample buffer. Samples were analyzed by Western using antibodies recognizing PP2A$_A$, the FLAG epitope (*Bδ-FLAG*), or PP2A$_C$ (n = 2). *, DSP crosslinked Bδ-FLAG.

Proteomic analysis of ReCLIP'd samples

To identify novel ABδC and Raf1 interacting proteins that could be important in regulating PP2A•Raf1 complexes, we performed proteomic analyses on samples isolated from cells treated with crosslinker. The reversible nature of the thiol bond within DSP and DTME allowed us to selectively release crosslinked binding partners and discard the beads, conjugated antibody, and antibody bound Bδ-FLAG itself. FLAG immune complexes from control and $B\delta_{FLAG}$-expressing cells treated with crosslinker (DSP, DTME, and DSP plus DTME) were incubated with 50 mM DTT to release crosslinked proteins. An aliquot of each eluate was subjected to SDS-PAGE followed by Colloidal Blue staining, which revealed several potential Bδ-FLAG binding partners (Fig. 33). The remainder of the eluates were submitted for analysis by the Proteomics Core of the Mass Spectrometry Research Center at Vanderbilt University. A high number of peptides matching the PP2A Aα, Aβ, Cα, and Bδ subunits were identified in the DTT eluates from Bδ-FLAG immune complexes (Table 1). After taking into account peptides identified in the DTT eluates from control immune complexes, we identified 76 proteins that were crosslinked to Bδ-FLAG: 26 proteins identified with DSP, 52 with DTME, and 43 with DSP plus DTME (Fig. 34). A short list of putative Bδ-FLAG binding proteins, including some that were unique to each crosslinker treatment group, is shown in Table 1; a full list of putative binding proteins can be obtained from Dr. Brian Wadzinski at Vanderbilt University.

Since peptides corresponding to Raf1 were not identified in the previous screen, a second set of proteomic samples was generated using only DTME as the crosslinker, which drastically enhanced the association of Bδ-FLAG with Raf1 (Fig. 30). Three sets

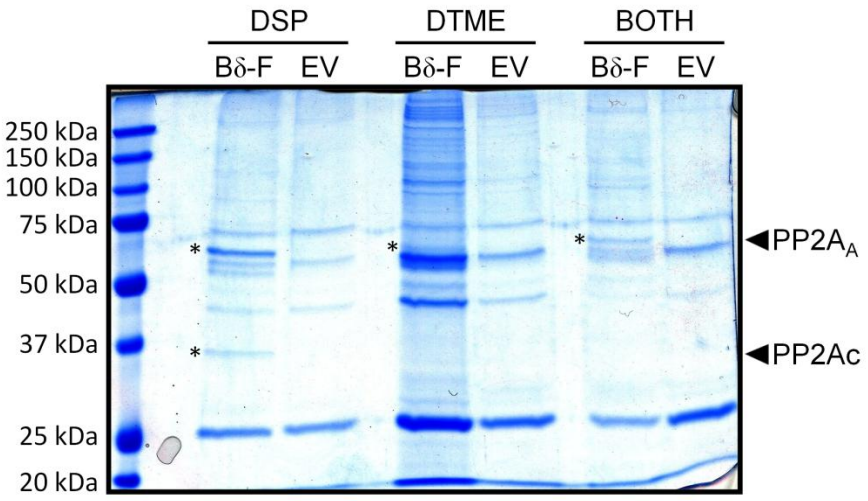

Figure 33. Colloidal Blue analysis of DTT-eluted FLAG immune complexes isolated from crosslinker treated Bδ-FLAG cells.

Bδ-FLAG (*Bδ-F*) and control (*EV*) cells were incubated with tetracycline for 36-48 h and then treated with crosslinker (1.0 mM DSP, 0.5 mM DTME, or 1.0 mM DSP and 0.5 mM DTME (*BOTH*)). Solubilized extracts were incubated with anti-FLAG resin and bound proteins were washed with lysis buffer prior to elution with 25 µl lysis buffer containing 50 mM DTT. Samples were run on SDS-polyacrylamide gels and stained with Collodial Blue. *, denotes bands predicted to be PP2A$_A$ and PP2A$_C$.

Table 1. Abbreviated list of Bδ-FLAG binding partners identified using ReCLIP and mass spectrometry.
ReCLIP experiments performed with 1.0 mM DSP, 0.5 mM DTME, or 1.0 mM DSP and 0.5 mM DTME (*BOTH*) from tetracycline treated Bδ-FLAG and control (*EV*) cells. Only peptide matches with a confidence ≥ 95% were considered.

Gene Name	Protein	% Coverage	Bδ-FLAG				EV			
			Total Peptides	DSP	DTME	BOTH	Total Peptides	DSP	DTME	BOTH
PPP2R1A	PP2A/Aα	45	58	31	8	19	3	2	0	1
PPP2R1B	PP2A/Aβ	25	18	12	1	5	0	0	0	0
PPP2CA	PP2A/Cα	34	14	10	2	2	0	0	0	0
PPP2R2D	PP2A/Bδ	19	18	8	6	4	0	0	0	0
YWHAQ	14-3-3 θ	10	4	1	1	3	0	0	0	0
YWHAH	14-3-3 η	10	2	0	1	1	0	0	0	0
YWHAG	14-3-3 γ	10	2	0	1	1	0	0	0	0
PFN1	Profilin	29	6	1	4	1	0	0	0	0
CKB	Creatine kinase B-type	14	4	2	1	1	0	0	0	0
HNRNPA2B1	Heterogeneous nuclear ribonucleoproteins A2/B1	6	3	3	0	0	0	0	0	0
SKA1	Spindle and kinetochore-associated protein 1	10	2	0	2	0	0	0	0	0
PCBP2	Poly(rC)-binding protein 2	10	2	0	0	2	0	0	0	0
EIF4A1	Eukaryotic translation initiation factor 4A-1	6	4	0	3	1	0	0	0	0
CCT2	T-complex protein 1 subunit beta	13	6	1	2	3	0	0	0	0

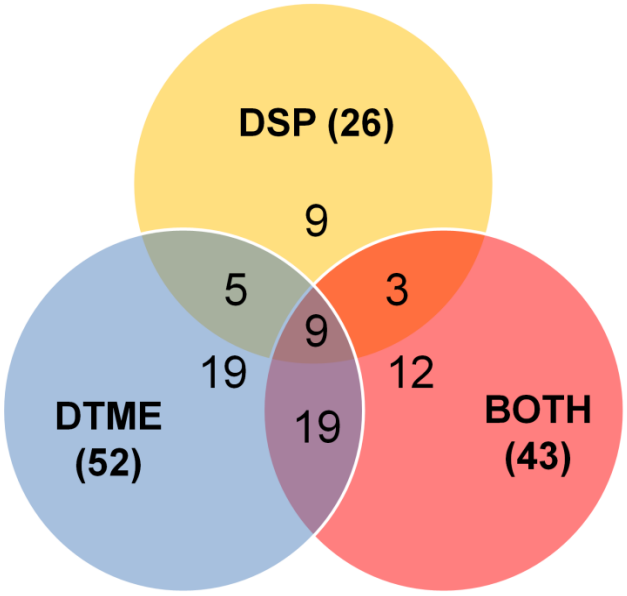

Figure 34. Chemical crosslinkers generate overlapping, but distinct Bδ-FLAG interactomes.

Venn-diagram depicting the intersections of putative Bδ-FLAG-interacting proteins isolated using the indicated chemical crosslinking reagents. Numbers represent candidate proteins remaining after accounting for peptides identified in ReCLIP samples from control cells. The total number of candidate proteins identified with each chemical crosslinker is denoted parenthetically (n = 1).

of samples were generated: i) FLAG immune complexes from Bδ-FLAG and empty vector stable cells, ii) Raf1 and control IgG immune complexes from Bδ-FLAG cells, and iii) tandem affinity-purified (TAP) complexes from Bδ-FLAG and empty vector stable cells. FLAG and Raf1 immunoprecipitations were performed in succession to obtain TAP complexes, as evidenced by the detection of Bδ-FLAG, $PP2A_C$, and Raf1 following each purification step (Fig. 35). Western analysis of non-reduced and reduced extracts showed a loss of both Raf1 and Bδ-FLAG signal (Nonreduced) that could be regained in the presence of DTT (Reduced), demonstrating the functionality of the crosslinker. Proteomic analysis identified 229 putative Bδ-FLAG binding proteins, 222 putative Raf1 binding proteins, and 57 putative interacting partners for the ABδC•Raf1 complex. After accounting for the 159 proteins common to both Bδ-FLAG and Raf1 samples, there were 70 binding proteins unique to Bδ-FLAG and 63 binding proteins unique to Raf1. An abbreviated list of these proteins highlights the presence of various phosphatases (e.g., PP2A subunits, PP1 subunits, Cdc37), chaperonins (e.g., HSP90, HSP70), kinases (e.g., CDK4), and cytoskeletal elements (e.g., vimentin, alpha-actinin-1) (Table 2). Heterogeneous nuclear ribonucleoprotein A2 (HNRNPA2) was identified in both proteomic analyses as a $B\delta_{FLAG}$- and Raf1-interacting protein, has been previously shown to associate with PP2A and inhibit phosphatase activity (239). Notable proteins identified in the TAP complex include PP1γ, IQGAP1, vimentin, Pin1, STRAP, and eIF4A. Interested researchers may contact Dr. Brian Wadzinski at Vanderbilt University for a full list of the proteins identified in this screen.

We employed STRAP (Software Tool for Researching Annotations of Proteins) to classify the proteins by biological process gene ontology terms (240). Bδ-FLAG and

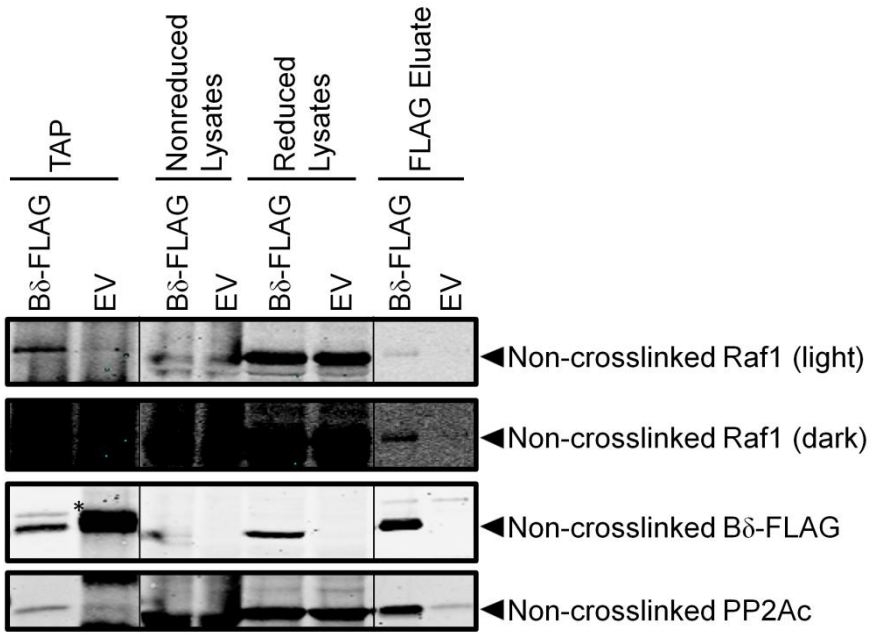

Figure 35. Tandem affinity purification (TAP) of ABδC•Raf1 complexes.
Bδ-FLAG (*Bδ-F*) and control (*EV*) cells were cultured with tetracycline for 36-48 h and then treated with 0.5 mM DTME. Clarified cell extracts were incubated with FLAG resin for 4 h 4^{o}C with rotation. Bound proteins were washed, eluted with excess FLAG peptide, and subsequently incubated with anti-Raf1 antibodies overnight. Raf1 immune complexes were captured with Protein G sepharose, washed, and eluted with SDS sample buffer. Western analysis of the TAP complex, FLAG peptide eluted material, and lysates prepared under Nonreducing and Reducing conditions were analyzed by Western using antibodies recognizing Raf1, the FLAG epitope (*Bδ-FLAG*), and PP2A$_C$ (n = 2). *, denotes a non-specific band.

Table 2. Abbreviated list of Bδ-FLAG, Raf1, and ABδC•Raf1 binding partners identified using ReCLIP and mass spectrometry.
ReCLIP experiments performed with 0.5 mM DTME-treated Bδ-FLAG and control (*EV*) cells. Putative $B\delta_{FLAG}$-interacting proteins were isolated from FLAG immune complexes from Bδ-FLAG and EV cells. Putative Raf1-interacting proteins were purified from Raf1 and control IgG immunoprecipitations from Bδ-FLAG cells. Candidate ABδC•Raf1-interacting proteins were isolated by tandem affinity purification (*TAP*) from Bδ-FLAG and EV cells. Numbers represent the peptides counts for the listed proteins. Only peptide matches with a confidence ≥ 95% were considered.

Gene Name	Protein	Bδ-FLAG	EV	Bδ-FLAG	Bδ-FLAG	Bδ-FLAG	EV
		FLAG	FLAG	Raf1	IgG	TAP	TAP
PPP2R1A	PP2A/Aα	24	1	3	2	0	0
PPP2R1B	PP2A/Aβ	10	0	0	0	0	0
PPP2R2A	PP2A/Bα	9	1	2	0	0	1
PPP2R2D	PP2A/Bδ	8	0	0	1	0	1
PPP1CC	PP1γ	2	0	2	0	1	0
PPP1R9B	Neurabin	0	0	5	0	0	0
STIP1	Stress-induced phosphoprotein 1	8	0	3	0	0	0
CDC37	Cell division cycle 37	3	0	1	0	0	0
HSP90AA	HSP90α	15	0	13	0	0	0
HSP90AB	HSP90β	25	0	19	0	4	0
HSPA1A	HSP70 1A	28	1	29	1	2	0
HSPA8	HSP70 type 8	22	0	13	0	1	0
IQGAP1	IQ motif containing GTPase activating protein 1	0	0	9	0	5	0
VIM	Vimentin	0	0	19	0	4	0
PIN1	Pin1	3	1	2	0	1	0
YWHAE	14-3-3 ε	11	0	11	0	0	0
CDK4	Cyclin-dependent kinase 4	1	0	2	0	0	0
ACTN1	α-actinin-1	0	0	47	0	0	0
RBM10	RNA-binding protein 10	12	0	0	0	0	0
STRAP	Serine/threonine kinase receptor-associated protein	6	0	4	1	0	0
eIF4A	Eukaryotic translation initiation factor 4A	8	1	7	0	5	0
HNRNPA2B1	Heterogeneous nuclear ribonucleoproteins A2/B1	3	1	8	0	0	0

Raf1 interacting partners could be classified in distinct, but largely overlapping cellular functions, while ABδC•Raf1 complex-interacting proteins are equally involved in a multitude of biological processes (Fig. 36). We further parsed the TAP complex interacting proteins by cellular compartment gene ontology terms, which revealed that these proteins are primarily localized to the cytoplasm (17%), nucleus (16%), cytoskeleton (12%), and plasma membrane (9%) (Fig. 37). We also utilized DAVID (Database for Annotation, Visualization, and Integrated Discovery) (241) to perform pathway mapping of the TAP-interacting proteins across several databases (i.e, Reactome, PANTHER, KEGG) and found several pathways enriched in the data, including (Benjamini corrected enrichment score indicated in parenthesis): regulation of actin cytoskeleton (5.00E-02), 3'-UTR-mediated translational regulation (1.10E-03), ribosome (1.20E-03), and metabolism of proteins (1.90E-05).

Our initial studies examining the association of different PP2A holoenzymes (i.e., $AB\delta_{FLAG}C$, $AB\alpha_{FLAG}C$, $AB'\beta_{FLAG}C$) with Raf1 demonstrated that more Raf1 co-purified with $AB\delta_{FLAG}C$ than with the other PP2A holoenzymes (data not shown). Therefore, we focused our analysis on the $AB\delta_{FLAG}C$•Raf1 complex and its possible regulation by EGF. However, these initial studies led to the serendipitous identification of an $AB'\beta_{FLAG}C$-Raf1 interaction following cell treatment with crosslinking reagents. Empty vector, Bδ-FLAG, Bα-FLAG, and FLAG-B′β cell lines were treated with nothing, vehicle (i.e., DMSO), or DTME and then solubilized in Buffer B or RIPA. Analysis of FLAG immune complexes isolated from extracts of untreated cells solubilized in Buffer B revealed that more endogenous Raf1 co-precipitated with Bδ-FLAG than with Bα-FLAG, and much less Raf1 associated with FLAG-B′β (~1/3 of that seen in Bδ-FLAG) (Fig. 38). Although

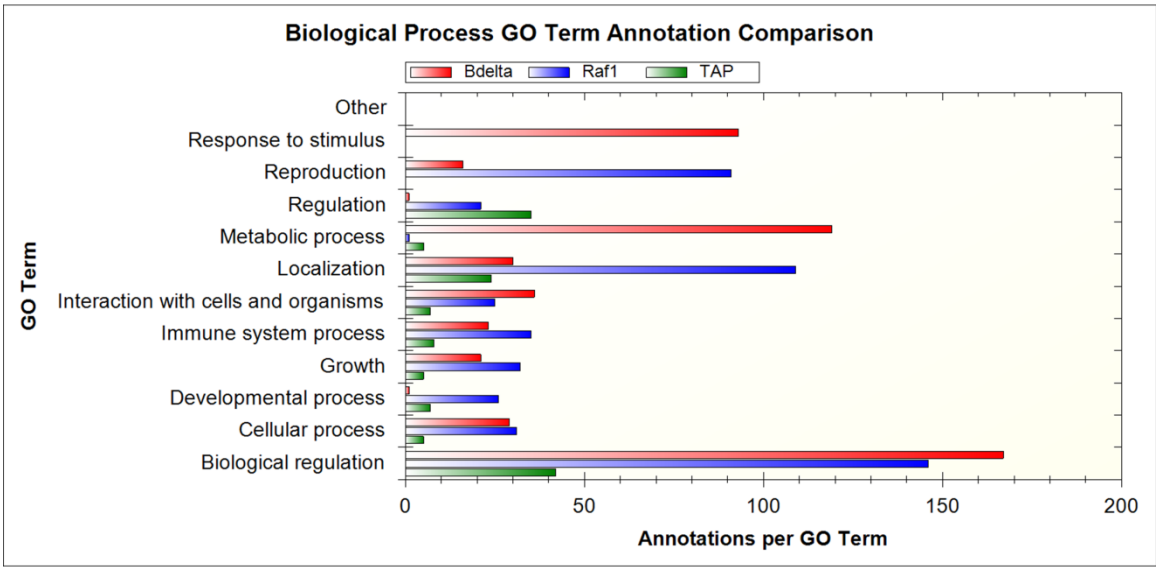

Figure 36. Biological Process Gene Ontology (GO) annotation analysis of candidate Bδ-FLAG, Raf1, and ABδC•Raf1 binding partners.

Bar graph showing the Biological Process GO annotation analysis performed with STRAP and the list of biological process gene ontology (GO) terms. GO terms associated with Bδ-FLAG, Raf1, and ABδC•Raf1 (*TAP*) binding partners identified using ReCLIP and mass spectrometry are represented by red, blue, and green bars, respectively, where the length of the bars is proportional to the number of genes in the term.

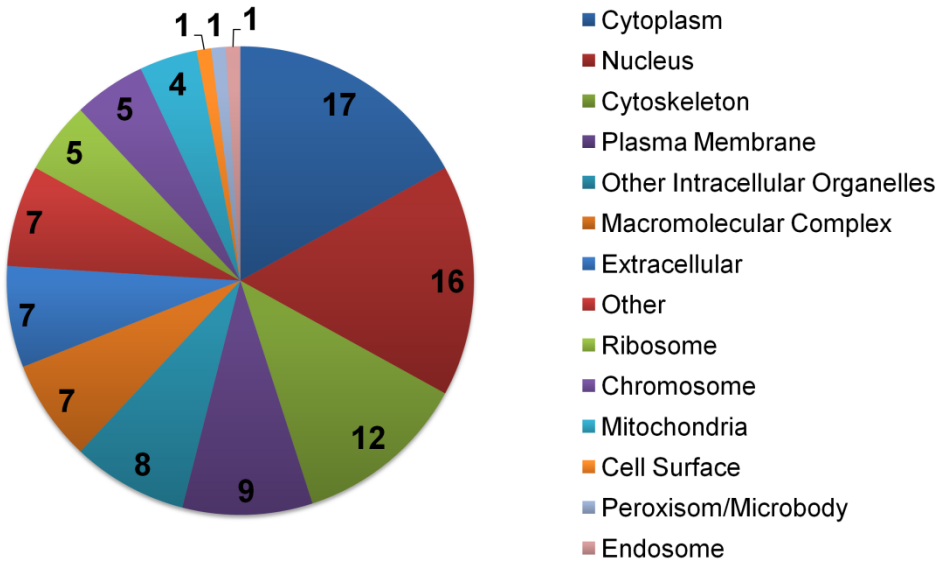

Figure 37. Cellular Component Gene Ontology (GO) annotation analysis of candidate ABδC•Raf1 binding partners.

Pie chart showing the Cellular Component GO annotation analysis performed with STRAP and list of cellular component gene ontology (GO) terms. Each ABδC•Raf1 (*TAP*) binding partner can have multiple cellular component GO terms associated with it. The proportion of each term represented by all putative interacting proteins is shown.

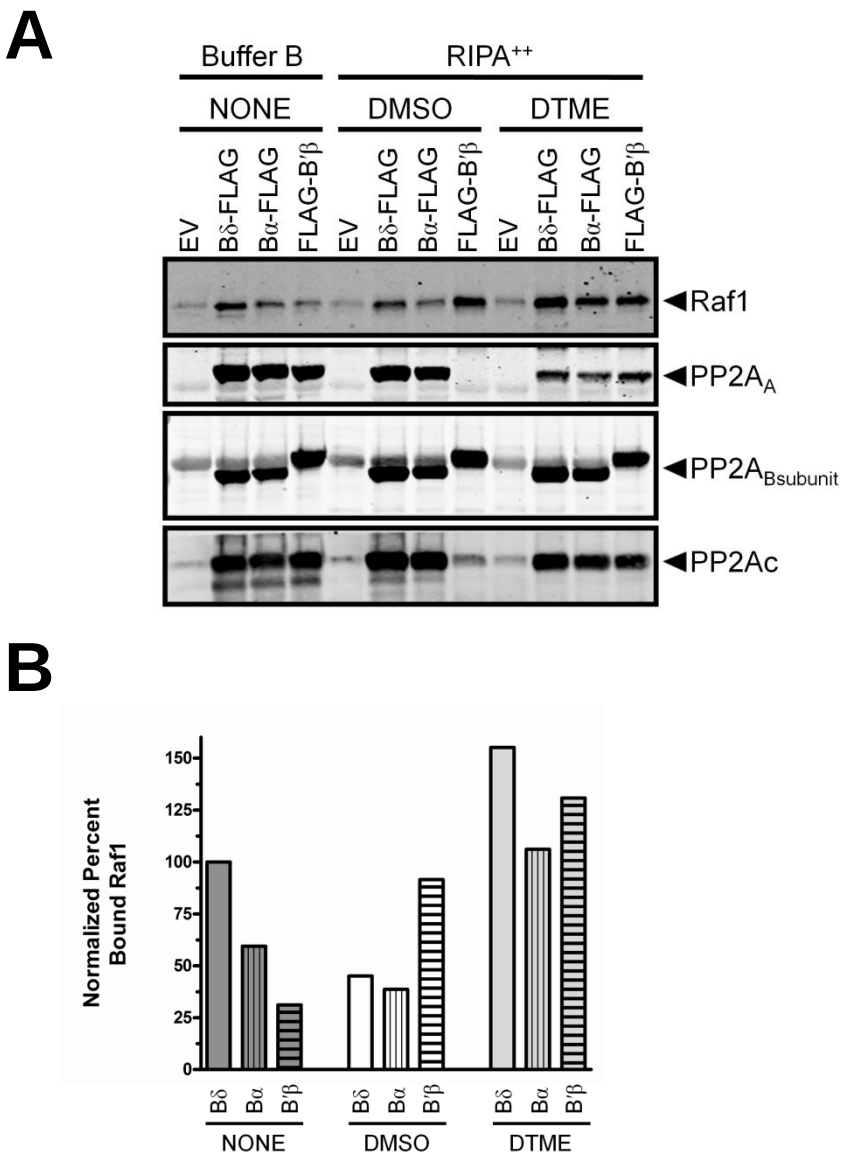

Figure 38. AB′βC interacts with Raf1.

A, Control (*EV*), Bδ-FLAG, Bα-FLAG, and FLAG-B′β cells were treated with tetracycline for 36-48 h and then solubilized without treatment (*NONE*) using a low stringency buffer (*Buffer B*) or following incubation with solutions lacking (*DMSO*) or containing 0.5 mM DTME with subsequent solubilization in a high stringency buffer (*RIPA*$^{++}$). Extracts were incubated with FLAG resin and bound proteins were washed prior to elution with SDS sample buffer. Samples were analyzed by Western using antibodies recognizing Raf1, $PP2A_A$, the FLAG epitope, and $PP2A_C$ (n = 2). ***B***, Quantification of the immunoblot in *A* for FLAG resin bound Raf1 normalized to FLAG-Bsubunit levels and compared to FLAG immune complexes from untreated Bδ-FLAG cells (*NONE*), which were set to 100.

RIPA solubilization of cells reduced the association of Raf1 with Bδ-FLAG and Bα-FLAG in the absence of any crosslinker (i.e., DMSO treated cells), we saw a surprising increase in the association of Raf1 with FLAG-B′β. DTME treatment enhanced the binding of endogenous Raf1 to all three regulatory B subunits and stabilized the interaction of the PP2A core dimer with FLAG-B′β in the presence of RIPA. These data not only confirmed the binding of $AB\delta_{FLAG}C$ and $AB\alpha_{FLAG}C$ to Raf1 but also revealed that Raf1 can associate with $AB'\beta_{FLAG}C$ holoenzymes. It is unclear what role $AB'\beta_{FLAG}C$ plays in modulating Raf1 function; previous studies from our laboratory have demonstrated that it does not regulate the phospho-state of Ser259 *in vitro* (137).

Discussion

Raf1 is critical in relaying upstream receptor-mediated signaling events to downstream MAPKs involved in cell growth, proliferation, and differentiation. Given that dysregulated MAPK signaling gives rise to a number of developmental disorders, collectively termed RASopathies, and has an oncogenic role in many tumor types, understanding the molecular mechanisms that regulate Raf1 function can provide insight into potential therapeutic modalities (242,243). The complex series of steps leading to Raf1 activation requires i) PP2A-mediated dephosphorylation of the inhibitory phospho-Ser259 site, ii) recruitment to the plasma membrane, and iii) interaction with RAS. The coordinated mechanism(s) by which RAS and PP2A displace 14-3-3 to allow dephosphorylation of phospho-Ser259 has not been well delineated (136,147,226). To better characterize the signaling events that affect PP2A-mediated regulation of Raf1, we monitored changes in $AB\delta_{FLAG}C$-Raf1 interactions following activation of the RAS-RAF-MEK-ERK pathway. Although it was evident that overexpression of Bδ-FLAG

enhanced downstream ERK signaling in response to EGF, we observed only subtle changes in the association of $AB\delta_{FLAG}C$ and Raf1 following cell stimulation with EGF (Figs. 24 and 25). Previous studies have demonstrated that amplification occurs in the RAS-RAF-MEK-ERK pathway. For example, PDGF stimulation of Swiss 3T3 cells activated 8% of the pool of MEK protein, which in turn fully activated 48% of ERK2 (244). Thus, incremental changes in Raf1 binding to PP2A could promote large changes in ERK activation. Likewise, we observed small increases in Raf1 activity in the presence of overexpressed Bδ-FLAG and limited formation of $AB\delta_{FLAG}C$•Raf1 complexes in the presence of constitutively active MEK (data not shown). However, the relatively small changes and variability seen in these experiments indicated to us that the immunoprecipitation approach lacked the sensitivity to capture dynamic changes in $AB\delta_{FLAG}C$-Raf1 interactions.

We attempted to trap potential transient changes in $AB\delta_{FLAG}C$-Raf1 interactions in response to EGF stimulation using DSP and DTME, two crosslinkers that have been successfully used to study transient protein-protein interactions (Fig. 26) (238). Properties inherent to each crosslinker (e.g., spacer arm length, presence of homo- or hetero-bifunctional reactive groups, and type of crosslinking target) and protein (e.g., surface accessibility of crosslinker targeted residues and location of crosslinking targets within a protein or between proteins) not only affects the ability of any one protein to be crosslinked, but also impacts whether particular protein-protein interactions are stabilized or destabilized (Fig. 27). Studies examining the susceptibility of PP2A holoenzymes to the thiol-reactive electrophile BMCC (biotinamido-4-[4′-(maleimidomethyl) cyclohexanecarboxamido]butane) demonstrated that treating cells with BMCC results in

the alkylation of all three PP2A subunits (data not shown) (245), thereby confirming that solvent-accessible cysteines in $AB\delta_{FLAG}C$ could be targeted for crosslinking. We performed a series of experiments to empirically determine the optimal conditions needed to crosslink both Raf1 and $AB\delta_{FLAG}C$ with DSP, DTME, or a combination of DSP and DTME and then subsequently analyzed how these crosslinkers alter the $AB\delta_{FLAG}C$-Raf1 interaction (Fig. 29). DSP treatment enhanced the binding of the PP2A core dimer to Bδ-FLAG (Fig. 30). Interestingly, DTME treatment induced a decrease in binding between Bδ-FLAG and the PP2A core dimer, while concomitantly enhancing $B\delta_{FLAG}$-Raf1 interactions (Figs. 30 and 31). The decrease in $PP2A_A$ and $PP2A_C$ subunit binding to Bδ-FLAG was less severe when cells were co-treated with both DSP and DTME, suggesting a balance was achieved between DSP-mediated stabilization and DTME-induced destabilization of the B subunit-core dimer interaction (Fig. 30). Surprisingly, the DTME-dependent loss in AC-$B\delta_{FLAG}$ interactions could not be replicated *in vitro* (Fig. 32). Since a less stringent buffer (Buffer B) was used in the *in vitro* assay washes, one interpretation of the data obtained from treating cells with DTME is that a synergistic DTME/RIPA effect may be responsible for the reduced binding between Bδ-FLAG and the core dimer. Alternatively, an unknown cellular component may work in concert with DTME to disrupt some PP2A holoenzymes, or prevent their formation, in cells. Crosslinker studies seeking to trap EGF-dependent changes in $AB\delta_{FLAG}C$-Raf1 interactions heavily depended upon the timing of stimulus treatment and application of chemical crosslinkers. Although the cell-permeable crosslinkers effectively crosslink a large portion of the Raf1 and Bδ-FLAG proteins within minutes, this may not be rapid enough to trap interactions that are occurring at faster timescales. Furthermore, crosslinking interacting proteins within a

signal transduction pathway could prohibit, as well as promote, further downstream signaling, which could affect the ability of EGF to modulate $AB\delta_{FLAG}C$-Raf1 interactions.

We performed a series of proteomic studies to identify novel $AB\delta_{FLAG}C$ and/or Raf1 interacting proteins that may be involved in regulating PP2A•Raf1 complexes. Treatment of $B\delta_{FLAG}$-expressing cells with reversible crosslinkers not only stabilized different amounts and types of protein-protein interactions but also yielded exceptionally low background in our proteomic data sets (Table 1 and Figs. 33 and 34). In line with our co-immunoprecipitation data, the highest number of peptides belonging to $PP2A_A$ and $PP2A_C$ was in the DSP-treated samples, followed by DSP plus DTME, and then DTME alone (Table 1 and Fig. 30). Although our analysis of these putative $AB\delta_{FLAG}C$ binding proteins did not reveal any obvious candidates that may regulate PP2A•Raf1 complexes, nineteen proteins identified in our initial screen also happened to be identified in a screen for ubiquitinated proteins from MCF-7 cells (246). This finding is in line with a growing body of evidence indicating that phosphorylation and ubiquitination crosstalk to modulate protein function (247), and indicates Bδ-FLAG containing holoenzymes may function to indirectly regulate the ubiquitination of certain proteins. A second proteomic screen of DTME-stabilized $AB\delta_{FLAG}C$ and Raf1 complexes revealed some overlap in the binding partners associating with these proteins (e.g., 14-3-3ε, HSP90α, HNRNPA2B1) (Table 2). Importantly, several proteins were identified in the $AB\delta_{FLAG}C$•Raf1 complex isolated by TAP, including PP1γ, Pin1, vimentin, IQGAP1, and eIF4A (Table 2 and Fig. 35). While a specific isoform of $PP1_C$ has not been implicated in the regulation of phospho-Ser259-Raf1 in cells (226), the Pin1 isomerase has been shown to act in concert with PP2A to

modulate the phosphorylation state of several Raf1 sites and re-prime Raf1 for subsequent signaling events (248). Although not a Raf1-substrate, the intermediate filament protein vimentin identified in our TAP screen can be phosphorylated by Raf1-associated vimentin kinases, such as CK2 (249). Interestingly, the existence of PP2A•CK2 complexes, in conjunction with data showing CK2 regulates RAS-RAF-MEK-ERK signaling, could implicate CK2 in the regulation of Raf1-associated PP2A (141,227). The scaffold IQGAP1 has been shown to bind all three MAPK elements (i.e., BRaf/Raf1, MEK, and ERK) simultaneously to facilitate signaling (250,251) and it is possible that IQGAP1 could play a role in the PP2A-mediated activation of Raf1. First characterized by Dr. Hal Moses's group at Vanderbilt University, serine/threonine kinsase receptor-associated protein (STRAP) was found in our crosslinking assays to associate with both Bδ-FLAG and Raf1 (252). Although STRAP lacks enzymatic activity, it appears to modulate various biological processes via its associations with cellular proteins (253). For example, the association of STRAP with the RNA helicase eukaryotic translation initiation factor 4A (eIF4A) promotes the translation of type 1 collagen mRNAs (254). The identification of eIF4A peptides in both proteomic screens (Tables 1 and 2), as well as our pathway mapping analysis, suggests that PP2A•Raf1 complexes may have a role in modulating STRAP-regulated translation. Raf1 is no stranger to the eIF proteins, as other reports indicate Raf1 dictates the stability of eIF1A by targeting Ser21 for phosphorylation, and association of eIF3A with Raf1 reduces ERK activation (255,256).

CHAPTER IV

SMALL G PROTEINS, RAC1 AND RAS, REGULATE PP5•ERK COMPLEXES INVOLVED IN THE FEEDBACK REGULATION OF RAF1

RAS background and signaling

The first *RAS* gene products (generically named $p21^{src}$) were identified from rodent leukaemia retroviruses in the 1960s (257-259). Designated *RAS* for their ability to form rat sarcomas, the H-*RAS* and K-*RAS* genes were confirmed to be of rat origin and inadvertently incorporated into the genomes of these oncoviruses (260). The relevance of these genes to human health, as well as a third gene termed N-*RAS*, was established following the identification of mutations in *RAS* genes in human tumors (261-264). Excluding the two processed *RAS* pseudogenes, H-*RAS*-2 and K-*RAS*-1, and accounting for the alternative splicing of exon 4 of the K-*RAS*-2 locus, four different isoforms of RAS proteins are expressed within the human proteome (H-Ras, N-Ras, K-Ras4A, K-Ras4B) (265). The RAS subfamily of small G proteins is an important regulator of cellular biology and these four RAS isoforms, which are highly homologous at the primary amino acid level, play significant roles in cellular growth, differentiation, and apoptosis (266,267). Related in structure to the Gα subunit of heterotrimeric G proteins and possessing intrinsic guanosine triphosphate (GTP) hydrolysis (GTPase) activity, RAS proteins function as molecular switches; active when bound to GTP and inactive when bound to GDP. In their conformationally active GTP-bound state, these small GTPases transiently display an effector binding domain that reorients following hydrolysis of GTP

to GDP, resulting in decreased effector protein binding and reduced downstream signaling (268). This GTPase cycle is catalyzed by interactions of RAS proteins with guanine nucleotide exchange factors (GEFs) and GTPase activating proteins (GAPs), but repressed through associations with guanine nucleotide dissociation inhibitors (GDIs) (269).

Despite the high homology, H-Ras, N-Ras, K-Ras4A, and K-Ras4B differ greatly in their C-terminal 23-24 amino acids, termed the hypervariable region (HVR). The HVR contains a CAAX motif (where C stands for cysteine, A for an aliphatic amino acid, and X for any amino acid) subject to a series of posttranslational modifications that are important in the localization of RAS to lipid membranes. Following farnesylation of the cysteine residue, proteolytic cleavage of the -AAX motif allows the new C-terminal prenylcysteine to become carboxymethylated (270). A second signal is necessary to allow RAS to associate with lipid membranes. This includes either palmitoylation of cysteines immediately upstream of the CAAX motif (H-Ras, N-Ras, and K-Ras4A) or the presence of a string of positively-charged lysine residues (K-Ras4B). Mutant RAS proteins with defective membrane targeting sequences accumulate in the membranes of the endoplasmic reticulum (ER) and Golgi, highlighting the important role these posttranslational modifications have in the trafficking of RAS proteins. However, these endomembrane platforms may not simply be pit stops en route to the plasma membrane and may serve as important sites of RAS signaling. Restricting the subcellular localization of activated H-Ras to the ER promotes ERK signaling, but tethering H-Ras to the Golgi induces activation of c-Jun N-terminal Kinase (JNK) (271). Activated K-Ras promotes cellular transformation when it is recruited to the plasma membrane and

apoptosis when localized at mitochondria (272). While the signaling role(s) of RAS on intracellular membranes continues to be elucidated, the majority of RAS signaling is predominately associated with the inner leaflet of the plasma membrane.

Following delivery of the RAS proteins to specific, mutually exclusive plasma membrane microdomains, they are further segregated laterally in response to GTP-loading (273-275). GDP-bound H-Ras resides in microenvironments containing actin and cholesterol but redistributes to actin- and cholesterol-independent regions following GTP-loading, while inactive N-Ras translocates from cholesterol-independent to cholesterol-dependent domains upon GTP-binding. K-Ras appears to localize to cholesterol-independent domains that are enriched in anionic phospholipids and does not appear to laterally segregate following activation. K-Ras associates with a lectin protein, galectin-3, which stabilizes K-Ras binding to the plasma membrane and regulates downstream signaling; an analogous association occurs between galectin-1 and H-Ras (276).

Recent studies have begun to elucidate how nanoscale protein clusters, termed nanoclusters, of EGFRs and RAS proteins contribute to high fidelity MAPK signaling. Approximately 32% of EGFRs are spatially organized as monomers in quiescent cells and the remaining ~67% as higher-ordered oligomers ranging from dimers to hexamers (277). The presence of EGF reduces the number of EGFR monomers to ~17% and modifies the local lipid environment by stimulating phospholipase D2-mediated production of phosphatidic acid (PA). Production of PA subsequently enhances the average radius of EGFR nanoclusters to generate clusters of up to nine oligomers. Likewise, ~40% of GTP-bound K-Ras forms short-lived nanoclusters (~0.4 s) composed

of ~7 RAS-GTP molecules, while ~60% of active RAS randomly distributes as monomers (278,279). Importantly, K-Ras nanoclusters, but not K-Ras monomers, have been shown to recruit ~3.5 Raf1 molecules per nanocluster, leading to the activation of a fixed quantum of ERK molecules per nanocluster (278). Thus, these RAS nanoclusters act as high-fidelity nanoswitches converting growth factor signaling into a graded ERK response that dictates cell fate decisions (280-282).

In addition to activating RAF kinases, several other RAS effector proteins have been described, including the p110 catalytic subunit of the class I phosphoinositide 3-kinases (PI3Ks), RAS-like (Ral) GEFs, phospholipase C-ε (PLCε), T-cell lymphoma invasion and metastasis-1 (TIAM1), RAS interaction/interference protein-1 (RIN1), and the RAS association domain-containing family (RASSF) proteins (283). As noted in Chapter III, the four RAS isoforms exhibit different affinities for each of the RAF kinases, creating diversity and selectivity in RAS signaling to downstream effectors (212,213). Notably, K-Ras has a greater capacity than H-Ras to activate Rac-dependent signaling as well as Raf1-MEK-ERK signaling (284,285). Preferential activation of Raf1 by K-Ras may be explained, in part, by the predilection of Raf1's lipid binding domains for PA (produced by EGFR nanoclusters) and phosphatidylserine (PS)/PIP_2 (enriched in the lipid microdomains to which K-Ras localizes) (198,200,201,286). In fact, fusing the C-terminal membrane targeting domain of K-Ras (i.e., CAAX) to Raf1 (i.e., Raf1-CAAX) generates a plasma membrane bound, active kinase that is completely RAS-independent (287). Therefore, RAS primarily serves to recruit Raf1 to the plasma membrane for further activation and allow downstream signaling to MEK1/2.

ERK background and signaling

Active Raf1 phosphorylates two serines within the activation segment of MEK1/2 (Ser218/Ser222 in MEK1 and Ser222/Ser226 in MEK2) (288,289). Although highly homologous (~85%), the MEK isoforms are not functionally interchangeable during development. MEK2 is approximately 7-fold more active than MEK1 towards ERK1/2 *in vitro*, but MEK2$^{-/-}$ mice exhibit no phenotypic abnormalities (290). In contrast, MEK1$^{-/-}$ mice are embryonic lethal with placental defects, suggesting that MEK1 may have a predominate role in MAPK signaling (291). Normally, MEK1/2 monomers promote downstream ERK activity by phosphorylating both regulatory Thr and Tyr residues in the activation segment of ERK1 (44 kDa) and ERK2 (42 kDa) (Thr202/Tyr204 in ERK1 and Thr185/Tyr187 in ERK2) (292). In addition to existing as monomers, and possibly homodimers, the recent identification of MEK1•MEK2 heterodimers revealed that MEK1 also functions to negatively regulate MEK2-dependent ERK1/2 signaling (291). An alternatively spliced isoform of MEK1, MEK1b (lacking 26 amino acids within the kinase domain), was originally classified as kinase dead because it failed to phosphorylate ERK1/2 (290,293). However, subsequent studies revealed that MEK1b could phosphorylate an ERK1 splice variant termed ERK1c (294,295) (Fig. 39). Thus, the MEK1b-ERK1c signaling cascade is distinct from the prototypical MEK1/2-ERK1/2 cascade. Whereas alternative splicing of ERK1 in primates yields ERK1c (42 kDa), which co-migrates with ERK2, alternative splicing of ERK1 in rodents produces ERK1b (46 kDa), which exhibits distinct signaling kinetics following its activation by MEK1 (296,297).

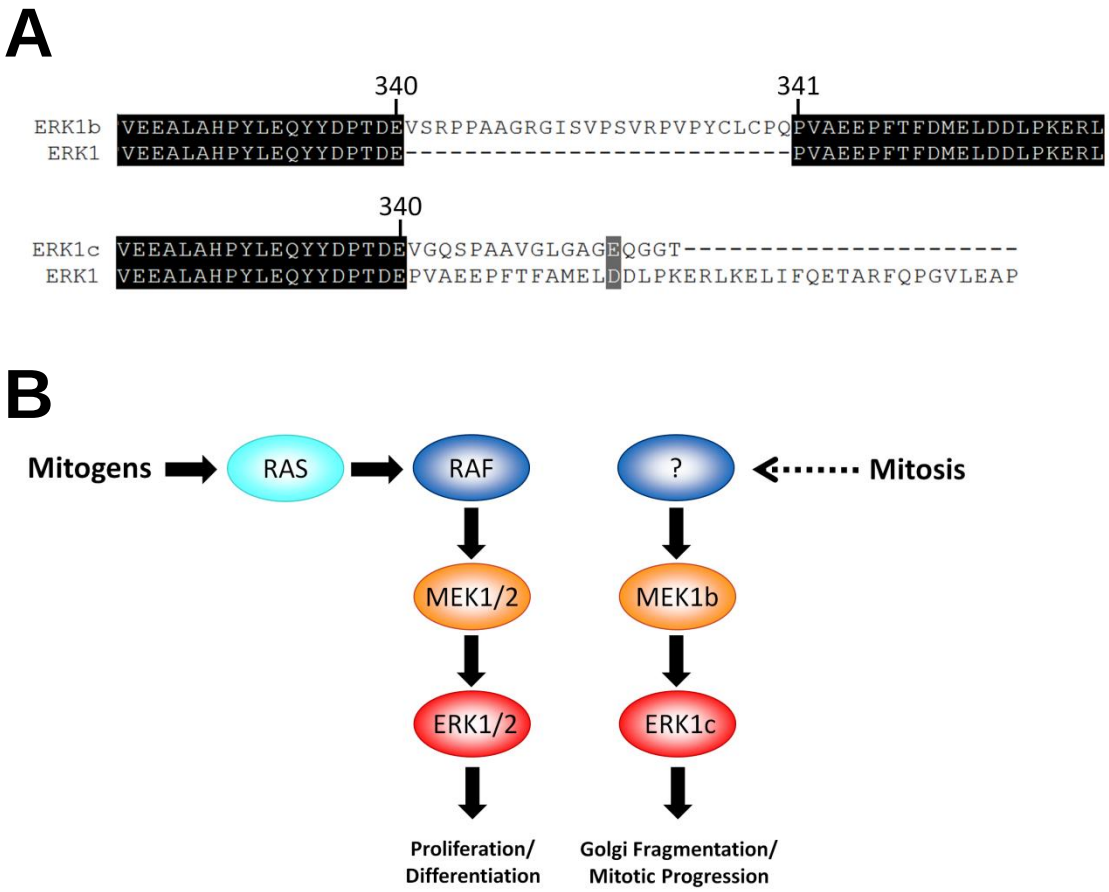

Figure 39. ERK1 splice variants.

A, Sequence alignment of human ERK1 and alternative splice variants of ERK1, rodent ERK1b and primate ERK1c. Rodent ERK1b contains an insert between exon 7 and exon 8 of rodent ERK1. The 78-base pair insertion encodes 26 amino acids that are localized between Glu340 and Pro341 of rodent ERK1. Alternative splicing of primate ERK1 creates a 103-base pair insertion. However, a stop codon within the insert leads to a substitution of the last 40 amino acids of ERK1 with 18 amino acids from the insert, forming a distinct C-terminus in ERK1c. Identical amino acids are shaded black and similar amino acids are shaded grey. The alignment was made at http://www.bioinformatics.org/sms2/pairwise_align_protein.html and shaded at http://www.bioinformatics.org/SMS/multi_align.html. ***B***, The RAS/RAF/MEK/ERK signaling pathway is activated by a number of stimuli, including mitogens, to regulate cellular processes like proliferation and differentiation. In contrast, the MEK1b/ERK1c transduction pathway is activated during mitosis and is responsible for Golgi fragmentation and mitotic progression.

Historically, the cellular functions attributed to ERK1 and ERK2 were initially viewed as redundant because: 1) at the level of their primary amino acid sequences ERK1 and ERK2 share ~83% identity in humans, 2) both ERK1 and ERK2 display parallel activation in response to a variety of stimuli, 3) they share common mechanisms for activation as well as similar kinase activity following activation, and 4) ERK1 and ERK2 exhibit comparable spatiotemporal expression patterns during development (298-300). Although ERK1 and ERK2 do indeed possess many overlapping properties, genetic studies have shown that their functions are not developmentally interchangeable. Notably, $ERK1^{-/-}$ mice are viable with deficits in thymocyte maturation (301), whereas the genetic disruption of ERK2 is lethal. $ERK2^{-/-}$ mice display embryonic lethality before E8.5 due to defects in placental development and mesoderm differentiation (300,302). Therefore, the preferential roles for ERK1 or ERK2 in the regulation of cell differentiation, proliferation, and growth are likely the result of distinct ERK-regulated gene targets and non-overlapping ERK-interacting proteins (302-304). Consistent with this idea, knockdown studies of ERK1/2 in zebrafish revealed uniquely regulated ERK1 and ERK2 genes and demonstrated that select genes are regulated in an anti-correlated manner (i.e., increased expression following ERK1 knockdown but decreased following ERK2 knockdown) (305). Moreover, the identification of proteins that uniquely associate with ERK1 (e.g., $\alpha_v\beta_3$ integrin, MEK Partner 1) or ERK2 (e.g., NIPA, Bmf, Sec16) provides additional support that ERK1 and ERK2 possess distinct functions (306-310).

PP5•Raf1 and other PP5•kinase complexes

A screen for proteins that regulate RAF-MEK-ERK signaling identified PP5 as a candidate Raf1-interacting protein (133). Biochemical analysis of the PP5•Raf1 complex

revealed that PP5 associates with Raf1 and inhibits kinase activity by dephosphorylating phospho-Ser338, without affecting levels of Raf1 phosphorylation at Ser259, Thr491, Ser494, or Ser621 (133) (Fig. 40). Additionally, mutation of a single PP5 residue important in promoting contact with HSP90 (i.e., Lys97) abolished binding to both HSP90 and Raf1, indicating that association of PP5 with Raf1 is mediated via HSP90. Interestingly, PP5 is known to associate with several protein kinases besides Raf1, including: ASK1, ATM, ATR/Chk1, DNA-PKcs, eIF2α kinase, and IKKβ (123-127,131,133,134). The role of PP5 in the regulation of these kinases is unclear, and in some instances controversial. Many protein kinases that associate with PP5 are HSP90 clients (311) and it has been proposed that PP5 may affect kinase function indirectly via its interactions with HSP90, possibly via modulating the chaperone function of HSP90 that then alters the maturation and activity of the associated client kinase (134,312,313). Conversely, given that HSP90 binding enhances PP5-mediated dephosphorylation of the co-chaperone Cdc37, PP5 could alter kinase function by regulating the phospho-state of the associated kinase (312).

Studies by our group and others previously established the existence of PP5•Raf1 and PP2A•Raf1 complexes in cells (133,137). Therefore, we explored the possibility that these two phosphatases associate with Raf1 to form a trimeric signaling complex. Data presented in this chapter indicate that both PSTPs can interact with Raf1 concurrently to form a multiprotein PP5•Raf1•ABαC complex. I also demonstrate that several protein kinases, including ERK1/1b/1c/2, form stable complexes with PP5 and that these PP5-kinase interactions are facilitated, in part, via HSP90. Further analyses of the PP5•ERK1 and PP5•ERK2 complexes reveal that the assembly of these complexes in unstimulated

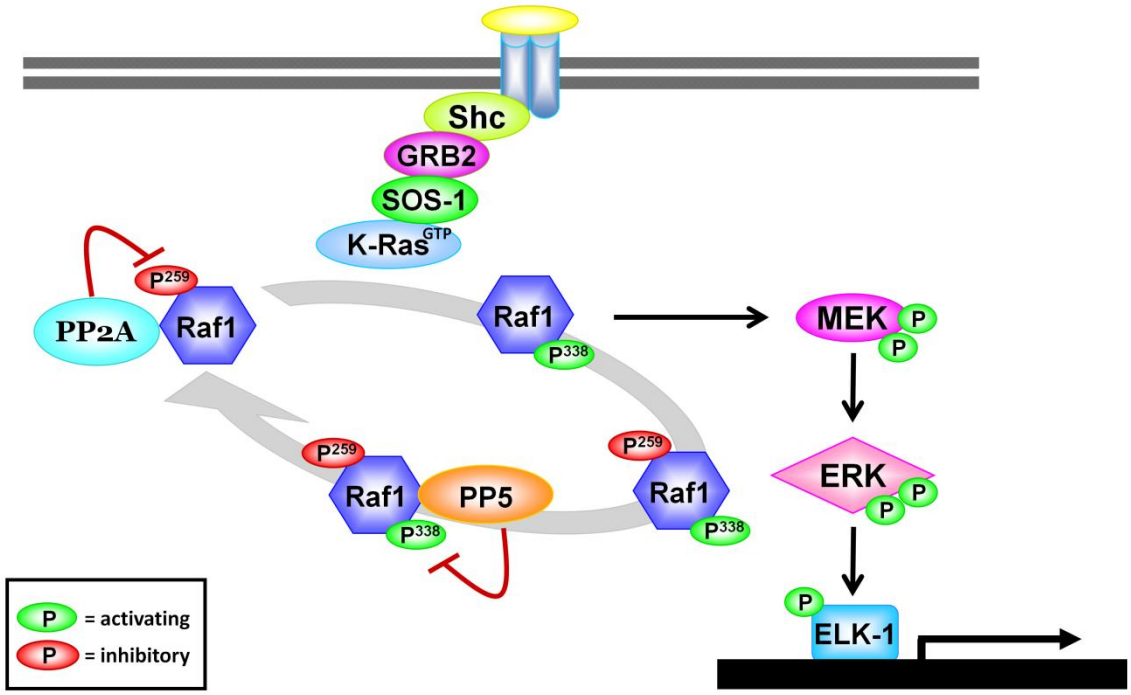

Figure 40. Raf1 signaling is positively regulated by PP2A and negatively regulated by PP5.

Growth factor signaling stimulates changes in Raf1 phosphorylation. Under unstimulating conditions, Raf1 is basally phosphorylated at several inhibitory sites, including phospho-Ser259 (P^{259}). Following stimulation, the dephosphorylation of P^{259} by PP2A precedes increases in phosphorylation at activating residues required for kinase activation, including phospho-Ser338 (P^{338}) (335). The dephosphorylation of P^{259} is transient and increases in P^{259} are followed by dephosphorylation of P^{338} by PP5, which suppresses Raf1 activity. Whereas PP2A activates Raf1 signaling by dephosphorylating an inhibitory site (i.e., P^{259}), PP5 inhibits Raf1 signaling by dephosphorylating an activating residue (i.e., P^{338}).

cells is independent of both phosphatase and kinase activity. However, the PP5-ERK interactions are regulated by constitutively active variants of the small G proteins Rac1 and RAS. Whereas $Rac1^{L61}$ enhances the assembly of both PP5•ERK1 and PP5•ERK2 complexes, oncogenic $HRas^{V12}$ and $KRas^{L61}$ decreases PP5-ERK2 interactions, without affecting PP5-ERK1 interactions. The selective alteration in PP5-ERK2 binding induced by $HRas^{V12}$ is independent of both MEK and PP5 activity, but paradoxically requires ERK2 kinase activity. Our studies also support a novel role for PP5•ERK complexes in regulating the feedback phosphorylation of Raf1 at Ser289, Ser296, and/or Ser301 (151).

Materials and Methods

Plasmids, antibodies, and other reagents

FLAG-K97A-PP5/pcDNA3 (FLAG-$PP5^{HBD}$) and FLAG-H304Q-PP5/pcDNA3 (FLAG-$PP5^{PD}$) were generated using the QuikChange site-directed mutagenesis kit (Stratagene; La Jolla, CA), mismatched primers (Integrated DNA Technologies; Coralville, IA), and wildtype FLAG-PP5/pcDNA3 (FLAG-$PP5^{WT}$) as the template (a gift from Dr. Hidenori Ichijo; Tokyo Medical and Dental University, Bunkyo-ku, Tokyo). HA-ERK1/pCEP4 was a gift from Dr. Melanie Cobb (University of Texas Southwestern Medical Center; Dallas, TX). Wildtype HA-ERK1/pcDNA3 (HA-$ERK1^{WT}$) was generated by excising the HA-ERK1 insert from HA-ERK1/pCEP4 with NotI and subsequent ligation into NotI-digested pcDNA3. HA-K71R-ERK1/pcDNA3 (HA-$ERK1^{KD}$) was generated by site-directed mutagenesis of HA-ERK1/pCEP4 followed by excision with NotI and subsequent ligation of the HA-K71R-ERK1 insert into NotI-digested pcDNA3. HA-K52R-ERK2/pcDNA3 (HA-$ERK2^{KD}$) was generated by site-

directed mutagenesis of wildtype HA-ERK2/pcDNA3 (HA-ERK2^{WT}) (a gift from Dr. Vsevolod Gurevich; Vanderbilt University, Nashville, TN). Dr. Melanie Cobb provided G12V-HaRas/pRc/CMV (HRas^{V12}), which was mutated to generate wildtype HaRas/pRc/CMV (HRas^{WT}). Wildtype HA-KRas4B/pEF hybrid (HA-KRas^{WT}) (a gift from Dr. Richard Marais; The Institute of Cancer Research, London, England) was used as a template to create HA-G12V-KRas4B/pEF hybrid (HA-KRas^{V12}) and HA-Q61L-KRas4B/pEF hybrid (HA-KRas^{L61}) by site-directed mutagenesis. HA-ERK1b/pcDNA3 and HA-ERK1c/pcDNA3 were from Dr. Rony Seger (The Weizmann Institute of Science; Rehovot, Israel), while Q61L-Rac1/pcDNA IIIB (Rac1^{L61}) and Myc-T17N-Rac1/pcDNA3.1 (Myc-Rac^{N17}) were from Dr. Ann Richmond (Vanderbilt University; Nashville, TN). HA$_3$-IKK1/pRcBactin and Src^{Y529F}/pRc/CMV were from Drs. Dean Ballard and Steve Hanks (Vanderbilt University; Nashville, TN), respectively. Strep-HA-MST2/pcDNA5/FRT/TO/SH/GW was from Dr. John Kyriakis (Tufts Medical Center; Boston, MA). The construction of HA-CaMKIV/pCMV-HA was previously described (150). Drs. Joseph Avruch and John Blenis (Harvard Medical School; Boston, MA) provided Myc-Raf1/pMT2 and HA-p70S6K/pRK7, respectively. GST-Bα/pGEMX-T2 was a kind gift from Dr. Verle Janssens (KU Leuven; Leuven, Belgium). Proper construction of all plasmids was verified by automated DNA sequencing (Vanderbilt University VANTAGE Sequencing Core).

The mouse anti-FLAG M2 antibody, rabbit anti-FLAG antibody, mouse anti-FLAG M2 affinity gel and FLAG peptide were from Sigma-Aldrich (St. Louis, MO). The rat IgG1 anti-HA (Clone 3F10) antibody and rat anti-HA (Clone 3F10) affinity matrix were from Roche Diagnostics (Indianapolis, IN). Protein G-Sepharose 4B conjugate was

from Invitrogen (Carlsbad, CA). Anti-Myc Tag (Clone 4A6) agarose conjugate and microcystin-agarose was from EMD Millipore Corporation (Billerica, MA). The mouse anti-HSP90α/β (F-8), goat anti-ERK1 (C-16-G), goat anti-ERK2 (C-14-G), rabbit anti-ERK2 (K-23), normal rabbit IgG, normal goat IgG, and rabbit anti-Rac1 (C-11) antibodies were from Santa Cruz Biotechnology, Inc. (Santa Cruz, CA). The mouse anti-Myc, rabbit anti-RAS (3965), rabbit anti-phospho-p44/42 MAPK (ERK1/2; pThr202/pTyr204), rabbit anti-phospho-Raf1 (pSer289/pSer296/pSer301), and rabbit anti-phospho-Raf1 (pSer338) (56A6) antibodies were from Cell Signaling Technology, Inc. (Danvers, MA). The mouse anti-PP5 and mouse anti-Raf1 antibodies were from BD Biosciences (San Jose, CA). The rabbit anti-PP5 antibody was from Bethyl Laboratories, Inc. (Montgomery, TX). The Alexa Fluor 680 conjugated goat anti-mouse IgG, donkey anti-goat IgG, and goat anti-rat IgG secondary antibodies were from Molecular Probes (Eugene, OR). The donkey anti-rabbit IRDye 800CW secondary antibody was from LI-COR (Lincoln, NE).

The MEK1/2 inhibitor U0126 was from Cell Signaling Technology, Inc. (Danvers, MA). Epidermal growth factor (EGF) and phorbol 12-myristate 13-acetate (PMA) were from Invitrogen (Carlsbad, CA) and Sigma-Aldrich (St. Louis, MO), respectively. The phosphatase substrate, DiFMUP, was from Molecular Probes (Eugene, OR). Odyssey Blocking Buffer was from LI-COR (Lincoln, NE). TransIT-293 transfection reagent was from Mirus (Madison,WI) and X-tremeGENE 9 DNA transfection reagent was from Roche Diagnostics (Indianapolis, IN). Bio-Safe Coomassie G-250 Stain was from Bio-Rad Laboratories, Inc. (Hercules, CA). Arachidonic acid was

from Nu-Chek Prep, Inc. (Elysian, MN). All other reagents were purchased from Sigma-Aldrich (St. Louis, MO) or Thermo Fisher Scientific Inc. (Lafayette, CO).

Cell culture, transfection, and treatments

HEK-293FT cells were maintained at 37^{o}C and 5% CO_2 in DMEM supplemented with 10% fetal calf serum. Cells (6-well plates) were transfected with the indicated plasmids using the Mirus TransIT-293 transfection reagent (2.5 µl:1 µg ratio of reagent to DNA) according to the manufacturer's protocol unless otherwise noted. For the PP5•Raf1•ABαC complex experiments, a plasmid ratio of 1:2:2 (kinase:phosphatase:phosphatase) was used. For co-transfections, 350 ng of wildtype FLAG-PP5 or FLAG-PP5^{HBD} were combined with the following amounts of each kinase construct: 350 ng of HA-p70S6K, HA-CaMKIV, and HA-ERK2; 500 ng of HA_3-IKK1; 900 ng of Src^{Y529F}; 1200 ng of Myc-Raf1 and HA-MST2. The appropriate amount of pcDNA3 was added to ensure equivalent amounts of DNA were transfected within each group. For the reciprocal immunoprecipitation experiments (anti-FLAG and anti-HA), cells (6-cm plates) were transfected with 500 ng of wildtype FLAG-PP5 or FLAG-PP5^{HBD}, 500 ng of wildtype HA-ERK1 or HA-ERK2, and pcDNA3, as needed, to equalize the amount of DNA. For all the other FLAG immunoprecipitation experiments, cells (6-well plates) were transfected with the following constructs: 350 ng each of wildtype FLAG-PP5, FLAG-PP5^{HBD}, FLAG-PP5^{PD}, wildtype HA-ERK1, HA-ERK1^{KD}, HA-ERK1b, HA-ERK1c, wildtype HA-ERK2, or HA-ERK2^{KD}; 200 ng each of wildtype HRas, HRas^{V12}, wildtype HA-KRas, HA-KRas^{V12}, or HA-KRas^{L61}; 500 ng each of Rac1^{L61} or Myc-Rac1^{N17}; and the appropriate amount of pcDNA3 to ensure equivalent amounts of total DNA across samples within experiments. For cell stimulation studies, at

40-48 h post-transfection, cells were treated with 50 ng/ml EGF for 5 min, 100 nM PMA for 20 min, or an equivalent volume of DMSO for 20 min prior to lysis. In some experiments, cells were treated with U0126 (50 μM) or an equivalent volume of DMSO for 30 min prior to cell harvesting. To isolate FLAG-PP5•endogenous ERK complexes, cells (6-cm plates) were transfected with a combination of 700 ng wildtype FLAG-PP5, 1000 ng $Rac1^{L61}$, and the appropriate amount of pcDNA3 to equalize amounts of DNA. Cells were subsequently treated with 100 ng/ml EGF (for $Rac1^{L61}$ expressing cells) or an equivalent volume of solvent for 5 min prior to lysis. To isolate endogenous PP5•HA-ERK2 complexes, cells (10-cm plates) were transfected with a combination of 2100 ng wildtype HA-ERK2, 3000 ng $Rac1^{L61}$, and the appropriate amount of pcDNA3 to equalize the amounts of DNA in the transfections. X-tremeGENE 9 DNA was used as the transfection reagent (3 μl:1 μg ratio of reagent to DNA). To examine Raf1 feedback phosphorylation, cells (6-well plates) were co-transfected with 1000 ng Myc-Raf1, 350 ng wildtype FLAG-PP5 or FLAG-$PP5^{PD}$, 350 ng wildtype HA-ERK2 or HA-$ERK2^{KD}$, 500 ng $Rac1^{L61}$ or 200 ng $HRas^{V12}$, and the appropriate amount of pcDNA3 to equalize amounts of DNA using X-tremeGENE 9 DNA; EGF-dependent feedback phosphorylation of Raf1 was monitored in cells transfected 40-48 h and then treated with solvent lacking or containing 100 ng/ml EGF for 30 min prior to lysis.

Cell extraction, immunoprecipitations, and pulldowns

Cells were washed twice with ice-cold PBS and then lysed using ice-cold Buffer B (20 mM Tris-HCl, pH 8.0, 137 mM NaCl, 10% glycerol, and 1% Igepal CA-630) or RIPA (50 mM Tris-HCl, pH 8.0, 150 mM NaCl, 1% Igepal CA-630, 0.5% sodium deoxycholate, and 0.1% SDS) containing inhibitors (17 μg/ml aprotinin, 10 μM

leupeptin, 1 mM phenylmethylsulfonyl fluoride, and 1 mM Na_3VO_4). For Raf1 phosphorylation experiments, cells were lysed in Phospho-Buffer (20 mM Tris-HCl, pH 7.2, 2 mM EGTA, 5 mM EDTA, 30 mM sodium fluoride, 20 mM sodium pyrophosphate, and 0.5% Igepal CA-630) containing inhibitors (40 mM β-glycerophosphate, 1 mM Na_3VO_4, 3 mM benzamidine, 5 µM pepstatin A, 10 µM leupeptin, and 1 mM phenylmethylsulfonyl fluoride). Clarified lysates were generated following centrifugation at 16,300xg for 10 min at 4^{o}C. For FLAG and HA immunoprecipitations, the clarified lysates were gently rotated with 10 µl of a 50% slurry of resin for 4 h at 4^{o}C. Immunoprecipitations of endogenous ERK (400 ng of goat anti-ERK2 and 1000 ng of goat anti-ERK1 antibody) and endogenous PP5 (800 ng rabbit anti-PP5) were performed by incubating antibodies with the clarified lysates overnight at 4^{o}C with rotation followed by subsequent incubation with protein G-Sepharose 4B (15 µl of a 50% slurry), rotating for 1 h at 4^{o}C. Microcystin-agarose pulldowns were performed by incubating the resin (20 µl of a 50% slurry) with the clarified lysates overnight at 4^{o}C with rotation. Bound proteins were washed five times with 350 µl Buffer B/RIPA lacking inhibitors or Phospho-Buffer containing inhibitors, and eluted with 25 µl (FLAG and HA immune complexes), 15 µl (ERK and PP5 immune complexes), or 18 µl (microcystin pulldowns) of 2xSDS sample buffer.

Expression and purification of recombinant S100A1 and S100B proteins

Recombinant rat S100A1 and bovine S100B proteins were overexpressed in *Escherichia coli* as previously described (314,315). Recombinant S100A1 was purified under reducing conditions using a modification of the procedure described by Landar *et al*. (314). Following removal of cellular debris by centrifugation, bacterial lysates were

incubated for 30 min with a 10% solution of streptomycin sulfate and DNA precipitates were removed by centrifugation. Heat-labile proteins were removed by heating to 60^{o}C, boiling for 4 min, and centrifugation at 15,000xg for 45 min at 4^{o}C. After the addition of 0.1 M NaCl, the heat stable fraction was fractionated on a Diethylaminoethyl Fast Flow (HiPrep DEAE FF 16/10) column (GE Healthcare Life Sciences; Pittsburgh, PA). S100A1-containing fractions (260 ± 90 mM NaCl) were dialyzed and loaded on a Phenyl Sepharose 6 Fast Flow 16/10 column (GE Healthcare Life Sciences; Pittsburgh, PA). S100A1 containing fractions were eluted with 10 mM EDTA (>95% purity by SDS-PAGE), concentrated (<5 ml), and fractionated on a Superdex S200-PG size exclusion column equilibrated with Chelex-treated buffer (10 mM Tris-HCl, pH 7.5, 50 mM NaCl, 1 mM DTT). Yields of S100A1 protein (>99% pure) were typically 40-50 mg of purified protein per liter of bacterial culture. Recombinant S100B was purified using a modification of the procedure described by Amburgey *et al*. (315). Following removal of cellular debris by centrifugation, bacterial lysates were incubated for 30 min with a 10% solution of streptomycin sulfate and DNA precipitates were removed by centrifugation. The S100B containing fraction (80% supernatant) from ammonium sulfate precipitation was dialyzed and loaded on a DEAE Fast Flow column. After concentration (<5 ml), the S100B-containing fraction (0.3 M NaCl) (>95% purity by SDS-PAGE) was fractionated on a Superdex S200-PG size exclusion column equilibrated with Chelex-treated buffer. Yields of S100B protein (>99% pure) were typically 20-30 mg per liter of bacterial culture. The identity and purity of recombinant S100A1 and S100B were confirmed by amino acid analysis and electrospray mass spectrometry.

Purification and quantification of PP5

HEK-293FT cells (10-cm plate) were transfected with 3 µg of wildtype FLAG-PP5 or FLAG-PP5^{HBD}. At 40-48 h post-transfection, cells were washed twice with 4 ml of ice-cold PBS and subsequently lysed with 1 ml of Buffer B plus inhibitors. Clarified lysates from two plates were pooled and then incubated with 40 µl of a 50% slurry of anti-FLAG resin and rotated overnight at 4^{o}C. Bound proteins were washed three times with 800 µl Buffer B lacking inhibitors, once with 1 ml of PP5 Storage Buffer (20 mM Tris-HCl, pH 7.5, 0.1% βME, 0.2 mM $MnCl_2$), and then eluted from the beads by washing 3x90 µl PP5 Storage Buffer containing 100 µg/ml FLAG peptide; for each elution the beads were gently rotated for 60-90 min at 4^{o}C. The pooled eluates were combined with an equivalent volume of 100% glycerol and stored at -20^{o}C. The amount of PP5 protein was determined by SDS-PAGE and Colloidal Blue staining (Invitrogen; Carlsbad, CA) using serial dilutions of bovine serum albumin (Pierce; Rockford, IL) as standards. Quantification was accomplished using the Odyssey infrared imaging system and Odyssey application software version 3.0 (LI-COR; Lincoln, NE).

Phosphatase assays

PP5 activity was measured by adapting a previously described protocol (316). Briefly, purified wildtype FLAG-PP5 or FLAG-PP5^{HBD} (25 nM) was incubated in 80 µl of PP5 Activity Buffer (100 mM MOPS, pH 7.0, 0.1% βME, 0.1 mg/ml BSA) lacking or containing 250 µM arachidonic acid or 5 µM S100B/S100A1 plus 1 mM $CaCl_2$ for 30 min at 4^{o}C, with agitation every 5 min, before being transferred to a 96-well assay plate [Corning/Costar 3691 black with clear, flat bottom (Corning; Corning, NY)]. DiFMUP substrate (167 µM) was freshly prepared in PP5 Activity Buffer; 1 mM $CaCl_2$ (final

concentration) was included for the assays containing S100B/S100A1. DiFMUP substrate (125 µl) was transferred to a 96-well compound plate [Falcon Microtest U-Bottom 353077 (Becton Dickinson; Franklin Lakes, NJ)]. Both 96-well plates were placed in a FLEXstation III (Molecular Devices; Sunnyvale, CA) and samples were allowed to equilibrate to 30^{o}C for 5 min prior to the assay. The substrate (120 µl) and phosphatase (80 µl) mixtures were combined and triturated by the FLEXstation III, resulting in final concentrations of 10 nM phosphatase, 100 µM arachidonic acid, 200 nM S100B/S100A1, 1 mM $CaCl_2$, and 100 µM DiFMUP. The assays were carried out at 30^{o}C for 15 min and the conversion of DiFMUP to DiFMU was monitored as previously described, with the PMT sensitivity setting set to low (317). The data were recorded and analyzed by SoftMax Pro software version 5.4 (Molecular Devices; Sunnyvale, CA).

S100 displacement of ERK from PP5 complexes

HEK-293FT cells (10-cm plates) were untransfected or transfected with 1400 ng wildtype HA-ERK2 using X-tremeGENE 9 DNA. At 40-48 h post-transfection, cells were lysed in Buffer B containing inhibitors and clarified by centrifugation. The cell lysates were incubated with 30 µl of a 50% slurry of microcystin-agarose overnight with rotation at 4^{o}C. Bound proteins were washed five times with 350 µl Buffer B lacking inhibitors and then once with 350 µl S100 Binding Buffer (20 mM Tris-HCl, pH 7.5, 100 mM KCl, 0.01% Tween 20, and 1 mM $CaCl_2$). The beads were then split in half into separate tubes and incubated in a final volume of 50 µl S100 Binding Buffer lacking or containing 20 µg S100A1 for 1 h at room temperature with agitation. Proteins immobilized on the resin were washed four times with 350 µl S100 Binding Buffer and eluted with 15 µ1 2xSDS sample buffer.

Western analysis

SDS-solubilized cell lysates and immune complexes were subjected to SDS-PAGE (10% Tris-glycine gels), transferred to 0.2 μm or 0.45 μm Optitran BA-S 85 reinforced nitrocellulose (Whatman; Dassel, Germany), blocked with Odyssey Blocking Buffer, and immunoblotted with the indicated primary antibodies and corresponding secondary antibodies. Phospho-specific antibodies were diluted 1:1000 in Odyssey Blocking Buffer containing 0.1% Tween-20. All other primary and secondary antibodies were diluted in Tris-buffered saline containing 0.5% BSA and 0.1% Tween-20; secondary antibodies were diluted 1:10,000. Visualization and quantification of the immunolabeled proteins was accomplished using the Odyssey infrared imaging system (LI-COR; Lincoln, NE) and Odyssey application software version 3.0.

Statistics

Statistical comparisons were performed using GraphPad Prism version 4.03 (GraphPad Software; San Diego, CA).

Results

Identification of a PP5•Raf1•ABαC complex

The association of PP5 and PP2A (i.e., ABα/δC) with Raf1 has been shown to regulate the Raf1-MEK-ERK pathway by promoting the inactivation and activation of Raf1 signaling, respectively (133,137,248). To better understand the regulation of Raf1 by PP5 and ABαC, we examined Raf1 binding with these PSTPs by performing immunoprecipitations and pulldowns from extracts of HEK-293FT cells expressing Myc-

Raf1, GST-Bα, or FLAG-PP5. Western analysis of the bound proteins revealed that PP5•Raf1•ABαC complexes were present in Myc-bound, GST-bound, and FLAG-bound eluates, indicating that this complex can be isolated regardless of which protein in the complex is targeted for precipitation (Fig. 41). Little to no non-specific binding with these resins was observed. We next sought to determine the molecular organization of this trimeric protein complex and tested whether Raf1 interacts with one of the phosphatases, which then interacts with the second phosphatase, or if Raf1 can associate with both phosphatases concurrently. Pulldowns and immunoprecipitations were performed from extracts of HEK-293FT cells expressing GST, GST-Bα, FLAG-PP5, or Myc-Raf1 individually or in the indicated combinations. Western analysis of GST pulldowns revealed the co-precipitation of Myc-Raf1 and FLAG-PP5 only in the triple transfected cells expressing GST-Bα (Fig. 42). Notably, FLAG-PP5 did not co-precipitate with either GST-Bα or GST. Analysis of FLAG immune complexes revealed the co-precipitation of GST-Bα and endogenous $PP2A_C$ only when Myc-Raf1 was co-expressed, again demonstrating the formation of trimeric PP5•Raf1•ABαC complexes. The addition of 150 mM NaCl to the lysis buffer enhanced purification of the trimeric complex via GST-Bα, but had no effect when purifying the complex via FLAG-PP5. Together, these data indicate that both PP5 and ABαC can interact with Raf1 concurrently, and that Raf1 serves as the scaffold in this multiprotein complex.

PP5 interacts with multiple protein kinases

The eukaryotic protein kinase superfamily can be subdivided into classes, families, and subfamilies based upon the sequence similarities of their kinase domains (4), and PP5 has been reported to associate with and/or regulate a number of protein

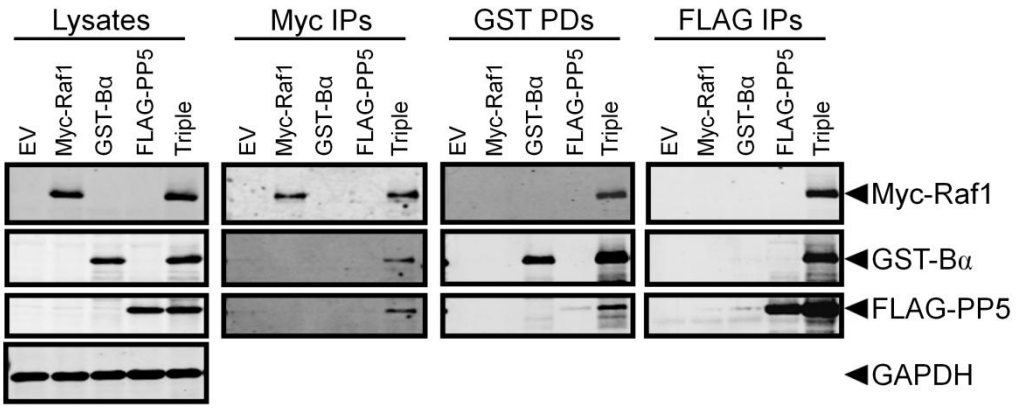

Figure 41. Isolation of a multiprotein PP5•Raf1•ABαC complex from cells.
HEK-293FT cells were transfected to express Myc-Raf1, GST-Bα, FLAG-PP5, or all three (Triple). Solubilized cell extracts were divided, incubated with Myc, GST, or FLAG resin, and bound proteins eluted with SDS sample buffer. Samples of starting material (Lysates), Myc eluates (Myc IPs), GST eluates (GST PDs), and FLAG eluates (FLAG IPs) were analyzed by Western using Myc, GST, FLAG, and $PP2A_C$ antibodies (n = 2).

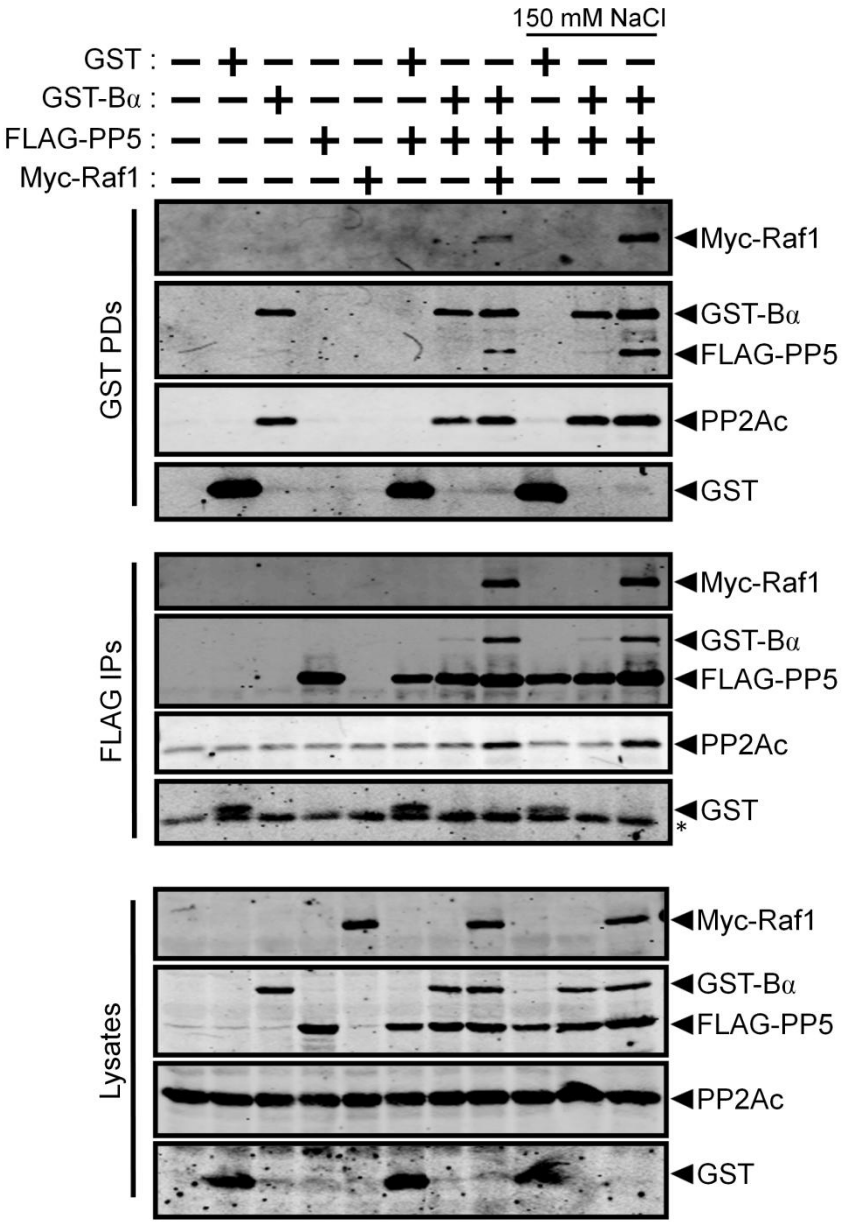

Figure 42. Raf1 serves as the scaffold for both PP5 and ABαC.
HEK-293FT cells were transfected to express GST, GST-Bα, FLAG-PP5, or Myc-Raf1 as indicated, and solubilized in lysis buffer lacking or containing 150 mM NaCl. GST-tagged proteins were pulled-down from cell extracts with a GST affinity resin (*GST PDs*), while FLAG-tagged proteins were immunoprecipitated from cell extracts with a FLAG affinity resin (*FLAG IPs*). Proteins contained in the GST PDs, FLAG IPs, and cell lysates were analyzed by immunoblotting with antibodies recognizing Myc, GST, FLAG, and $PP2A_C$ (n = 1).

kinases that mediate signaling cascades controlling cell growth and cellular responses to stress (123-127,131,134). However, the precise role(s) of PP5 in these biological events is unclear and it is unknown if the interactions of PP5 are restricted to a particular class of kinases. Therefore, we systematically tested kinases representing several classes to determine which could form stable complexes with PP5. To detect PP5-kinase interactions, FLAG immunoprecipitations were performed from lysates of HEK-293FT cells co-expressing FLAG-PP5 and a differentially epitope-tagged protein kinase that included (kinase class indicated in parenthesis): HA-p70S6K (AGC), HA-ERK2 (CMGC), HA_3-IKK1 (Other), HA-CaMKIV (CaMK), Src^{Y529F} (TK), Myc-Raf1 (TKL), and HA-MST2 (STE). Western analysis of the FLAG immune complexes revealed that at least one kinase from each class could form a stable complex with PP5 (Fig. 43). No kinase was detected in any of the control immunoprecipitations and, for all of the kinases tested, endogenous HSP90 co-precipitated with FLAG-PP5.

The binding of PP5 with many interacting proteins is mediated by HSP90 (318), and some of the kinases tested are known HSP90 clients (311). Therefore, we next examined the ability of each kinase to interact with a mutated form of PP5, which contains a single point mutation that disrupts the association of PP5 with HSP90 (HSP90 binding-deficient; FLAG-$PP5^{HBD}$) (Fig. 44) (108). Under conditions where both the expression of the kinases and the levels of immunopurified phosphatase were comparable, the binding of CaMKIV, Raf1 and MST2 to $PP5^{HBD}$ was abolished or dramatically impaired relative to wildtype PP5, indicating HSP90 likely plays a role in these PP5-kinase interactions (Fig. 43). Likewise, HSP90 appears to facilitate the binding of PP5 to p70S6K, ERK2, IKK1 and Src^{Y529F} because the association of each kinase with

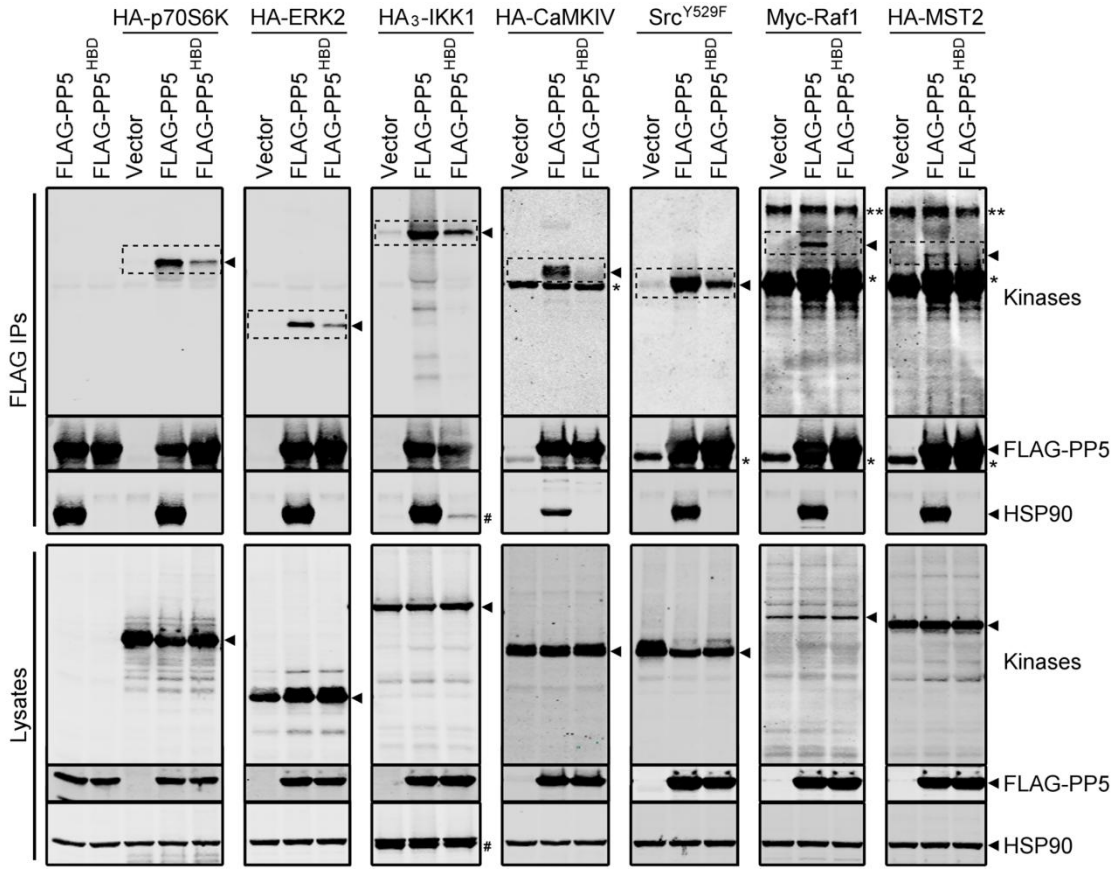

Figure 43. Multiple kinases associate with PP5 in an HSP90-dependent manner. HEK-293FT cells were transfected with wildtype FLAG-PP5 (*FLAG-PP5^{WT}*) or an HSP90 binding-deficient point mutant of PP5 (*FLAG-PP5^{HBD}*) alone or together with HA-p70S6K, HA-ERK2, HA_3-IKK1, HA-CaMKIV, Src^{Y529F}, Myc-Raf1, or HA-MST2; cells were also co-transfected with the indicated epitope tagged kinase and pcDNA3 (*Vector*). FLAG-tagged proteins were immunoprecipitated from cell extracts with a FLAG affinity resin (*FLAG IPs*), and proteins contained in the FLAG IPs and cell lysates were detected by Western analysis using antibodies recognizing HA, Myc, FLAG, Src, and HSP90. ** and *, denote a non-specific band and IgG heavy chain, respectively. #, denotes HA_3-IKK1 that migrates just below HSP90. The data are representative of experiments performed at least three independent times with similar results.

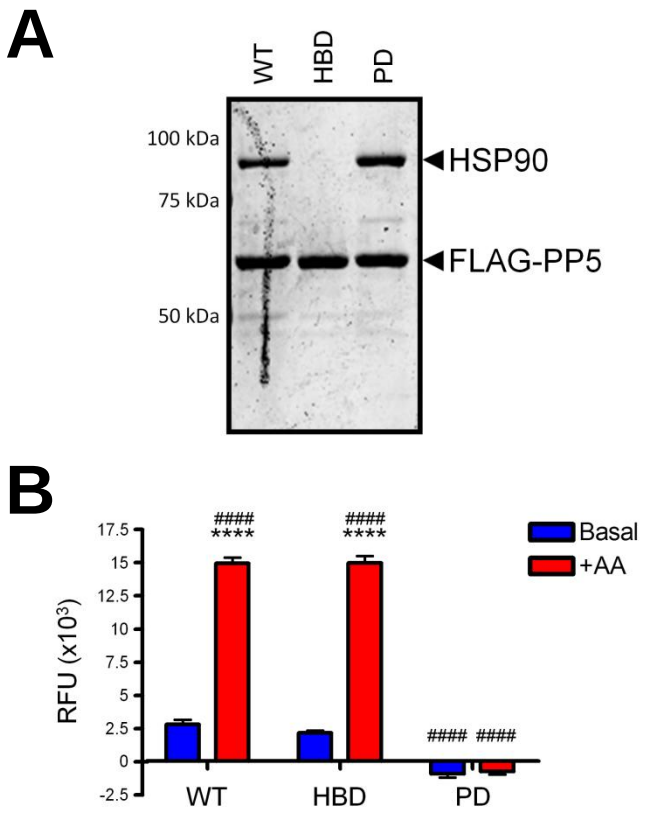

Figure 44. HSP90 binding and phosphatase activity levels of mutant PP5 proteins.

HEK-293FT cells were transfected to express wildtype FLAG-PP5 (*WT*), FLAG-K97A-PP5 [a point mutant that disrupts the association of PP5 with HSP90 (HSP90 binding-deficient; *HSB*)], or FLAG-H304Q-PP5 [a point mutant that is catalytically inactive (phosphatase dead; *PD*)]. Solubilized extracts were incubated with anti-FLAG resin and bound proteins eluted with excess FLAG peptide. Purified proteins were subjected to SDS-PAGE and Colloidal Blue staining to monitor PP5-HSP90 interactions (***A***) and *in vitro* phosphatase assays to analyze catalytic activity in the presence of buffer (*Basal*) or 100 μM arachidonic acid (*+AA*) (***B***). Phosphatase activity toward DiFMUP [Relative Fluorescent Units (*RFU*)] was continuously assayed over 900 s. Quantification of phosphatase activity at the 900 s time point is presented. Background fluorescence was measured and subtracted from the corresponding fluorescent values of the phosphatase-containing samples. One-way analysis of variance followed by Tukey multiple comparison tests identified statistically significant differences in PP5 activity: **** Basal vs. +AA, $p < .0001$; #### vs. WT-Basal, $p < .0001$ ($n = 3$).

PP5^{HBD} was reduced relative to their association with wildtype PP5. However, in PP5^{HBD} immune complexes that lacked HSP90, p70S6K, ERK2, IKK1 and Src^{Y529F} were still detected. This suggests that not all PP5•kinase complexes require the presence of HSP90.

PP5 forms stable complexes with ERKs

Our Western analysis of FLAG-PP5 immune complexes isolated from HEK-293FT cells revealed a number of novel PP5 interacting proteins, which included ERK2 (Fig. 43). Therefore we performed additional experiments to determine if PP5 could interact with ERK2, ERK1, and two ERK1 splice variants (rodent ERK1b and primate ERK1c; refs. 294,296). Western analysis of FLAG immune complexes from HEK-293FT cells co-expressing FLAG-PP5 and HA-ERK1, HA-ERK1b, HA-ERK1c, or HA-ERK2 revealed that PP5 is capable of interacting with each of the MAPKs (Fig. 45). The binding of these MAPKs to PP5 does not appear to involve the extreme C-terminus of the kinases, as this region is very divergent amongst the ERKs (294,296). No kinase was detected in the control immunoprecipitations and endogenous HSP90 was found to co-precipitate with FLAG-PP5. Under conditions where both the expression of the kinases and the levels of immunopurified phosphatase were comparable, we observed that the amount of ERK1/2 bound to PP5^{HBD} was dramatically reduced relative to wildtype PP5 (Fig. 46), indicating that HSP90 plays a role in facilitating these interactions. However, in PP5^{HBD} immune complexes that contain no HSP90, ERK1/2 was still detected, suggesting that not all PP5•ERK complexes require the presence of HSP90.

To ensure the functionality of the FLAG-PP5^{HBD} mutant, we analyzed its activity in the presence of two different activators of PP5, arachidonic acid and S100 family members (99,110). Both wildtype PP5 and PP5^{HBD} exhibited comparable basal and

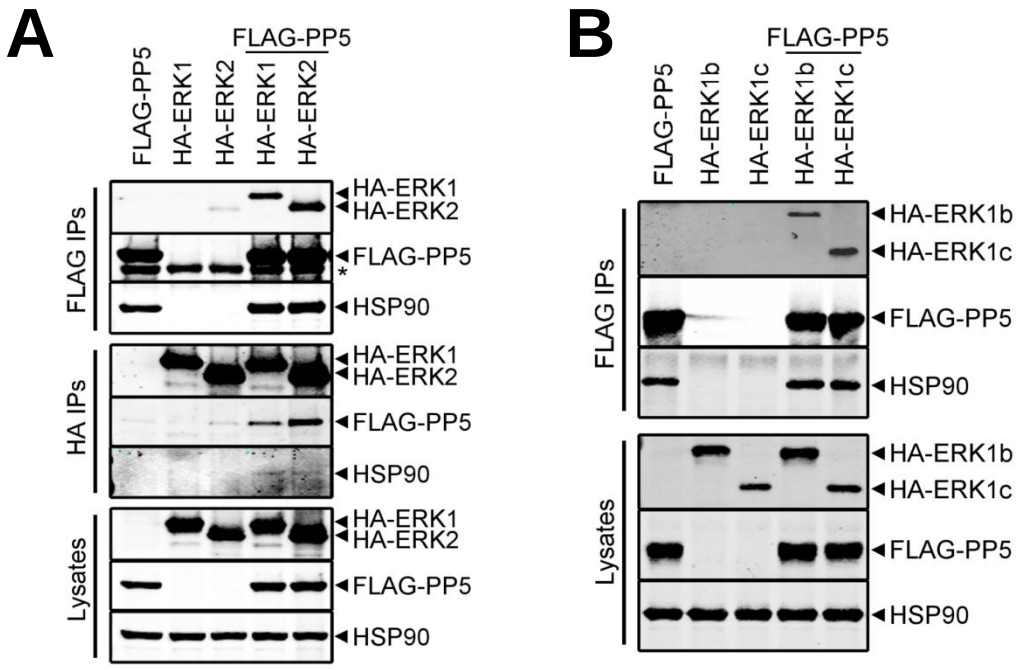

Figure 45. PP5 interacts with ERK2, ERK1, and ERK1 splice variants.
A, HEK-293FT cells were transfected with FLAG-PP5, HA-ERK1, or HA-ERK2 alone or in combination, as indicated. Western analysis of FLAG immune complexes (*FLAG IPs*), HA immune complexes (*HA IPs*), and cell lysates were performed using FLAG, HA, and HSP90 antibodies (n = 3). *, denotes IgG heavy chain. ***B***, HEK-293FT cells were transfected with FLAG-PP5, HA-ERK1b, or HA-ERK1c alone or in combination, as indicated. FLAG IPs and cell lysates were analyzed by Western as in *A* (n = 3).

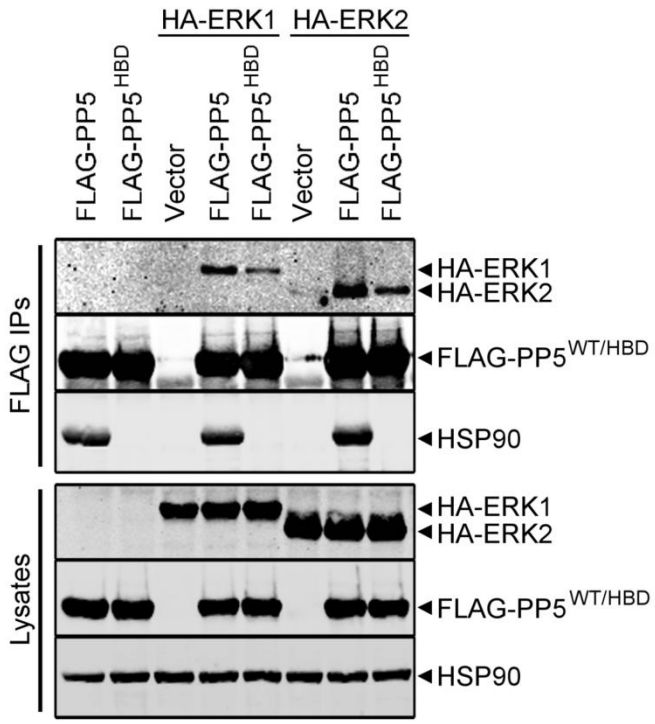

Figure 46. Not all PP5•ERK1/2 complexes require the presence of HSP90.
HEK-293FT cells were transfected with wildtype FLAG-PP5 or FLAG-PP5^{HBD} alone or together with HA-ERK1 or HA-ERK2; cells were also transfected with the indicated HA-tagged kinase and pcDNA3 (*Vector*). FLAG IPs and cell lysates were analyzed as described in *A*. A significant reduction in the binding of HA-ERK1 (88.21% ± 3.01%, p<.0001) and HA-ERK2 (77.3% ± 8.97%, p=.0003) to FLAG-PP5^{HBD} was found when ERK signals were normalized to levels of mutant PP5 in the IPs and compared to the corresponding values in the wildtype FLAG-PP5 conditions, which were set to 100. The results represent the means ± S.E. analyzed by one sample t-test using two-tailed p values (n = 6).

arachidonic acid-stimulated activities (Fig. 47). In addition, both S100B and S100A1 induced the activation of $PP5^{HBD}$ to a level comparable to the activation observed following treatment with arachidonic acid (Fig. 47, and data not shown). Studies from our laboratory have established that FLAG-PP5 immunopurified from RIPA Buffer-solubilized cell lysates lacks HSP90 (unpublished data). To further substantiate the ability of PP5 to bind ERK1/2 in the absence of HSP90, we examined the association of HA-ERK2 with wildtype FLAG-PP5 immune complexes isolated from cells that were lysed in different buffers (i.e., Buffer B or RIPA Buffer). As shown in Fig. 48, RIPA Buffer solubilization maintains the interaction of ERK2 with an HSP90-uncoupled, monomeric form of PP5. Collectively, these data indicate that PP5 binding to ERK can occur in the absence of HSP90.

To determine if PP5-ERK1/2 interactions are dependent on kinase or phosphatase activity, we performed binding experiments using catalytically inactive forms of these enzymes. Western analysis of FLAG immune complexes from lysates of unstimulated cells co-expressing wildtype FLAG-PP5 and kinase dead ERK1 (HA-$ERK1^{KD}$) or ERK2 (HA-$ERK2^{KD}$) (319) revealed that catalytically inactive kinases retained their ability to associate with wildtype PP5 (Fig. 49). Likewise, analysis of FLAG immune complexes from lysates of cells co-expressing catalytically inactive PP5 (FLAG-$PP5^{PD}$) (Fig. 44) (103,111,320) and wildtype HA-ERK1 or HA-ERK2 revealed that PP5-ERK1/2 interactions were maintained in the absence of PP5 activity (Fig. 49). Together, these findings demonstrate that neither kinase nor phosphatase activity is required for the assembly of PP5•ERK1 and PP5•ERK2 complexes in unstimulated cells.

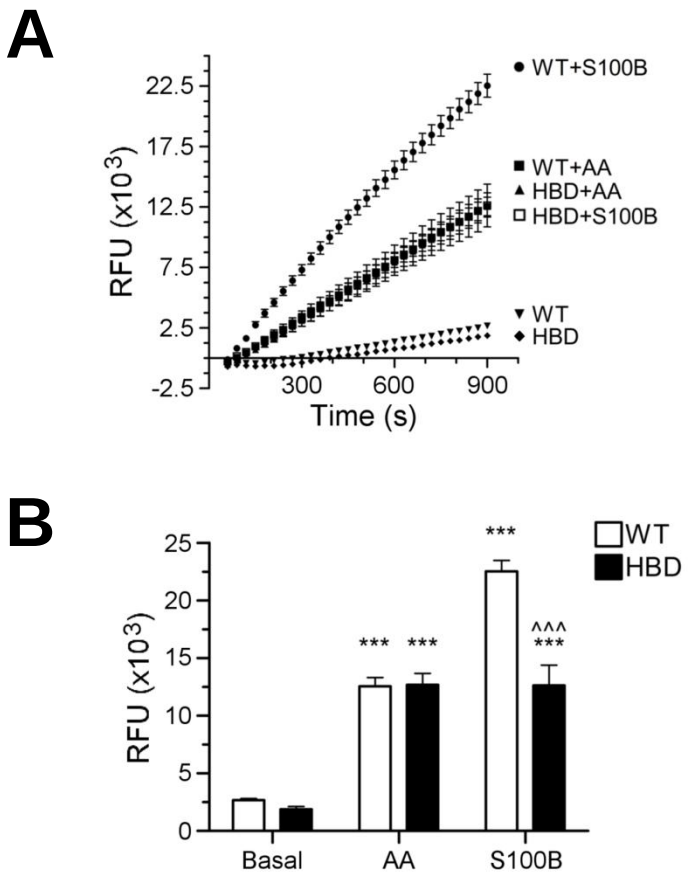

Figure 47. Analysis of PP5^{HBD} activity.
A, Approximately 118 ng (10 nM) of purified wildtype FLAG-PP5 (*WT*) or HSP90 binding-deficient mutant of FLAG-PP5 (*HBD*) were continuously assayed over 900 s for phosphatase activity toward DiFMUP [Relative Fluorescent Units (*RFU*)] in the presence of only buffer (*Basal*), 100 µM arachidonic acid (*AA*), or 200 nM S100B plus 1 mM $CaCl_2$ (*S100B*). Background fluorescence (i.e., samples containing only DiFMUP+AA or DiFMUP+S100B+$CaCl_2$) was measured and subtracted from the corresponding fluorescent values of the phosphatase-containing samples. Levels of fluorescence in WT+AA, HBD+AA, and HBD+S100B preparations were virtually identical. The results represent the means ± S.E. from six independent experiments; three experiments performed with duplicates from each of two separate purifications of WT and HBD. Standard error of the mean bars are obscured by the symbols for most data points. ***B***, Quantification of phosphatase activity at the 900 s time point. Two-way ANOVA identified a statistically significant genotype vs. activator interaction ($F(5,30)=61.83$, $p<.0001$). Tukey post-tests: *** vs. Basal, $p<.0001$; ^^^ WT vs. HBD, $p<.0001$.

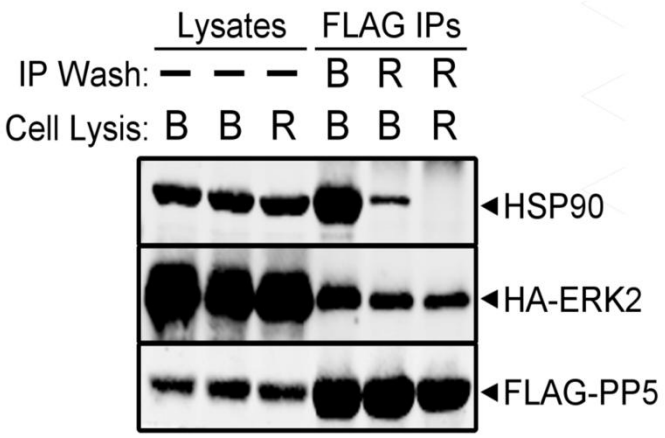

Figure 48. PP5-ERK2 interactions are maintained following RIPA-mediated disruption of PP5-HSP90 binding.
HEK-293FT cells expressing FLAG-PP5 and HA-ERK2 were lysed in Buffer B (*B*) or RIPA buffer (*R*) (*Lysates*). FLAG immunoprecipitations (*FLAG IPs*) were performed from the cell lysates and washed (*IP Wash*) in either B or R, as indicated. The FLAG IPs and corresponding cell lysates were analyzed by Western using HSP90, HA, and FLAG antibodies (n = 2).

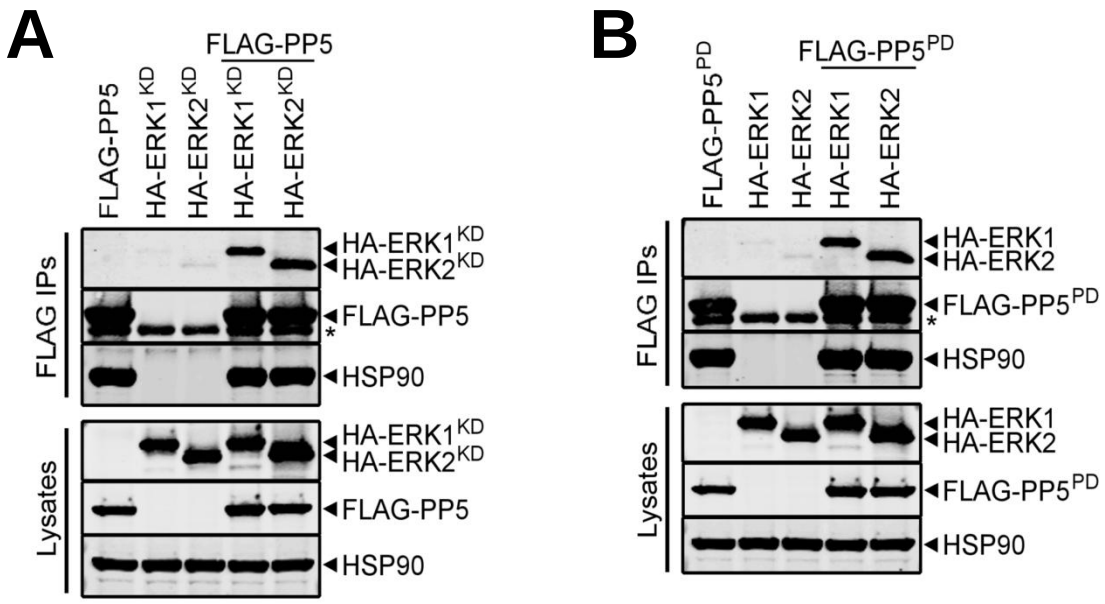

Figure 49. The interaction of PP5 with ERK1/2 is independent of kinase and phosphatase activity.

A, FLAG immunoprecipitations (*FLAG IPs*) were performed from lysates of HEK-293FT cells transfected with wildtype FLAG-PP5, kinase dead ERK1 (*HA-ERK1^{KD}*), or kinase dead ERK2 (*HA-ERK2^{KD}*) alone or in combination, as indicated. The cell lysates and FLAG IPs were subjected to Western analysis using FLAG, HA, and HSP90 antibodies (n = 3). ***B***, FLAG IPs were performed from lysates of HEK-293FT cells transfected with phosphatase dead PP5 (*FLAG-PP5^{PD}*), wildtype HA-ERK1, or wildtype HA-ERK2 alone or in combination, as indicated. The cell lysates and FLAG IPs were analyzed as described in *A* (n = 3). *, denotes IgG heavy chain.

Active Rac1 promotes assembly of PP5•ERK1 and PP5•ERK2 complexes

Activated Rac1 has been shown to promote the translocation of PP5 to the plasma membrane (111), one of several subcellular sites where the compartmentalization of ERK1/2 forms spatially distinct pockets of ERK activity that are important in creating diversity in cellular responses to stimuli (321). To determine if PP5-ERK1/2 interactions could be altered in the presence of active Rac1, we evaluated the binding of PP5 to ERK1/2 in cells co-expressing constitutively active Rac1 ($Rac1^{L61}$). Significantly enhanced binding of PP5 to both ERK1 and ERK2 (5.2 and 2.8 fold increases, respectively) was observed in cells expressing $Rac1^{L61}$, relative to control cells (Fig. 50). Moreover, the interaction of PP5 with ERK1/2 was unaffected by expression of a dominant negative form of Rac1 (Myc-$Rac1^{N17}$) (Fig. 50). Given that $Rac1^{L61}$ augmented the interaction of the ectopic proteins, we next tested whether $Rac1^{L61}$ could promote increased interaction of endogenous-ectopic proteins. Indeed, the expression of $Rac1^{L61}$ enhanced the interaction of endogenous ERK1/2 with FLAG-PP5 (Fig. 51). Likewise, the expression of $Rac1^{L61}$ led to increased interaction of endogenous PP5 with HA-ERK2, as visualized by Western analysis of both endogenous PP5 immune complexes and microcystin-agarose pulldowns (an affinity resin for protein serine/threonine phosphatases such as PP5) (Fig. 51). To test whether endogenous PP5 interacts with endogenous ERK, we performed microcystin-agarose pulldowns from lysates of untransfected cells. As shown in Fig. 52A, endogenous ERK1/2 co-purified with endogenous PP5 on this phosphatase affinity resin. To demonstrate that the binding of ERK1/2 to microcystin-agarose is due to its interaction with PP5, we performed an *in vitro* displacement assay using S100A1, a PP5 regulatory protein that competitively

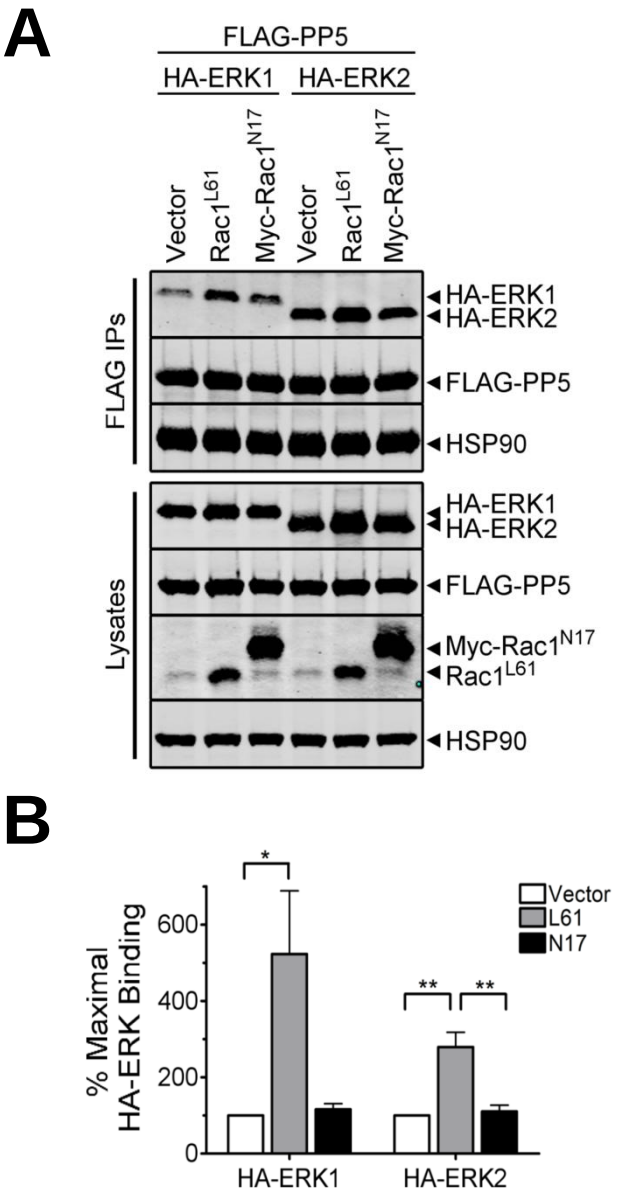

Figure 50. Active Rac1 promotes assembly of ectopic PP5•ERK1 and PP5•ERK2 complexes.

A, HEK-293FT cells were co-transfected with FLAG-PP5 and either HA-ERK1 or HA-ERK2 together with pcDNA3 (*Vector*), constitutively active Rac1 (*Rac1^{L61}*), or dominant negative Rac1 (*Myc-Rac1^{N17}*) as indicated. Western analysis of FLAG immune complexes (*FLAG IPs*) and cell lysates were performed using the HA, FLAG, HSP90, and Rac1 antibodies (n = 3). ***B***, Quantification of percent maximal HA-ERK binding normalized to the FLAG-PP5 signal in FLAG IPs, with binding in the Vector samples set to 100. One-way ANOVA identified a significant increase in PP5-ERK1 ($F(2,6)=6.222$, $p=.0344$) and PP5-ERK2 ($F(2,6)=17.28$, $p=.0032$) association in the presence of Rac1^{L61}. Tukey post-tests: *, $p<.05$; **, $p<.01$. Data are mean ± S.E. No significant differences in the expression levels of FLAG-PP5, HA-ERK1, or HA-ERK2 were detected following normalization to HSP90 levels.

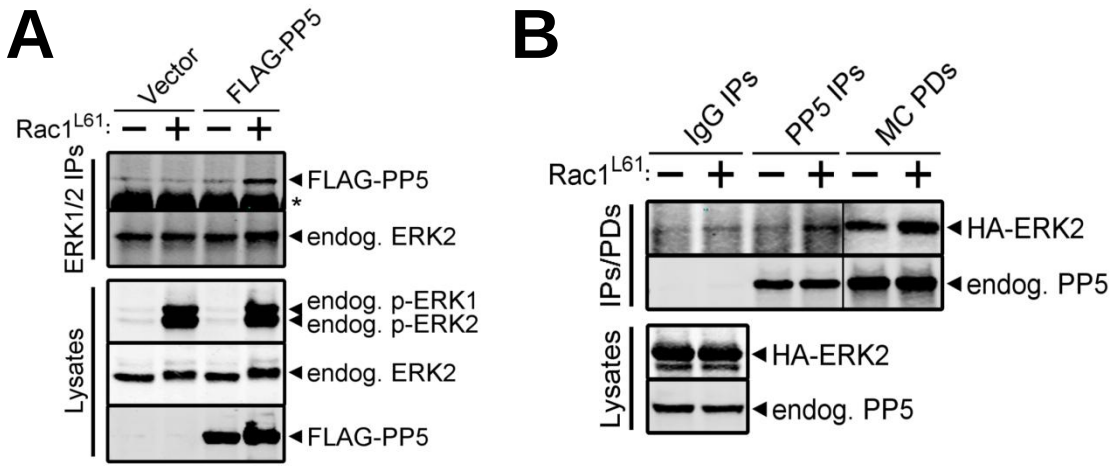

Figure 51. Active Rac1 promotes assembly of endogenous-ectopic PP5•ERK1 and PP5•ERK2 complexes.

A, HEK-293FT cells were transfected with pcDNA3 (*Vector*) or FLAG-PP5 in the absence (-) or presence (+) of constitutively active Rac1 (*Rac1^{L61}*). Cells transfected with Rac1^{L61} were also treated with 100 ng/mL EGF for 5 min prior to lysis. Endogenous ERK1/2 immune complexes (*ERK1/2 IPs*) and cell lysates were analyzed by Western using phospho-ERK1/2 (*p-ERK1/2*), ERK2, PP5, and FLAG antibodies (n = 3). *, denotes IgG heavy chain. ***B***, HEK-293FT cells were co-transfected with HA-ERK2 and pcDNA3 (-) or Rac1^{L61} (+). Western analysis of cell lysates, and proteins purifying with normal rabbit IgG (IgG IPs), rabbit anti-PP5 antibody (PP5 IPs), and microcystin-agarose (MC PDs), were performed using ERK2 and PP5 antibodies (n = 2).

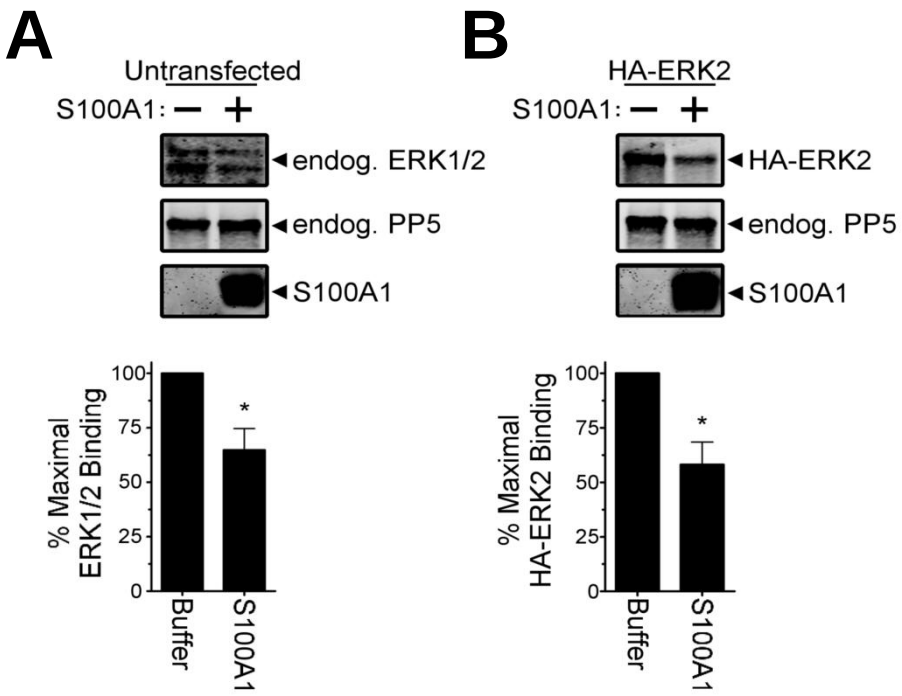

Figure 52. Endogenous PP5•ERK1 and PP5•ERK2 complexes form in cells.
Lysates from untransfected (***A***) and HA-ERK2-expressing (***B***) HEK-293FT cells were incubated with microcystin-agarose and bound proteins were extensively washed prior to splitting the resin into separate tubes, which were then incubated with buffer lacking (-) or containing (+; 20µg) purified S100A1. A fraction of the reaction mixture was collected and analyzed by SDS-PAGE (15% Tris-glycine gels), and stained with Coomassie G-250 to detect S100A1. Following incubation, bound proteins were extensively washed and eluted for analysis by Western with antibodies detecting the ERK1/2 and PP5 proteins. Unpaired, one-tailed t tests identified a significant decrease in the levels of bound ERK following incubation with S100A1 (left panel: *, p=.0117; right panel: *, p=.0279). The data are representative of experiments performed three (***A***) and two (***B***) independent times with similar results.

inhibits the association of PP5 with other interacting partners (110). S100A1 significantly displaced endogenous ERK1/2 from the resin without affecting the binding of endogenous PP5 (Fig. 52A). S100A1 also disrupted the interaction of HA-ERK2 with endogenous PP5 (Fig. 52B), thus reinforcing that our overexpression system recapitulates the native condition. The co-purification of PP5 and ERK with microcystin-agarose also supports our observations that phosphatase activity is not required for the PP5-ERK interaction since microcystin is a potent inhibitor of PP5 activity (322). Moreover, analysis of microcystin pulldowns from a variety of other cell types (e.g., MCF7, MDCK, MDA-MB-435) also revealed co-purification of endogenous ERK1/2 and PP5 (data not shown).

Oncogenic RAS alters the interaction of PP5 with ERK2 but not ERK1

To address whether activation of the RAS-RAF-MEK-ERK signaling cascade influences PP5-ERK1/2 interactions, we treated cells with a variety of stimuli and monitored binding by co-immunoprecipitation assays coupled with Western analysis. Acute treatment of cells with epidermal growth factor (EGF) potently stimulated this pathway, as visualized in the cell lysates using a phospho-ERK1/2 antibody, but failed to alter PP5-ERK1/2 interactions (Fig. 53). Likewise, acute treatment of cells with phorbol 12-myristate 13-acetate (PMA), which activates ERK in a RAS-independent manner via activation of PKC (323), also failed to impact the PP5•ERK1/2 complexes. Interestingly, introduction of constitutively active HRas ($HRas^{V12}$), which chronically activates ERK signaling, led to a loss of PP5-ERK2 binding, without influencing the association of PP5 and ERK1. To determine if the $HRas^{V12}$-induced effect was specific to the gain-of-function G12V mutation, we compared the ability of wildtype HRas ($HRas^{WT}$) and

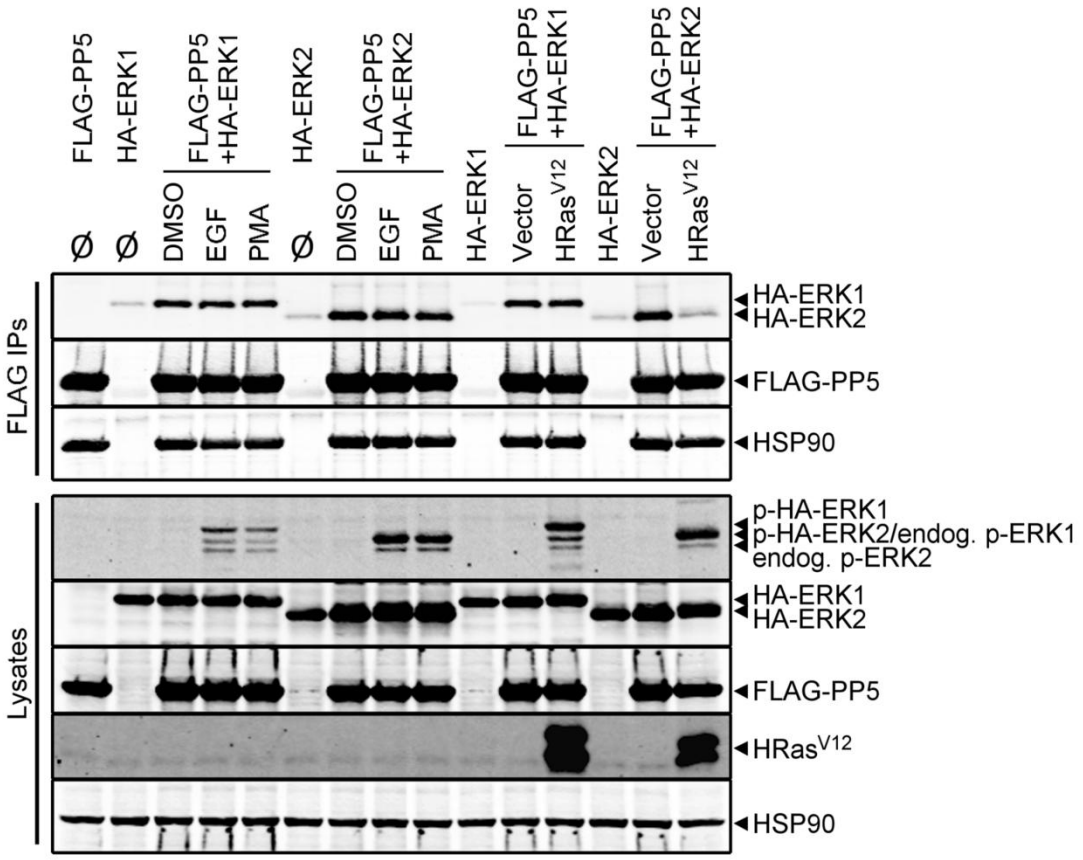

Figure 53. HRas^{V12}, but not acute ERK activation, selectively decreases PP5-ERK2, but not PP5-ERK1, interactions.
HEK-293FT cells were transfected with HA-ERK1, HA-ERK2, or FLAG-PP5 alone or in combination and treated with nothing (*Ø*), 50 ng/mL EGF (5 min), 100 nM PMA (20 min), or an equivalent volume of DMSO (20 min) as a vehicle control. HEK-293FT cells transfected with FLAG-PP5 and HA-ERK1 or HA-ERK2 in combination with pcDNA3 (*Vector*) or HRas^{V12} were not treated prior to lysis. Western analysis of the FLAG immune complexes (*FLAG IPs*) and cell lysates was done using antibodies recognizing phospho-ERK1/2 (*p-ERK1/2*), Ras, HSP90, HA, and FLAG (n = 4). Note that phospho-HA-ERK2 (*p-HA-ERK2*) and endogenous phospho-ERK1 (*endog. p-ERK1*) co-migrate.

$HRas^{V12}$ to influence the PP5-ERK2 interaction. Although $HRas^{WT}$ and $HRas^{V12}$ expression led to comparable increases in ERK1/2 phosphorylation, relative to cells lacking RAS expression, only the oncogenic variant was capable of decreasing the association of PP5 and ERK2 (Fig. 54). These observations prompted us to examine another RAS isoform, namely KRas4B, and two of its oncogenic variants (i.e., $KRas^{V12}$ and $KRas^{L61}$) for their ability to modulate the interaction of PP5 with ERK2. Introduction of wildtype KRas4B ($KRas^{WT}$), $KRas^{V12}$, and $KRas^{L61}$ each resulted in enhanced levels of ERK phosphorylation and, analogous to $HRas^{V12}$, $KRas^{L61}$ was fully capable of modifying this phosphatase-kinase interaction (Fig. 54). Surprisingly, despite similar levels of activated ERK in cells expressing $KRas^{L61}$, oncogenic $KRas^{V12}$ did not decrease the PP5-ERK2 interaction (Fig. 54). These findings reveal novel stimulus-induced differences in PP5-ERK1/2 binding and indicate that the PP5•ERK2 complex is selectively regulated in response to specific oncogenic RAS-initiated signaling events.

Kinase activity, but not phosphatase activity, is required for $HRas^{V12}$-induced alteration of PP5•ERK2 complexes

We next performed experiments to determine if the $HRas^{V12}$-induced reduction in PP5-ERK2 interactions is dependent on the enzymatic activity of PP5 and/or ERK2. The impact of phosphatase activity on this event was assessed by immunoblotting for ERK2 in FLAG immune complexes from cells co-expressing FLAG-$PP5^{PD}$ and wildtype HA-ERK2 in the absence or presence of $HRas^{V12}$. As shown in Fig. 55, $HRas^{V12}$ decreased the interaction between $PP5^{PD}$ and wildtype ERK2, similar to what was observed for the wildtype PP5-ERK2 interaction (Fig. 53), thus demonstrating that phosphatase activity was not required for this effect. To ascertain if ERK2 activity was important for the

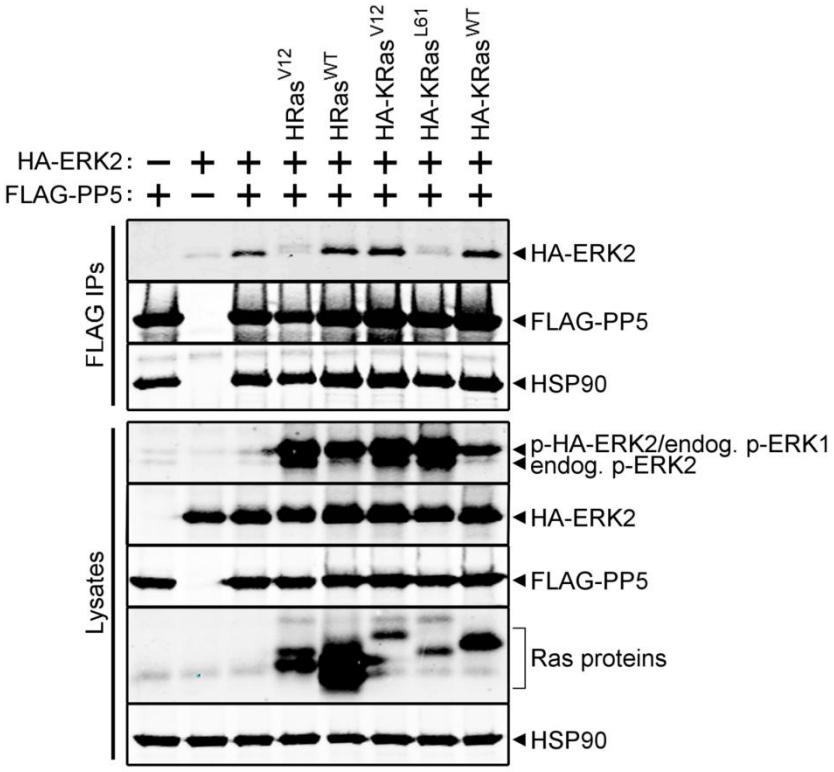

Figure 54. Specific oncogenic Ras variants selectively decrease PP5-ERK2 interactions.
HEK-293FT cells transfected with (+) or without (-) HA-ERK2 or FLAG-PP5 were co-transfected with HRas^{V12}, wildtype HRas (HRas^{WT}), HA-KRas^{V12}, HA-KRas^{L61}, or wildtype HA-KRas (HA-KRas^{WT}). FLAG IPs and cell lysates were analyzed by Western as in Fig. 53 (n = 3).

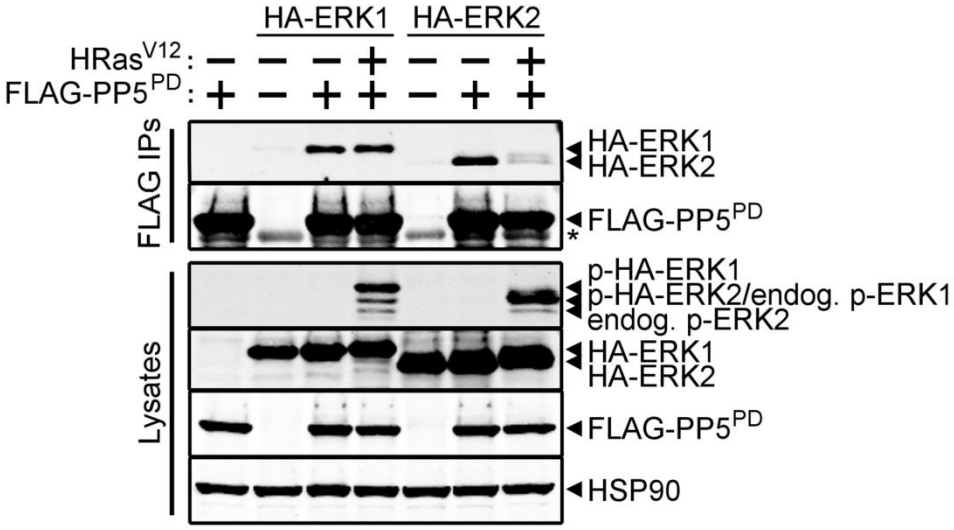

Figure 55. Phosphatase activity is not required for HRas^{V12}-dependent disruption of the PP5•ERK2 complex.
HEK-293FT cells were transfected with wildtype HA-ERK1 or wildtype HA-ERK2 together with (+) or without (-) phosphatase dead FLAG-PP5 (*FLAG-PP5^{PD}*) and HRas^{V12}. FLAG immune complexes (*FLAG IPs*) and cell lysates were analyzed by Western using antibodies recognizing the indicated proteins (n = 3). *, denotes IgG heavy chain.

HRas^{V12}-induced changes in the PP5•ERK2 complex, we evaluated the binding of both wildtype HA-ERK2 and HA-ERK2^{KD} to wildtype FLAG-PP5 in the absence or presence of HRas^{V12}. As predicted by previous observations, HRas^{V12} expression diminished the interaction of PP5 and wildtype ERK2; however, the interaction of wildtype PP5 and ERK2^{KD} was maintained in HRas^{V12} expressing cells (Fig. 56). Consistent with the results shown in Figs. 49 and 53, the PP5-ERK1 interaction was independent of phosphatase and kinase activity in both the absence and presence of HRas^{V12}. Collectively, these data demonstrate that the association of PP5 with ERK1/2 is independent of both phosphatase and kinase activity, while the HRas^{V12}-mediated reduction of PP5-ERK2 binding requires ERK2 activity.

Disruption of the PP5-ERK2 interaction by HRas^{V12} is independent of MEK activity

Because the data indicate that ERK2 activity is necessary for the HRas^{V12}-induced decrease in PP5-ERK2 interactions, we wanted to determine if MEK1/2 plays a role in this process. To address this question, cells co-expressing wildtype HA-ERK2, wildtype FLAG-PP5, and oncogenic HRas were treated with the MEK1/2 inhibitor, U0126, or solvent as a control. Western analysis of cell lysates and FLAG immune complexes revealed that MEK inhibition potently abrogated ERK phosphorylation but did not influence the loss of PP5-ERK2 binding caused by HRas^{V12} (Fig. 57). Quantification of these data revealed that expression of HRas^{V12} produced a dramatic reduction in the association of PP5 and ERK2, regardless of the activation state of MEK (reductions of 86.08% ± 1.62% and 81.95% ± 2.26% in the absence or presence of U0126, respectively) (Fig. 57). Therefore, it appears that acute inhibition of ERK, in the context of HRas^{V12} signaling, does not allow reassembly of PP5•ERK2 complexes. Collectively, these data

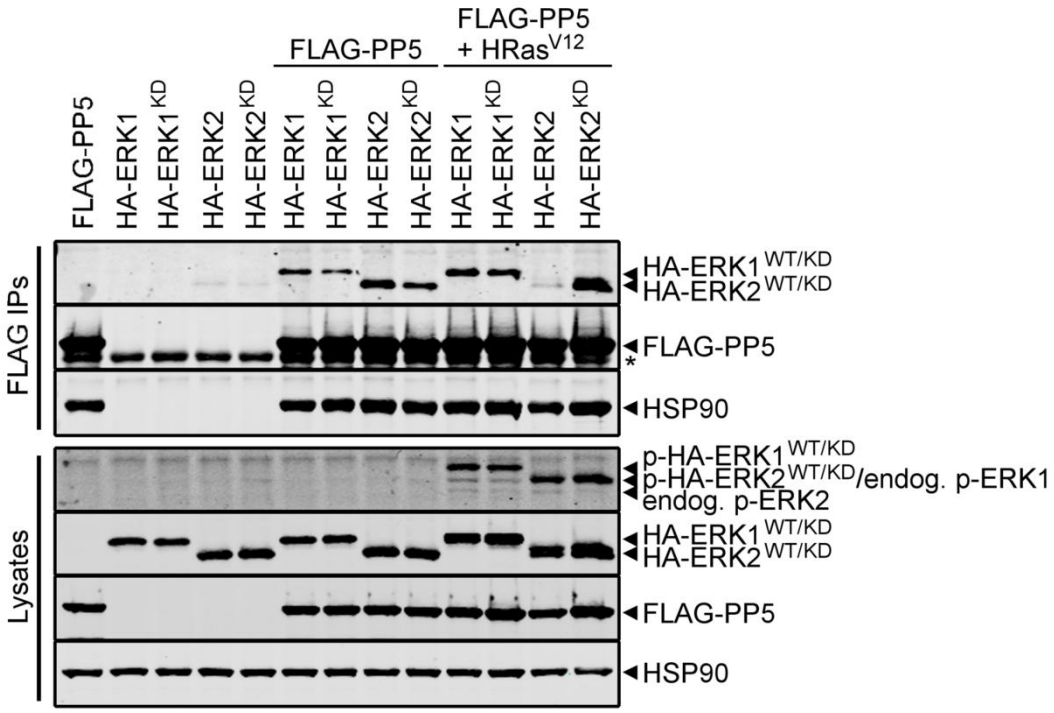

Figure 56. Kinase activity is required for HRas^{V12}-dependent disruption of the PP5•ERK2 complex.
Wildtype HA-ERK1 (*HA-ERK1^{WT}*), kinase dead HA-ERK1 (*HA-ERK1^{KD}*), wildtype HA-ERK2 (*HA-ERK2^{WT}*), and kinase dead HA-ERK2 (*HA-ERK2^{KD}*) were transfected into HEK-293FT cells alone or together with wildtype FLAG-PP5 in the absence or presence of HRas^{V12}. FLAG IPs and cell lysates were analyzed as described in Fig. 55 (n = 5). *, denotes IgG heavy chain.

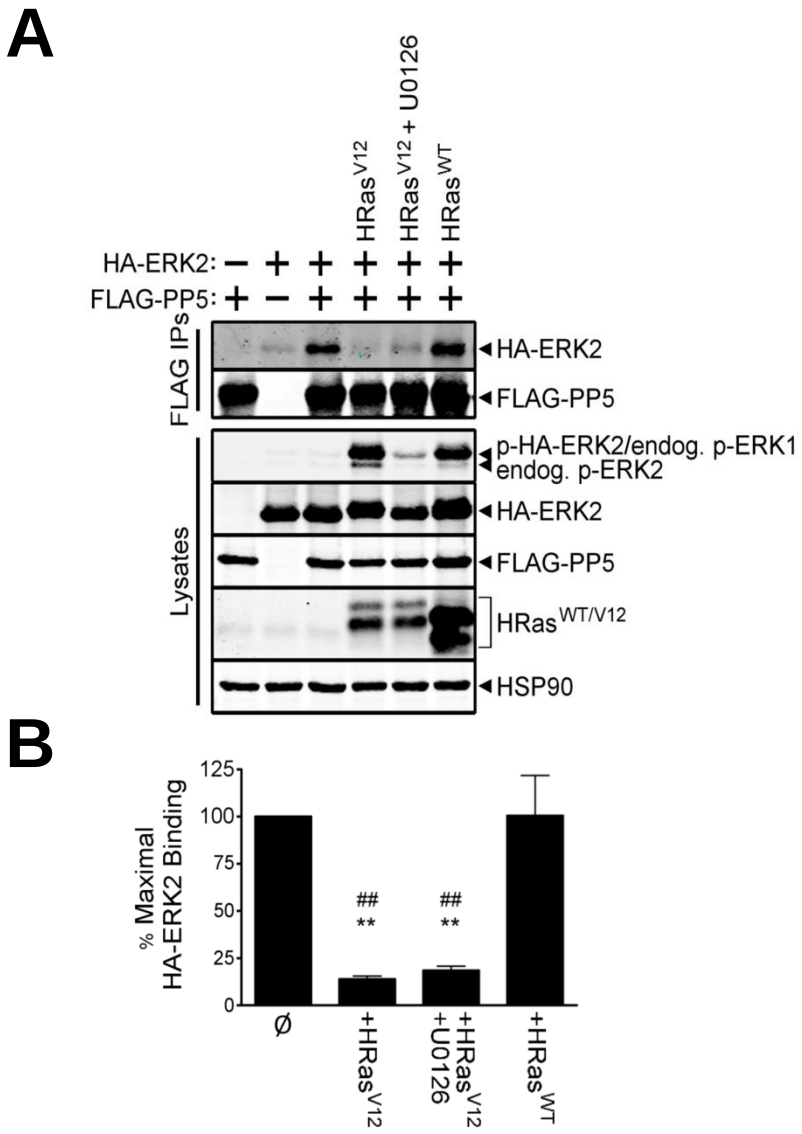

Figure 57. HRas^{V12}-induces disruption of the PP5•ERK2 complex independently of the activation state of ERK2.

A, HEK-293FT cells were transfected with (+) or without (-) HA-ERK2 and FLAG-PP5 together with HRas^{V12} or wildtype HRas (*HRas^{WT}*); cells were treated with the MEK inhibitor U0126 or DMSO for 30 min prior to lysis. FLAG immune complexes (*FLAG IPs*) and cell lysates were analyzed by Western using antibodies recognizing the indicated proteins. ***B***, Percent maximal binding of HA-ERK2 to FLAG-PP5. ERK2 binding signals, quantified for cells in *A* that co-expressed HA-ERK2 and FLAG-PP5, were normalized to levels of PP5 in the FLAG IPs and compared to the corresponding values in the absence of any Ras expression (*Ø*), which were set to 100. Significant reductions in PP5 binding to ERK2 were observed in the presence of HRas^{V12} (86.08% ± 1.62%) and following acute treatment with U0126 (81.95% ± 2.26%), while HRas^{WT} expression failed to disrupt the interaction. The results represent the means ± S.E. based on one-way ANOVA ($F(3,8)=20.42$, $p=.0004$). Tukey post-tests: ** vs. Ø, $p<.01$; ## vs. HRas^{WT}, $p<.01$. The data are representative of experiments performed three independent times with similar results.

support the idea that the $HRas^{V12}$/$KRas^{L61}$-mediated regulation of the PP5•ERK2 complex is independent of the activation state of ERK, yet paradoxically requires ERK2 activity.

PP5•ERK2 complexes regulate Raf1 phosphorylation

RAS-RAF-MEK-ERK signaling pathways acquire their highly adaptive character, in part, from multiple, ERK-mediated feedback phosphorylation loops that act to promote or suppress the activity of upstream components (324,325). While several feedback phosphorylation events on Raf1 are mediated by ERK1/2, the mechanism(s) that dictates the recruitment of ERK to Raf1 are unknown (248,326). Since PP5 dephosphorylation of Raf1 at pSer338 (133) temporally overlaps with the phosphorylation of Raf1 by ERK (248,326), we explored the possibility that PP5•ERK2 complexes play a role in the feedback phosphorylation state of Raf1. This question was addressed by examining the phospho-state of PP5-associated Raf1 from unstimulated and EGF-stimulated HEK-293FT cells transfected with combinations of Myc-Raf1, wildtype or kinase dead HA-ERK2, and wildtype or catalytically inactive FLAG-PP5. Western analysis of the FLAG immune complexes from cells expressing wildtype HA-ERK2 and FLAG-PP5 revealed an EGF-dependent increase in the phosphorylation of ERK-dependent sites (EDS) (i.e., Ser289/Ser296/Ser301) and the activating site (Ser338) on Raf1 (Fig. 58, Lanes 3 vs. 4). Expression of $PP5^{PD}$, in lieu of wildtype PP5, resulted in increased phosphorylation of EDS and Ser338 in unstimulated cells (Fig. 58, Lanes 3 vs. 6), which was augmented by treatment with EGF (Fig. 58, Lanes 6 vs. 7). In contrast to wildtype ERK2-expressing cells, EGF failed to promote increased phosphorylation of EDS in $ERK2^{KD}$-expressing cells, and in cells lacking wildtype HA-ERK2; however, the phosphorylation of Ser338

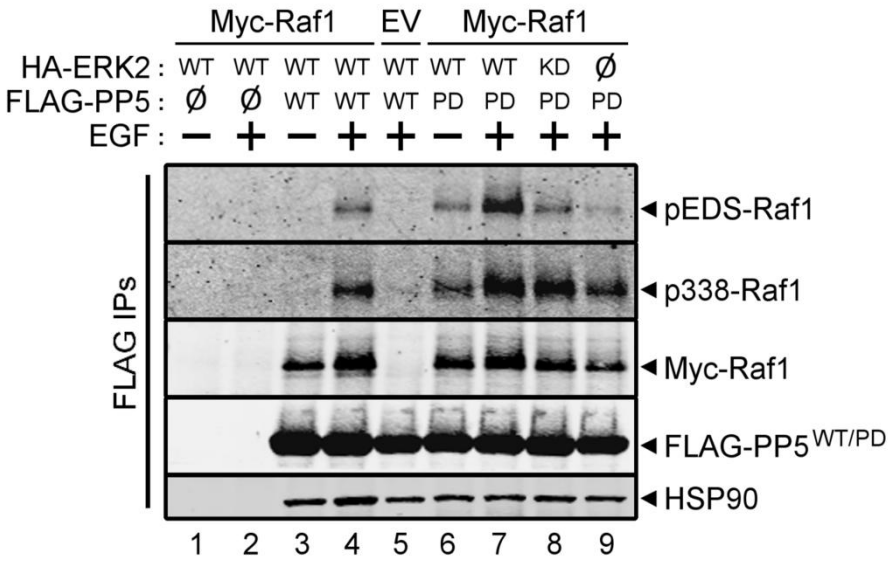

Figure 58. PP5•ERK2 complexes regulate EGF-dependent feedback phosphorylation of Raf1.
HEK-293FT cells were co-transfected with Myc-Raf1 or pcDNA3 (*EV*) together with the indicated combinations of nothing (*Ø*), wildtype (*WT*) or kinase dead HA-ERK2 (*KD*), and wildtype (*WT*) or catalytically inactive FLAG-PP5 (*PD*). Cells were treated with solvent containing (+) or lacking (-) 100 ng/mL EGF for 30 min prior to lysis. FLAG immune complexes (*FLAG IPs*) were analyzed by Western using phospho-Ser289/296/301-Raf1 (*pEDS-Raf1*), phospho-Ser338-Raf1 (*p338-Raf1*), Raf1, HSP90, and FLAG antibodies (n = 2).

remained elevated (Fig. 58, Lanes 7 vs. 8 vs. 9). Together, these findings indicate that ERK2 phosphorylates EDS but not Ser338 and that PP5 activity modulates the phosphorylation state of both EDS and Ser338.

To determine if $Rac1^{L61}$ or $HRas^{V12}$ influence the phosphorylation of PP5-associated Raf1 by modulating the PP5-ERK2 interaction, we co-expressed each small G protein in combination with wildtype or catalytically inactive forms of HA-ERK2 and FLAG-PP5. Western analysis of the FLAG immune complexes revealed very little phosphorylation of either EDS or Ser338 in the PP5-associated Raf1 in $Rac1^{L61}$-expressing cells containing wildtype PP5 (Fig. 59, Lanes 1 vs. 5). In contrast, the phosphorylation of both EDS and Ser338 in the PP5-associated Raf1 complexes were drastically elevated in cells expressing catalytically inactive PP5 (Fig. 59, Lanes 5 vs. 6). Comparable levels of Raf1 Ser338 phosphorylation were observed in cells co-expressing $PP5^{PD}$ and either wildtype ERK2 or $ERK2^{KD}$; however, only the phosphorylation of EDS was altered in $ERK2^{KD}$-expressing cells relative to wildtype ERK2-expressing cells (Fig. 59, Lanes 6 vs. 7). Surprisingly, the co-expression of $HRas^{V12}$ also promoted phosphorylation of EDS (Fig. 59, Lanes 1 vs. 10), via a mechanism that required ERK2 (Fig. 59, Lanes 9 vs. 10). Consistent with the EGF and $Rac1^{L61}$ data, loss of PP5 activity dramatically enhanced phosphorylation of both EDS and Ser338 in $HRas^{V12}$-expressing cells (Fig. 59, Lanes 10 vs. 11), while the additional loss of ERK2 activity partially reduced phosphorylation of EDS but not Ser338 (Fig. 59, Lanes 11 vs. 12). Together, these data support a dynamic role for PP5•ERK2 complexes in regulating Raf1 phosphorylation.

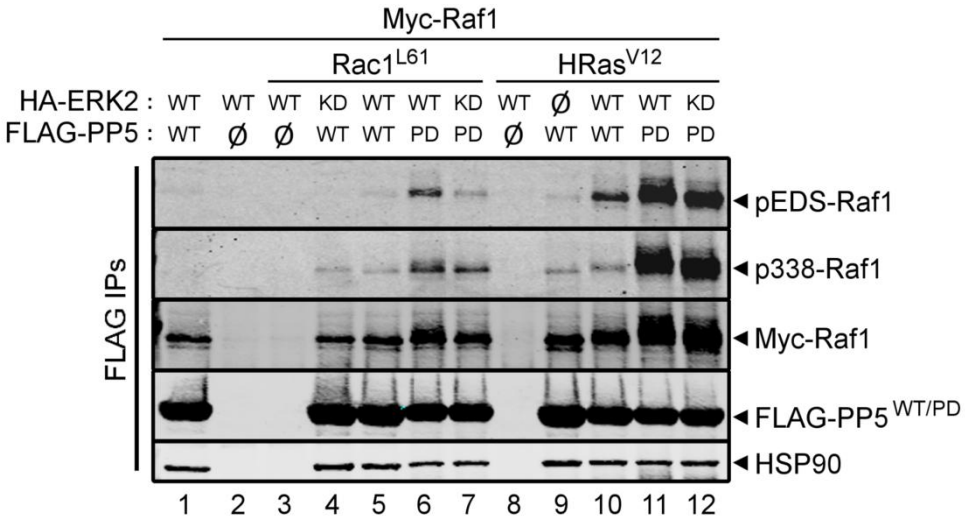

Figure 59. PP5•ERK2 complex-regulated feedback phosphorylation of Raf1 is elevated in Rac1^{L61}- and HRas^{V12}-expressing cells.
HEK-293FT cells were co-transfected to express Myc-Raf1, in the presence or absence of Rac1^{L61} or HRas^{V12}, together with the indicated combinations of nothing (*Ø*), wildtype (*WT*) or kinase dead HA-ERK2 (*KD*), and wildtype (*WT*) or catalytically inactive FLAG-PP5 (*PD*). FLAG IPs were analyzed as in Fig. 58 (n = 2).

Discussion

HSP90•PP5•protein kinase complexes

The studies herein confirm the known interactions of PP5 with HSP90 and Raf1 (133,318). In addition, we identify nine protein kinases as novel interacting partners for PP5. Since several of these kinases are HSP90 chaperone clients (311), we examined the relationship further to determine if the interaction of PP5 with each kinase could be detected in a complex that did not also contain HSP90. Our studies comparing HSP90-bound PP5 and monomeric forms of PP5 that are completely devoid of HSP90 (i.e., FLAG-PP5^{HBD} and RIPA-disrupted PP5•HSP90) revealed that the association of PP5 with some kinases (e.g., HA-CaMKIV, Myc-Raf1, HA-MST2) only occurs in the presence of HSP90, while other kinases (e.g., HA-p70S6K, HA-ERK1/2, HA_3-IKK1, Src^{Y529F}) associate with PP5 independently of HSP90, albeit to a lesser extent than observed in HSP90•PP5•protein kinase complexes (Figs. 43 and 46). This may indicate that the autoinhibitory conformation of monomeric PP5 yields an encounter complex with a reduced capacity to interact with the kinases (327). Alternatively, kinase binding sites on HSP90, which regulate HSP90-Akt interactions (328), may facilitate the association of PP5 with certain kinases when HSP90 is present. Our data also support the possibility that kinase binding determinants are located on PP5. Our data indicate monomeric PP5 can directly interact with ERK1/2 in the absence of HSP90; accordingly, analysis of the primary sequence of PP5 has revealed the presence of putative ERK docking domains and reverse D domains (329). Future studies will be needed to determine the precise role of HSP90 in the assembly, maintenance, or maturation of PP5•kinase complexes.

Regulation of PP5•ERK complexes and Raf1 feedback phosphorylation

Phosphatase•kinase complexes can be regulated by intramolecular reversible phosphorylation (135,137,141,149), and we observed that the $HRas^{V12}$-induced reduction in PP5-ERK2 binding required ERK2 activity (Fig. 56). It is unlikely that ERK1/2 phosphorylates PP5 directly, because PP5 lacks both the proline-directed serine/threonine (P-X-S/T) motif and the secondary DEF (Docking site for ERK, F-X-F-P) domain found in many ERK1/2 substrates (330). In addition, *in vitro* phosphorylation assays failed to detect ERK1/2-mediated phosphorylation of PP5 (data not shown). Nonetheless, our studies clearly demonstrate that the formation of PP5•ERK1/2 complexes can occur in a phosphatase and kinase activity-independent manner in unstimulated cells (Fig. 49). Thus, although PP5 activity is not required for its interaction with ERK1/2, PP5-mediated dephosphorylation could regulate the activity of the associated kinase, either directly or indirectly via HSP90. Consistent with a prior study (133), we did not detect any direct dephosphorylation of residues within the T-loop of ERK1/2 in our *in vitro* assays containing arachidonic acid-activated PP5 (data not shown). However, our data do not rule out the possibility that PP5-mediates dephosphorylation of residues outside the T-loop of ERK, which may directly impact kinase function. Moreover, as first reported for HSP90•heme-regulated eIF2α kinase (134), and also observed for Cdc37•HSP90•protein kinase complexes (312), PP5 may function to alter HSP90 chaperone activity, which in turn may regulate kinase maturation/activity.

The formation of macromolecular complexes containing protein kinases and phosphatases is important for maintaining the proper phosphorylation state of target proteins within key cell signaling pathways (331), including the RAS-RAF-MEK-ERK

cascade. Recent investigations indicate Raf1 activity is modulated via its association with two different protein phosphatases, PP2A and PP5. The extant data indicate PP2A functions as a positive regulator of Raf1, acting to dephosphorylate an inhibitory phospho-Ser259 site (137). In contrast, PP5 acts as a negative regulator of Raf1, by dephosphorylating a site (phospho-Ser338) that helps maintain Raf1 activity (133). In addition to Ser259 and Ser338 phosphorylation, Raf1 is subject to ERK-mediated feedback phosphorylation at several sites, including Ser289, Ser296, and Ser301 (collectively termed ERK Dependent Sites, EDS), which can either enhance or inhibit Raf1 function (248,326). Given the similar temporal relationship between ERK phosphorylation of EDS (248,326) and PP5 dephosphorylation of pSer338 (133), PP5•ERK complexes may be involved in coordinating these processes. Our current observations validate both the role of ERK in the regulation of EDS phosphorylation and the role of PP5 in the dephosphorylation of Raf1 at pSer338 (Figs. 58 and 59). In addition, our data reveal a novel role for PP5 in modulating the phosphorylation state of Raf1 at EDS (Figs. 58 and 59). PP2A has also been implicated in the dephosphorylation of pEDS (248), suggesting both phosphatases may act in concert to fine tune Raf1 activity. Interestingly, both PP5 and PP2A appear to play a similar role in the activation and feedback regulation of the dual specificity phosphatase CDC25 (125,332). Collectively, these findings suggest PP5•ERK complexes provide an additional control mechanism that regulates the phosphorylation status of Raf1 (Fig. 60).

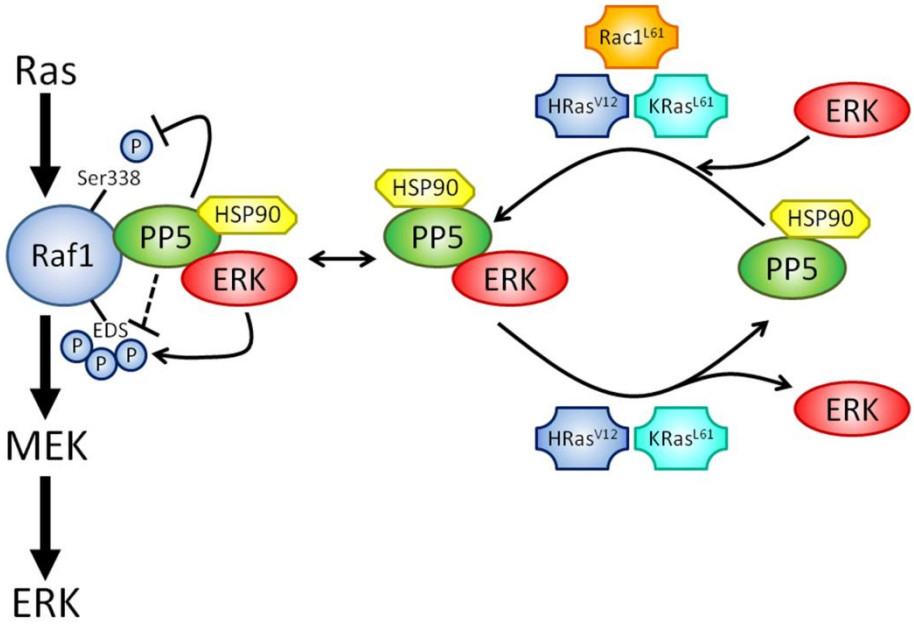

Figure 60. A model depicting the role and regulation of PP5•ERK complexes.
PP5 suppresses Raf1 signaling by dephosphorylating Ser338, a site important in making Raf1 permissive to further phosphorylation for full activation. Our studies support an additional role for PP5 in regulating the phosphorylation state of several ERK-dependent sites (EDS) on Raf1, and suggest that PP5•ERK complexes coordinate Raf1 feedback phosphorylation events. Furthermore, we find that PP5-ERK interactions are modulated by active small G proteins. Active Rac1 ($Rac1^{L61}$) promotes PP5-ERK1/2 interactions. In contrast, active HRas ($HRas^{V12}$) and KRas4B ($KRas^{L61}$), but not $KRas^{V12}$, promote rapid turnover of PP5•ERK2 complexes without affecting PP5•ERK1 complexes.

Small G protein-dependent regulation of PP5•ERK complexes and their potential involvement in oncogenic processes

The identification of PP5•ERK1/2 complexes in unstimulated cells prompted us to examine the possibility that PP5-ERK1/2 interactions can be altered in response to cell stimulation. Acute activation of the RAS-RAF-MEK-ERK signaling cascade with EGF did not affect the binding of PP5 with ERK1/2. However, chronic activation of this pathway, via expression of constitutively active small G proteins, drastically altered the levels of PP5•ERK1/2 complexes (Figs. 50, 51, 53, and 54). Expression of $Rac1^{L61}$ promoted the interaction of PP5 with both ERK1 and ERK2 (Figs. 50 and 51), while the expression of $HRas^{V12}$ led to decreased PP5-ERK2 binding without affecting PP5-ERK1 binding (Figs. 53 and 54). These observations suggest the two small G proteins likely utilize separate mechanisms and/or signaling pathways to modulate the assembly of PP5•ERK complexes in cells.

The expression of $HRas^{V12}$ and $KRas^{L61}$ greatly suppressed PP5-ERK2 binding, while the expression of $HRas^{WT}$ or $KRas^{WT}$ had no apparent affect (Fig. 54). This indicates that the diminishment in PP5-ERK2 interactions produced by $HRas^{V12}$ and $KRas^{L61}$ may not simply be the result of RAS proteins serving as a scaffold, rather it may reflect a consequence of the oncogenic activity of these RAS variants. Interestingly, $KRas^{V12}$ expression does not alter the binding between ERK2 and PP5, despite its potent activation of ERK (Fig. 54). This observation, together with the MEK inhibitor data (Fig. 57), indicate that chronic activation of the RAS-RAF-MEK-ERK pathway is not sufficient to alter the PP5-ERK2 interaction and suggests a different RAS effector pathway (e.g., PI3K, Tiam1, PLCε, RalGEF) may be involved in modulating PP5-ERK2

interactions. Although it has been known for some time that the various RAS isoforms demonstrate bias in their capacity to activate downstream effectors (284), recent work has revealed that variants of the same RAS isoform are also capable of differentially activating downstream effectors (333). Thus, it is unclear if the $HRas^{V12}$- and $KRas^{L61}$-dependent loss of PP5-ERK2 binding occurs through an undefined, shared effector pathway that is unaffected by $KRas^{V12}$ signaling or through unique pathways that eventually converge on PP5•ERK2, but not PP5•ERK1, complexes.

Active Rac1 promotes both the assembly of PP5•ERK2 complexes (Fig. 50), and PP5- and ERK2-coordinated regulation of Raf1 phosphorylation (Fig. 59). Surprisingly, oncogenic $HRas^{V12}$ expression also enhanced phosphorylation of EDS (Fig. 59, Lane 1 vs. 10), which seemingly contradicts our data showing that $HRas^{V12}$ decreased PP5-ERK2 binding (Figs. 53 and 54). Since co-immunoprecipitation assays only capture a single moment in a dynamic equilibrium, one possible explanation for the apparent decrease in the PP5-ERK2 interaction is that $HRas^{V12}$ promotes enhanced turnover of the PP5•ERK2 complex (Fig. 60), creating a false impression that the binding is decreased. A hallmark of protein kinase complexes subject to rapid turnover is increased phosphorylation of substrates (334). Consistent with this idea, we observe high levels of EDS phosphorylation on the PP5-associated Raf1 in cells expressing $HRas^{V12}$ (Figs. 58 and 59).

The ERK1/2 pathway integrates various cytosolic signals to regulate cellular proliferation, differentiation, growth, and apoptosis. Thus, it is no surprise that abnormal ERK signaling contributes to the formation and development of a variety of tumors and RASopathies (242,335). Although nearly 30% of all human tumors contain a gain-of-

function mutation in a *RAS* gene (336) (Fig. 61), several recent reports demonstrate that ERK2 - and not ERK1 - predominantly, if not exclusively, regulates several oncogenic properties of certain human tumors (337-340). We observed a striking difference in the responsiveness of PP5-ERK2 complexes to various oncogenic RAS proteins (Figs. 53 and 54). This not only highlights the contextually kaleidoscopic nature of the ERK interactome, but also hints at a potential mechanism through which oncogenic RAS mutants regulate signaling selectivity via the ERK2 isoform. Given that PP5 has been implicated in tumor development (341,342), it is possible that particular PP5 and ERK2 properties, such as their binding with one another, are dysregulated in the context of aberrant RAS signaling and contribute to particular oncogenic characteristics that define certain human tumors.

In summary, our studies identify novel PP5-ERK interactions and uncover a new role for small G proteins in regulating PP5•ERK1/2 complexes. Future studies of the mechanism(s) by which Rac1 and RAS modulate PP5-ERK1/2 interactions may shed light on the selective regulation of PP5•ERK2 complexes by constitutively active $HRas^{V12}$ and $KRas^{L61}$ and their role in tumor development. Raf1 was recently identified as one of the top ten essential genes in a model for murine embryonic $HRas^{V12}$-mediated epidermal hyperplasia (343). Our data support a role for PP5•ERK1/2 complexes in modulating the feedback phosphorylation of Raf1. As such, characterization of the ERK-mediated hyperphosphorylation of Raf1 in tumors harboring oncogenic mutations of the *RAS* gene may provide insight on the individual diversity of cancers as well as their susceptibility to signal transduction-modulating drugs. Given that protein phosphatases shape the spatiotemporal dynamics of signaling cascades and have emerged as attractive

A

Incidence Rates of *RAS* Gene Mutations in all Cancers		
K-*RAS*	H-*RAS*	N-*RAS*
25-30%	3%	8%

B

Frequency of *RAS* Codon Mutations in all Cancers			
	Gly12	Gly13	Gln61
K-*RAS*	86	13	1
H-*RAS*	54	9	34.5
N-*RAS*	24.4	12.7	60

Figure 61. Mutation rates of *RAS* genes and codons in all cancers.

A, Approximately 30% of all screened human tumors carry a somatic mutation in any 1 of the 3 *RAS* genes: K-*RAS*, H-*RAS*, or N-*RAS*. The highest incidence rate of oncogenic mutation occurs within the K-*RAS* locus. ***B***, Oncogenic mutations of the *RAS* genes are concentrated within three codons: Gly12, Gly13, or Gln61. The frequency rate of mutations within these codons varies among the three *RAS* genes (336).

targets for the treatment of diabetes, obesity, and cancer (344,345), it may be interesting to investigate the PP5•ERK complex as a therapeutic target of diseases characterized by aberrant ERK signaling.

CHAPTER V

SUMMARY AND FUTURE DIRECTIONS

Summary

The phosphorylation profile of signaling intermediates is determined by a dynamic equilibrium of protein kinase and phosphatase activities (346). Whereas protein kinases control signal magnitude more than duration, protein phosphatases modulate both the amplitude and duration of signal transduction (347), as well as restrict spontaneous pulses of signaling in the absence of stimulus (348). The macromolecular assembly of phosphatase•kinase complexes provides a mechanism to enhance the speed and selectivity of enzyme-substrate and protein-protein interactions to generate high fidelity cell signaling events. Moreover, the formation of phosphatase•kinase signaling modules allows for acute regulation of common substrate and intramolecular regulation of kinase activity by the associated phosphatase (or vice versa). The studies outlined in this dissertation examine the composition, regulation, and function of various protein serine/threonine phosphatase•kinase complexes, with a focus on the CaMKIV•PP2A (Chapter II), PP2A•Raf1 (Chapter III), and PP5•ERK1/2 (Chapter IV) complexes.

Although PP2A had been implicated in the regulation of CaMKIV phosphorylation *in vitro* (165), it was not until the purification of a CaMKIV•PP2A complex that we could attribute the rapid inactivation of CaMKIV activity in Jurkat T lymphocytes to a stably associated protein phosphatase (135). The CaMKIV-associated PP2A contains a regulatory Bα subunit, whose function in negatively regulating CaMKIV signaling was validated in cell-based CREB reporter assays using SV40 small t

antigen. However, these studies did not address the identity of the phospho-residue in CaMKIV targeted by PP2A. The phosphorylation of CaMKIV at multiple residues (Ser11, Ser12, and Thr200) fully activates the kinase and eliminates its dependence on Ca^{2+}/CaM binding (156). We hypothesized that PP2A regulated CaMKIV activity by targeting the phospho-site important for autonomous activity (i.e., phospho-Thr200). To address this hypothesis, we collaborated with Bethyl Laboratories, Inc. to generate an antibody that specifically recognizes the phospho-Thr200 epitope within CaMKIV (Fig. 8). Our analysis of the kinetics of CaMKIV signaling revealed that the activation of endogenous CaMKIV was acutely regulated by an associated phosphatase, which needed to be inhibited with okadaic acid in order to observe phosphorylation of Thr200 (Figs. 9 and 12). However, ectopically-expressed CaMKIV exhibited a distinct phosphorylation profile, characterized by rapid dephosphorylation of phospho-Thr200, even in the presence of okadaic acid (Fig. 12).

Our studies also revealed that the ectopically-expressed CaMKIV did not associate with endogenous $PP2A_C$ (Fig. 13), which probably accounted for the insensitivity of Thr200 dephosphorylation to okadaic acid (Fig. 12). Although the PP2A regulatory Bα and Bδ subunits associated with CaMKIV and promoted the recruitment of endogenous $PP2A_C$ to the kinase, we did not observe a change in p-Thr200 levels in ionomycin-stimulated cells overexpressing the Bα subunit (Figs. 14-16). We subsequently tested the ability of Bα-containing holoenzymes to regulate the phosphorylation state of CaMKIV *in vitro*, and found that this PP2A holoenzyme failed to dephosphorylate p-Thr200 (Fig. 17). These data suggest that Bα- and Bδ-containing PP2A holoenzymes may play a different role in regulating CaMKIV function. Since we

observed dephosphorylation of p-Thr200 *in vitro* following the addition of purified $PP2A_C$, we hypothesized that a different form of PP2A may regulate p-Thr200 levels (Fig. 18). In support of this idea, we demonstrated that the association of alpha4•$PP2A_C$ complexes with CaMKIV is regulated in a stimulus-dependent manner (Figs. 11, 19, and 20). Future studies aimed at addressing the roles of different oligomeric forms of PP2A in the regulation of CaMKIV signaling will be addressed below in "Future Directions."

Reports from us and others have clarified the roles specific PP2A holoenzymes play in the control of Raf1-MEK-ERK signaling. In contrast to our CaMKIV studies, Bα- and Bδ-containing PP2A holoenzymes function as positive regulators of Raf1-MEK-ERK signaling. These holoenzymes associate with Raf1 and catalyze the dephosphorylation of an inhibitory site in this kinase (phospho-Ser259), thereby promoting Raf1 activation and the subsequent activation of MEK1/2 and ERK1/2 (137). However, the regulatory mechanisms controlling ABαC-Raf1 and ABδC-Raf1 interactions in response to various stimuli is unknown. Although EGF-stimulated ERK phosphorylation was enhanced in cells overexpressing Bδ (Fig. 24), we could only detect relatively small changes in the ABδC-Raf1 interaction (Fig. 25). Furthermore, these changes did not temporally correlate with the stimulus-induced increases in ERK activity. Given the relatively small difference and variability of these assays, we utilized cell-permeable chemical crosslinking reagents in an attempt to trap transient $AB\delta_{FLAG}C$-Raf1 interactions following EGF stimulation.

Although crosslinking with DTME enhanced $B\delta_{FLAG}$-Raf1 interactions (Fig. 30), we did not observe a difference in the EGF-stimulated PP2A-Raf1 interaction profiles between noncrosslinked and crosslinked samples (data not shown). Interestingly, these studies revealed that the association of the PP2A core dimer with Bδ-FLAG was

disrupted in the presence of DTME in cells but not *in vitro* (Figs. 30-32). Utilizing the recently developed method of ReCLIP (238), we subjected ABδC, Raf1, and ABδC•Raf1 complexes isolated from crosslinked cells to mass spectrometry to identify novel binding partners that could potentially regulate ABδC-Raf1 interactions in a stimulus-dependent manner. Although DSP, DTME, and both DSP and DTME treatments yielded overlapping, but distinct ABδC interactomes (Table 1 and Figs. 33 and 34), we narrowed our focus to studying candidate proteins co-purifying with the ABδC•Raf1 complex following DTME treatment (Fig. 35). These proteomic studies identified several putative candidates that may regulate, or be regulated by, ABδC•Raf1 signaling modules (Table 2). Analysis of these ABδC•Raf1-interacting proteins indicated an enrichment for proteins localized to particular subcellular compartments as well as specific cellular processes, hinting at novel signaling events that involve ABδC•Raf1 complexes (Figs. 36 and 37). The rationale behind further characterizing ABδC•Raf1 complex candidate interacting proteins was presented in the Discussion of Chapter III. Experiments performed in preparation for the ReCLIP/mass spectrometry studies serendipitously revealed an interaction between AB′βC and Raf1, suggesting that AB′βC may be involved in the regulation of other Raf1 phospho-sites (Fig. 38). Future studies to examine the functional role of AB′βC in Raf1-MEK-ERK signaling will be addressed below in "Future Directions."

Serine/threonine protein phosphatase 5 (PP5, *PPP5C*) is known to interact with the chaperonin heat shock protein 90 (HSP90), and is involved in the regulation of multiple cellular signaling cascades that control diverse cellular processes such as cell growth, differentiation, proliferation, motility, and apoptosis. We showed that PP5

associates with multiple protein kinases, including the PP2A-associated Raf1 and ERKs (Figs. 41-43 and 45). Studies using mutant forms of PP5 revealed that the formation of PP5•ERK1 and PP5•ERK2 complexes partially depends on HSP90 binding to PP5, but does not require PP5 or ERK1/2 activity (Figs. 46 and 49). However, PP5 and ERK activity regulated the phosphorylation state of Raf1 kinase, an upstream activator of ERK signaling (Fig. 58). While expression of constitutively active Rac1 promoted the assembly of PP5•ERK1/2 complexes, acute activation of ERK1/2 failed to influence the phosphatase-kinase interaction (Figs. 50, 51, and 53). Introduction of oncogenic HRas ($HRas^{V12}$) had no effect on PP5-ERK1 binding but selectively decreased the interaction of PP5 with ERK2, in a manner that was independent of PP5 and MAPK/ERK kinase (MEK) activity, yet paradoxically required ERK2 activity (Figs. 53, 56, and 57). Additional studies conducted with oncogenic variants of KRas4B revealed that $KRas^{L61}$, but not $KRas^{V12}$, also decreased the PP5-ERK2 interaction (Fig. 54). The expression of wildtype HRas or KRas proteins failed to reduce PP5-ERK2 binding, indicating that the effect was specific to $HRas^{V12}$ and $KRas^{L61}$ gain-of-function mutations (Fig. 54). These findings revealed a novel, differential responsiveness of PP5-ERK1 and PP5-ERK2 interactions to select oncogenic RAS variants, and also support a role for PP5•ERK complexes in regulating the feedback phosphorylation of PP5-associated Raf1 (Fig. 58 and 59) (151). Future studies regarding the PP5-ERK interaction were briefly presented in the Discussion of Chapter IV. More detailed experiments on this topic will be presented below in "Future Directions."

Future Directions

My studies on the CaMKIV•PP2A, PP2A•Raf1, PP2A•Raf1•PP5, and PP5•ERK signaling modules have afforded a better understanding of the composition, regulation, and function of these protein serine/threonine phosphatase•kinase complexes. Although these studies have provided key insights, several questions still remain.

CaMKIV•PP2A Studies

Does alpha4 regulate CaMKIV function?

Jurkat T lymphocytes are an ideal system for testing if alpha4 plays a role in regulating CaMKIV function, as these cells express high levels of CaMKIV and alpha4. To test if alpha4 modulates CaMKIV function, RNAi technologies can be exploited to specifically knockdown alpha4 in unstimulated and CD3 receptor-stimulated Jurkat T cells. Changes in CaMKIV signaling at the molecular (phosphorylation of CaMKIV and CREB) and cellular (cytokine production (e.g., interleukin-2 (IL-2)) and differentiation into T helper subtypes) levels can be monitored to assess whether alpha4 regulates CaMKIV signaling in a positive or negative manner. Changes in p-Thr200 would indicate that the effect of alpha4 is occurring at the level of, or upstream of, CaMKIV. In parallel with these RNAi studies to suppress alpha4 expression, we could diminish alpha4 function by overexpressing the B-box1 domain of Mid1 (a domain in the Mid1 protein responsible for binding alpha4) to competitively inhibit the association of alpha4 with CaMKIV.

Does CaMKIV alter alpha4 function?

Alpha4 plays an important role in regulating the stability of $PP2A_C$ (83). It may be that alpha4 does not regulate CaMKIV function, but rather CaMKIV modulates the function of alpha4 via phosphorylation. Scanning the alpha4 primary amino acid sequence for putative CaMKIV targeting motifs (consensus: Hyd-X-R-X-X-S/T) revealed a candidate phospho-site, Ser224. To determine if alpha4 is targeted for CaMKIV phosphorylation, *in vitro* assays using [γ-^{32}P]ATP and CaMKK-activated CaMKIV in the presence or absence of phosphatase inhibitors can be performed. Both purified alpha4 and alpha4•$PP2A_C$ complexes would be tested as potential substrates, and CREB would be used as a positive control. Should the *in vitro* studies reveal that alpha4 is a substrate of CaMKIV, additional experiments will be carried out to analyze the ability of CaMKIV to phosphorylate alpha4 in cells. Following cellular stimulation with CD3 antibody or PMA changes in the phospho-state of immunopurified alpha4 can be monitored by Western (using phospho-Ser and phospho-Thr antibodies) and verified by mass spectrometry. One way to determine if CaMKIV alters the ability of alpha4 to modulate the stability of $PP2A_C$ in cells is to monitor $PP2A_C$ turnover in cycloheximide treated cells in the presence or absence of the CaMKIV inhibitor KN93.

Identify the oligomeric forms of PP2A that dephosphorylate the N-terminal phospho-serines and phospho-Thr200 in CaMKIV.

Given the prerequisite phosphorylation of N-terminal serines (i.e., Ser12 and Ser13) in the activation of CaMKIV, the phospho-state of these residues should dictate the ability of CaMKK to phosphorylate Thr200. Bα-containing PP2A holoenzymes have

been presumed to catalyze the dephosphorylation of phospho-Thr200; however, our *in vitro* and in cell data suggest that ABαC does not regulate this particular residue. One possibility is that ABαC instead regulates the N-terminal phospho-serines, which would represent a paradigm shift in our understanding of the role of the PP2A-associated CaMKIV. *In vitro* kinase assays with radiolabeled ATP can be carried out to examine the ability of CaMKIV to autophosphorylate these serine sites in the absence or presence of ABαC holoenzymes together without or with okadaic acid. Since CaMKK is absent in this assay, Thr200 should not be phosphorylated and loss of radiolabeled phosphate from CaMKIV in the absence of okadaic acid would indicate that the dephosphorylation of sites other than Thr200 is occurring.

Mutation of the N-terminal serines in CaMKIV with phospho-mimetic residues (e.g., Asp, Glu) would allow us to assess Thr200 phosphorylation in ionomycin-stimulated cells expressing SV40 small t. We would predict that levels of phospho-Thr200 in the CaMKIV mutants would be insensitive to SV40 small t expression, providing additional support that Bα- and Bδ-containing PP2A holoenzymes indirectly regulate Thr200 phosphorylation via the direct modulation of phosphorylation state of the N-terminal serines.

Since we can observe dephosphorylation of phospho-Thr200 with purified $PP2A_C$, it is possible that a different oligomeric form of PP2A regulates phospho-Thr200 (e.g., alpha4•$PP2A_C$). Given the interaction of CaMKIV with alpha4, it would be prudent to couple *in vitro* CaMKK phosphorylation assays using CaMKIV as the substrate with dephosphorylation assays performed in the presence or absence of alpha4•$PP2A_C$ complexes together with or without okadaic acid. Loss of radiolabeled phosphate from

CaMKK-phosphorylated CaMKIV in the absence of okadaic acid would indicate that alpha4•PP2A$_C$ can dephosphorylate residues in CaMKIV. Dephosphorylation assays can also be performed with the phospho-mimetic CaMKIV mutants, which would eliminate the N-terminal serines as a source of the liberated radiolabeled phosphate. Alpha4•PP2A$_C$ may be unable to dephosphorylate CaMKIV *in vitro*, which could suggest alpha4 plays a role in the biogenesis of PP2A holoenzymes that regulate the phospho-state of CaMKIV.

PP2A•Raf1 Studies

Do AB′βC holoenzymes regulate Raf1-MEK-ERK signaling?

To determine if AB′βC holoenzymes play a role in modulating Raf1-MEK-ERK signaling, a comparison of ERK phosphorylation profiles can be made between empty vector control cells and cells overexpressing FLAG-B′β following treatment with stimulus (e.g., EGF, PDGF, PMA, insulin). An increase in ERK phosphorylation would suggest that AB′βC holoenzymes positively regulate MAPK signaling, while a decrease would indicate AB′βC negatively regulates this pathway. In parallel with the overexpression studies, the reciprocal experiment to analyze ERK phosphorylation in cells where endogenous B′β expression has been reduced using RNAi can be carried out.

Does AB′βC affect Raf1 signaling?

AB′βC holoenzymes may regulate MAPK signaling by dephosphorylating ERK1/2 or upstream signaling components (e.g., MEK1/2 or Raf1). We can assess the step at which AB′βC modulates signaling by overexpressing B′β in the presence of constitutively active (CA) mutants of RAS, Raf1, or MEK1/2. An augmentation in ERK

phosphorylation with certain CA mutants but not others would indicate AB′βC positively regulates signaling. Likewise, a decrease in ERK phosphorylation is expected if AB′βC inhibits MAPK signaling in the presence of select CA mutants. In addition, a panel of chemical inhibitors could be used to selectively inhibit each step in the signaling cascade in stimulated cells overexpressing B′β. Such experiments would allow us to narrow in on the step in the pathway modulated by AB′βC.

Does AB′βC modulate kinase-independent targets of Raf1?

We may not observe any alterations in Raf1-MEK-ERK signaling following overexpression or knockdown of B′β; however, there are other Raf1 interacting proteins that could be regulated by AB′βC. *Raf1*$^{-/-}$ mice die in embryogenesis, but replacing the *Raf1* locus with a catalytically inactive *Raf1* gene, in which tyrosines 340 and 341 are mutated to phenylalanines, allows the embryos to survive for over a year with no noticeable defects (349). These data indicate that Raf1 likely has kinase-independent, scaffolding functions. Several proteins have been identified as being regulated by Raf1 in a catalytically-independent manner, including apoptosis signal-regulating kinase 1 (ASK1) (350). Raf1 has been shown to interact with ASK1 and inhibit ASK1-mediated apoptosis; however, the mechanism of inhibition is not yet known (351). To assess if AB′βC regulates ASK1-mediated apoptosis, B′β levels can be overexpressed or knocked down in cells to monitor the effect on apoptosis following cellular stress (e.g., hypoxia, DNA-damage, oxidative stress). An alteration in the phosphorylation of ASK1 would indicate that the AB′βC effect occurs upstream of ASK1 or implicate AB′βC in the regulation of apoptosis via the modulation of phosphorylated ASK1. Should modulating

the levels of B′β affect ASK1-mediated apoptosis and ASK1 phosphorylation, the ability of AB′βC to directly dephosphorylate phospho-ASK1 will be assessed by performing *in vitro* dephosphorylation assays, which may require the presence of Raf1 for dephosphorylation to occur. Likewise, studies to examine the interaction of AB′βC and ASK1 may require the presence of Raf1. To ascertain if the modulation of apoptosis by AB′βC is Raf1-dependent, apoptosis can be monitored in cells overexpressing B′β in the absence or presence of Raf1 knockdown. We would predict that knockdown of Raf1 expression would prevent the B′β-mediated reduction in apoptosis, indicating that AB′βC•Raf1 complexes play an important role in regulating ASK1-mediated apoptosis.

PP5•ERK Studies

Does PP5 directly dephosphorylate the ERK-dependent sites (EDS) in Raf1?

Our data reveal a novel role for PP5 in modulating the phosphorylation state of Raf1 at EDS. ERK-mediated phosphorylation of Raf1 is enhanced in the presence of catalytically inactive PP5, but it is currently unclear if PP5 directly dephosphorylates EDS. To address this, *in vitro* dephosphorylation assays using ERK-phosphorylated Raf1 and active PP5 can be carried out. Alterations in Raf1 phosphorylation can be monitored by Western analysis using phospho-specific antibodies recognizing the EDS.

Mapping the PP5-ERK1/2 interaction sites.

Future studies to address the functional role(s) of the PP5•ERK1 and PP5•ERK2 complexes will require methods to selectively disrupt the PP5-ERK1/2 interaction (e.g., peptide competition, binding site mutations). PP5 contains several putative ERK docking (D) and reverse D domains, present in both the N-terminal and C-terminal globular

domains. The list of candidate ERK-binding sites within PP5 can be narrowed down by assessing the ability of PP5 deletion mutants, which lack the N- or C-terminal globular domain, to interact with ERK in immunoprecipitation assays. Subsequent mutation to reverse the charge on key basic residues these potential ERK-binding sites within PP5 is predicted to reduce or eliminate the binding of PP5 to ERK. Once we have identified a PP5 mutant unable to associate with ERK, we can generate a GST-fusion protein containing a peptide spanning the ERK binding site of PP5 and determine if the fusion protein can act as bait to pulldown ERK, thereby validating the ability of the peptide to associate with ERK. Finally, we can ensure that excess peptide blocks the interaction of ERK with the GST-fusion protein and, ultimately, PP5 *in vitro* and in cells (352).

What is the RAS effector pathway responsible for destabilizing the PP5-ERK2 interaction?

The $HRas^{V12}$- and $KRas^{L61}$-dependent alteration in PP5•ERK2 complexes is independent of MEK activity but requires ERK2 activity. To address which effector pathway(s) downstream of $HRas^{V12}$ and $KRas^{L61}$ is involved, genetic and pharmacologic tools can be used to ascertain the candidate signaling pathway(s) (e.g., PI3K, Tiam1, PLCε, and/or RalGEF) that may be responsible for this effect. One genetic approach to this question is to use RAS effector domain mutants (353,354), such as $HRas^{12V/35S}$, $HRas^{12V/37G}$, and $HRas^{12V/40C}$, which differentially activate Raf1 kinase, RalGEF, and PI3K effector signaling, respectively. A decrease in PP5-ERK binding in the presence of one mutant Ras but not the others would implicate that signaling pathway to which the Ras can signal to in the $HRas^{V12}$ effect. Dominant negative effector mutants could also be

expressed to stabilize the PP5-ERK2 interaction in the presence of oncogenic RAS, but a more selective genetic approach involves using RNAi to knockdown the expression of particular RAS effectors. As an alternative to genetic disruption of RAS effector pathways, pharmacological inhibitors could be used. Such approaches can also be used to determine if $HRas^{V12}$ and $KRas^{L61}$ mediate their effects through the same effector pathway or through different pathways that ultimately converge upon PP5•ERK2, but not PP5•ERK1, signaling complexes.

REFERENCES

1. Bairoch, A., and Apweiler, R. (2000) The SWISS-PROT protein sequence database and its supplement TrEMBL in 2000. *Nucleic acids research* **28**, 45-48
2. Khoury, G. A., Baliban, R. C., and Floudas, C. A. (2011) Proteome-wide post-translational modification statistics: frequency analysis and curation of the swiss-prot database. *Scientific reports* **1**
3. Hanks, S. K., and Hunter, T. (1995) Protein kinases 6. The eukaryotic protein kinase superfamily: kinase (catalytic) domain structure and classification. *FASEB journal : official publication of the Federation of American Societies for Experimental Biology* **9**, 576-596
4. Manning, G., Whyte, D. B., Martinez, R., Hunter, T., and Sudarsanam, S. (2002) The Protein Kinase Complement of the Human Genome. *Science* **298**, 1912-1934
5. Hanks, S. K. (2003) Genomic analysis of the eukaryotic protein kinase superfamily: a perspective. *Genome biology* **4**, 111
6. Olsen, J. V., Blagoev, B., Gnad, F., Macek, B., Kumar, C., Mortensen, P., and Mann, M. (2006) Global, in vivo, and site-specific phosphorylation dynamics in signaling networks. *Cell* **127**, 635-648
7. Oppermann, F. S., Gnad, F., Olsen, J. V., Hornberger, R., Greff, Z., Keri, G., Mann, M., and Daub, H. (2009) Large-scale proteomics analysis of the human kinome. *Molecular & cellular proteomics : MCP* **8**, 1751-1764
8. Shi, Y. (2009) Serine/threonine phosphatases: mechanism through structure. *Cell* **139**, 468-484
9. Lammers, T., and Lavi, S. (2007) Role of type 2C protein phosphatases in growth regulation and in cellular stress signaling. *Critical reviews in biochemistry and molecular biology* **42**, 437-461
10. Fjeld, C. C., and Denu, J. M. (1999) Kinetic analysis of human serine/threonine protein phosphatase 2Calpha. *The Journal of biological chemistry* **274**, 20336-20343
11. Pan, C., Liu, H. D., Gong, Z., Yu, X., Hou, X. B., Xie, D. D., Zhu, X. B., Li, H. W., Tang, J. Y., Xu, Y. F., Yu, J. Q., Zhang, L. Y., Fang, H., Xiao, K. H., Chen, Y. G., Wang, J. Y., Pang, Q., Chen, W., and Sun, J. P. (2013) Cadmium is a potent inhibitor of PPM phosphatases and targets the M1 binding site. *Scientific reports* **3**, 2333
12. Pato, M. D., and Kerc, E. (1991) Regulation of smooth muscle phosphatase-II by divalent cations. *Molecular and cellular biochemistry* **101**, 31-41
13. Cohen, P. T. W. (2011) Phosphatase Families Dephosphorylating Serine and Threonine Residues in Proteins. in *Transduction Mechanisms in Cellular Signaling: Cell Signaling Collection* (Edward A. Dennis, R. A. B. ed.), First Ed., Academic Press. pp 105-122
14. Zhang, Y., Kim, Y., Genoud, N., Gao, J., Kelly, J. W., Pfaff, S. L., Gill, G. N., Dixon, J. E., and Noel, J. P. (2006) Determinants for dephosphorylation of the RNA polymerase II C-terminal domain by Scp1. *Molecular cell* **24**, 759-770
15. Ingebritsen, T. S., and Cohen, P. (1983) The Protein Phosphatases Involved in Cellular Regulation. *European Journal of Biochemistry* **132**, 255-261

16. Ingebritsen, T. S., Foulkes, J. G., and Cohen, P. (1983) The protein phosphatases involved in cellular regulation. 2. Glycogen metabolism. *European journal of biochemistry / FEBS* **132**, 263-274
17. Cohen, P. T. W. (1994) Nomenclature and chromosomal localization of human protein serine/threonine phosphatase genes. *Adv Protein Phosphat* **8**, 371-376
18. Mumby, M. C., and Walter, G. (1993) Protein serine/threonine phosphatases: structure, regulation, and functions in cell growth. *Physiological reviews* **73**, 673-699
19. Walter, G., and Mumby, M. (1993) Protein serine/threonine phosphatases and cell transformation. *Biochimica et biophysica acta* **1155**, 207-226
20. Cohen, P. T. (1997) Novel protein serine/threonine phosphatases: variety is the spice of life. *Trends in biochemical sciences* **22**, 245-251
21. Honkanen, R. E., and Golden, T. (2002) Regulators of serine/threonine protein phosphatases at the dawn of a clinical era? *Current medicinal chemistry* **9**, 2055-2075
22. Honkanen, R. E., Zwiller, J., Daily, S. L., Khatra, B. S., Dukelow, M., and Boynton, A. L. (1991) Identification, purification, and characterization of a novel serine/threonine protein phosphatase from bovine brain. *The Journal of biological chemistry* **266**, 6614-6619
23. Chen, M. X., McPartlin, A. E., Brown, L., Chen, Y. H., Barker, H. M., and Cohen, P. T. (1994) A novel human protein serine/threonine phosphatase, which possesses four tetratricopeptide repeat motifs and localizes to the nucleus. *The EMBO journal* **13**, 4278-4290
24. Chinkers, M. (1994) Targeting of a distinctive protein-serine phosphatase to the protein kinase-like domain of the atrial natriuretic peptide receptor. *Proceedings of the National Academy of Sciences of the United States of America* **91**, 11075-11079
25. Becker, W., Kentrup, H., Klumpp, S., Schultz, J. E., and Joost, H. G. (1994) Molecular cloning of a protein serine/threonine phosphatase containing a putative regulatory tetratricopeptide repeat domain. *The Journal of biological chemistry* **269**, 22586-22592
26. da Cruz e Silva, O. B., da Cruz e Silva, E. F., and Cohen, P. T. (1988) Identification of a novel protein phosphatase catalytic subunit by cDNA cloning. *FEBS Lett* **242**, 106-110
27. Brewis, N. D., Street, A. J., Prescott, A. R., and Cohen, P. T. (1993) PPX, a novel protein serine/threonine phosphatase localized to centrosomes. *The EMBO journal* **12**, 987-996
28. Bastians, H., and Ponstingl, H. (1996) The novel human protein serine/threonine phosphatase 6 is a functional homologue of budding yeast Sit4p and fission yeast ppe1, which are involved in cell cycle regulation. *Journal of cell science* **109 (Pt 12)**, 2865-2874
29. Dombradi, V., Axton, J. M., Glover, D. M., and Cohen, P. T. (1989) Molecular cloning and chromosomal localization of a novel Drosophila protein phosphatase. *FEBS Lett* **247**, 391-395
30. Huang, X., and Honkanen, R. E. (1998) Molecular cloning, expression, and characterization of a novel human serine/threonine protein phosphatase, PP7, that

is homologous to Drosophila retinal degeneration C gene product (rdgC). *The Journal of biological chemistry* **273**, 1462-1468
31. Sherman, P. M., Sun, H., Macke, J. P., Williams, J., Smallwood, P. M., and Nathans, J. (1997) Identification and characterization of a conserved family of protein serine/threonine phosphatases homologous to Drosophila retinal degeneration C. *Proceedings of the National Academy of Sciences of the United States of America* **94**, 11639-11644
32. Montini, E., Rugarli, E. I., Van de Vosse, E., Andolfi, G., Mariani, M., Puca, A. A., Consalez, G. G., den Dunnen, J. T., Ballabio, A., and Franco, B. (1997) A novel human serine-threonine phosphatase related to the Drosophila retinal degeneration C (rdgC) gene is selectively expressed in sensory neurons of neural crest origin. *Human molecular genetics* **6**, 1137-1145
33. Alonso, A., Sasin, J., Bottini, N., Friedberg, I., Osterman, A., Godzik, A., Hunter, T., Dixon, J., and Mustelin, T. (2004) Protein tyrosine phosphatases in the human genome. *Cell* **117**, 699-711
34. Lin, X. H., Walter, J., Scheidtmann, K., Ohst, K., Newport, J., and Walter, G. (1998) Protein phosphatase 2A is required for the initiation of chromosomal DNA replication. *Proceedings of the National Academy of Sciences of the United States of America* **95**, 14693-14698
35. Ruediger, R., Van Wart Hood, J. E., Mumby, M., and Walter, G. (1991) Constant expression and activity of protein phosphatase 2A in synchronized cells. *Molecular and cellular biology* **11**, 4282-4285
36. Janssens, V., and Goris, J. (2001) Protein phosphatase 2A: a highly regulated family of serine/threonine phosphatases implicated in cell growth and signalling. *The Biochemical journal* **353**, 417-439
37. Kinoshita, K., Nemoto, T., Nabeshima, K., Kondoh, H., Niwa, H., and Yanagida, M. (1996) The regulatory subunits of fission yeast protein phosphatase 2A (PP2A) affect cell morphogenesis, cell wall synthesis and cytokinesis. *Genes to cells : devoted to molecular & cellular mechanisms* **1**, 29-45
38. Snaith, H. A., Armstrong, C. G., Guo, Y., Kaiser, K., and Cohen, P. T. (1996) Deficiency of protein phosphatase 2A uncouples the nuclear and centrosome cycles and prevents attachment of microtubules to the kinetochore in Drosophila microtubule star (mts) embryos. *Journal of cell science* **109 (Pt 13)**, 3001-3012
39. Gotz, J., Probst, A., Ehler, E., Hemmings, B., and Kues, W. (1998) Delayed embryonic lethality in mice lacking protein phosphatase 2A catalytic subunit Calpha. *Proceedings of the National Academy of Sciences of the United States of America* **95**, 12370-12375
40. Fujiki, H., and Suganuma, M. (2011) Tumor promoters--microcystin-LR, nodularin and TNF-alpha and human cancer development. *Anti-cancer agents in medicinal chemistry* **11**, 4-18
41. Pallas, D. C., Shahrik, L. K., Martin, B. L., Jaspers, S., Miller, T. B., Brautigan, D. L., and Roberts, T. M. (1990) Polyoma small and middle T antigens and SV40 small t antigen form stable complexes with protein phosphatase 2A. *Cell* **60**, 167-176
42. Shtrichman, R., Sharf, R., Barr, H., Dobner, T., and Kleinberger, T. (1999) Induction of apoptosis by adenovirus E4orf4 protein is specific to transformed

cells and requires an interaction with protein phosphatase 2A. *Proceedings of the National Academy of Sciences of the United States of America* **96**, 10080-10085
43. Tung, H. Y., De Rocquigny, H., Zhao, L. J., Cayla, X., Roques, B. P., and Ozon, R. (1997) Direct activation of protein phosphatase-2A0 by HIV-1 encoded protein complex NCp7:vpr. *FEBS Lett* **401**, 197-201
44. Eichhorn, P. J., Creyghton, M. P., and Bernards, R. (2009) Protein phosphatase 2A regulatory subunits and cancer. *Biochimica et biophysica acta* **1795**, 1-15
45. Kowluru, A., and Matti, A. (2012) Hyperactivation of protein phosphatase 2A in models of glucolipotoxicity and diabetes: potential mechanisms and functional consequences. *Biochemical pharmacology* **84**, 591-597
46. Rudrabhatla, P., and Pant, H. C. (2011) Role of protein phosphatase 2A in Alzheimer's disease. *Current Alzheimer research* **8**, 623-632
47. Torrent, L., and Ferrer, I. (2012) PP2A and Alzheimer disease. *Current Alzheimer research* **9**, 248-256
48. Cohen, P. (1989) The structure and regulation of protein phosphatases. *Annual review of biochemistry* **58**, 453-508
49. Kerk, D., Bulgrien, J., Smith, D. W., Barsam, B., Veretnik, S., and Gribskov, M. (2002) The complement of protein phosphatase catalytic subunits encoded in the genome of Arabidopsis. *Plant physiology* **129**, 908-925
50. Orgad, S., Brewis, N. D., Alphey, L., Axton, J. M., Dudai, Y., and Cohen, P. T. (1990) The structure of protein phosphatase 2A is as highly conserved as that of protein phosphatase 1. *FEBS Lett* **275**, 44-48
51. Khew-Goodall, Y., Mayer, R. E., Maurer, F., Stone, S. R., and Hemmings, B. A. (1991) Structure and transcriptional regulation of protein phosphatase 2A catalytic subunit genes. *Biochemistry* **30**, 89-97
52. Gotz, J., Probst, A., Mistl, C., Nitsch, R. M., and Ehler, E. (2000) Distinct role of protein phosphatase 2A subunit Calpha in the regulation of E-cadherin and beta-catenin during development. *Mechanisms of development* **93**, 83-93
53. Hemmings, B. A., Adams-Pearson, C., Maurer, F., Muller, P., Goris, J., Merlevede, W., Hofsteenge, J., and Stone, S. R. (1990) alpha- and beta-forms of the 65-kDa subunit of protein phosphatase 2A have a similar 39 amino acid repeating structure. *Biochemistry* **29**, 3166-3173
54. Zhou, J., Pham, H. T., Ruediger, R., and Walter, G. (2003) Characterization of the Aalpha and Abeta subunit isoforms of protein phosphatase 2A: differences in expression, subunit interaction, and evolution. *The Biochemical journal* **369**, 387-398
55. Zhou, J., Pham, H. T., and Walter, G. (2003) The formation and activity of PP2A holoenzymes do not depend on the isoform of the catalytic subunit. *The Journal of biological chemistry* **278**, 8617-8622
56. Xing, Y., Xu, Y., Chen, Y., Jeffrey, P. D., Chao, Y., Lin, Z., Li, Z., Strack, S., Stock, J. B., and Shi, Y. (2006) Structure of protein phosphatase 2A core enzyme bound to tumor-inducing toxins. *Cell* **127**, 341-353
57. Lambrecht, C., Haesen, D., Sents, W., Ivanova, E., and Janssens, V. (2013) Structure, regulation, and pharmacological modulation of PP2A phosphatases. *Methods Mol Biol* **1053**, 283-305

58. Xu, Y., Chen, Y., Zhang, P., Jeffrey, P. D., and Shi, Y. (2008) Structure of a protein phosphatase 2A holoenzyme: insights into B55-mediated Tau dephosphorylation. *Molecular cell* **31**, 873-885
59. Xu, Y., Xing, Y., Chen, Y., Chao, Y., Lin, Z., Fan, E., Yu, J. W., Strack, S., Jeffrey, P. D., and Shi, Y. (2006) Structure of the protein phosphatase 2A holoenzyme. *Cell* **127**, 1239-1251
60. Wlodarchak, N., Guo, F., Satyshur, K. A., Jiang, L., Jeffrey, P. D., Sun, T., Stanevich, V., Mumby, M. C., and Xing, Y. (2013) Structure of the Ca2+-dependent PP2A heterotrimer and insights into Cdc6 dephosphorylation. *Cell research* **23**, 931-946
61. Tanti, G. K., Singarapu, N., Muthuswami, R., and Goswami, S. K. (2014) Among the three striatin family members, SG2NA was first to arise during evolution. *Frontiers in bioscience (Scholar edition)* **6**, 1-15
62. Li, X., and Virshup, D. M. (2002) Two conserved domains in regulatory B subunits mediate binding to the A subunit of protein phosphatase 2A. *European journal of biochemistry / FEBS* **269**, 546-552
63. Ruediger, R., Roeckel, D., Fait, J., Bergqvist, A., Magnusson, G., and Walter, G. (1992) Identification of binding sites on the regulatory A subunit of protein phosphatase 2A for the catalytic C subunit and for tumor antigens of simian virus 40 and polyomavirus. *Molecular and cellular biology* **12**, 4872-4882
64. Cho, U. S., and Xu, W. (2007) Crystal structure of a protein phosphatase 2A heterotrimeric holoenzyme. *Nature* **445**, 53-57
65. Sontag, J. M., Nunbhakdi-Craig, V., and Sontag, E. (2013) Leucine carboxyl methyltransferase 1 (LCMT1)-dependent methylation regulates the association of protein phosphatase 2A and Tau protein with plasma membrane microdomains in neuroblastoma cells. *The Journal of biological chemistry* **288**, 27396-27405
66. De Baere, I., Derua, R., Janssens, V., Van Hoof, C., Waelkens, E., Merlevede, W., and Goris, J. (1999) Purification of porcine brain protein phosphatase 2A leucine carboxyl methyltransferase and cloning of the human homologue. *Biochemistry* **38**, 16539-16547
67. Longin, S., Zwaenepoel, K., Louis, J. V., Dilworth, S., Goris, J., and Janssens, V. (2007) Selection of protein phosphatase 2A regulatory subunits is mediated by the C terminus of the catalytic Subunit. *The Journal of biological chemistry* **282**, 26971-26980
68. Xing, Y., Li, Z., Chen, Y., Stock, J. B., Jeffrey, P. D., and Shi, Y. (2008) Structural mechanism of demethylation and inactivation of protein phosphatase 2A. *Cell* **133**, 154-163
69. Stanevich, V., Jiang, L., Satyshur, K. A., Li, Y., Jeffrey, P. D., Li, Z., Menden, P., Semmelhack, M. F., and Xing, Y. (2011) The structural basis for tight control of PP2A methylation and function by LCMT-1. *Molecular cell* **41**, 331-342
70. Cayla, X., Van Hoof, C., Bosch, M., Waelkens, E., Vandekerckhove, J., Peeters, B., Merlevede, W., and Goris, J. (1994) Molecular cloning, expression, and characterization of PTPA, a protein that activates the tyrosyl phosphatase activity of protein phosphatase 2A. *The Journal of biological chemistry* **269**, 15668-15675

71. Li, M., Guo, H., and Damuni, Z. (1995) Purification and characterization of two potent heat-stable protein inhibitors of protein phosphatase 2A from bovine kidney. *Biochemistry* **34**, 1988-1996
72. Li, M., Makkinje, A., and Damuni, Z. (1996) Molecular identification of I1PP2A, a novel potent heat-stable inhibitor protein of protein phosphatase 2A. *Biochemistry* **35**, 6998-7002
73. Arnaud, L., Chen, S., Liu, F., Li, B., Khatoon, S., Grundke-Iqbal, I., and Iqbal, K. (2011) Mechanism of inhibition of PP2A activity and abnormal hyperphosphorylation of tau by I2(PP2A)/SET. *FEBS Lett* **585**, 2653-2659
74. Adachi, Y., Pavlakis, G. N., and Copeland, T. D. (1994) Identification of in vivo phosphorylation sites of SET, a nuclear phosphoprotein encoded by the translocation breakpoint in acute undifferentiated leukemia. *FEBS Lett* **340**, 231-235
75. Junttila, M. R., Puustinen, P., Niemela, M., Ahola, R., Arnold, H., Bottzauw, T., Ala-aho, R., Nielsen, C., Ivaska, J., Taya, Y., Lu, S. L., Lin, S., Chan, E. K., Wang, X. J., Grenman, R., Kast, J., Kallunki, T., Sears, R., Kahari, V. M., and Westermarck, J. (2007) CIP2A inhibits PP2A in human malignancies. *Cell* **130**, 51-62
76. McConnell, J. L., Gomez, R. J., McCorvey, L. R., Law, B. K., and Wadzinski, B. E. (2007) Identification of a PP2A-interacting protein that functions as a negative regulator of phosphatase activity in the ATM/ATR signaling pathway. *Oncogene* **26**, 6021-6030
77. Jiang, Y., and Broach, J. R. (1999) Tor proteins and protein phosphatase 2A reciprocally regulate Tap42 in controlling cell growth in yeast. *The EMBO journal* **18**, 2782-2792
78. Murata, K., Wu, J., and Brautigan, D. L. (1997) B cell receptor-associated protein alpha4 displays rapamycin-sensitive binding directly to the catalytic subunit of protein phosphatase 2A. *Proceedings of the National Academy of Sciences of the United States of America* **94**, 10624-10629
79. Kloeker, S., Reed, R., McConnell, J. L., Chang, D., Tran, K., Westphal, R. S., Law, B. K., Colbran, R. J., Kamoun, M., Campbell, K. S., and Wadzinski, B. E. (2003) Parallel purification of three catalytic subunits of the protein serine/threonine phosphatase 2A family (PP2A(C), PP4(C), and PP6(C)) and analysis of the interaction of PP2A(C) with alpha4 protein. *Protein expression and purification* **31**, 19-33
80. Chen, J., Peterson, R. T., and Schreiber, S. L. (1998) Alpha 4 associates with protein phosphatases 2A, 4, and 6. *Biochem Biophys Res Commun* **247**, 827-832
81. McConnell, J. L., Watkins, G. R., Soss, S. E., Franz, H. S., McCorvey, L. R., Spiller, B. W., Chazin, W. J., and Wadzinski, B. E. (2010) Alpha4 is a ubiquitin-binding protein that regulates protein serine/threonine phosphatase 2A ubiquitination. *Biochemistry* **49**, 1713-1718
82. LeNoue-Newton, M., Watkins, G. R., Zou, P., Germane, K. L., McCorvey, L. R., Wadzinski, B. E., and Spiller, B. W. (2011) The E3 ubiquitin ligase- and protein phosphatase 2A (PP2A)-binding domains of the Alpha4 protein are both required for Alpha4 to inhibit PP2A degradation. *The Journal of biological chemistry* **286**, 17665-17671

83. Watkins, G. R., Wang, N., Mazalouskas, M. D., Gomez, R. J., Guthrie, C. R., Kraemer, B. C., Schweiger, S., Spiller, B. W., and Wadzinski, B. E. (2012) Monoubiquitination promotes calpain cleavage of the protein phosphatase 2A (PP2A) regulatory subunit alpha4, altering PP2A stability and microtubule-associated protein phosphorylation. *The Journal of biological chemistry* **287**, 24207-24215
84. Wang, N., Leung, H. T., Mazalouskas, M. D., Watkins, G. R., Gomez, R. J., and Wadzinski, B. E. (2012) Essential roles of the Tap42-regulated protein phosphatase 2A (PP2A) family in wing imaginal disc development of Drosophila melanogaster. *PloS one* **7**, e38569
85. Kong, M., Fox, C. J., Mu, J., Solt, L., Xu, A., Cinalli, R. M., Birnbaum, M. J., Lindsten, T., and Thompson, C. B. (2004) The PP2A-associated protein alpha4 is an essential inhibitor of apoptosis. *Science* **306**, 695-698
86. Cygnar, K. D., Gao, X., Pan, D., and Neufeld, T. P. (2005) The phosphatase subunit tap42 functions independently of target of rapamycin to regulate cell division and survival in Drosophila. *Genetics* **170**, 733-740
87. Jiang, L., Stanevich, V., Satyshur, K. A., Kong, M., Watkins, G. R., Wadzinski, B. E., Sengupta, R., and Xing, Y. (2013) Structural basis of protein phosphatase 2A stable latency. *Nature communications* **4**, 1699
88. Trockenbacher, A., Suckow, V., Foerster, J., Winter, J., Krauss, S., Ropers, H. H., Schneider, R., and Schweiger, S. (2001) MID1, mutated in Opitz syndrome, encodes an ubiquitin ligase that targets phosphatase 2A for degradation. *Nature genetics* **29**, 287-294
89. Ogris, E., Gibson, D. M., and Pallas, D. C. (1997) Protein phosphatase 2A subunit assembly: the catalytic subunit carboxy terminus is important for binding cellular B subunit but not polyomavirus middle tumor antigen. *Oncogene* **15**, 911-917
90. Guo, H., and Damuni, Z. (1993) Autophosphorylation-activated protein kinase phosphorylates and inactivates protein phosphatase 2A. *Proceedings of the National Academy of Sciences of the United States of America* **90**, 2500-2504
91. Chen, J., Martin, B. L., and Brautigan, D. L. (1992) Regulation of protein serine-threonine phosphatase type-2A by tyrosine phosphorylation. *Science* **257**, 1261-1264
92. Chen, J., Parsons, S., and Brautigan, D. L. (1994) Tyrosine phosphorylation of protein phosphatase 2A in response to growth stimulation and v-src transformation of fibroblasts. *The Journal of biological chemistry* **269**, 7957-7962
93. Nunbhakdi-Craig, V., Schuechner, S., Sontag, J. M., Montgomery, L., Pallas, D. C., Juno, C., Mudrak, I., Ogris, E., and Sontag, E. (2007) Expression of protein phosphatase 2A mutants and silencing of the regulatory B alpha subunit induce a selective loss of acetylated and detyrosinated microtubules. *Journal of neurochemistry* **101**, 959-971
94. Ohama, T., and Brautigan, D. L. (2010) Endotoxin conditioning induces VCP/p97-mediated and inducible nitric-oxide synthase-dependent Tyr284 nitration in protein phosphatase 2A. *The Journal of biological chemistry* **285**, 8711-8718

95. Sikorski, R. S., Boguski, M. S., Goebl, M., and Hieter, P. (1990) A repeating amino acid motif in CDC23 defines a family of proteins and a new relationship among genes required for mitosis and RNA synthesis. *Cell* **60**, 307-317
96. Hirano, T., Kinoshita, N., Morikawa, K., and Yanagida, M. (1990) Snap helix with knob and hole: essential repeats in S. pombe nuclear protein nuc2+. *Cell* **60**, 319-328
97. D'Andrea, L. D., and Regan, L. (2003) TPR proteins: the versatile helix. *Trends in biochemical sciences* **28**, 655-662
98. Das, A. K., Cohen, P. W., and Barford, D. (1998) The structure of the tetratricopeptide repeats of protein phosphatase 5: implications for TPR-mediated protein-protein interactions. *The EMBO journal* **17**, 1192-1199
99. Yang, J., Roe, S. M., Cliff, M. J., Williams, M. A., Ladbury, J. E., Cohen, P. T., and Barford, D. (2005) Molecular basis for TPR domain-mediated regulation of protein phosphatase 5. *The EMBO journal* **24**, 1-10
100. Silverstein, A. M., Galigniana, M. D., Chen, M. S., Owens-Grillo, J. K., Chinkers, M., and Pratt, W. B. (1997) Protein phosphatase 5 is a major component of glucocorticoid receptor.hsp90 complexes with properties of an FK506-binding immunophilin. *The Journal of biological chemistry* **272**, 16224-16230
101. Fung, J. J., and Starzl, T. E. (1995) FK506 in solid organ transplantation. *Therapeutic drug monitoring* **17**, 592-595
102. Barton, G. J., Cohen, P. T., and Barford, D. (1994) Conservation analysis and structure prediction of the protein serine/threonine phosphatases. Sequence similarity with diadenosine tetraphosphatase from Escherichia coli suggests homology to the protein phosphatases. *European journal of biochemistry / FEBS* **220**, 225-237
103. Swingle, M. R., Honkanen, R. E., and Ciszak, E. M. (2004) Structural basis for the catalytic activity of human serine/threonine protein phosphatase-5. *The Journal of biological chemistry* **279**, 33992-33999
104. Chen, M. X., and Cohen, P. T. (1997) Activation of protein phosphatase 5 by limited proteolysis or the binding of polyunsaturated fatty acids to the TPR domain. *FEBS Lett* **400**, 136-140
105. Sinclair, C., Borchers, C., Parker, C., Tomer, K., Charbonneau, H., and Rossie, S. (1999) The tetratricopeptide repeat domain and a C-terminal region control the activity of Ser/Thr protein phosphatase 5. *The Journal of biological chemistry* **274**, 23666-23672
106. Kang, H., Sayner, S. L., Gross, K. L., Russell, L. C., and Chinkers, M. (2001) Identification of amino acids in the tetratricopeptide repeat and C-terminal domains of protein phosphatase 5 involved in autoinhibition and lipid activation. *Biochemistry* **40**, 10485-10490
107. Zeytuni, N., and Zarivach, R. (2012) Structural and Functional Discussion of the Tetra-Trico-Peptide Repeat, a Protein Interaction Module. *Structure* **20**, 397-405
108. Russell, L. C., Whitt, S. R., Chen, M. S., and Chinkers, M. (1999) Identification of conserved residues required for the binding of a tetratricopeptide repeat domain to heat shock protein 90. *The Journal of biological chemistry* **274**, 20060-20063
109. Connarn, J. N., Assimon, V. A., Reed, R. A., Tse, E., Southworth, D. R., Zuiderweg, E. R., Gestwicki, J. E., and Sun, D. (2013) The Molecular Chaperone

Hsp70 Activates Protein Phosphatase 5 (PP5) By Binding the Tetratricopeptide Repeat (TPR) Domain. *The Journal of biological chemistry*

110. Yamaguchi, F., Umeda, Y., Shimamoto, S., Tsuchiya, M., Tokumitsu, H., Tokuda, M., and Kobayashi, R. (2012) S100 proteins modulate protein phosphatase 5 function: a link between CA2+ signal transduction and protein dephosphorylation. *The Journal of biological chemistry* **287**, 13787-13798
111. Chatterjee, A., Wang, L., Armstrong, D. L., and Rossie, S. (2010) Activated Rac1 GTPase translocates protein phosphatase 5 to the cell membrane and stimulates phosphatase activity in vitro. *The Journal of biological chemistry* **285**, 3872-3882
112. Yamaguchi, Y., Katoh, H., Mori, K., and Negishi, M. (2002) Galpha(12) and Galpha(13) interact with Ser/Thr protein phosphatase type 5 and stimulate its phosphatase activity. *Current biology : CB* **12**, 1353-1358
113. Borthwick, E. B., Zeke, T., Prescott, A. R., and Cohen, P. T. (2001) Nuclear localization of protein phosphatase 5 is dependent on the carboxy-terminal region. *FEBS Lett* **491**, 279-284
114. Golden, T., Swingle, M., and Honkanen, R. E. (2008) The role of serine/threonine protein phosphatase type 5 (PP5) in the regulation of stress-induced signaling networks and cancer. *Cancer metastasis reviews* **27**, 169-178
115. Freeman, A. K., and Monteiro, A. N. (2010) Phosphatases in the cellular response to DNA damage. *Cell communication and signaling : CCS* **8**, 27
116. Kumar, R., Grammatikakis, N., and Chinkers, M. (2001) Regulation of the atrial natriuretic peptide receptor by heat shock protein 90 complexes. *The Journal of biological chemistry* **276**, 11371-11375
117. Ikeda, K., Ogawa, S., Tsukui, T., Horie-Inoue, K., Ouchi, Y., Kato, S., Muramatsu, M., and Inoue, S. (2004) Protein phosphatase 5 is a negative regulator of estrogen receptor-mediated transcription. *Molecular endocrinology (Baltimore, Md.)* **18**, 1131-1143
118. Chen, M. S., Silverstein, A. M., Pratt, W. B., and Chinkers, M. (1996) The tetratricopeptide repeat domain of protein phosphatase 5 mediates binding to glucocorticoid receptor heterocomplexes and acts as a dominant negative mutant. *The Journal of biological chemistry* **271**, 32315-32320
119. Chinkers, M. (2001) Protein phosphatase 5 in signal transduction. *Trends in endocrinology and metabolism: TEM* **12**, 28-32
120. Gentile, S., Darden, T., Erxleben, C., Romeo, C., Russo, A., Martin, N., Rossie, S., and Armstrong, D. L. (2006) Rac GTPase signaling through the PP5 protein phosphatase. *Proceedings of the National Academy of Sciences of the United States of America* **103**, 5202-5206
121. Duerson, K., White, R. E., Jiang, F., Schonbrunn, A., and Armstrong, D. L. (1996) Somatostatin stimulates BKCa channels in rat pituitary tumor cells through lipoxygenase metabolites of arachidonic acid. *Neuropharmacology* **35**, 949-961
122. Smith, J., Tho, L. M., Xu, N., and Gillespie, D. A. (2010) The ATM-Chk2 and ATR-Chk1 pathways in DNA damage signaling and cancer. *Advances in cancer research* **108**, 73-112
123. Ali, A., Zhang, J., Bao, S., Liu, I., Otterness, D., Dean, N. M., Abraham, R. T., and Wang, X. F. (2004) Requirement of protein phosphatase 5 in DNA-damage-induced ATM activation. *Genes Dev* **18**, 249-254

124. Zhang, J., Bao, S., Furumai, R., Kucera, K. S., Ali, A., Dean, N. M., and Wang, X. F. (2005) Protein phosphatase 5 is required for ATR-mediated checkpoint activation. *Molecular and cellular biology* **25**, 9910-9919
125. Amable, L., Grankvist, N., Largen, J. W., Ortsater, H., Sjoholm, A., and Honkanen, R. E. (2011) Disruption of serine/threonine protein phosphatase 5 (PP5:PPP5c) in mice reveals a novel role for PP5 in the regulation of ultraviolet light-induced phosphorylation of serine/threonine protein kinase Chk1 (CHEK1). *The Journal of biological chemistry* **286**, 40413-40422
126. Wechsler, T., Chen, B. P., Harper, R., Morotomi-Yano, K., Huang, B. C., Meek, K., Cleaver, J. E., Chen, D. J., and Wabl, M. (2004) DNA-PKcs function regulated specifically by protein phosphatase 5. *Proceedings of the National Academy of Sciences of the United States of America* **101**, 1247-1252
127. Morita, K., Saitoh, M., Tobiume, K., Matsuura, H., Enomoto, S., Nishitoh, H., and Ichijo, H. (2001) Negative feedback regulation of ASK1 by protein phosphatase 5 (PP5) in response to oxidative stress. *The EMBO journal* **20**, 6028-6036
128. Zhou, G., Golden, T., Aragon, I. V., and Honkanen, R. E. (2004) Ser/Thr protein phosphatase 5 inactivates hypoxia-induced activation of an apoptosis signal-regulating kinase 1/MKK-4/JNK signaling cascade. *The Journal of biological chemistry* **279**, 46595-46605
129. Huang, S., Shu, L., Easton, J., Harwood, F. C., Germain, G. S., Ichijo, H., and Houghton, P. J. (2004) Inhibition of mammalian target of rapamycin activates apoptosis signal-regulating kinase 1 signaling by suppressing protein phosphatase 5 activity. *The Journal of biological chemistry* **279**, 36490-36496
130. Lubert, E. J., Hong, Y., and Sarge, K. D. (2001) Interaction between protein phosphatase 5 and the A subunit of protein phosphatase 2A: evidence for a heterotrimeric form of protein phosphatase 5. *The Journal of biological chemistry* **276**, 38582-38587
131. Chiang, C. W., Liu, W. K., and Chou, C. K. (2011) Phosphorylation-dependent association of the G4-1/G5PR regulatory subunit with IKKbeta negatively modulates NF-kappaB activation through recruitment of protein phosphatase 5. *The Biochemical journal* **433**, 187-196
132. Katayama, K., Yamaguchi, M., Noguchi, K., and Sugimoto, Y. (2014) Protein phosphatase complex PP5/PPP2R3C dephosphorylates P-glycoprotein/ABCB1 and down-regulates the expression and function. *Cancer letters* **345**, 124-131
133. von Kriegsheim, A., Pitt, A., Grindlay, G. J., Kolch, W., and Dhillon, A. S. (2006) Regulation of the Raf-MEK-ERK pathway by protein phosphatase 5. *Nature cell biology* **8**, 1011-1016
134. Shao, J., Hartson, S. D., and Matts, R. L. (2002) Evidence that protein phosphatase 5 functions to negatively modulate the maturation of the Hsp90-dependent heme-regulated eIF2alpha kinase. *Biochemistry* **41**, 6770-6779
135. Westphal, R. S., Anderson, K. A., Means, A. R., and Wadzinski, B. E. (1998) A signaling complex of Ca2+-calmodulin-dependent protein kinase IV and protein phosphatase 2A. *Science* **280**, 1258-1261
136. Abraham, D., Podar, K., Pacher, M., Kubicek, M., Welzel, N., Hemmings, B. A., Dilworth, S. M., Mischak, H., Kolch, W., and Baccarini, M. (2000) Raf-1-

associated protein phosphatase 2A as a positive regulator of kinase activation. *The Journal of biological chemistry* **275**, 22300-22304
137. Adams, D. G., Coffee, R. L., Jr., Zhang, H., Pelech, S., Strack, S., and Wadzinski, B. E. (2005) Positive regulation of Raf1-MEK1/2-ERK1/2 signaling by protein serine/threonine phosphatase 2A holoenzymes. *The Journal of biological chemistry* **280**, 42644-42654
138. Charlton, L. A., Sayed, M., Clark-Lewis, I., Aebersold, R., and Pelech, S. L. (1999) Characterization of an activated ribosomal S6 kinase variant from maturing sea star oocytes: association with phosphatase 2A and substrate specificity. *Journal of cellular biochemistry* **75**, 310-326
139. Peterson, R. T., Desai, B. N., Hardwick, J. S., and Schreiber, S. L. (1999) Protein phosphatase 2A interacts with the 70-kDa S6 kinase and is activated by inhibition of FKBP12-rapamycinassociated protein. *Proceedings of the National Academy of Sciences of the United States of America* **96**, 4438-4442
140. Westphal, R. S., Coffee, R. L., Jr., Marotta, A., Pelech, S. L., and Wadzinski, B. E. (1999) Identification of kinase-phosphatase signaling modules composed of p70 S6 kinase-protein phosphatase 2A (PP2A) and p21-activated kinase-PP2A. *The Journal of biological chemistry* **274**, 687-692
141. Heriche, J. K., Lebrin, F., Rabilloud, T., Leroy, D., Chambaz, E. M., and Goldberg, Y. (1997) Regulation of protein phosphatase 2A by direct interaction with casein kinase 2alpha. *Science* **276**, 952-955
142. Petritsch, C., Beug, H., Balmain, A., and Oft, M. (2000) TGF-beta inhibits p70 S6 kinase via protein phosphatase 2A to induce G(1) arrest. *Genes Dev* **14**, 3093-3101
143. Boudreau, R. T., Garduno, R., and Lin, T. J. (2002) Protein phosphatase 2A and protein kinase Calpha are physically associated and are involved in Pseudomonas aeruginosa-induced interleukin 6 production by mast cells. *The Journal of biological chemistry* **277**, 5322-5329
144. Kuo, Y. C., Huang, K. Y., Yang, C. H., Yang, Y. S., Lee, W. Y., and Chiang, C. W. (2008) Regulation of phosphorylation of Thr-308 of Akt, cell proliferation, and survival by the B55alpha regulatory subunit targeting of the protein phosphatase 2A holoenzyme to Akt. *The Journal of biological chemistry* **283**, 1882-1892
145. Beaulieu, J. M., Sotnikova, T. D., Marion, S., Lefkowitz, R. J., Gainetdinov, R. R., and Caron, M. G. (2005) An Akt/beta-arrestin 2/PP2A signaling complex mediates dopaminergic neurotransmission and behavior. *Cell* **122**, 261-273
146. Fuhrer, D. K., and Yang, Y. C. (1996) Complex formation of JAK2 with PP2A, P13K, and Yes in response to the hematopoietic cytokine interleukin-11. *Biochem Biophys Res Commun* **224**, 289-296
147. Ory, S., Zhou, M., Conrads, T. P., Veenstra, T. D., and Morrison, D. K. (2003) Protein Phosphatase 2A Positively Regulates Ras Signaling by Dephosphorylating KSR1 and Raf-1 on Critical 14-3-3 Binding Sites. *Current Biology* **13**, 1356-1364
148. Fu, D. X., Kuo, Y. L., Liu, B. Y., Jeang, K. T., and Giam, C. Z. (2003) Human T-lymphotropic virus type I tax activates I-kappa B kinase by inhibiting I-kappa B kinase-associated serine/threonine protein phosphatase 2A. *The Journal of biological chemistry* **278**, 1487-1493

149. Kray, A. E., Carter, R. S., Pennington, K. N., Gomez, R. J., Sanders, L. E., Llanes, J. M., Khan, W. N., Ballard, D. W., and Wadzinski, B. E. (2005) Positive regulation of IkappaB kinase signaling by protein serine/threonine phosphatase 2A. *The Journal of biological chemistry* **280**, 35974-35982
150. Reece, K. M., Mazalouskas, M. D., and Wadzinski, B. E. (2009) The Balpha and Bdelta regulatory subunits of PP2A are necessary for assembly of the CaMKIV.PP2A signaling complex. *Biochem Biophys Res Commun* **386**, 582-587
151. Mazalouskas, M. D., Godoy-Ruiz, R., Weber, D. J., Zimmer, D. B., Honkanen, R. E., and Wadzinski, B. E. (2013) Small G proteins, Rac1 and Ras, regulate serine/threonine protein phosphatase 5 (PP5)-extracellular signal-regulated (ERK) complexes involved in the feedback regulation of Raf1. *The Journal of biological chemistry*
152. Wayman, G. A., Tokumitsu, H., Davare, M. A., and Soderling, T. R. (2011) Analysis of CaM-kinase signaling in cells. *Cell calcium* **50**, 1-8
153. Sakagami, H., and Kondo, H. (1993) Cloning and sequencing of a gene encoding the beta polypeptide of Ca2+/calmodulin-dependent protein kinase IV and its expression confined to the mature cerebellar granule cells. *Brain research. Molecular brain research* **19**, 215-218
154. Murphy, A. J., Kemp, F., and Love, J. (2008) Surface plasmon resonance characterization of calspermin-calmodulin binding kinetics. *Analytical biochemistry* **376**, 61-72
155. Anderson, K. A., and Kane, C. D. (1998) Ca2+/calmodulin-dependent protein kinase IV and calcium signaling. *Biometals : an international journal on the role of metal ions in biology, biochemistry, and medicine* **11**, 331-343
156. Chatila, T., Anderson, K. A., Ho, N., and Means, A. R. (1996) A unique phosphorylation-dependent mechanism for the activation of Ca2+/calmodulin-dependent protein kinase type IV/GR. *The Journal of biological chemistry* **271**, 21542-21548
157. Tokumitsu, H., Brickey, D. A., Glod, J., Hidaka, H., Sikela, J., and Soderling, T. R. (1994) Activation mechanisms for Ca2+/calmodulin-dependent protein kinase IV. Identification of a brain CaM-kinase IV kinase. *The Journal of biological chemistry* **269**, 28640-28647
158. Selbert, M. A., Anderson, K. A., Huang, Q. H., Goldstein, E. G., Means, A. R., and Edelman, A. M. (1995) Phosphorylation and activation of Ca(2+)-calmodulin-dependent protein kinase IV by Ca(2+)-calmodulin-dependent protein kinase Ia kinase. Phosphorylation of threonine 196 is essential for activation. *The Journal of biological chemistry* **270**, 17616-17621
159. Chow, F. A., Anderson, K. A., Noeldner, P. K., and Means, A. R. (2005) The autonomous activity of calcium/calmodulin-dependent protein kinase IV is required for its role in transcription. *The Journal of biological chemistry* **280**, 20530-20538
160. Sun, P., Enslen, H., Myung, P. S., and Maurer, R. A. (1994) Differential activation of CREB by Ca2+/calmodulin-dependent protein kinases type II and type IV involves phosphorylation of a site that negatively regulates activity. *Genes Dev* **8**, 2527-2539

161. Sun, P., Lou, L., and Maurer, R. A. (1996) Regulation of activating transcription factor-1 and the cAMP response element-binding protein by Ca2+/calmodulin-dependent protein kinases type I, II, and IV. *The Journal of biological chemistry* **271**, 3066-3073
162. Misra, R. P., Bonni, A., Miranti, C. K., Rivera, V. M., Sheng, M., and Greenberg, M. E. (1994) L-type voltage-sensitive calcium channel activation stimulates gene expression by a serum response factor-dependent pathway. *The Journal of biological chemistry* **269**, 25483-25493
163. Wu, J. Y., and Means, A. R. (2000) Ca(2+)/calmodulin-dependent protein kinase IV is expressed in spermatids and targeted to chromatin and the nuclear matrix. *The Journal of biological chemistry* **275**, 7994-7999
164. Means, A. R., Ribar, T. J., Kane, C. D., Hook, S. S., and Anderson, K. A. (1997) Regulation and properties of the rat Ca2+/calmodulin-dependent protein kinase IV gene and its protein products. *Recent progress in hormone research* **52**, 389-406; discussion 406-387
165. Park, I. K., and Soderling, T. R. (1995) Activation of Ca2+/calmodulin-dependent protein kinase (CaM-kinase) IV by CaM-kinase kinase in Jurkat T lymphocytes. *The Journal of biological chemistry* **270**, 30464-30469
166. Anderson, K. A., Noeldner, P. K., Reece, K., Wadzinski, B. E., and Means, A. R. (2004) Regulation and function of the calcium/calmodulin-dependent protein kinase IV/protein serine/threonine phosphatase 2A signaling complex. *The Journal of biological chemistry* **279**, 31708-31716
167. Strack, S., Westphal, R. S., Colbran, R. J., Ebner, F. F., and Wadzinski, B. E. (1997) Protein serine/threonine phosphatase 1 and 2A associate with and dephosphorylate neurofilaments. *Brain research. Molecular brain research* **49**, 15-28
168. Strack, S., Chang, D., Zaucha, J. A., Colbran, R. J., and Wadzinski, B. E. (1999) Cloning and characterization of B delta, a novel regulatory subunit of protein phosphatase 2A. *FEBS Lett* **460**, 462-466
169. Hanissian, S. H., Frangakis, M., Bland, M. M., Jawahar, S., and Chatila, T. A. (1993) Expression of a Ca2+/calmodulin-dependent protein kinase, CaM kinase-Gr, in human T lymphocytes. Regulation of kinase activity by T cell receptor signaling. *The Journal of biological chemistry* **268**, 20055-20063
170. Wu, J. Y., Gonzalez-Robayna, I. J., Richards, J. S., and Means, A. R. (2000) Female fertility is reduced in mice lacking Ca2+/calmodulin-dependent protein kinase IV. *Endocrinology* **141**, 4777-4783
171. Wu, J. Y., Ribar, T. J., and Means, A. R. (2001) Spermatogenesis and the regulation of Ca(2+)-calmodulin-dependent protein kinase IV localization are not dependent on calspermin. *Molecular and cellular biology* **21**, 6066-6070
172. Fukushima, H., Maeda, R., Suzuki, R., Suzuki, A., Nomoto, M., Toyoda, H., Wu, L. J., Xu, H., Zhao, M. G., Ueda, K., Kitamoto, A., Mamiya, N., Yoshida, T., Homma, S., Masushige, S., Zhuo, M., and Kida, S. (2008) Upregulation of calcium/calmodulin-dependent protein kinase IV improves memory formation and rescues memory loss with aging. *The Journal of neuroscience : the official journal of the Society for Neuroscience* **28**, 9910-9919

173. Anderson, K. A., Ribar, T. J., Illario, M., and Means, A. R. (1997) Defective survival and activation of thymocytes in transgenic mice expressing a catalytically inactive form of Ca2+/calmodulin-dependent protein kinase IV. *Molecular endocrinology (Baltimore, Md.)* **11**, 725-737
174. Van Kanegan, M. J., and Strack, S. (2009) The protein phosphatase 2A regulatory subunits B'beta and B'delta mediate sustained TrkA neurotrophin receptor autophosphorylation and neuronal differentiation. *Molecular and cellular biology* **29**, 662-674
175. Yamashita, T., Inui, S., Maeda, K., Hua, D. R., Takagi, K., Fukunaga, K., and Sakaguchi, N. (2006) Regulation of CaMKII by alpha4/PP2Ac contributes to learning and memory. *Brain research* **1082**, 1-10
176. Hua, D. R., Inui, S., Yamashita, T., Maeda, K., Takagi, K., Takeda, J., and Sakaguchi, N. (2003) T cell-specific gene targeting reveals that alpha4 is required for early T cell development. *European journal of immunology* **33**, 1899-1906
177. Inui, S., Maeda, K., Hua, D. R., Yamashita, T., Yamamoto, H., Miyamoto, E., Aizawa, S., and Sakaguchi, N. (2002) BCR signal through alpha 4 is involved in S6 kinase activation and required for B cell maturation including isotype switching and V region somatic hypermutation. *International immunology* **14**, 177-187
178. Yamashita, T., Inui, S., Maeda, K., Hua, D. R., Takagi, K., and Sakaguchi, N. (2005) The heterodimer of alpha4 and PP2Ac is associated with S6 kinase1 in B cells. *Biochem Biophys Res Commun* **330**, 439-445
179. Kong, M., Bui, T. V., Ditsworth, D., Gruber, J. J., Goncharov, D., Krymskaya, V. P., Lindsten, T., and Thompson, C. B. (2007) The PP2A-associated protein alpha4 plays a critical role in the regulation of cell spreading and migration. *The Journal of biological chemistry* **282**, 29712-29720
180. Nanahoshi, M., Nishiuma, T., Tsujishita, Y., Hara, K., Inui, S., Sakaguchi, N., and Yonezawa, K. (1998) Regulation of protein phosphatase 2A catalytic activity by alpha4 protein and its yeast homolog Tap42. *Biochem Biophys Res Commun* **251**, 520-526
181. Nien, W. L., Dauphinee, S. M., Moffat, L. D., and Too, C. K. (2007) Overexpression of the mTOR alpha4 phosphoprotein activates protein phosphatase 2A and increases Stat1alpha binding to PIAS1. *Molecular and cellular endocrinology* **263**, 10-17
182. Prickett, T. D., and Brautigan, D. L. (2006) The alpha4 regulatory subunit exerts opposing allosteric effects on protein phosphatases PP6 and PP2A. *The Journal of biological chemistry* **281**, 30503-30511
183. Kong, M., Ditsworth, D., Lindsten, T., and Thompson, C. B. (2009) Alpha4 is an essential regulator of PP2A phosphatase activity. *Molecular cell* **36**, 51-60
184. Green, M. F., Anderson, K. A., and Means, A. R. (2011) Characterization of the CaMKKbeta-AMPK signaling complex. *Cellular signalling* **23**, 2005-2012
185. Rapp, U. R., Goldsborough, M. D., Mark, G. E., Bonner, T. I., Groffen, J., Reynolds, F. H., Jr., and Stephenson, J. R. (1983) Structure and biological activity of v-raf, a unique oncogene transduced by a retrovirus. *Proceedings of the National Academy of Sciences of the United States of America* **80**, 4218-4222

186. Moelling, K., Heimann, B., Beimling, P., Rapp, U. R., and Sander, T. (1984) Serine- and threonine-specific protein kinase activities of purified gag-mil and gag-raf proteins. *Nature* **312**, 558-561
187. Bonner, T. I., Kerby, S. B., Sutrave, P., Gunnell, M. A., Mark, G., and Rapp, U. R. (1985) Structure and biological activity of human homologs of the raf/mil oncogene. *Molecular and cellular biology* **5**, 1400-1407
188. Sithanandam, G., Druck, T., Cannizzaro, L. A., Leuzzi, G., Huebner, K., and Rapp, U. R. (1992) B-raf and a B-raf pseudogene are located on 7q in man. *Oncogene* **7**, 795-799
189. Sithanandam, G., Kolch, W., Duh, F. M., and Rapp, U. R. (1990) Complete coding sequence of a human B-raf cDNA and detection of B-raf protein kinase with isozyme specific antibodies. *Oncogene* **5**, 1775-1780
190. Beck, T. W., Huleihel, M., Gunnell, M., Bonner, T. I., and Rapp, U. R. (1987) The complete coding sequence of the human A-raf-1 oncogene and transforming activity of a human A-raf carrying retrovirus. *Nucleic acids research* **15**, 595-609
191. Eychene, A., Barnier, J. V., Apiou, F., Dutrillaux, B., and Calothy, G. (1992) Chromosomal assignment of two human B-raf(Rmil) proto-oncogene loci: B-raf-1 encoding the p94Braf/Rmil and B-raf-2, a processed pseudogene. *Oncogene* **7**, 1657-1660
192. Huebner, K., ar-Rushdi, A., Griffin, C. A., Isobe, M., Kozak, C., Emanuel, B. S., Nagarajan, L., Cleveland, J. L., Bonner, T. I., Goldsborough, M. D., and et al. (1986) Actively transcribed genes in the raf oncogene group, located on the X chromosome in mouse and human. *Proceedings of the National Academy of Sciences of the United States of America* **83**, 3934-3938
193. Marais, R., and Marshall, C. J. (1996) Control of the ERK MAP kinase cascade by Ras and Raf. *Cancer surveys* **27**, 101-125
194. Patschinsky, T., and Bister, K. (1988) Structural analysis of normal and transforming mil(raf) proteins: effect of 5'-truncation on phosphorylation in vivo or in vitro. *Oncogene* **3**, 357-364
195. Cutler, R. E., Stephens, R. M., Saracino, M. R., and Morrison, D. K. (1998) Autoregulation of the Raf-1 serine/threonine kinase. *Proceedings of the National Academy of Sciences* **95**, 9214-9219
196. Tran, N. H., Wu, X., and Frost, J. A. (2005) B-Raf and Raf-1 are regulated by distinct autoregulatory mechanisms. *The Journal of biological chemistry* **280**, 16244-16253
197. Vojtek, A. B., Hollenberg, S. M., and Cooper, J. A. (1993) Mammalian Ras interacts directly with the serine/threonine kinase Raf. *Cell* **74**, 205-214
198. Hekman, M., Hamm, H., Villar, A. V., Bader, B., Kuhlmann, J., Nickel, J., and Rapp, U. R. (2002) Associations of B- and C-Raf with cholesterol, phosphatidylserine, and lipid second messengers: preferential binding of Raf to artificial lipid rafts. *The Journal of biological chemistry* **277**, 24090-24102
199. Johnson, L. M., James, K. M., Chamberlain, M. D., and Anderson, D. H. (2005) Identification of key residues in the A-Raf kinase important for phosphoinositide lipid binding specificity. *Biochemistry* **44**, 3432-3440
200. Ghosh, S., Strum, J. C., Sciorra, V. A., Daniel, L., and Bell, R. M. (1996) Raf-1 kinase possesses distinct binding domains for phosphatidylserine and

phosphatidic acid. Phosphatidic acid regulates the translocation of Raf-1 in 12-O-tetradecanoylphorbol-13-acetate-stimulated Madin-Darby canine kidney cells. *The Journal of biological chemistry* **271**, 8472-8480
201. Ghosh, S., Xie, W. Q., Quest, A. F., Mabrouk, G. M., Strum, J. C., and Bell, R. M. (1994) The cysteine-rich region of raf-1 kinase contains zinc, translocates to liposomes, and is adjacent to a segment that binds GTP-ras. *The Journal of biological chemistry* **269**, 10000-10007
202. Baljuls, A., Mueller, T., Drexler, H. C., Hekman, M., and Rapp, U. R. (2007) Unique N-region determines low basal activity and limited inducibility of A-RAF kinase: the role of N-region in the evolutionary divergence of RAF kinase function in vertebrates. *The Journal of biological chemistry* **282**, 26575-26590
203. Carpenter, G., and Cohen, S. (1979) Epidermal growth factor. *Annual review of biochemistry* **48**, 193-216
204. Edwin, F., Wiepz, G. J., Singh, R., Peet, C. R., Chaturvedi, D., Bertics, P. J., and Patel, T. B. (2006) A historical perspective of the EGF receptor and related systems. *Methods Mol Biol* **327**, 1-24
205. Linggi, B., and Carpenter, G. (2006) ErbB receptors: new insights on mechanisms and biology. *Trends in cell biology* **16**, 649-656
206. Qian, X., LeVea, C. M., Freeman, J. K., Dougall, W. C., and Greene, M. I. (1994) Heterodimerization of epidermal growth factor receptor and wild-type or kinase-deficient Neu: a mechanism of interreceptor kinase activation and transphosphorylation. *Proceedings of the National Academy of Sciences of the United States of America* **91**, 1500-1504
207. Wada, T., Qian, X. L., and Greene, M. I. (1990) Intermolecular association of the p185neu protein and EGF receptor modulates EGF receptor function. *Cell* **61**, 1339-1347
208. Batzer, A. G., Rotin, D., Urena, J. M., Skolnik, E. Y., and Schlessinger, J. (1994) Hierarchy of binding sites for Grb2 and Shc on the epidermal growth factor receptor. *Molecular and cellular biology* **14**, 5192-5201
209. Hashimoto, A., Kurosaki, M., Gotoh, N., Shibuya, M., and Kurosaki, T. (1999) Shc regulates epidermal growth factor-induced activation of the JNK signaling pathway. *The Journal of biological chemistry* **274**, 20139-20143
210. Keshet, Y., and Seger, R. (2010) The MAP kinase signaling cascades: a system of hundreds of components regulates a diverse array of physiological functions. *Methods Mol Biol* **661**, 3-38
211. Li, N., Batzer, A., Daly, R., Yajnik, V., Skolnik, E., Chardin, P., Bar-Sagi, D., Margolis, B., and Schlessinger, J. (1993) Guanine-nucleotide-releasing factor hSos1 binds to Grb2 and links receptor tyrosine kinases to Ras signalling. *Nature* **363**, 85-88
212. Weber, C. K., Slupsky, J. R., Herrmann, C., Schuler, M., Rapp, U. R., and Block, C. (2000) Mitogenic signaling of Ras is regulated by differential interaction with Raf isozymes. *Oncogene* **19**, 169-176
213. Rodriguez-Viciana, P., Sabatier, C., and McCormick, F. (2004) Signaling specificity by Ras family GTPases is determined by the full spectrum of effectors they regulate. *Molecular and cellular biology* **24**, 4943-4954

214. Yoon, S., and Seger, R. (2006) The extracellular signal-regulated kinase: multiple substrates regulate diverse cellular functions. *Growth factors (Chur, Switzerland)* **24**, 21-44
215. Galaktionov, K., Jessus, C., and Beach, D. (1995) Raf1 interaction with Cdc25 phosphatase ties mitogenic signal transduction to cell cycle activation. *Genes Dev* **9**, 1046-1058
216. Wang, S., Ghosh, R. N., and Chellappan, S. P. (1998) Raf-1 physically interacts with Rb and regulates its function: a link between mitogenic signaling and cell cycle regulation. *Molecular and cellular biology* **18**, 7487-7498
217. Li, S., and Sedivy, J. M. (1993) Raf-1 protein kinase activates the NF-kappa B transcription factor by dissociating the cytoplasmic NF-kappa B-I kappa B complex. *Proceedings of the National Academy of Sciences of the United States of America* **90**, 9247-9251
218. Janosch, P., Schellerer, M., Seitz, T., Reim, P., Eulitz, M., Brielmeier, M., Kolch, W., Sedivy, J. M., and Mischak, H. (1996) Characterization of IkappaB kinases. IkappaB-alpha is not phosphorylated by Raf-1 or protein kinase C isozymes, but is a casein kinase II substrate. *The Journal of biological chemistry* **271**, 13868-13874
219. Wellbrock, C., Karasarides, M., and Marais, R. (2004) The RAF proteins take centre stage. *Nature reviews. Molecular cell biology* **5**, 875-885
220. Pritchard, C. A., Samuels, M. L., Bosch, E., and McMahon, M. (1995) Conditionally oncogenic forms of the A-Raf and B-Raf protein kinases display different biological and biochemical properties in NIH 3T3 cells. *Molecular and cellular biology* **15**, 6430-6442
221. Ebisuya, M., Kondoh, K., and Nishida, E. (2005) The duration, magnitude and compartmentalization of ERK MAP kinase activity: mechanisms for providing signaling specificity. *Journal of cell science* **118**, 2997-3002
222. Morrison, D. K., Heidecker, G., Rapp, U. R., and Copeland, T. D. (1993) Identification of the major phosphorylation sites of the Raf-1 kinase. *The Journal of biological chemistry* **268**, 17309-17316
223. Chong, H., and Guan, K. L. (2003) Regulation of Raf through phosphorylation and N terminus-C terminus interaction. *The Journal of biological chemistry* **278**, 36269-36276
224. Noble, C., Mercer, K., Hussain, J., Carragher, L., Giblett, S., Hayward, R., Patterson, C., Marais, R., and Pritchard, C. A. (2008) CRAF autophosphorylation of serine 621 is required to prevent its proteasome-mediated degradation. *Molecular cell* **31**, 862-872
225. Dhillon, A. S., Yip, Y. Y., Grindlay, G. J., Pakay, J. L., Dangers, M., Hillmann, M., Clark, W., Pitt, A., Mischak, H., and Kolch, W. (2009) The C-terminus of Raf-1 acts as a 14-3-3-dependent activation switch. *Cellular signalling* **21**, 1645-1651
226. Jaumot, M., and Hancock, J. F. (2001) Protein phosphatases 1 and 2A promote Raf-1 activation by regulating 14-3-3 interactions. *Oncogene* **20**, 3949-3958
227. Ritt, D. A., Zhou, M., Conrads, T. P., Veenstra, T. D., Copeland, T. D., and Morrison, D. K. (2007) CK2 Is a component of the KSR1 scaffold complex that contributes to Raf kinase activation. *Current biology : CB* **17**, 179-184

228. Zang, M., Gong, J., Luo, L., Zhou, J., Xiang, X., Huang, W., Huang, Q., Luo, X., Olbrot, M., Peng, Y., Chen, C., and Luo, Z. (2008) Characterization of Ser338 phosphorylation for Raf-1 activation. *The Journal of biological chemistry* **283**, 31429-31437
229. Tran, N. H., and Frost, J. A. (2003) Phosphorylation of Raf-1 by p21-activated kinase 1 and Src regulates Raf-1 autoinhibition. *The Journal of biological chemistry* **278**, 11221-11226
230. Xiang, X., Zang, M., Waelde, C. A., Wen, R., and Luo, Z. (2002) Phosphorylation of 338SSYY341 regulates specific interaction between Raf-1 and MEK1. *The Journal of biological chemistry* **277**, 44996-45003
231. Mason, C. S., Springer, C. J., Cooper, R. G., Superti-Furga, G., Marshall, C. J., and Marais, R. (1999) Serine and tyrosine phosphorylations cooperate in Raf-1, but not B-Raf activation. *The EMBO journal* **18**, 2137-2148
232. Sieburth, D. S., Sundaram, M., Howard, R. M., and Han, M. (1999) A PP2A regulatory subunit positively regulates Ras-mediated signaling during Caenorhabditis elegans vulval induction. *Genes Dev* **13**, 2562-2569
233. Kubicek, M., Pacher, M., Abraham, D., Podar, K., Eulitz, M., and Baccarini, M. (2002) Dephosphorylation of Ser-259 regulates Raf-1 membrane association. *The Journal of biological chemistry* **277**, 7913-7919
234. Kloeker, S., Bryant, J. C., Strack, S., Colbran, R. J., and Wadzinski, B. E. (1997) Carboxymethylation of nuclear protein serine/threonine phosphatase X. *The Biochemical journal* **327 (Pt 2)**, 481-486
235. Blum, H., Beier, H., and Gross, H. J. (1987) Improved silver staining of plant proteins, RNA and DNA in polyacrylamide gels. *ELECTROPHORESIS* **8**, 93-99
236. Yates, J. R., 3rd, Eng, J. K., McCormack, A. L., and Schieltz, D. (1995) Method to correlate tandem mass spectra of modified peptides to amino acid sequences in the protein database. *Analytical chemistry* **67**, 1426-1436
237. Zhang, B., Chambers, M. C., and Tabb, D. L. (2007) Proteomic parsimony through bipartite graph analysis improves accuracy and transparency. *Journal of proteome research* **6**, 3549-3557
238. Smith, A. L., Friedman, D. B., Yu, H., Carnahan, R. H., and Reynolds, A. B. (2011) ReCLIP (reversible cross-link immuno-precipitation): an efficient method for interrogation of labile protein complexes. *PloS one* **6**, e16206
239. Vera, J., Jaumot, M., Estanyol, J. M., Brun, S., Agell, N., and Bachs, O. (2006) Heterogeneous nuclear ribonucleoprotein A2 is a SET-binding protein and a PP2A inhibitor. *Oncogene* **25**, 260-270
240. Bhatia, V. N., Perlman, D. H., Costello, C. E., and McComb, M. E. (2009) Software tool for researching annotations of proteins: open-source protein annotation software with data visualization. *Analytical chemistry* **81**, 9819-9823
241. Huang da, W., Sherman, B. T., and Lempicki, R. A. (2009) Systematic and integrative analysis of large gene lists using DAVID bioinformatics resources. *Nature protocols* **4**, 44-57
242. Tidyman, W. E., and Rauen, K. A. (2009) The RASopathies: developmental syndromes of Ras/MAPK pathway dysregulation. *Current opinion in genetics & development* **19**, 230-236

243. Pritchard, A. L., and Hayward, N. K. (2013) Molecular pathways: mitogen-activated protein kinase pathway mutations and drug resistance. *Clinical cancer research : an official journal of the American Association for Cancer Research* **19**, 2301-2309
244. Alessi, D. R., Cuenda, A., Cohen, P., Dudley, D. T., and Saltiel, A. R. (1995) PD 098059 is a specific inhibitor of the activation of mitogen-activated protein kinase kinase in vitro and in vivo. *The Journal of biological chemistry* **270**, 27489-27494
245. Codreanu, S. G., Adams, D. G., Dawson, E. S., Wadzinski, B. E., and Liebler, D. C. (2006) Inhibition of protein phosphatase 2A activity by selective electrophile alkylation damage. *Biochemistry* **45**, 10020-10029
246. Vasilescu, J., Smith, J. C., Ethier, M., and Figeys, D. (2005) Proteomic analysis of ubiquitinated proteins from human MCF-7 breast cancer cells by immunoaffinity purification and mass spectrometry. *Journal of proteome research* **4**, 2192-2200
247. Hunter, T. (2007) The Age of Crosstalk: Phosphorylation, Ubiquitination, and Beyond. *Molecular cell* **28**, 730-738
248. Dougherty, M. K., Muller, J., Ritt, D. A., Zhou, M., Zhou, X. Z., Copeland, T. D., Conrads, T. P., Veenstra, T. D., Lu, K. P., and Morrison, D. K. (2005) Regulation of Raf-1 by direct feedback phosphorylation. *Molecular cell* **17**, 215-224
249. Janosch, P., Kieser, A., Eulitz, M., Lovric, J., Sauer, G., Reichert, M., Gounari, F., Buscher, D., Baccarini, M., Mischak, H., and Kolch, W. (2000) The Raf-1 kinase associates with vimentin kinases and regulates the structure of vimentin filaments. *FASEB journal : official publication of the Federation of American Societies for Experimental Biology* **14**, 2008-2021
250. Sbroggio, M., Carnevale, D., Bertero, A., Cifelli, G., De Blasio, E., Mascio, G., Hirsch, E., Bahou, W. F., Turco, E., Silengo, L., Brancaccio, M., Lembo, G., and Tarone, G. (2011) IQGAP1 regulates ERK1/2 and AKT signalling in the heart and sustains functional remodelling upon pressure overload. *Cardiovascular research* **91**, 456-464
251. Ren, J. G., Li, Z., and Sacks, D. B. (2008) IQGAP1 integrates Ca2+/calmodulin and B-Raf signaling. *The Journal of biological chemistry* **283**, 22972-22982
252. Datta, P. K., Chytil, A., Gorska, A. E., and Moses, H. L. (1998) Identification of STRAP, a novel WD domain protein in transforming growth factor-beta signaling. *The Journal of biological chemistry* **273**, 34671-34674
253. Reiner, J. E., and Datta, P. K. (2011) TGF-beta-dependent and -independent roles of STRAP in cancer. *Frontiers in bioscience (Landmark edition)* **16**, 105-115
254. Vukmirovic, M., Manojlovic, Z., and Stefanovic, B. (2013) Serine-threonine kinase receptor-associated protein (STRAP) regulates translation of type I collagen mRNAs. *Molecular and cellular biology* **33**, 3893-3906
255. Sanges, C., Scheuermann, C., Zahedi, R. P., Sickmann, A., Lamberti, A., Migliaccio, N., Baljuls, A., Marra, M., Zappavigna, S., Reinders, J., Rapp, U., Abbruzzese, A., Caraglia, M., and Arcari, P. (2012) Raf kinases mediate the phosphorylation of eukaryotic translation elongation factor 1A and regulate its stability in eukaryotic cells. *Cell death & disease* **3**, e276
256. Xu, T. R., Lu, R. F., Romano, D., Pitt, A., Houslay, M. D., Milligan, G., and Kolch, W. (2012) Eukaryotic translation initiation factor 3, subunit a, regulates

the extracellular signal-regulated kinase pathway. *Molecular and cellular biology* **32**, 88-95
257. Harvey, J. J. (1964) AN UNIDENTIFIED VIRUS WHICH CAUSES THE RAPID PRODUCTION OF TUMOURS IN MICE. *Nature* **204**, 1104-1105
258. Kirsten, W. H., and Mayer, L. A. (1969) Malignant lymphomas of extrathymic origin induced in rats by murine erythroblastosis virus. *Journal of the National Cancer Institute* **43**, 735-746
259. Malumbres, M., and Barbacid, M. (2003) RAS oncogenes: the first 30 years. *Nature reviews. Cancer* **3**, 459-465
260. Scolnick, E. M., Rands, E., Williams, D., and Parks, W. P. (1973) Studies on the nucleic acid sequences of Kirsten sarcoma virus: a model for formation of a mammalian RNA-containing sarcoma virus. *Journal of virology* **12**, 458-463
261. Marshall, C. J., Hall, A., and Weiss, R. A. (1982) A transforming gene present in human sarcoma cell lines. *Nature* **299**, 171-173
262. Hall, A., Marshall, C. J., Spurr, N. K., and Weiss, R. A. (1983) Identification of transforming gene in two human sarcoma cell lines as a new member of the ras gene family located on chromosome 1. *Nature* **303**, 396-400
263. Der, C. J., Krontiris, T. G., and Cooper, G. M. (1982) Transforming genes of human bladder and lung carcinoma cell lines are homologous to the ras genes of Harvey and Kirsten sarcoma viruses. *Proceedings of the National Academy of Sciences of the United States of America* **79**, 3637-3640
264. Shimizu, K., Goldfarb, M., Suard, Y., Perucho, M., Li, Y., Kamata, T., Feramisco, J., Stavnezer, E., Fogh, J., and Wigler, M. H. (1983) Three human transforming genes are related to the viral ras oncogenes. *Proceedings of the National Academy of Sciences of the United States of America* **80**, 2112-2116
265. Chang, E. H., Gonda, M. A., Ellis, R. W., Scolnick, E. M., and Lowy, D. R. (1982) Human genome contains four genes homologous to transforming genes of Harvey and Kirsten murine sarcoma viruses. *Proceedings of the National Academy of Sciences of the United States of America* **79**, 4848-4852
266. Rojas, A. M., Fuentes, G., Rausell, A., and Valencia, A. (2012) The Ras protein superfamily: evolutionary tree and role of conserved amino acids. *The Journal of cell biology* **196**, 189-201
267. Reuther, G. W., and Der, C. J. (2000) The Ras branch of small GTPases: Ras family members don't fall far from the tree. *Current opinion in cell biology* **12**, 157-165
268. Colicelli, J. (2004) Human RAS superfamily proteins and related GTPases. *Science's STKE : signal transduction knowledge environment* **2004**, RE13
269. Cherfils, J., and Zeghouf, M. (2013) Regulation of small GTPases by GEFs, GAPs, and GDIs. *Physiological reviews* **93**, 269-309
270. Wright, L. P., and Philips, M. R. (2006) Thematic review series: lipid posttranslational modifications. CAAX modification and membrane targeting of Ras. *Journal of lipid research* **47**, 883-891
271. Chiu, V. K., Bivona, T., Hach, A., Sajous, J. B., Silletti, J., Wiener, H., Johnson, R. L., 2nd, Cox, A. D., and Philips, M. R. (2002) Ras signalling on the endoplasmic reticulum and the Golgi. *Nature cell biology* **4**, 343-350

272. Bivona, T. G., Quatela, S. E., Bodemann, B. O., Ahearn, I. M., Soskis, M. J., Mor, A., Miura, J., Wiener, H. H., Wright, L., Saba, S. G., Yim, D., Fein, A., Perez de Castro, I., Li, C., Thompson, C. B., Cox, A. D., and Philips, M. R. (2006) PKC regulates a farnesyl-electrostatic switch on K-Ras that promotes its association with Bcl-XL on mitochondria and induces apoptosis. *Molecular cell* **21**, 481-493
273. Plowman, S. J., and Hancock, J. F. (2005) Ras signaling from plasma membrane and endomembrane microdomains. *Biochimica et biophysica acta* **1746**, 274-283
274. Plowman, S. J., Muncke, C., Parton, R. G., and Hancock, J. F. (2005) H-ras, K-ras, and inner plasma membrane raft proteins operate in nanoclusters with differential dependence on the actin cytoskeleton. *Proceedings of the National Academy of Sciences of the United States of America* **102**, 15500-15505
275. Abankwa, D., Gorfe, A. A., and Hancock, J. F. (2007) Ras nanoclusters: molecular structure and assembly. *Seminars in cell & developmental biology* **18**, 599-607
276. Elad-Sfadia, G., Haklai, R., Balan, E., and Kloog, Y. (2004) Galectin-3 augments K-Ras activation and triggers a Ras signal that attenuates ERK but not phosphoinositide 3-kinase activity. *The Journal of biological chemistry* **279**, 34922-34930
277. Ariotti, N., Liang, H., Xu, Y., Zhang, Y., Yonekubo, Y., Inder, K., Du, G., Parton, R. G., Hancock, J. F., and Plowman, S. J. (2010) Epidermal growth factor receptor activation remodels the plasma membrane lipid environment to induce nanocluster formation. *Molecular and cellular biology* **30**, 3795-3804
278. Tian, T., Harding, A., Inder, K., Plowman, S., Parton, R. G., and Hancock, J. F. (2007) Plasma membrane nanoswitches generate high-fidelity Ras signal transduction. *Nature cell biology* **9**, 905-914
279. Tian, T., Plowman, S. J., Parton, R. G., Kloog, Y., and Hancock, J. F. (2010) Mathematical modeling of K-Ras nanocluster formation on the plasma membrane. *Biophysical journal* **99**, 534-543
280. Marshall, C. J. (1995) Specificity of receptor tyrosine kinase signaling: transient versus sustained extracellular signal-regulated kinase activation. *Cell* **80**, 179-185
281. Nagashima, T., Shimodaira, H., Ide, K., Nakakuki, T., Tani, Y., Takahashi, K., Yumoto, N., and Hatakeyama, M. (2007) Quantitative transcriptional control of ErbB receptor signaling undergoes graded to biphasic response for cell differentiation. *The Journal of biological chemistry* **282**, 4045-4056
282. McCawley, L. J., Li, S., Wattenberg, E. V., and Hudson, L. G. (1999) Sustained activation of the mitogen-activated protein kinase pathway. A mechanism underlying receptor tyrosine kinase specificity for matrix metalloproteinase-9 induction and cell migration. *The Journal of biological chemistry* **274**, 4347-4353
283. Karnoub, A. E., and Weinberg, R. A. (2008) Ras oncogenes: split personalities. *Nature reviews. Molecular cell biology* **9**, 517-531
284. Yan, J., Roy, S., Apolloni, A., Lane, A., and Hancock, J. F. (1998) Ras isoforms vary in their ability to activate Raf-1 and phosphoinositide 3-kinase. *The Journal of biological chemistry* **273**, 24052-24056
285. Walsh, A. B., and Bar-Sagi, D. (2001) Differential activation of the Rac pathway by Ha-Ras and K-Ras. *The Journal of biological chemistry* **276**, 15609-15615

286. McPherson, R. A., Harding, A., Roy, S., Lane, A., and Hancock, J. F. (1999) Interactions of c-Raf-1 with phosphatidylserine and 14-3-3. *Oncogene* **18**, 3862-3869
287. Stokoe, D., Macdonald, S. G., Cadwallader, K., Symons, M., and Hancock, J. F. (1994) Activation of Raf as a result of recruitment to the plasma membrane. *Science* **264**, 1463-1467
288. Kyriakis, J. M., App, H., Zhang, X. F., Banerjee, P., Brautigan, D. L., Rapp, U. R., and Avruch, J. (1992) Raf-1 activates MAP kinase-kinase. *Nature* **358**, 417-421
289. Alessi, D. R., Saito, Y., Campbell, D. G., Cohen, P., Sithanandam, G., Rapp, U., Ashworth, A., Marshall, C. J., and Cowley, S. (1994) Identification of the sites in MAP kinase kinase-1 phosphorylated by p74raf-1. *The EMBO journal* **13**, 1610-1619
290. Zheng, C. F., and Guan, K. L. (1993) Properties of MEKs, the kinases that phosphorylate and activate the extracellular signal-regulated kinases. *The Journal of biological chemistry* **268**, 23933-23939
291. Catalanotti, F., Reyes, G., Jesenberger, V., Galabova-Kovacs, G., de Matos Simoes, R., Carugo, O., and Baccarini, M. (2009) A Mek1-Mek2 heterodimer determines the strength and duration of the Erk signal. *Nature structural & molecular biology* **16**, 294-303
292. Payne, D. M., Rossomando, A. J., Martino, P., Erickson, A. K., Her, J. H., Shabanowitz, J., Hunt, D. F., Weber, M. J., and Sturgill, T. W. (1991) Identification of the regulatory phosphorylation sites in pp42/mitogen-activated protein kinase (MAP kinase). *The EMBO journal* **10**, 885-892
293. Seger, R., Seger, D., Lozeman, F. J., Ahn, N. G., Graves, L. M., Campbell, J. S., Ericsson, L., Harrylock, M., Jensen, A. M., and Krebs, E. G. (1992) Human T-cell mitogen-activated protein kinase kinases are related to yeast signal transduction kinases. *The Journal of biological chemistry* **267**, 25628-25631
294. Aebersold, D. M., Shaul, Y. D., Yung, Y., Yarom, N., Yao, Z., Hanoch, T., and Seger, R. (2004) Extracellular signal-regulated kinase 1c (ERK1c), a novel 42-kilodalton ERK, demonstrates unique modes of regulation, localization, and function. *Molecular and cellular biology* **24**, 10000-10015
295. Shaul, Y. D., Gibor, G., Plotnikov, A., and Seger, R. (2009) Specific phosphorylation and activation of ERK1c by MEK1b: a unique route in the ERK cascade. *Genes Dev* **23**, 1779-1790
296. Yung, Y., Yao, Z., Hanoch, T., and Seger, R. (2000) ERK1b, a 46-kDa ERK isoform that is differentially regulated by MEK. *The Journal of biological chemistry* **275**, 15799-15808
297. Yung, Y., Yao, Z., Aebersold, D. M., Hanoch, T., and Seger, R. (2001) Altered regulation of ERK1b by MEK1 and PTP-SL and modified Elk1 phosphorylation by ERK1b are caused by abrogation of the regulatory C-terminal sequence of ERKs. *The Journal of biological chemistry* **276**, 35280-35289
298. Boulton, T. G., Nye, S. H., Robbins, D. J., Ip, N. Y., Radziejewska, E., Morgenbesser, S. D., DePinho, R. A., Panayotatos, N., Cobb, M. H., and Yancopoulos, G. D. (1991) ERKs: a family of protein-serine/threonine kinases

that are activated and tyrosine phosphorylated in response to insulin and NGF. *Cell* **65**, 663-675
299. Lefloch, R., Pouyssegur, J., and Lenormand, P. (2008) Single and combined silencing of ERK1 and ERK2 reveals their positive contribution to growth signaling depending on their expression levels. *Molecular and cellular biology* **28**, 511-527
300. Saba-El-Leil, M. K., Vella, F. D., Vernay, B., Voisin, L., Chen, L., Labrecque, N., Ang, S. L., and Meloche, S. (2003) An essential function of the mitogen-activated protein kinase Erk2 in mouse trophoblast development. *EMBO reports* **4**, 964-968
301. Pages, G., Guerin, S., Grall, D., Bonino, F., Smith, A., Anjuere, F., Auberger, P., and Pouyssegur, J. (1999) Defective thymocyte maturation in p44 MAP kinase (Erk 1) knockout mice. *Science* **286**, 1374-1377
302. Yao, Y., Li, W., Wu, J., Germann, U. A., Su, M. S., Kuida, K., and Boucher, D. M. (2003) Extracellular signal-regulated kinase 2 is necessary for mesoderm differentiation. *Proceedings of the National Academy of Sciences of the United States of America* **100**, 12759-12764
303. Li, J., and Johnson, S. E. (2006) ERK2 is required for efficient terminal differentiation of skeletal myoblasts. *Biochem Biophys Res Commun* **345**, 1425-1433
304. Vantaggiato, C., Formentini, I., Bondanza, A., Bonini, C., Naldini, L., and Brambilla, R. (2006) ERK1 and ERK2 mitogen-activated protein kinases affect Ras-dependent cell signaling differentially. *Journal of biology* **5**, 14
305. Krens, S. F., Corredor-Adamez, M., He, S., Snaar-Jagalska, B. E., and Spaink, H. P. (2008) ERK1 and ERK2 MAPK are key regulators of distinct gene sets in zebrafish embryogenesis. *BMC genomics* **9**, 196
306. Roberts, M. S., Woods, A. J., Shaw, P. E., and Norman, J. C. (2003) ERK1 associates with alpha(v)beta 3 integrin and regulates cell spreading on vitronectin. *The Journal of biological chemistry* **278**, 1975-1985
307. Schaeffer, H. J. (1998) MP1: A MEK Binding Partner That Enhances Enzymatic Activation of the MAP Kinase Cascade. *Science* **281**, 1668-1671
308. Shao, Y., and Aplin, A. E. (2012) ERK2 phosphorylation of serine 77 regulates Bmf pro-apoptotic activity. *Cell death & disease* **3**, e253
309. Farhan, H., Wendeler, M. W., Mitrovic, S., Fava, E., Silberberg, Y., Sharan, R., Zerial, M., and Hauri, H. P. (2010) MAPK signaling to the early secretory pathway revealed by kinase/phosphatase functional screening. *The Journal of cell biology* **189**, 997-1011
310. Illert, A. L., Zech, M., Moll, C., Albers, C., Kreutmair, S., Peschel, C., Bassermann, F., and Duyster, J. (2012) Extracellular signal-regulated kinase 2 (ERK2) mediates phosphorylation and inactivation of nuclear interaction partner of anaplastic lymphoma kinase (NIPA) at G2/M. *The Journal of biological chemistry* **287**, 37997-38005
311. Echeverria, P. C., Bernthaler, A., Dupuis, P., Mayer, B., and Picard, D. (2011) An interaction network predicted from public data as a discovery tool: application to the Hsp90 molecular chaperone machine. *PloS one* **6**, e26044
312. Vaughan, C. K., Mollapour, M., Smith, J. R., Truman, A., Hu, B., Good, V. M., Panaretou, B., Neckers, L., Clarke, P. A., Workman, P., Piper, P. W., Prodromou,

C., and Pearl, L. H. (2008) Hsp90-dependent activation of protein kinases is regulated by chaperone-targeted dephosphorylation of Cdc37. *Molecular cell* **31**, 886-895
313. Soroka, J., Wandinger, S. K., Mausbacher, N., Schreiber, T., Richter, K., Daub, H., and Buchner, J. (2012) Conformational switching of the molecular chaperone Hsp90 via regulated phosphorylation. *Molecular cell* **45**, 517-528
314. Landar, A., Rustandi, R. R., Weber, D. J., and Zimmer, D. B. (1998) S100A1 utilizes different mechanisms for interacting with calcium-dependent and calcium-independent target proteins. *Biochemistry* **37**, 17429-17438
315. Amburgey, J. C., Abildgaard, F., Starich, M. R., Shah, S., Hilt, D. C., and Weber, D. J. (1995) 1H, 13C and 15N NMR assignments and solution secondary structure of rat Apo-S100 beta. *Journal of biomolecular NMR* **6**, 171-179
316. Ni, L., Swingle, M. S., Bourgeois, A. C., and Honkanen, R. E. (2007) High yield expression of serine/threonine protein phosphatase type 5, and a fluorescent assay suitable for use in the detection of catalytic inhibitors. *Assay and drug development technologies* **5**, 645-653
317. Wegner, A. M., McConnell, J. L., Blakely, R. D., and Wadzinski, B. E. (2007) An automated fluorescence-based method for continuous assay of PP2A activity. *Methods Mol Biol* **365**, 61-69
318. Skarra, D. V., Goudreault, M., Choi, H., Mullin, M., Nesvizhskii, A. I., Gingras, A. C., and Honkanen, R. E. (2011) Label-free quantitative proteomics and SAINT analysis enable interactome mapping for the human Ser/Thr protein phosphatase 5. *Proteomics* **11**, 1508-1516
319. Robinson, M. J., Harkins, P. C., Zhang, J., Baer, R., Haycock, J. W., Cobb, M. H., and Goldsmith, E. J. (1996) Mutation of position 52 in ERK2 creates a nonproductive binding mode for adenosine 5'-triphosphate. *Biochemistry* **35**, 5641-5646
320. Borthwick, E. B., Zeke, T., Prescott, A. R., and Cohen, P. T. W. (2001) Nuclear localization of protein phosphatase 5 is dependent on the carboxy-terminal region. *FEBS Letters* **491**, 279-284
321. Wortzel, I., and Seger, R. (2011) The ERK Cascade: Distinct Functions within Various Subcellular Organelles. *Genes & cancer* **2**, 195-209
322. Swingle, M., Ni, L., and Honkanen, R. E. (2007) Small-molecule inhibitors of ser/thr protein phosphatases: specificity, use and common forms of abuse. *Methods Mol Biol* **365**, 23-38
323. Schonwasser, D. C., Marais, R. M., Marshall, C. J., and Parker, P. J. (1998) Activation of the mitogen-activated protein kinase/extracellular signal-regulated kinase pathway by conventional, novel, and atypical protein kinase C isotypes. *Molecular and cellular biology* **18**, 790-798
324. Sturm, O. E., Orton, R., Grindlay, J., Birtwistle, M., Vyshemirsky, V., Gilbert, D., Calder, M., Pitt, A., Kholodenko, B., and Kolch, W. (2010) The mammalian MAPK/ERK pathway exhibits properties of a negative feedback amplifier. *Science signaling* **3**, ra90
325. Shin, S. Y., Rath, O., Choo, S. M., Fee, F., McFerran, B., Kolch, W., and Cho, K. H. (2009) Positive- and negative-feedback regulations coordinate the dynamic

behavior of the Ras-Raf-MEK-ERK signal transduction pathway. *Journal of cell science* **122**, 425-435
326. Balan, V., Leicht, D. T., Zhu, J., Balan, K., Kaplun, A., Singh-Gupta, V., Qin, J., Ruan, H., Comb, M. J., and Tzivion, G. (2006) Identification of novel in vivo Raf-1 phosphorylation sites mediating positive feedback Raf-1 regulation by extracellular signal-regulated kinase. *Molecular biology of the cell* **17**, 1141-1153
327. Uversky, V. N., and Dunker, A. K. (2013) The case for intrinsically disordered proteins playing contributory roles in molecular recognition without a stable 3D structure. *F1000 biology reports* **5**, 1
328. Sato, S., Fujita, N., and Tsuruo, T. (2000) Modulation of Akt kinase activity by binding to Hsp90. *Proceedings of the National Academy of Sciences of the United States of America* **97**, 10832-10837
329. Garai, A., Zeke, A., Gogl, G., Toro, I., Fordos, F., Blankenburg, H., Barkai, T., Varga, J., Alexa, A., Emig, D., Albrecht, M., and Remenyi, A. (2012) Specificity of linear motifs that bind to a common mitogen-activated protein kinase docking groove. *Science signaling* **5**, ra74
330. Fantz, D. A., Jacobs, D., Glossip, D., and Kornfeld, K. (2001) Docking sites on substrate proteins direct extracellular signal-regulated kinase to phosphorylate specific residues. *The Journal of biological chemistry* **276**, 27256-27265
331. Szomolay, B., and Shahrezaei, V. (2012) Bell-shaped and ultrasensitive dose-response in phosphorylation-dephosphorylation cycles: the role of kinase-phosphatase complex formation. *BMC systems biology* **6**, 26
332. Leung-Pineda, V., Ryan, C. E., and Piwnica-Worms, H. (2006) Phosphorylation of Chk1 by ATR is antagonized by a Chk1-regulated protein phosphatase 2A circuit. *Molecular and cellular biology* **26**, 7529-7538
333. Buhrman, G., Kumar, V. S., Cirit, M., Haugh, J. M., and Mattos, C. (2011) Allosteric modulation of Ras-GTP is linked to signal transduction through RAF kinase. *The Journal of biological chemistry* **286**, 3323-3331
334. Dhillon, A. S., Meikle, S., Yazici, Z., Eulitz, M., and Kolch, W. (2002) Regulation of Raf-1 activation and signalling by dephosphorylation. *The EMBO journal* **21**, 64-71
335. Deng, Y., Atri, D., Eichmann, A., and Simons, M. (2013) Endothelial ERK signaling controls lymphatic fate specification. *The Journal of clinical investigation* **123**, 1202-1215
336. Fernandez-Medarde, A., and Santos, E. (2011) Ras in cancer and developmental diseases. *Genes & cancer* **2**, 344-358
337. Radtke, S., Milanovic, M., Rosse, C., De Rycker, M., Lachmann, S., Hibbert, A., Kermorgant, S., and Parker, P. J. (2013) ERK2 but not ERK1 mediates HGF-induced motility in non-small cell lung carcinoma cell lines. *Journal of cell science* **126**, 2381-2391
338. Shin, S., Dimitri, C. A., Yoon, S. O., Dowdle, W., and Blenis, J. (2010) ERK2 but not ERK1 induces epithelial-to-mesenchymal transformation via DEF motif-dependent signaling events. *Molecular cell* **38**, 114-127
339. Aceves-Luquero, C. I., Agarwal, A., Callejas-Valera, J. L., Arias-Gonzalez, L., Esparis-Ogando, A., del Peso Ovalle, L., Bellon-Echeverria, I., de la Cruz-Morcillo, M. A., Galan Moya, E. M., Moreno Gimeno, I., Gomez, J. C.,

Deininger, M. W., Pandiella, A., and Sanchez Prieto, R. (2009) ERK2, but not ERK1, mediates acquired and "de novo" resistance to imatinib mesylate: implication for CML therapy. *PloS one* **4**, e6124
340. von Thun, A., Birtwistle, M., Kalna, G., Grindlay, J., Strachan, D., Kolch, W., von Kriegsheim, A., and Norman, J. C. (2012) ERK2 drives tumour cell migration in three-dimensional microenvironments by suppressing expression of Rab17 and liprin-beta2. *Journal of cell science* **125**, 1465-1477
341. Golden, T., Aragon, I. V., Rutland, B., Tucker, J. A., Shevde, L. A., Samant, R. S., Zhou, G., Amable, L., Skarra, D., and Honkanen, R. E. (2008) Elevated levels of Ser/Thr protein phosphatase 5 (PP5) in human breast cancer. *Biochimica et biophysica acta* **1782**, 259-270
342. Golden, T., Aragon, I. V., Zhou, G., Cooper, S. R., Dean, N. M., and Honkanen, R. E. (2004) Constitutive over expression of serine/threonine protein phosphatase 5 (PP5) augments estrogen-dependent tumor growth in mice. *Cancer letters* **215**, 95-100
343. Beronja, S., Janki, P., Heller, E., Lien, W. H., Keyes, B. E., Oshimori, N., and Fuchs, E. (2013) RNAi screens in mice identify physiological regulators of oncogenic growth. *Nature*
344. Nguyen, L. K., Matallanas, D., Croucher, D. R., von Kriegsheim, A., and Kholodenko, B. N. (2013) Signalling by protein phosphatases and drug development: a systems-centred view. *The FEBS journal* **280**, 751-765
345. McConnell, J. L., and Wadzinski, B. E. (2009) Targeting protein serine/threonine phosphatases for drug development. *Molecular pharmacology* **75**, 1249-1261
346. Kumar, D., Dua, R., Srikanth, R., Jayaswal, S., Siddiqui, Z., and Rao, K. V. (2008) Cellular phosphatases facilitate combinatorial processing of receptor-activated signals. *BMC research notes* **1**, 81
347. Hornberg, J. J., Bruggeman, F. J., Binder, B., Geest, C. R., de Vaate, A. J., Lankelma, J., Heinrich, R., and Westerhoff, H. V. (2005) Principles behind the multifarious control of signal transduction. ERK phosphorylation and kinase/phosphatase control. *The FEBS journal* **272**, 244-258
348. Costa, M., Marchi, M., Cardarelli, F., Roy, A., Beltram, F., Maffei, L., and Ratto, G. M. (2006) Dynamic regulation of ERK2 nuclear translocation and mobility in living cells. *Journal of cell science* **119**, 4952-4963
349. Huser, M., Luckett, J., Chiloeches, A., Mercer, K., Iwobi, M., Giblett, S., Sun, X. M., Brown, J., Marais, R., and Pritchard, C. (2001) MEK kinase activity is not necessary for Raf-1 function. *The EMBO journal* **20**, 1940-1951
350. Rauch, J., Volinsky, N., Romano, D., and Kolch, W. (2011) The secret life of kinases: functions beyond catalysis. *Cell communication and signaling : CCS* **9**, 23
351. Chen, J., Fujii, K., Zhang, L., Roberts, T., and Fu, H. (2001) Raf-1 promotes cell survival by antagonizing apoptosis signal-regulating kinase 1 through a MEK-ERK independent mechanism. *Proceedings of the National Academy of Sciences of the United States of America* **98**, 7783-7788
352. Bardwell, A. J., Abdollahi, M., and Bardwell, L. (2003) Docking sites on mitogen-activated protein kinase (MAPK) kinases, MAPK phosphatases and the

Elk-1 transcription factor compete for MAPK binding and are crucial for enzymic activity. *The Biochemical journal* **370**, 1077-1085
353. McFall, A., Ulku, A., Lambert, Q. T., Kusa, A., Rogers-Graham, K., and Der, C. J. (2001) Oncogenic Ras blocks anoikis by activation of a novel effector pathway independent of phosphatidylinositol 3-kinase. *Molecular and cellular biology* **21**, 5488-5499
354. White, M. A., Nicolette, C., Minden, A., Polverino, A., Van Aelst, L., Karin, M., and Wigler, M. H. (1995) Multiple Ras functions can contribute to mammalian cell transformation. *Cell* **80**, 533-541
355. Le, S. Q., and Gascuel, O. (2008) An improved general amino acid replacement matrix. *Molecular biology and evolution* **25**, 1307-1320
356. Hall, B. G. (2013) Building phylogenetic trees from molecular data with MEGA. *Molecular biology and evolution* **30**, 1229-1235
357. Tamura, K., Stecher, G., Peterson, D., Filipski, A., and Kumar, S. (2013) MEGA6: Molecular Evolutionary Genetics Analysis version 6.0. *Molecular biology and evolution* **30**, 2725-2729